



HAL
open science

**Nouvelles approches thérapeutiques pour réduire les
réponses au stress associées aux dysfonctions
cérébrovasculaires et réparatrices en situation diabétique
par des principes actifs vectorisés**

Sai Sandhya Narra

► **To cite this version:**

Sai Sandhya Narra. Nouvelles approches thérapeutiques pour réduire les réponses au stress associées aux dysfonctions cérébrovasculaires et réparatrices en situation diabétique par des principes actifs vectorisés. Biochimie, Biologie Moléculaire. Université de la Réunion; Central University of Tamil Nadu (Inde), 2022. Français. NNT : 2022LARE0005 . tel-03675252

HAL Id: tel-03675252

<https://theses.hal.science/tel-03675252>

Submitted on 23 May 2022

HAL is a multi-disciplinary open access archive for the deposit and dissemination of scientific research documents, whether they are published or not. The documents may come from teaching and research institutions in France or abroad, or from public or private research centers.

L'archive ouverte pluridisciplinaire **HAL**, est destinée au dépôt et à la diffusion de documents scientifiques de niveau recherche, publiés ou non, émanant des établissements d'enseignement et de recherche français ou étrangers, des laboratoires publics ou privés.



THÈSE

Présenté pour l'obtention du titre de Docteur de l'Université de La Réunion

Spécialité - **Biologie cellulaire et Biochimie**

Par

Sai Sandhya NARRA

Nouvelles approches thérapeutiques pour réduire les réponses au stress associées aux dysfonctions cérébrovasculaires et réparatrices en situation diabétique par des principes actifs vectorisés

Soutenue publiquement le Mercredi 6 avril 2022

Composition du jury:

Pr. Archana Bhaw-Luximon	University of Mauritius	Rapporteur
Pr. Sonia Athina Karabina	Sorbonne Université	Rapporteur
Pr. Philippe Gasque	Université de La Réunion	Examinateur et Président
Pr. Muthukalingan Krishnan	Central University of Tamil Nadu	Examinateur
Assoc. Pr. Ravanan Palaniyandi	Central University of Tamil Nadu	Co-directeur
Pr. Christian Lefebvre d'Hellencourt	Université de La Réunion	Directeur



THESIS

To obtain the title of Doctor of Philosophy from the Université de La Réunion

Speciality : **Cell Biology and Biochemistry**

By

Sai Sandhya NARRA

New therapeutic approaches to reduce the stress responses related to cerebrovascular dysfunction and regenerative wound healing in diabetes condition by the use of vector encapsulated active compounds

Presented and defended publicly on April 6, 2022

Composition of the jury

Pr. Archana Bhaw-Luximon	University of Mauritius	Reviewer
Pr. Sonia Athina Karabina	Sorbonne Université	Reviewer
Pr. Philippe Gasque	Université de La Réunion	Examiner and President
Pr. Muthukalingan Krishnan	Central University of Tamil Nadu	Examiner
Assoc. Pr. Ramanan Palaniyandi	Central University of Tamil Nadu	Co-director
Pr. Christian Lefebvre d'Hellencourt	Université de La Réunion	Director

To my family,

To my friends

And god

Acknowledgements

This work was carried out in the Joint Research Unit - 1188 Diabetes atherothrombosis Thérapies Réunion Océan Indien (DÉTROI) which is directed by Dir. Olivier Meilhac, whom I sincerely thank for welcoming me to DÉTROI laboratory for my research training.

A special thanks to the Region Reunion of National Education of Higher Education and Research for their financial support through a doctoral contract from the University of La Reunion that made this research work possible. This work was in collaboration with Associate Pr. Ramanan Palaniyandi of Central University of Tamil Nadu (India).

I would like to thank Pr. Sonia Athina Karabina and Pr. Archana Bhaw-Luximon for doing me the honor of judging this thesis work as rapporteurs and examiners. I also express my sincere thanks to Pr. Muthukalingan Krishnan and Pr. Philippe Gasque for agreeing to be the examiners of my thesis work.

I would like to express my deep gratitude to my thesis director Pr. Christian Lefebvre d'Hellencourt and Co-director Associate Pr. Ramanan Palaniyandi, thank you so much for giving me this opportunity to finish my thesis and for having taught me so much in my research journey. Your advice and your encouragement enabled me to complete this work. Pr. Christian Lefebvre d'Hellencourt, thank you for your positivity and support for my work and my stay in Reunion Island. Special thanks to Associate Pr. Ramanan Palaniyandi for giving me this opportunity to apply for my thesis at University of La Reunion at the first place.

I would like to specially thank all the members of my thesis committee for their valuable support, encouragement with their wise and benevolent advices. Special thanks to Dir. Olivier Meilhac co-supervisor of my work who has supported, taught many things and encouraged me to complete this work gracefully.

I would like to express my sincere gratitude to all the members of DÉTROI laboratory and to all the people who have directly or indirectly contributed for the inspiration of completing this work.

Special thanks to Dr. Nicolas for your support and encouragement. I also thank the members of PIMIT laboratory and CYROI platform.

I would like to thank and show my affection to my friends, from here and elsewhere:

Special thanks to Chloe, Batoul, Latufa for being there for me during my happy and hard days.

Thank you for your presence, support and being part of my life.

Chloe, you have made my journey in Reunion Island very beautiful and special. I will cherish every moment of this experience.

Batoul, Thank you for being there for me always to help and support me.

I thank my lovely family for their unconditional love, support and encouragement for all these years. Mom and Dad, thank you for your unfailing trust and love for me. Thanks for guiding me so far in my life and hope to receive the same in the coming years.

Table of Contents

Résumé.....	11
Abstract.....	12
Scientific Publications	13
List of figures.....	14
List of tables	15
List of Abbreviations	17
General Introduction.....	20
Bibliographic studies	22
I. Diabetes and its pathophysiology in vascular complications	23
1.1 Diabetes and its prevalence	23
1.2.1 Microvascular complications of diabetes	25
Diabetic Neuropathy.....	25
Diabetic Retinopathy	25
Diabetic Nephropathy.....	25
1.2.2 Macrovascular complications of diabetes.....	26
Coronary heart disease.....	26
Peripheral artery disease.....	26
Cerebrovascular disease in diabetes	26
1.3 Pathophysiology of diabetic vascular complications.....	27
1.3.1 Role of hyperglycemia in diabetic vascular complications	27
1.3.3 Role of advanced glycation end products in diabetic vascular complications.....	31
1.3.4 Role of Oxidative stress in diabetic vascular complications	35
1.3.5 Role of inflammation in diabetic vascular complications	37
II. Diabetic Stroke and impaired wound healing, pathophysiology and therapeutics	44
2.1 Diabetic stroke.....	44
2.1.1 Ischemic stroke.....	44
2.1.2 Haemorrhagic stroke.....	44
2.2 Pathophysiology of diabetic Stroke	45
2.3 Therapeutics for diabetic stroke.....	49
III Curcumin, its therapeutics benefits.....	54
3.3 Bioactive properties of curcumin.....	56
3.3.1 Anti-inflammatory activity of curcumin.....	57

3.3.2	Antioxidant activity of curcumin.....	57
3.3.3	Antimicrobial activity of curcumin	58
3.3.4	Anti-cancer mechanism	58
3.3.5	Role of curcumin in metabolic disorders and wound healing	59
3.4	Metabolism of curcumin.....	59
3.5	Bioavailability and Biodistribution of curcumin	61
3.5.1	Oral administration	61
3.5.2	Intravenous (IV) administration	62
3.5.3	Intraperitoneal administration (IP)	62
3.5.5	Topical and nasal administration.....	62
3.6	Therapeutic formulations of curcumin	63
IV.	HDL and its therapeutic properties in vascular complications.....	66
4.1	Structure of HDL	66
4.2	HDL sub types.....	68
4.3	Biogenesis and function of HDL	69
4.4	HDL cargo.....	71
4.5	HDL in the pathophysiology of vascular diseases.....	71
4.5.1	HDL anti-inflammatory role.....	71
4.5.2	HDL antioxidant role.....	72
4.5.3	HDL anti-apoptotic role.....	73
4.6	Cellular uptake of HDL	73
4.7	HDL molecules in therapeutics	75
	HDL in drug delivery	75
V	Marine Algae and their use in therapeutics	78
5.1	Marine algae and their bioactive properties.....	78
	Green algae.....	78
	Brown algae.....	79
	Red algae.....	79
5.2	Composition of marine algae.....	80
5.2.1	Polysaccharides of marine algae.....	80
5.3	Marine algae use in nutraceuticals.....	81
5.4	Pharmacological use of marine algae in cosmetic industry	82
5.5	Use of marine algae in food and agricultural industry.....	83
5.6	Use of marine algae in biomedical field	84
	Purpose of the work: Aim and objectives.....	86

Experimental results	87
Part 1: Impact of curcumin loaded rHDL nanoparticles on methylglyoxal mediated cytotoxicity and stress in cerebral endothelial cells	88
I. Introduction	88
I. introduction	88
II. Methods	89
III. Results	90
IV. Discussion	91
V. Conclusion	92
Part 2. Impact of curcumin nanomicelles on zebrafish tail regeneration.....	94
I. Introduction	94
II. Methods	94
III. Results	98
IV. Discussion	99
V. Conclusion	99
Perspectives and conclusion	101
References	111
Annexe.....	130
Résumé	131
Abstract.....	132

Résumé

Le diabète est un problème majeur de santé publique. Il est caractérisé par une hyperglycémie, une résistance à l'insuline et est associé à des complications macro et micro vasculaires. En situation de diabète, la concentration de méthylglyoxal (MGO) est augmentée. Le MGO est un précurseur des produits avancés de glycation (AGE) et il induit un stress oxydatif, une inflammation et un stress du réticulum endoplasmique. Ces Stress jouent un rôle important dans les dysfonctions endothéliales et de la barrière hématoencéphalique ainsi que dans le retard de réparation des lésions.

L'objectif de ma thèse a été d'améliorer la délivrance de curcumine, une molécule d'origine végétale. La curcumine a plusieurs effets bénéfiques tel que des activités anti oxydantes et anti inflammatoires, mais ces effets sont limités par son hydrophobicité. Des nanovecteurs tel que des protéines de hautes densités (HDL) ou des micelles peuvent améliorer la délivrance de la curcumine.

L'effet de la curcumine, vectorisée par des HDL ou par des micelles, a été évaluée dans deux modèles différents : la protection de cellules endothéliales en présence de MGO *in vitro* et *in vivo*, la régénération de la nageoire caudale chez le poisson zèbre.

Des nanoparticules de rHDL associées avec la curcumine (Cur-rHDLs) ont été préparées par ultracentrifugation après avoir mélangé brièvement les HDL avec la curcumine. Une analyse par LC-MS/MS a permis de quantifier la curcumine associée aux HDL. Les cellules endothéliales cérébrales Bend3 ont été prétraitées 1 heure en présence de rHDL, de curcumine ou de Cur-rHDLs puis incubées en présence de MGO. Sur des cellules traitées par du MGO, la Cur-rHDLs a montré un effet protecteur en réduisant la cytotoxicité, la production d'espèces radicalaires d'oxygène, le stress du réticulum endoplasmique et la condensation de la chromatine. Elle améliore également l'intégrité des cellules endothéliales compromise par le MGO. La Cur-rHDLs a un effet synergique en comparaison des effets de la curcumine ou des rHDLs seuls.

Des micelles de polysaccharide d'algues (des carraghénanes) associées avec de la curcumine (Cur-micelles) ont été préparées en copolymérisant des oligocarraghénanes (carraghénanes digérées) avec du polycaprolactone. La curcumine a été associée aux micelles par la méthode d'évaporation de l'acétone. Les Cur-micelles ont été caractérisées par des analyses de spectroscopie de résonance magnétique nucléaire et de diffusion dynamique de la lumière. Dans ce modèle, les Cur-micelles augmentent le recrutement des macrophages et des neutrophiles au site de la lésion ainsi que la taille de la surface de la nageoire régénérée. Les Cur-micelles ont également un effet synergique en comparaison des effets de la curcumine ou des micelles seules.

Ces travaux montrent les effets bénéfiques des Cur- rHDLs sur des cellules endothéliales en présence de MGO et des Cur-micelles sur la régénérescence de la nageoire caudale des poissons zèbres. Ils permettent une meilleure compréhension de ces approches et ouvrent de nouvelles perspectives de recherche pour le développement de thérapies dans le cadre de complications vasculaires associées au diabète.

Abstract

Diabetes is a major health issue worldwide. It is characterized by hyperglycemia, insulin resistance and is associated with many microvascular and macrovascular complications. In diabetic conditions, methylglyoxal (MGO) levels are increased. MGO is a major precursor of advanced glycation end products (AGE) formation and it induces cellular oxidative stress, inflammation and endoplasmic reticulum (ER) stress. These cellular stresses play a crucial role in endothelial and blood brain barrier (BBB) dysfunctions and also delay the wound healing.

My thesis objective was to improve the drug delivery of a plant derived compound (Curcumin). Curcumin has several beneficial properties such as antioxidant and anti-inflammatory properties but its effects are limited due to its hydrophobic nature. Nano-vectors such as High Density Lipoprotein (HDL) or micelles may help to improve the delivery of curcumin.

Curcumin vectorized by HDL or micelles were evaluated in two different models: *in vitro* brain endothelial cell protection from methylglyoxal and *in vivo* tail regeneration in Zebra fish.

Curcumin loaded rHDL nanoparticles (Cur-rHDLs) were prepared by mixing HDL and curcumin briefly followed by ultracentrifugation. Amount of curcumin loaded was quantified by LC-MS/MS analysis. Brain endothelial cells (Bend3), were pre-treated with rHDL, curcumin and Cur-rHDLs for 1h before co-incubating with MGO. Cur-rHDLs showed a protective effect by reducing the cytotoxicity, reactive oxygen species (ROS) production, ER stress, and chromatin condensation induced by MGO. It also improved the endothelial cell integrity impaired by MGO. Cur-rHDLs showed a synergistic effect compared to curcumin or rHDL alone.

Curcumin loaded carrageenan polysaccharide micelles (Cur-micelles) were prepared by using oligocarrageenan (digested carrageenan) copolymerized with polycaprolactone. Curcumin was loaded by acetone volatilization method. Cur-micelles were characterized by nuclear magnetic resonance analysis and dynamic light scattering analysis. On the Zebrafish tail amputation model, Cur-micelles increased macrophages and neutrophils recruitment to the site of tail injury and had a positive impact on the tail regeneration by increasing the tail regenerative area. Cur-micelles also showed a synergistic effect compared to curcumin or micelles alone.

These studies show the potential beneficial effects of Cur-rHDLs and Cur-micelles on MGO stimulated endothelial cells and on zebrafish tail regeneration, respectively. They open new research perspectives to further investigate and understand the mechanisms that can be used to develop therapeutics for diabetic vascular complications.

Scientific Publications

Publications directly related to this work:

Sai Sandhya Narra , Philippe Rondeau , Jessica Patche , Bryan Veeren , Marie-Paule Gonthier, Wildriss Viranaicken , Nicolas Diotel , Ramanan Palaniyandi , Christian Lefebvre d' Hellencourt and Olivier Meilhac.

Apo-A1 nanoparticles as curcumin carriers for cerebral endothelial cells: improved cytoprotective effects against methylglyoxal. *Pharmaceutics MDPI (Published on March 13 2022.)*

Sai Sandhya Narra , Laura Gence , Latufa Youssouf, Joël Couprie , Pierre Giraud , Nicolas Diotel, Christian Lefebvre D' Hellencourt.

Curcumin-encapsulated nanomicelles promote tissue regeneration in zebrafish larva. (**Preparing for submission**).

Other publications associated with the work:

Sai Sandhya Narra , Philippe Rondeau, Danielle Fernezelian, Laura Gence, Batoul Ghaddar, Emmanuel Bourdon, Christian Lefebvre d' Hellencourt, Sepand Rastegar and Nicolas Diotel.

Microglial distribution in adult zebrafish brain: focus on oxidative stress implication during brain repair. (**Submitted to Journal of comparative neurology on Feb 24 2022**).

Sepand Rastegar, Avinash Parimisetty, Nora Cassam Sulliman, **Sai Sandhya Narra**, Sabrina Weber, Maryam Rastegar, Wildriss Viranaicken, David Couret, Cynthia Planesse, Uwe Strähle, Olivier Meilhac, Christian Lefebvre d' Hellencourt, Nicolas Diotel.

Expression of adiponectin receptors in the brain of adult zebrafish and mouse: Links with neurogenic niches and brain repair. *Journal of Comparative Neurology*, 527(14), 2317-2333, (2019).

List of figures

FIGURE 1: DIABETIC MICROVASCULAR AND MACROVASCULAR COMPLICATIONS	24
FIGURE 2: HYPERGLYCEMIA IN DIABETIC VASCULAR COMPLICATIONS	29
FIGURE 3: SCHEMATICS OF METHYLGLYOXAL FORMATION, DETOXIFICATION AND ROLE IN DIABETIC VASCULAR COMPLICATIONS	30
FIGURE 4: ADVANCED GLYCATION END PRODUCT FORMATION	31
FIGURE 5: INFLAMMATION ASSOCIATED WITH DIABETES	40
FIGURE 6: ENDOPLASMIC RETICULUM STRESS SENSOR MOLECULES AND THEIR PATHWAYS	42
FIGURE 7: TYPES OF STROKE: ISCHEMIC AND HAEMORRHAGIC STROKE	45
FIGURE 8: PATHOPHYSIOLOGY OF STROKE	46
FIGURE 9: OVERVIEW OF BBB NEUROVASCULAR UNIT	47
FIGURE 10: SCHEMATIC OF CEREBROVASCULATURE	49
FIGURE 11: WOUND HEALING PROCESS IN DIABETES.	52
FIGURE 12: CHEMICAL STRUCTURE OF CURCUMINOIDS OF TURMERIC	56
FIGURE 13: THERAPEUTIC PROPERTIES OF CURCUMIN	56
FIGURE 14: DIFFERENT METABOLITES OF CURCUMIN	61
FIGURE 15: BIODISTRIBUTION OF CURCUMIN AND ITS METABOLITES	63
FIGURE 16: DIFFERENT NANOFORMULATIONS OF CURCUMIN	65
FIGURE 17: STRUCTURE OF HDL	67
FIGURE 18: DIFFERENT SUB-TYPES OF HDL	69
FIGURE 19: SCHEMATIC OF HDL BIOGENESIS	70
FIGURE 20: CELLULAR UPTAKE OF HDL BY SR-B1 RECEPTORS	75
FIGURE 21: STRUCTURE OF KAPPA, IOTA AND LAMBDA CARRAGEENANS	81
FIGURE 22: CURCUMIN LOADED rHDL (CUR-rHDLs) PREPARATION METHOD	89
FIGURE 23: MECHANISM OF FORMATION OF COPOLYMER CAPROLACTONE GRAFTED CARRAGEENAN MICELLES	96
FIGURE 24: SCHEMATICS OF CURCUMIN DRUG LOADING METHOD	97
FIGURE 25: IN VIVO ZEBRAFISH TAIL AMPUTATION MODEL.	98
FIGURE 26: EFFECT OF FREE RESVERATROL ON BEND3 CEREBRAL ENDOTHELIAL CELLS TREATED WITH MGO.	103

FIGURE 27: EFFECT OF RESVERATROL LOADED rHDLs ON bEND3 CEREBRAL ENDOTHELIAL CELLS TREATED WITH MGO.	104
FIGURE 28: CYTOTOXICITY OF CURCUMIN OR RESVERATROL LOADED MICELLES ON bEND3 CEREBRAL ENDOTHELIAL CELLS.	106
FIGURE 29: CYTOTOXICITY OF CURCUMIN LOADED MICELLES ON RAW 264.7 MACROPHAGE CELLS.	107
FIGURE 30: ILLUSTRATION OF IN VIVO APPROACH OF USING DRUG ENCAPSULATED VECTORS.	107
FIGURE 31: ILLUSTRATION OF IN VIVO APPROACH OF USING DRUG ENCAPSULATED VECTORS IN MCAO MICE MODEL.....	109

List of tables

TABLE 1: DIFFERENT GLUCOSE TRANSPORTERS (ILLSLEY, 2000).	28
TABLE 2: DIFFERENT TYPES OF REACTIVE FREE RADICLE SPECIES (PHANIENDRA, JESTADI, & PERIYASAMY, 2015).	37
TABLE 3: QUANTIFICATION OF RESVERATROL BY LC-MS ANALYSIS.	104

List of Abbreviations

ABC: ATP binding cassette

AGE: Advanced glycation end products

ATF: Activating transcription factor

BBB: Blood brain barrier

CHOP: C/EBP homologous protein

CML: Carboxy methyl lysine

DHC: Dihydrocurcumin

ER: Endoplasmic reticulum

ERAD: ER associated protein degradation

GLUT: Glucose transporters

HDL: High density lipoprotein

HHS: Hyperosmolar hyperglycemic state

HHC: Hexahydrocurcumin

H₂O₂: Hydrogen peroxide

IL: Interleukin

IP: Intraperitoneal

IRE-1: Inositol requiring enzyme 1

IV: Intravenous

LCAT: Lecithin cholesterol transferase

LPS: Lipopolysaccharides

MAPK: Mitogen activated protein kinase

MCAO: Middle cerebral artery occlusion

MGO: Methylglyoxal

MMP: Matrix Metalloproteinase

NFκB: Nuclear factor kappa-B

NMR: Nuclear magnetic resonance

NO: Nitric oxide

OHC: Octahydrocurcumin

ONOO⁻: Peroxynitrite

PAD: Peripheral artery disease

PRRs: Pattern recognition receptors

RAGE: Receptor for advanced glycation end products

rHDL: Reconstituted HDL

RNS: Reactive nitrogen species

ROS: Reactive oxygen species

sRAGE: Soluble RAGE

SR-B1: Scavenger receptor class B type 1

THC: Tetrahydrocurcumin

TJ: Tight junctions

TLR: Toll-like receptors

TNF: Tumor necrosis factor

UPR: Unfolded protein responses

VEGF: Vascular endothelial growth factor

XBP-1: X-box binding protein 1

ZO: Zonula occludens

General Introduction

Diabetes is a serious metabolic disorder that is one of the major causes of mortality worldwide. Its prevalence is increasing rapidly throughout the world. It is associated with high blood glucose levels (hyperglycemia) and its abnormal regulation (insulin resistance) can trigger the inflammatory, oxidative stress and endoplasmic reticulum stress responses which play a key role in the progression and development of diabetic vascular complications. Vascular complications involve the structural and functional damage to blood vessels including the brain vessels, which can lead to the origin of stroke. Stroke is a condition where the brain is deprived of oxygen and nutrients supply due to the blockage of the brain blood vessels. Stroke is also a major issue of mortality worldwide. Stress associated with diabetes contributes to the damage of brain blood vessels (endothelial dysfunction) and permeability of blood-brain barrier (BBB). Endothelial cells line the blood vessels and maintain their proper functioning. BBB is composed of a neurovascular unit that includes endothelial cells associated with other cells (microglia, astrocytes, and pericytes) and is a selective barrier present in the brain region. BBB allows the passage of only certain molecules from the blood to the brain region to support the brain growth and function. Endothelial dysfunction is the major contributor to diabetic vascular complications.

Diabetic vascular complications also include peripheral artery disease (PAD). Prolonged diabetic condition is associated with PAD that involves the blockage and narrowing of blood vessels in the foot region due to fat deposition (atherosclerosis). PAD development and progression involves endothelial dysfunction, vascular inflammation, abnormalities in smooth muscle cells, blood cells and platelets that result in increased plaque formation and atherosclerosis. PAD is associated with stroke and mortality in diabetic conditions. It causes long-term disabilities in diabetic patients resulting in an increased risk of amputation of lower extremities. Diabetic foot ulcers, an outcome of PAD, is a chronic condition associated with failure of wound healing and results in foot amputation. Wound healing capacity is reduced or lost in diabetes condition. Oxidative stress and inflammatory processes are involved in the impaired diabetic wound healing.

Various polyphenol molecules derived from plant sources have many therapeutic properties including antioxidant, anti-inflammatory, anti-diabetic and wound healing properties. Therefore they are being widely used in therapeutics. Hydrophobic polyphenol molecules such as curcumin

and resveratrol use are limited in therapeutics due to their poor solubility and poor bioavailability. To overcome this limitation and improve the therapeutic benefits of hydrophobic drugs various nanoparticle drug delivery systems such as HDL and micelles are being developed for different pathophysiological conditions.

The use of HDL and micelles made of marine polysaccharides as drug delivery systems are newly emerging as they are biodegradable and less toxic.

This study focuses on preparing and characterization of HDL, micelles nanoparticles loaded with curcumin drug molecule. And these curcumin loaded nanoparticles were used to limit the impact of cellular stress on cerebrovascular damage concerning stroke and wound healing mechanisms in diabetic condition.

Bibliographic studies

I. Diabetes and its pathophysiology in vascular complications

1.1 Diabetes and its prevalence

Metabolic diseases, such as diabetes, are one of the major causes of deaths worldwide. Diabetes is caused by many factors including sedentary lifestyle, lack of physical exercise, age, junk food and genetics (Naslafkih & Sestier, 2003). It is one of the top 10 causes of death globally. The risk of diabetes is associated with cardiovascular diseases, stroke, chronic liver, kidney diseases, cancer and other infections (Bragg et al., 2017; Policardo et al., 2015).

Diabetes prevalence has reached pandemic proportions, reported to be 9% of the population affecting 463 million adults worldwide in 2019. By 2021 about 536.6 million adults are affected with diabetes and it is estimated that 783.2 million people will be affected by 2045. The global prevalence of diabetes (20-79 years adults) is 10.5 %. The prevalence of diabetes is variable with age, sex and region. Diabetes is found to be more prevalent in men (10.8%) than in women (10.2%) and found to be higher in 75-79 years adults (24%). The Prevalence of diabetes has increased in recent decades in most developed and developing countries (Dwyer-Lindgren, Mackenbach, van Lenthe, Flaxman, & Mokdad, 2016). The comparative prevalence of diabetes is higher in middle-income and low-income countries than high-income countries. The prevalence in urban areas is estimated to be 12.1 % and in rural areas 8.3 %. Global burden of diabetes has increased significantly in recent decades and is estimated to increase further in the coming years (H. Sun et al., 2022).

In France, prevalence of diabetes accounts for 8.6% (of adults) in 2022. Prevalence of diabetes mainly type 2 diabetes is increasing alarmingly in the French overseas than in mainland France. In India About 74.2 million people (adults) are by diabetes in 2021 (H. Sun et al., 2022).

Diabetes is a chronic metabolic disorder characterized by high blood glucose, impaired insulin secretion and insulin action (insulin resistance). The fasting glucose levels exceed 1.26g/L in the blood which is way beyond normal blood glucose levels (Gillett, 2009). Diabetes is classified as type-1, type-2, gestational diabetes and other specific types of diabetes (neonatal diabetes, diseases of exocrine pancreas and drug or chemical induced diabetes) (American Diabetes, 2021).

Type-1 diabetes is the deficiency of insulin production by pancreatic beta cells that can be due to the loss of beta cells by autoimmune destruction (Greenbaum et al., 2009; Hull, Peakman, &

Tree, 2017). It is known as insulin-dependent diabetes which accounts for 10% of the total diabetic cases. Various factors including environmental factors, reduced physical activity, genetic factors and immunogenic processes (including infiltration of lymphocytes and monocytes) (Babon et al., 2016; Michels et al., 2017) are associated with the progression of type-1 diabetes. Type-1 diabetic complications include hypoglycemia (Feltbower et al., 2008) and ketoacidosis (Skrivarhaug et al., 2006).

Type-2 diabetes is the loss of sensitivity to respond to insulin (insulin resistance) which impairs the regulation of insulin production by pancreatic beta cells (Mahler & Adler, 1999). It is known as non-insulin-dependent diabetes which is the most common type of diabetes that accounts for 90% of the total diabetic cases. It is characterized by insulin resistance (Botero & Wolfsdorf, 2005) and hyperglycemia (Cryer, 2012).

Gestational diabetes is the risk of development of diabetes in pregnant women during their pregnancy. It can either be a short-term prevalence until the delivery of the baby or prolongs after the delivery (Naylor, Sermer, Chen, & Sykora, 1996). However, it is a risk factor for both type1 and type 2 diabetes (Expert Committee on the & Classification of Diabetes, 2000). Women who develop type 1 and undiagnosed type 2 diabetes are classified under gestational diabetes. It develops mostly during the third trimester of pregnancy (Schmidt et al., 2001).

1.2 Diabetic complications

Diabetic complications include microvascular and macrovascular complications.

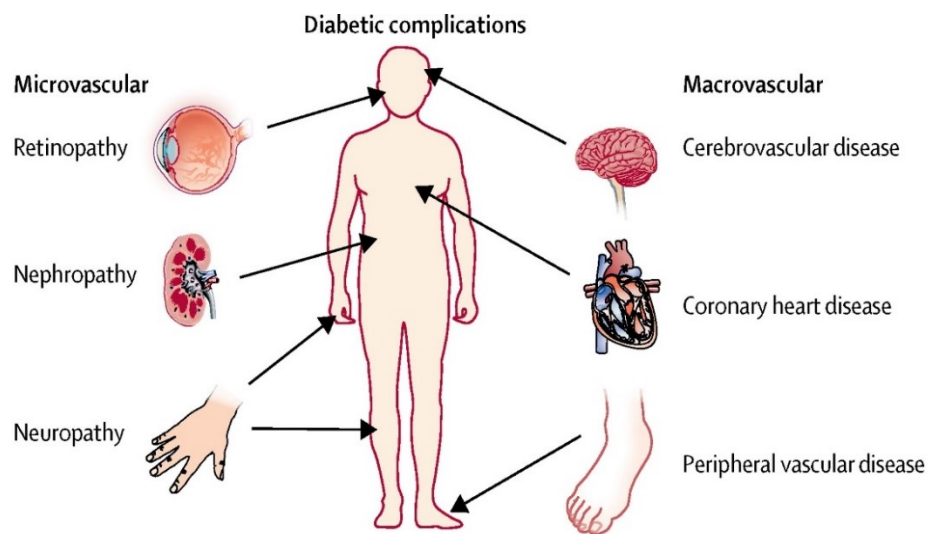


Figure 1: Diabetic microvascular and macrovascular complications (Gelfand & Wan, 2018).

1.2.1 Microvascular complications of diabetes

Diabetic microvascular complications include retinopathy, neuropathy and nephropathy (Fig 1). Diabetes is more associated with macrovascular complications than microvascular complications in terms of mortality rate. Microvascular complications are induced by different factors including oxidative stress, inflammation, hyperglycemia and advanced glycation end products (AGEs) (Peppia & Vlassara, 2005).

Diabetic Neuropathy

Diabetic Neuropathy is the damage caused to the nerves in diabetes condition. The peripheral nerve injury occurs at an early stage of diabetes during low glycaemic levels. Depending on the site of nerve damage the sensory symptoms include tingling, numbness and pain; motor symptoms include weakness and autonomic changes such as urinary symptoms (J. A. Cohen, Jeffers, Faldut, Marcoux, & Schrier, 1998). These symptoms are caused by small blood vessel dysfunction that supplies blood to the nerves, resulting in microvascular injury (Q. Yang et al., 2001). Advanced glycation end products (AGEs), oxidative stress and hyperglycemia are known to mediate nerve damage resulting in diabetic neuropathy (Eid et al., 2019; Vincent & Feldman, 2004).

Diabetic Retinopathy

Diabetic retinopathy is the damage of retinal blood vessels and neurons in diabetes, which is also known as diabetic eye disease. Long-term diabetes is associated with the development of retinopathy (Cheung, Mitchell, & Wong, 2010). Reduced blood flow due to the thinning of retinal arteries, dysfunction of the blood-retinal barrier and leakage of blood contents into the macular edema area results in blurred vision (Stitt et al., 2016). Hyperglycemia contributes to the damage of retinal blood vessels leading to blood loss, ischemia and dysfunction of retinal neurons and glial cells in the early non-proliferative diabetic stage (Frey & Antonetti, 2011). In the later advanced proliferative diabetic stage, new abnormal blood vessels are formed (neovascularization) which are fragile that can burst and bleed (vitreous haemorrhage) (X. Zhang, Zeng, Bao, Wang, & Gillies, 2014).

Diabetic Nephropathy

Diabetic nephropathy is the loss of kidney function due to damage of blood vessels in diabetes also known as diabetic kidney disease (Z. Zheng & Zheng, 2016). High blood glucose is involved

in the pathophysiology of diabetic nephropathy. Nephropathy involves many stages from hyperfiltration, microalbuminuria, macroalbuminuria and nephrotic proteinuria to end-stage renal disease. Damage to glomeruli blood vessels of the kidney leads to hypertension and hyperfiltration in the early stages of nephropathy and renal fibrosis is the major mechanism that leads to end-stage renal disease (Tervaert et al., 2010). Diabetes associated glucose metabolism deregulation, inflammation, over-activated renin-angiotensin-aldosterone system, oxidative stress and advanced glycation end products (AGEs) lead to renal fibrosis (Jude et al., 2002).

1.2.2 Macrovascular complications of diabetes

Macrovascular complications include stroke, peripheral artery disease, cerebrovascular disease and coronary heart disease (Fig 1).

Coronary heart disease

Coronary heart disease involves narrowing of coronary arteries, reduced blood flow and plaque formation in coronary arteries. It is also known as coronary artery/ischemic heart disease (Deedwania & Fonseca, 2005; Y. Wang, Yu, Fan, & Cao, 2012). The atherosclerotic plaque is formed by the accumulation of lipids, calcium and abnormal immune cells inside the coronary arteries (Nishio, 2016). Plaque formation hardens the arteries and partially obstructs the blood flow which can result in coronary heart disease (Onat, Donmez, Karadeniz, Cakir, & Kaya, 2014).

Peripheral artery disease

Peripheral artery disease involves the narrowing of the arteries that supply blood to the body except to the heart and brain regions (S. L. Yang et al., 2017). This mostly affects the leg region but also includes neck, kidneys and arms (Viigimaa et al., 2020). Peripheral artery disease associated with diabetes is involved in the high risk of amputations (Barnes, Eid, Creager, & Goodney, 2020). Atherosclerosis associated plaque formation in the arteries, and clot formation (thrombosis) together cause the narrowing of blood vessels resulting in the lack of oxygen (hypoxia) and blood supply to the various tissues of the body (Farber & Eberhardt, 2016).

Cerebrovascular disease in diabetes

Diabetic cerebrovascular disease involves the dysfunction of blood vessels and the blood circulation of the brain region resulting in stroke (McCrimmon, Ryan, & Frier, 2012). Atherosclerosis and hypertension contribute to the risk of cerebrovascular disease. Stroke is of

two types, ischemic stroke involves the blockage of blood vessels and reduced blood supply to the brain; hemorrhagic stroke involves rupture of the blood vessels and bleeding into the cerebrospinal fluid of the brain region (Shishkova & Adasheva, 2021). Atherosclerosis and thrombosis cause the narrowing of arteries that results in ischemic stroke and hypertension which can lead to hemorrhagic stroke (Chavda, Vashi, & Patel, 2021). This reduced blood flow to the brain (ischemia), if prolonged can result in hypoxia (lack of oxygen) that further causes brain cell damage (Zhou, Zhang, & Lu, 2014).

1.3 Pathophysiology of diabetic vascular complications

The Progression and development of vascular complications are associated with various factors of diabetes that lead to endothelial dysfunction (Fig 2) (Domingueti et al., 2016).

Hyperglycemia, by modifying the nitric oxide (NO) production and reactive oxygen species (ROS) accumulation leads to endothelial dysfunction (Tesfamariam, Brown, & Cohen, 1991). Nitric oxide is a key mediator secreted by the endothelium (R. A. Cohen, 2005). NO is a vasodilator that has anti-platelet, anti-proliferative and anti-inflammatory properties. Reduced NO biosynthesis and availability are associated with cardiovascular diseases (Schalkwijk & Stehouwer, 2005). Increased ROS production by mitochondria is linked to hyperglycemia which in turn triggers ROS mediated cellular mechanisms including increased intracellular levels of the glucose metabolite methylglyoxal, advanced glycation end products (AGE) synthesis and NFκB mediated inflammation that is involved in the development of vascular complications of diabetes (Nishikawa et al., 2000). Methylglyoxal plays a role in the pathophysiology of diabetic complications by AGEs accumulation, oxidative stress and endothelial dysfunction. AGE-RAGE signaling leads to cellular dysfunction by activation of ROS production and deregulation of enzymes involved in vascular homeostasis (Giacco & Brownlee, 2010).

1.3.1 Role of hyperglycemia in diabetic vascular complications

Glucose homeostasis is maintained by the neuroendocrine system which regulates the production, cellular uptake and utilization of glucose by the cells (Papachristoforou, Lambadiari, Maratou, & Makrilakis, 2020). Several hormones regulate the glucose levels in the body including insulin, epinephrine, cortisol, glucagon, growth hormone and glucagon like peptide-1. Glucose is mostly produced by the liver either by gluconeogenesis or glycogenolysis pathways. Pancreatic beta cells produce insulin that regulate glucose levels by increasing glucose uptake during glycogenolysis and reducing during gluconeogenesis (Crecil Dias, Kamath, &

Vidyasagar, 2020). Whereas during injury and stress conditions glucagon stimulates the upregulation of gluconeogenesis and raises the glucose levels to meet the cellular metabolic needs. Insulin and glucagon play a major role in glucose regulation via the liver and pancreatic islet cells that can directly sense the glucose concentrations in the blood. Imbalance in this hormonal regulation of glucose can result in increased blood glucose levels leading to hyperglycemia (Campbell & Drucker, 2015).

Glucose transporters	Location	Function
GLUT-1	Widespread	Responsible for basal glucose uptake. Insulin dependent
GLUT-2	Renal tubules, small intestine, liver, and pancreatic β cells	Ensures rapid glucose uptake by liver. Insulin independent
GLUT-3	Neurons and placenta	Possibly most important isoform in the central nervous system. Insulin independent
GLUT-4	Adipose, skeletal, and cardiac muscle	Located intracellularly, moving to plasma membrane promoted by insulin

Table 1: Different glucose transporters (Illsley, 2000).

GLUT transporters cellular expression and function details.

Glucose is a polar molecule that is transported to the cells by active or facilitated diffusion. Glucose is mostly transported by facilitated diffusion by transmembrane proteins called glucose transporters (GLUTs) either by insulin-dependent or insulin-independent mechanisms. GLUT 1-4 (Table 1) are the major glucose transport in the body (Lizak et al., 2019).

Hyperglycemia causes damage to the cells and tissues of the body but interestingly some cells have an internal efflux mechanism to remove excess glucose and regulate their intracellular glucose levels while some cells like endothelial cells, pancreatic beta cells and neuronal cells lack this mechanism and are more susceptible to excess glucose.

Hyperglycemia can cause acute or chronic diabetic complications (Orasanu & Plutzky, 2009). Acute complications include a hyperosmolar hyperglycemic state (HHS) and diabetic ketoacidosis (Umpierrez & Korytkowski, 2016). HHS occurs mostly in aged people while diabetic ketoacidosis occurs in young people. Both acute and chronic hyperglycemia is involved in the development of diabetic vascular complications (Steenkamp, Alexanian, & McDonnell, 2013).

Hyperglycemia is involved in the production of highly reactive dicarbonyl compounds and AGEs, which alter the function of macromolecules by post-translational modifications. These dicarbonyl compounds include mainly methylglyoxal (MGO), a well-known reactive metabolite involved in the pathophysiology of diabetic complications (Haik, Lo, & Thornalley, 1994).

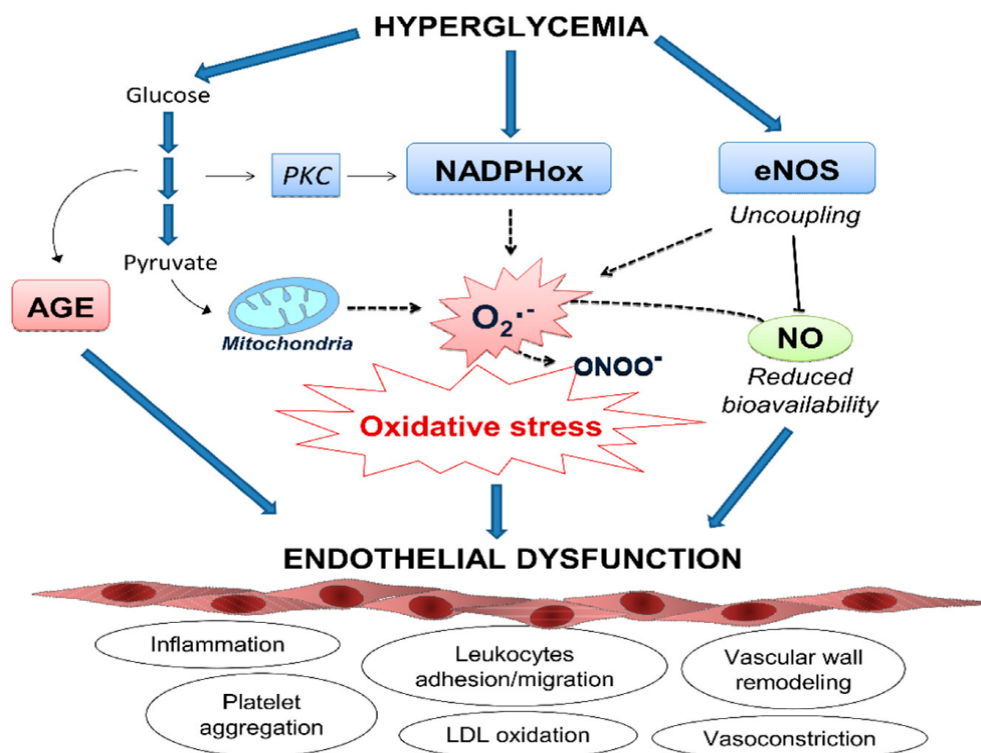


Figure 2: Hyperglycemia in diabetic vascular complications (Burgos-Moron et al., 2019). Mechanisms of ROS-induced endothelial dysfunction in response to hyperglycemia. Vascular damage caused by elevated glucose levels is mainly derived by an imbalance between ROS production and NO bioavailability in the endothelium and by the direct damaged caused by the accumulation of AGE. Resulting endothelial dysfunction is characterized by the activation of several deleterious mechanisms, including proinflammatory response, recruitment of leukocytes, accumulation of oxidized LDL particles and impaired vasodilatation, in the onset of cardiovascular complications. AGE: Advanced glycation end-products; eNOS: Endothelial nitric oxide synthase; LDL: Low density lipoprotein particles; NADPHox: Nicotinamide adenine

dinucleotide phosphate oxidase; NO: Nitric oxide; O₂^{•-}: Superoxide anion; ONOO⁻: Peroxynitrite; PKC: Protein kinase C; RNS: Radical nitrogen species.

1.3.2 Role of MGO in diabetic vascular complications

MGO is a physiological metabolite of the glycolytic pathway derived from triose phosphate intermediates. It is detoxified from the system after conversion to D-lactate by glyoxalase enzymes (Oya et al., 1999). MGO levels are low in a normal physiological condition whereas in pathophysiological conditions such as diabetes their levels significantly increase as the detoxification is impaired leading to their accumulation. It is a major precursor of AGE formation which contributes to endothelial dysfunction and diabetic vascular complications along with oxidative stress, inflammation. (Fiorentino, Prioletta, Zuo, & Folli, 2013).

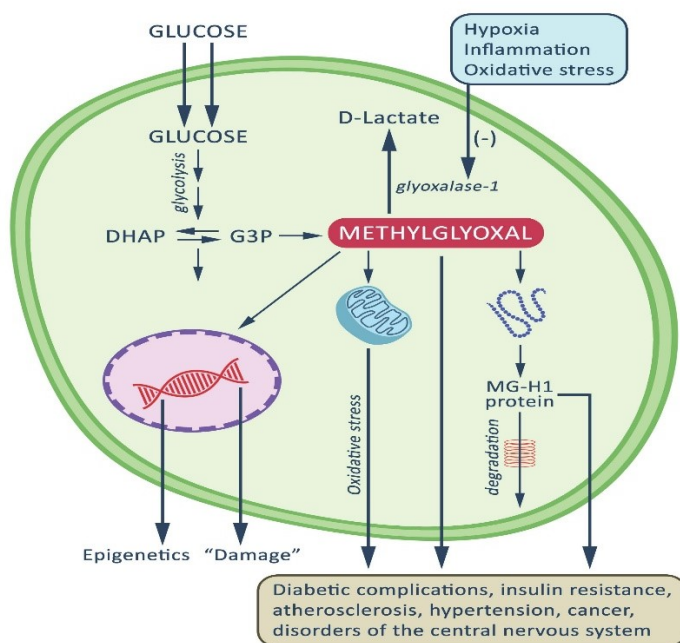


Figure 3: Schematics of methylglyoxal formation, detoxification and role in diabetic vascular complications (Schalkwijk & Stehouwer, 2020). The formation and accumulation of MGO have been implicated in the pathogenesis of type 2 diabetes, vascular complications of diabetes, and several other age-related chronic inflammatory diseases such as cardiovascular disease, cancer, and disorders of the central nervous system. MGO is mainly formed as a by-product of glycolysis and, under physiological circumstances, detoxified by the glyoxalase system. MGO is the major precursor of nonenzymatic glycation of proteins and DNA, subsequently leading to the formation of advanced glycation end products (AGEs). MGO and MGO-derived AGEs can impact organs and tissues affecting their functions and structure. Hypoxia, inflammation and oxidative stress are associated with MGO formation and impair its detoxification which is linked to the development of diabetes and vascular complications of diabetes.

1.3.3 Role of advanced glycation end products in diabetic vascular complications

1.3.3.1 AGE formation

Advanced glycation end products are heterogeneous toxic compounds that are formed from exogenous or endogenous sources. AGE formation is known to be enhanced in diabetes condition (R. Singh, Barden, Mori, & Beilin, 2001).

Endogenous AGEs are formed in the body by a non-enzymatic Maillard reaction that involves the interaction of reducing sugars like glucose, fructose and glucose-6-phosphate with macromolecules such as aminoacids of proteins, lipids and nucleic acids and form Schiff bases, Amadori products intermediates (Vistoli et al., 2013) (Fig 4). Methylglyoxal and 3 deoxyglucosone formed by non-oxidative mechanisms are some of the intermediates of Amadori product formation. Glucose-6-phosphate, fructose shows a faster rate of glycation compared to glucose. AGEs also include glycoxidation products resulting from both glycation and oxidation reactions including N^ε-(Carboxymethyl) lysine (CML) and pentosidine, pyralline, Furoyl-furanyl and imidazole (Takeuchi & Makita, 2001). CML is a biomarker for oxidative stress. Glycated hemoglobin HbA_{1c} is an Amadori product that is an indicator of glycemia in the early stages of diabetes. Immunologically AGEs bind to the carrier proteins such as hemoglobin, albumin and LDL protein, where the majority of them bind to albumin (Kuzan, 2021).

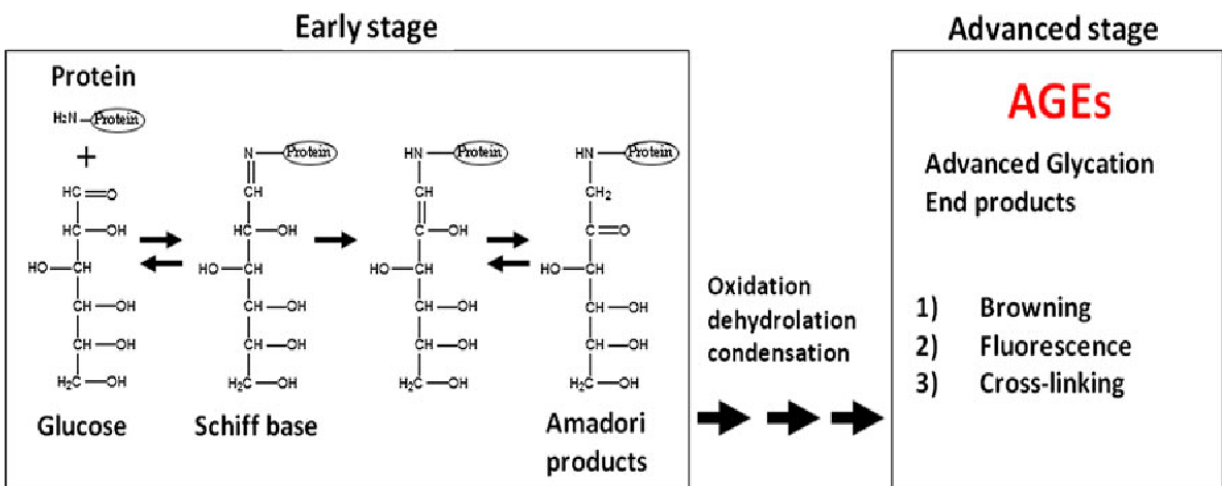


Figure 4: Advanced glycation end product formation (Nagai, Shirakawa, Ohno, Moroishi, & Nagai, 2014).

Exogenous AGEs are derived from outside sources like processed food, pollutants and tobacco smoke. Processed foods with heat treatment undergo a Maillard reaction (Fig 4) (Snelson & Coughlan, 2019). Although AGEs cross-links are resistant to chemical and enzymatic hydrolysis and are poorly absorbed by the gastrointestinal tract, processed foods still contribute to AGE formation (Q. Zhang, Wang, & Fu, 2020).

1.3.3.2 AGE cross-links and their role in vascular complications

AGE protein cross-links are a major form of AGE modifications including Arginine-lysine (CML, pentosidine) that play a role in pathological conditions. Arginine lysine cross-links include 3-deoxyglucosone derived imidazolium and methylglyoxal crosslinks (Fig 4). Intermediates of AGE cross-link formation include dicarbonyl intermediates (1-3-4-deoxyaldosuloses, arabinose and glyoxal) and glycerolaldehyde (α -hydroxyaldehydes) (Ajith & Vinodkumar, 2016). Pathophysiological consequences of AGE cross-linking involve atherosclerosis, endothelial dysfunction, thickening of capillary basement membrane and sclerosis of renal glomeruli. AGE cross-linking and lipoprotein trapping are shown to be involved in diabetic macrovascular complications by impairing cholesterol efflux from vessels resulting in cholesterol accumulation in the vessel walls. Tissue remodeling is affected by AGE cross-links as it stiffens the cellular basement membrane proteins such as collagen affecting its flexibility (Nash, Noh, Birch, & de Leeuw, 2021). AGE cross-linking is known to increase with age and in diabetes condition. Aortic stiffness was reported due to the accumulation of AGEs in human aorta. AGE cross-links pentosidine and pyrroline have also been shown to accumulate in diabetic kidney subjects (Yamagishi, 2012).

Tissue remodeling is defined as the renewal of living tissue. It involves the maintenance and adaptive alteration of organism tissue morphology. Tissue remodeling involves the alteration of extracellular matrix (ECM) by metalloproteinases triggering different signaling molecules including fibroblast growth factor (FGF), WNT, bone morphogenetic protein (BMP) and hedgehog. These signaling molecules promote the cell growth, proliferation, migration, differentiation or apoptosis at the site of tissue renewal. Tissue remodeling process is important for the survival of animals. It occurs either at a specific time during their life cycle (regeneration, metamorphosis) or continuously (adipose or cartilage remodelling) (Pinet & McLaughlin, 2019).

Physiological tissue remodeling

Physiological tissue remodeling is an endogenous process, whereas pathological tissue remodeling occurs post-injury or in a disease condition. Several processes in animal species fall within the category of physiological tissue remodeling (metamorphosis in *X. laevis* and mammary tissue remodeling in humans) (Cowin, 2004). It is crucial during embryonic development, growth and healing. It depends on the genetic information and its mechanical environment that is required for the development of proper tissue morphology (Fernandes, Barauna, Negrao, Phillips, & Oliveira, 2015).

Pathological tissue remodeling

Tissue remodeling is affected in pathologies involving joint atherosclerosis, cancer, asthma, ischemia, diabetic foot ulcers and tissue fibrosis.

Mimicking physical-mechanical stimuli is used in tissue engineering approach to encourage tissue growth and repair; especially for load-bearing applications (Vignola, Kips, & Bousquet, 2000).

Tissue growth and remodeling are associated with the wound healing mechanism that involves inflammation, migration, proliferation and maturation stages.

Different wound healing strategies have been developed in the recent years. They include, Cell therapy based on using stem cells and co-culture techniques to create new skin, Bioactive therapeutic delivery, which involves engineering the release of healing components to enhance the rate of wound repair and Application of biomaterial/scaffold for skin tissue engineering and regeneration. Few wound healing studies based on the above strategies are mentioned below (Nour et al., 2019).

For skin regeneration, various cells including adipose derived stem cells (ADSCs), MSCs, endothelial progenitor cells (EPCs) and induced pluripotent stem cells (iPSCs) are used. ADSCs and endothelial cells in gellan gum–HA (GG–HA) hydrogels promoted neovascularization and granulation tissue formation with greater wound closure, re-epithelialization, and resemblance of normal skin tissue (Cerqueira et al., 2014).

The microemulsion of Aloe vera extract encapsulated into Tragacanth gum showed wound healing properties (Ghayempour, Montazer, & Mahmoudi Rad, 2016).

Natural polymers such as collagen, gelatin, HA, chitosan, alginate, elastin, and silk fibroin were used in bioactive scaffolds in cellular interactions for healing (Stratton, Shelke, Hoshino, Rudraiah, & Kumbar, 2016).

Nanofibers improved adhesion and formed a porous structure by increasing the cellular interactions by simulating a native ECM microenvironment (X. Liu, Xu, Zhang, & Yu, 2021).

AGE receptors and cellular interactions

AGE activate several signaling pathways by interacting with receptor for advanced glycation end products (RAGE), AGE receptor complex and scavenger receptor family. Where RAGE is the most common multi-ligand receptor of AGE. AGE receptor expression depends on different cell or tissue type and metabolic changes like aging, hyperlipidaemia and diabetes.

RAGE receptors belong to the immunoglobulin superfamily. They are expressed in several cell types including fibroblasts, smooth muscle cells, dendritic cells, neuronal cells, glial cells, endothelial cells, chondrocytes, keratinocytes and T- lymphocytes. RAGEs have many ligands involving AGE, lipopolysaccharide, amyloid peptide and S 100/calgranuline protein (Sakaguchi et al., 2017). RAGE is membrane-bound and consists of an extracellular domain, a single transmembrane spanning helix and a cytoplasmic domain (Indyk, Bronowicka-Szydelko, Gamian, & Kuzan, 2021). It interacts with the ligands by the extracellular domain and activates downstream signaling pathways via the intracellular cytoplasmic domain. RAGE has two variants, an N-truncated RAGE lacking n-terminal V-type domain which is present in the cytoplasmic membrane and a soluble RAGE (sRAGE) lacking a c-terminal domain which is secreted extracellularly. The sRAGE is known to prevent ligands from interacting with RAGE or other cell surface receptors (Erusalimsky, 2021; Steenbeke et al., 2021). Low levels of sRAGE were detected in patients with coronary artery disease suggesting an increased AGE-RAGE interaction resulting in inflammatory and oxidative responses (Hudson & Lippman, 2018).

1.3.2.2 AGE in diabetic vascular complications

AGE formation is accelerated by hyperglycemia and it accumulates in various tissues and organs. As already mentioned, AGEs play a major role in arterial dysfunction by forming cross-links with collagen protein that causes vascular stiffness which can result in vascular complications. AGEs are known to play an important role in the progression and development of vascular complications prior to glycemic control (Yamagishi, Fukami, & Matsui, 2015). The advanced glycation process lasts over a long period for many weeks and is involved in the development of

metabolic memory and diabetic complications. In endothelial cells, AGE activates oxidative stress and inflammatory responses by interacting with RAGE receptors. It activates the NFκB pathway which leads to the production of various cytokines and adhesion factors (Yamagishi, 2009). AGE-RAGE interaction accelerates the production of oxidative stress by activating the Rac family small GTPase1 cell membrane transporters leading to endothelial cell dysfunction. RAGE expression levels are shown to be increased in atherosclerotic lesions, in diabetic patients. AGE-RAGE interaction is known to increase vascular endothelial growth factor (VEGF) production and is involved in the aggregation of inflammation in atherosclerotic plaques. Oxidized and denatured LDL (low density lipoprotein) by AGE play a role in the progression of atherosclerosis in patients with diabetes (Barbosa, Oliveira, & Seara, 2008).

1.3.4 Role of Oxidative stress in diabetic vascular complications

Oxidative stress is caused by the imbalance between the production, accumulation and detoxification of free radical species in the cells and tissues of the body. At low and moderate concentrations free radicals play an important role in regulating various cell signaling pathways including mitogen-activated protein kinase (MAPK) and extracellular-signal-regulated kinase that is involved in maintaining various cellular activities like proliferation, gene expression, cell division and migration (Betteridge, 2000). While excessive levels of free radicals cause the oxidation of macromolecules such as proteins, lipids and nucleic acids causing oxidative damage to their cell structure and functions (Ighodaro, 2018). Reduced antioxidant levels are associated with increased oxidative stress.

1.3.4.1 Free radicals and antioxidants

Free radicals are highly reactive and unstable molecules that are short-lived. They contain one or more paired electrons and induce cellular damage by the oxidation of cellular components. Free radicals include reactive oxygen species (ROS), reactive nitrogen species (RNS) and reactive chlorine species (RCS). ROS includes hydrogen peroxide (H₂O₂), superoxide (O₂^{•-}), hydroxyl (•OH), hydrochlorous acid (HOCL) and RNS includes nitrogen dioxide (NO₂), nitric oxide (NO) and non-radical peroxyntirite (ONOO⁻) (Table 2). Free radicals are produced by neutrophils, macrophages, mitochondria and chemicals, cigarette smoke and industrial effluents respectively (Jones, 2008). The endogenous source of free radicals include mitochondria and non-mitochondrial sources such as xanthine oxidase, lipoxygenases, monoamine oxidases, hemeoxygenases, cytochrome P450 reductase, nicotinamide adenine nucleotide phosphate oxidase (NOX), endothelial nitric oxide synthase (eNOS) and cyclooxygenases (Cadenas &

Davies, 2000; Cheeseman & Slater, 1993). Mitochondria produces free radicals by oxidative phosphorylation and the non-enzymatic reaction of organic compounds via oxygen and ionizing radiations. Peroxynitrite is formed when nitric oxide reacts with superoxide, is shown to elevate ROS and vascular dysfunction in type 2 diabetes. The eNOS and NOX have been shown to play a significant role in diabetic vascular diseases via ROS production.

The body has a natural antioxidant defense mechanism that prevents free radical formation by scavenging them. Antioxidants maintain the cellular redox state by balancing the formation and detoxification of free radicals (P. Zhang et al., 2020). It thereby reduces the elevated levels of free radicals by transforming them into less reactive molecules and protecting the cells from their toxic effects. Antioxidants can be from endogenous (superoxide dismutase, reduced glutathione and peroxidases) or exogenous (vitamin A, C, E, lipoic acid and polyphenols) sources (Hybertson, Gao, Bose, & McCord, 2011)

Free radical	Symbol	Half-life
Reactive oxygen species-ROS		
Radicals		
Superoxide	$O_2^{\cdot -}$	10^{-6} s
Hydroxyl	OH^{\cdot}	10^{-10} s
Alkoxyl radical	RO^{\cdot}	10^{-6}
Peroxyl Radical	ROO^{\cdot}	17 s
Non radicals		
Hydrogen peroxide	H_2O_2	Stable
Singlet oxygen	1O_2	10^{-6} s
Ozone	O_3	s
Organic peroxide	$ROOH$	Stable
Hypochlorous acid	$HOCl$	Stable (min)
Hypobromous acid	$HOBr$	Stable (min)
Reactive nitrogen species-RNS		
Radicals		
Nitric oxide	NO^{\cdot}	s^a
Nitrogen dioxide	NO_2^{\cdot}	s
Non radicals		
Peroxynitrite	$ONOO^-$	10^{-3} s
Nitrosyl cation	NO^+	s
Nitroxyl anion	NO^-	s
Dinitrogen trioxide	N_2O_3	s
Dinitrogen tetroxide	N_2O_4	s

Nitrous acid	HNO ₂	s
Peroxynitrous acid	ONOOH	Fairly stable
Nitryl chloride	NO ₂ Cl	s

Table 2: Different types of reactive free radicle species (Phaniendra, Jestadi, & Periyasamy, 2015). Details of stability and chemical formula of ROS and RNS.

Oxidative stress is involved in many pathophysiological conditions including cancer, rheumatoid arthritis and diabetes. It plays a major role in the vascular complications of type 2 diabetes by various biomarkers including Lipid peroxidation and DNA damage. Increased ROS and impaired antioxidant levels are the main culprits in diabetic β cell dysfunction and insulin resistance (Luc, Schramm-Luc, Guzik, & Mikolajczyk, 2019). Hyperglycaemia increases ROS production by activating NOX and dysfunction of mitochondrial oxygen consumption. Mitochondrial oxidative metabolism also plays a major role in diabetes (Hybertson et al., 2011). ROS and RNS are associated with insulin signaling and play a dual role. They are produced in response to insulin that regulates the cellular activities on one side and on the other side they negatively impact insulin signaling resulting in insulin resistance. Oxidized LDL by hydroxyl radical is shown to be responsible for oxidative damage in diabetic complications (Senoner & Dichtl, 2019).

Pathophysiology of diabetes includes impaired tissue repair and homeostasis restoration associated with persistent cellular stress that triggers chronic inflammatory changes. Both acute and chronic inflammatory states are known to be coupled with significant alterations of redox equilibrium associated with enhancement of reactive oxygen species (ROS) generation (Muriach, Flores-Bellver, Romero, & Barcia, 2014).

1.3.5 Role of inflammation in diabetic vascular complications

1.3.5.1 Inflammation

Inflammation is the body's defense mechanism to protect from harmful toxins, injuries and infections. It also modulates some cellular activities like growth, survival and differentiation. During inflammation immune cells or tissues of the body produce various inflammatory factors including C-reactive proteins, acute phase proteins, fibrinogen, sialic acid, hepatoglobin, cytokines and chemokines that trigger the inflammatory responses. Inflammatory responses result in increased blood flow to the area of injury or infection (Medzhitov, 2008). Cytokines and chemokines are the major inflammatory factors that modulate the immune responses throughout

the body involving chemoattraction and immune cells trafficking. Inflammatory factors trigger various downstream pathways such as phagocytosis, cell proliferation, cell adhesion, cytokine secretion, cell survival, apoptosis, angiogenesis and cell death.

1.3.5.2 Inflammatory factors

Cytokines are important inflammatory modulators that include tumor necrosis factor (TNF- α), interleukin-1 (IL-1), interleukin-6 (IL-6) and interleukin-8 (IL-8). These cytokines interact with various receptors such as pattern recognition receptors (PRRs), NOD-like receptors (NLRs) and Toll-like receptors (TLRs) and activate downstream signaling pathways including NF κ B and mitogen-activated protein kinase (Kuprash & Nedospasov, 2016).

Chemokines regulate the cell migration of leukocytes and other cell types in both physiological and pathological conditions. they plays a major role in the activation of immune responses. Chemokines include four major types of proteins CXC, CX3C, CC and C that interact mostly through G protein coupled receptors known as chemokine receptors. Chemokines and chemokine receptors together modulate and activate the signaling mechanisms to recruit the immune cells at the site of injury or infection (Roe, 2021).

1.3.5.3 Acute and chronic inflammation

Inflammation can either be acute short-lived or chronic-long lasting. Acute inflammation lasts for few hours to days while chronic inflammation lasts for few months or years. Chronic inflammation is involved in many pathological conditions like cancer, asthma, heart diseases and diabetes.

Acute inflammation is the first response by the immune system. Neutrophils phagocytose the microorganisms and foreign substances at the site of injury. As neutrophils are short-lived (24-48 h), macrophages that persist for few months further phagocytose the remaining cell or tissue debris. Acute inflammation is usually resolved within a week but if prolonged can be a sign of infection (Yeung, Aziz, Guerrero-Castilla, & Arguelles, 2018).

Chronic inflammation is an uncontrolled and continuous inflammatory response stimulated in the body even after the injury or infection is resolved. Low level of abnormal inflammation is known to alter insulin regulation and plays a role in metabolic diseases such as diabetes (Glass, Saijo, Winner, Marchetto, & Gage, 2010).

1.3.5.4 Inflammation in diabetic vascular complications

Insulin resistance and hyperglycemia of type 2 diabetes are associated with inflammation and it's a vicious cycle, where inflammation mediates more insulin resistance and vice versa. Low level of chronic inflammation is shown to be associated with diabetes. Metabolic and energetic distribution in cells regulates the normal inflammatory responses (Luc et al., 2019). Integration of immunity and metabolism is beneficial for good health but is deleterious under metabolic challenges. Targeting inflammation to improve the pathophysiology of diabetic complications is an emerging field of research (Domingueti et al., 2016).

Elevated levels of C-reactive proteins, IL-6 and IL-1 β are known to be found in type 2 diabetes. Gut microbiota is shown to interact with the immune system which triggers tissue metabolic modifications which may be the origin of low-grade inflammation that can lead to the onset of diabetes (Fig 5) and obesity (Nilsson, Bengtsson, Fredrikson, & Bjorkbacka, 2008). Altered gut microbiota can possibly affect and activate gut immune cells by the presence of lipopolysaccharides (LPS) and short-chain fatty acids to produce inflammatory responses (X. Wang, Antony, Wang, Wu, & Liang, 2020).

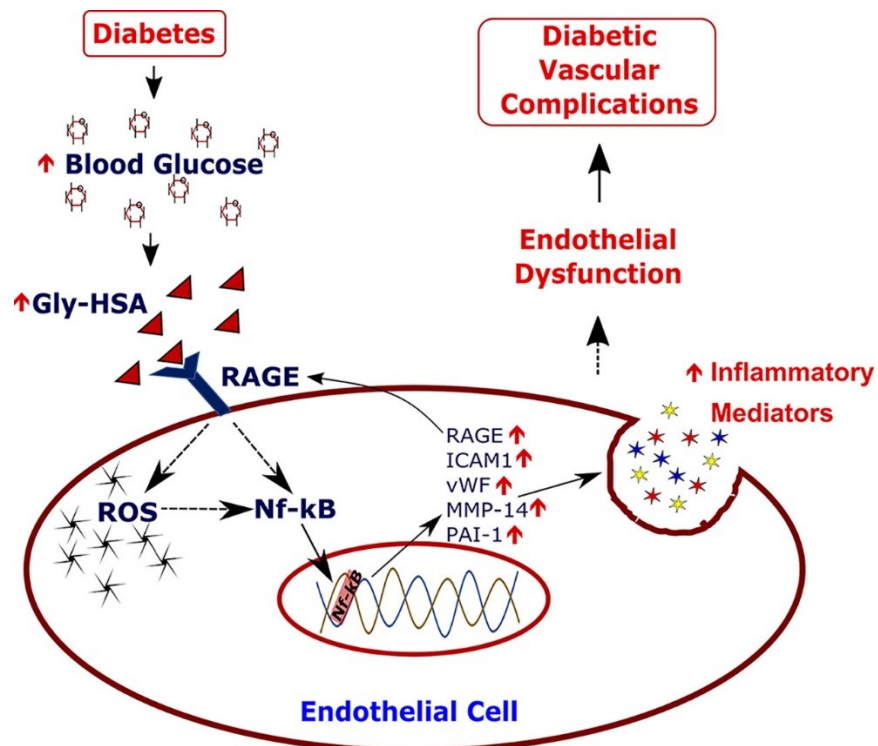


Figure 5: Inflammation associated with diabetes (Banarjee, Sharma, Bai, Deshmukh, & Kulkarni, 2018). Endothelial dysfunction is one of the primary steps in the development of diabetes associated vascular diseases. Hyperglycemic condition in diabetes promotes the accumulation of AGEs in the plasma that interacts with the receptor for AGEs (RAGE) present on the endothelial cells and negatively affect their function. Differentially regulated proteins were involved in various processes such as inflammation, oxidative stress and apoptosis that are associated with endothelial dysfunction. Inflammatory pathway NF- κ B downstream to AGE-RAGE and proteins including ICAM1, vWF and PAI-1 affect the important endothelial functions like cell adhesion and blood coagulation.

Chronic inflammation is associated with other intracellular stresses such as mitochondrial oxidative stress and endoplasmic reticulum (ER) stress. In a feedback manner, ER stress can also activate cellular inflammatory pathways and cellular accumulation of ROS associated with oxidative stress which, in turn, impair cellular functions and lead to metabolic disorders such as diabetes (Cullinan & Diehl, 2006).

Role of endoplasmic reticulum (ER) stress in diabetic vascular complications

Endoplasmic reticulum is a membrane-bound cellular component of cells that performs protein synthesis, maturation and transport. It is also a storehouse of calcium ions (Ca^{2+}) apart from mitochondria. It involves the proper folding of proteins assisted by ER chaperons and the improperly folded proteins are degraded by ER associated protein degradation (ERAD) machinery. When a load of improperly folded proteins exceeds the protein folding capacity of ER, the defence mechanisms known as ER stress responses or unfolded protein responses (UPR) are activated (Abdullah & Ravanan, 2018). Many factors can lead to the accumulation of misfolded or unfolded proteins including impaired Ca^{2+} homeostasis, post-translational (glycosylation, disulfide bond formation) modifications of protein folding, hypoxia condition and bacterial or viral infections that can lead to ER stress responses (Oakes & Papa, 2015). Improperly folded proteins can be harmful as they can interact with other proteins and inhibit their cellular functions. Accumulation of unfolded proteins in turn impairs calcium homeostasis of ER causing Ca^{2+} leakage out of the cell membrane inhibiting chaperones and proteosomal degradation systems. Impaired proteosomal degradation of misfolded proteins further can induce the UPR stress responses (Schroder & Kaufman, 2005a).

1.3.5.5 ER stress and unfolded protein responses

Mammalian cells have evolved a defence mechanism called unfolded protein responses (UPR) signaling pathways to reduce ER stress responses and maintain ER homeostasis (Hetz, Zhang,

& Kaufman, 2020). Initially, UPR activates pro-survival pathway to restore the cellular homeostasis by decreasing the protein overload by activating the expression of genes involved in ERAD machinery. But, if the ER stress prolongs the UPR responses trigger the cell death mostly by apoptosis.

UPR signaling is mediated by ER transmembrane proteins, PERK (RNA-like endoplasmic reticulum kinase), IRE-1 (inositol requiring enzyme 1 alpha) and ATF 6 (Activating transcription factor 6). These are the transducer proteins that are maintained in their inactive state associated with the chaperone GRP78/Bip (78 kDa glucose-regulated protein). When the ER stress is overloaded with unfolded proteins, GRP 78 dissociates to form the transducer proteins or misfolded proteins and activates the UPR responses by interacting with the luminal domain of transducer proteins (Abdullah & Ravanan, 2018; So, 2018) (Fig 6).

PERK is an ER transmembrane protein ubiquitously expresses but is more expressed in secretory cells. During ER stress PERK is activated which phosphorylates alpha subunit of eIF2 α involved in the eukaryotic protein translational initiation. Phosphorylated eIF2 α inhibits the protein translation that reduces the protein folding load of ER and allows to regain ER homeostasis. The eIF2 α further activates ATF-4 (activating factor-4) which mediates the expression of C/EBP homologous protein CHOP transcription factor which is involved in the ER stress mediated cell death (Fig 6).

ATF 6 transmembrane protein of ER which sense the unfolded proteins. It binds to Bip normally and during ER stress it is released from Bip and translocates to the Golgi apparatus where it is activated by cleavage of two proteases called S1P and S2P. Activated ATF 6 translocates to the nucleus and induces the expression of Bip chaperon and endoplasmic reticulum protein degradation genes (ERAD) (Fig 6).

There are two isoforms of mammalian IRE1 genes, IRE1 α and IRE1 β . They differ in luminal domain amino acid sequence and substrate specificity by their RNase domain. IRE1 α is a sensor molecule of ER stress which is a transmembrane domain with an N-terminal luminal domain in the ER lumen and C-terminal kinase and endoribonuclease domains in the cytosol. During ER stress IRE1 α is released and activated by dimerization and transphosphorylation. Upon activation, IRE1 α targets XBP 1 (X-box binding protein 1) and activates it by mRNA splicing mechanism. Activated XBP 1 gets translocated to the nucleus as an active transcription factor that activates genes involved in the UPR pathway which plays a role in re-establishing ER homeostasis (Hetz, 2012). IRE-1 α is mostly known to be associated with cell death as it activates

stress kinases including the c-Jun N- terminal pathway (JNK) which further modulates the activation of Bcl-2 family proteins. The IRE-1 mechanisms of regulating ER stress induced cell death has been well established while its non-apoptotic functions are not yet clearly established (Abdullah & Ravanan, 2018) (Fig 6). Prolonged activation of IRE1 β also is associated with apoptosis (X. Z. Wang et al., 1998).

All the downstream mediators of UPR pathway induce CHOP transcription factor that reduces the expression of anti-apoptotic Bcl-2 family proteins by inducing the expression of pro-apoptotic Bcl-2 interacting Mediator Of Cell Death and Death Receptor-5 that have been linked to ER stress-induced apoptosis (Abdullah & Ravanan, 2018).

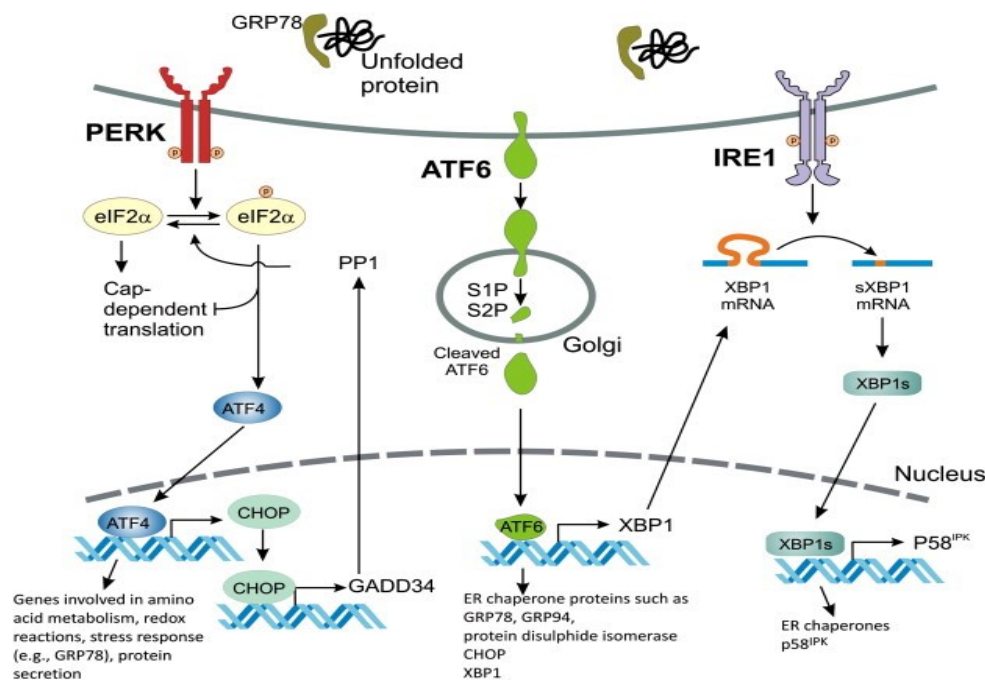


Figure 6: Endoplasmic reticulum stress sensor molecules and their pathways (Gorman, Healy, Jager, & Samali, 2012). The UPR is mediated by three ER stress sensors. The binding of unfolded proteins to GRP78 within the ER lumen allows activation of PERK, ATF6 and IRE1. PERK dimerises and autophosphorylates. It phosphorylates eIF2 α and thus general Cap-dependent translation is inhibited. Cap-independent translation allows the translation of certain proteins such as ATF4 which activates CHOP transcription. One of the genes induced by CHOP is GADD34 which regulates protein phosphatase 1 (PP1), which can dephosphorylate eIF2 α . Activation of ATF6 allows its translocation to the Golgi where it undergoes cleavage by S1P and S2P proteases. Cleaved ATF6 activates XBP1 transcription. Active IRE1 is a dual kinase and endonuclease. One of its targets is XBP1 mRNA which undergoes splicing to produce an active transcription factor, XBP1s. One of the targets of XBP1s is p58^{IPK}.

1.3.6.2 ER stress in diabetic vascular complications

Endoplasmic reticulum plays a major role in the regulation of many cellular processes. The first response of the cell during ER stress is to re-establish its homeostasis by upregulation of the chaperons GRP94 and Bip (Schroder & Kaufman, 2005b). UPR plays a central role in diabetes. ER stress is one of the cellular mechanisms that can influence the integrity of endothelial cells. Chronic ER stress and UPR pathways activation in endothelial cells leads to increased oxidative stress and inflammation and often results in cell death. UPR signaling has beneficial functions during transient ER stress rather than prolonged ER stress. Disturbances in its normal function trigger a network of signaling pathways to restore cellular homeostasis and prolonged ER stress trigger apoptotic responses (Sano & Reed, 2013). Prolonged ER stress is known to be involved in the progression of many diseases including diabetes type2, atherosclerosis, neurodegeneration and cancer (Ren, Bi, Sowers, Hetz, & Zhang, 2021). There is increased expression of adhesion molecules, increased chemokines and cytokine release and decreased anti-coagulant and ROS production in the endothelium. Prolonged ER stress is associated with increased inflammation triggering the switch from prosurvival to proapoptotic mode. ER stress is known to impact the physiology of endothelial cells and may lead to inflammation and apoptosis. Decreased expression of tight junction proteins may be correlated to ER stress (Maamoun, Benameur, Pintus, Munusamy, & Agouni, 2019).

This work focuses on diabetes associated stroke and impaired wound healing. The pathophysiology and clinical aspects are mentioned in the next section.

II. Diabetic Stroke and impaired wound healing, pathophysiology and therapeutics

Stroke is the second leading cause of mortality, and affected 15 million people worldwide. Stroke is of two types: ischemic stroke and haemorrhagic stroke (Fig 7). About 87% of strokes are ischemic strokes and 10-25% are haemorrhagic strokes. Till 2016 it has been shown that stroke occurrence doubled in low-and-middle-income groups and decreased in high-income countries (Lau, Lew, Borschmann, Thijs, & Ekinici, 2019). Stroke involves many risk factors, few of them are dyslipidaemia, diabetes, smoking and hypertension. Individuals with diabetes are 1.5 times more likely to have a stroke than non-diabetic individuals (Sarikaya, Ferro, & Arnold, 2015).

Stroke involves many pathophysiological changes in blood vessels at various locations including cerebral blood vessels. Various factors including hyperglycemia, AGEs, high blood pressure, protein and lipid deposits in the walls of blood vessels cause blood vessel damage associated with stroke (R. Chen, Ovbiagele, & Feng, 2016).

2.1 Diabetic stroke

Stroke is a serious life-threatening condition, where the blood supply to the brain is deprived, blocked or cut off. Oxygen and nutrients supplied to the brain tissue is reduced in stroke condition. It is mainly caused by either blockage of the artery or leakage and rupture of a blood vessel. The reduced blood flow to the brain region can be either for a short duration or a long duration. Stroke includes ischemic and haemorrhagic stroke (Smajlovic, 2015).

2.1.1 Ischemic stroke

Ischemic stroke involves the blockage of blood vessels and reduced blood supply to the brain. It is the most common type of stroke associated with diabetes. The blockage and narrowing of blood vessels are caused by the deposition of blood clots, fats or other debris that are travelled to the brain region mostly from heart or other parts of the body (Feske, 2021; Putaala, 2020) (Fig 7).

2.1.2 Haemorrhagic stroke

Haemorrhagic stroke involves the leakage and rupture of the blood vessel which results in the release of contents of the blood into the brain region. The leakage of blood into the brain region causes damage to the brain tissue. Ischemic stroke can lead to haemorrhagic stroke (Unnithan & Mehta, 2022) (Fig 7).

Haemorrhagic stroke is of two types, intracerebral haemorrhage and sub-arachnoid haemorrhage. Intra-cerebral stroke involves the rupture of an artery in the brain and leakage of blood into the surrounding tissues. It is the most common haemorrhagic stroke. Sub-arachnoid haemorrhage involves the rupture and leaking of blood vessels in between the brain and its membranes. It is less common (Montano, Hanley, & Hemphill, 2021).

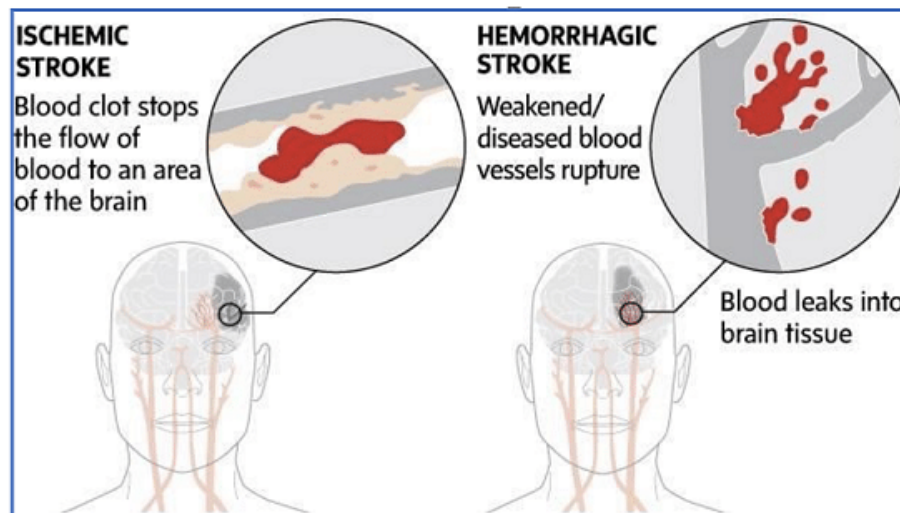


Figure 7: Types of stroke: ischemic and haemorrhagic stroke (Qureshi, Arooj Ahmed, et al.2018). In Ischemic Brain Stroke (left), a blood clot has blocked the flow of blood to a specific area of the brain.

2.2 Pathophysiology of diabetic Stroke

Type 2 diabetes increases and doubles the risk of acute and chronic complications of stroke. Diabetes is responsible for about 20-33% of ischemic strokes. Stress-induced hyperglycemia caused brain damage involving oxidative stress, pro-inflammatory responses and reperfusion injury that lead to a high risk of mortality after stroke. Stroke has short term early complications and long term late complications.

Nitric oxide (NO) mediated vasodilation of blood vessels is impaired in diabetes that leads to arterial stiffness, endothelial dysfunction and atherosclerosis. Atherosclerosis also adds to the risk of stroke. Diabetic nephropathy patients have shown thickening of vascular basement membrane and reduced blood flow to the surrounding tissues (van Sloten, Sedaghat, Carnethon, Launer, & Stehouwer, 2020). Hyperglycemia, oxidative stress, vasoconstrictor endothelin-1, matrix metalloproteinase-9 (MMP-9) mediated inflammatory responses and vascular remodelling can result in vascular complications and increased ischemic damage post-stroke (Baliga & Weinberger, 2006) (Fig 8).

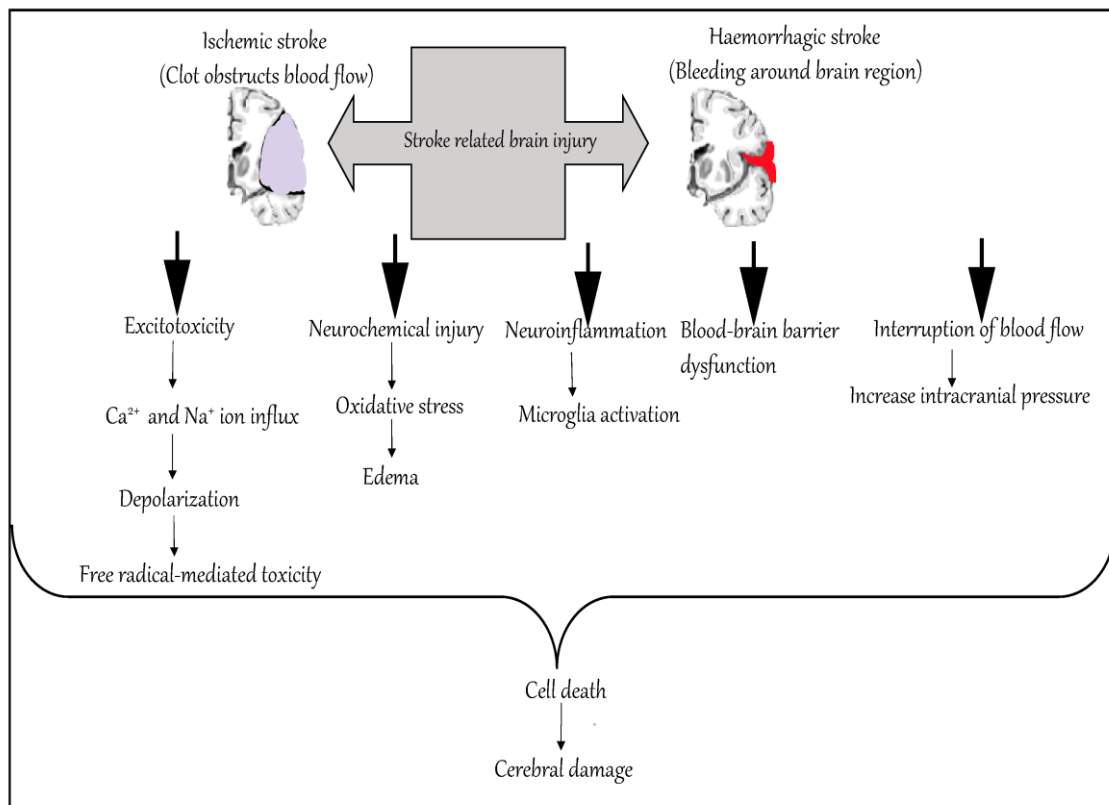


Figure 8: Pathophysiology of stroke (Kuriakose & Xiao, 2020).

2.2.1 Role of endothelial cells and blood brain barrier (BBB) in vascular dysfunction

Endothelial cells line the blood vessels and function as a permeability barrier between the blood and the blood vessels. Reactive oxygen species play a major role in the physiology pathology of the endothelial vasculature (Sturtzel, 2017). It plays a major role in vascular relaxation, contraction, and exchange of hormones, macromolecules and solutes. It maintains vascular homeostasis by balancing the release of relaxing and contracting substances, but an imbalance in this leads to endothelial dysfunction. Increased NO is released by the endothelium by up regulation of the eNOS gene in stress conditions (Godo & Shimokawa, 2017).

2.2.1.1 BBB structure and function

A blood-brain barrier is a neurovascular unit composed of neurons, microvascular endothelium, basement membrane, pericytes, astrocytes and microglia (Fig 9). BBB also interacts with circulating blood cells and intravascular signals (Daneman & Prat, 2015). BBB is formed by a

layer of microvascular endothelial cells that line the intraluminal space of brain capillaries. The endothelial cells are tightly packed together by tight junctions (Langen, Ayloo, & Gu, 2019). Tight junctions consist of ZO-1 (Zonula occludin), occludin and claudin proteins; adherent junctions, including catenins, actinin, cadherin and vinculin; and junctional adhesion molecules (Profaci, Munji, Pulido, & Daneman, 2020). The endothelial cell layer has an interior (luminal) and exterior compartments separated by cytoplasm between the blood and brain. On the outside surface, ECs are enveloped in a basement membrane and separated into regions associated with a pericyte. Pericytes surround brain capillaries and aid their growth and integrity. They also control the substances that cross the BBB along with macrophages by phagocytosis which act as a secondary barrier besides endothelial cells (Daneman & Prat, 2015).

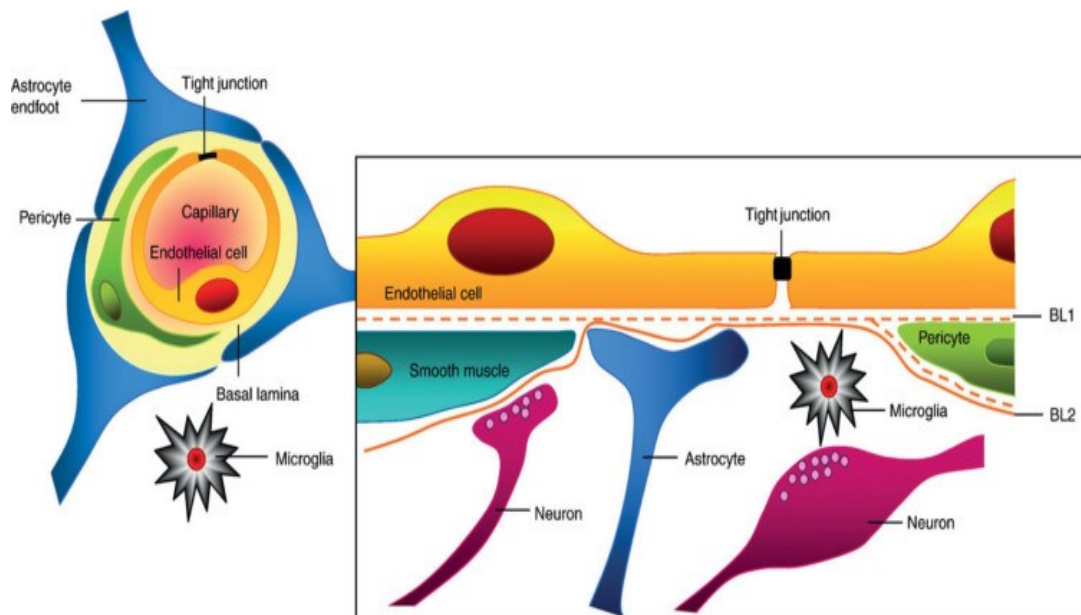


Figure 9: Overview of BBB neurovascular unit (Nian, Harding, Herman, & Ebong, 2020).

Structure of the neurovascular unit (NVU). Endothelial cells form the inner most layer of the NVU and are connected to each other by tight junctions. Surrounding the ECs are pericytes in the case of capillaries or smooth muscle cells in the case of larger cerebrovasculature such as veins and arteries. Additionally, astrocytes and neurons of the NVU extend foot-processes or axons, respectively, that also help regulate NVU function. Finally, microglia, which are the brain’s resident immune cells, also contribute to NVU regulation. Collectively, ECs and these supportive cells help maintain the proper function of the blood-brain barrier.

BBB is a selective barrier that ensures the exchange and transport of only essential compounds such as oxygen, glucose and other small molecules from the blood to the brain region by passive

and facilitated diffusion and active transport (Villasenor, Lampe, Schwaninger, & Collin, 2019). Thereby it protects the brain from deleterious substances in the peripheral circulation. The selective barrier function of BBB involves tight junctions (TJs), enzymatic reactions, and neurotransmitter signaling and selectively transports small and large (Sweeney, Zhao, Montagne, Nelson, & Zlokovic, 2019). Transportation across the BBB is regulated mainly by γ -glutamyl transpeptidase, alkaline phosphatase, and aromatic acid decarboxylase enzymes. The permeability of the BBB is determined by tight junction controlled paracellular integrity and is mediated by caveolae-mediated transcellular permeability (Andreone et al., 2017). The relationship between paracellular and transcellular permeability is important for the regulation of transendothelial permeability (Liebner et al., 2018).

2.2.1.2 BBB in stroke

Continuous regulation of tissue microenvironment is necessary for a proper barrier function. Impaired BBB function is associated with numerous pathologic processes including diabetic vascular complications. BBB also limits the delivery of drug molecules to the brain. Recently, novel therapeutic methods are being developed using nanoformulations to circumvent the BBB limitation and treat many neuropathophysiological conditions (Obermeier, Daneman, & Ransohoff, 2013; Pandit, Chen, & Gotz, 2020).

Ischemia and cerebrovascular diseases have deleterious effects on BBB including inflammation and depleting brain nutrients which causes vasogenic edema and degradation of the extracellular matrix by release of matrix metalloproteinases (C. Yang, Hawkins, Dore, & Candelario-Jalil, 2019). Stroke causes disruption of TJs (Fig 10) and destruction of basal lamina proteins, including collagen type IV, laminin, and fibronectin (Abdullahi, Tripathi, & Ronaldson, 2018). The severity of infarction is correlated with the degree of BBB dysfunction, which may place the patient at greater risk for hemorrhagic conversion after reperfusion (Abdullahi et al., 2018).

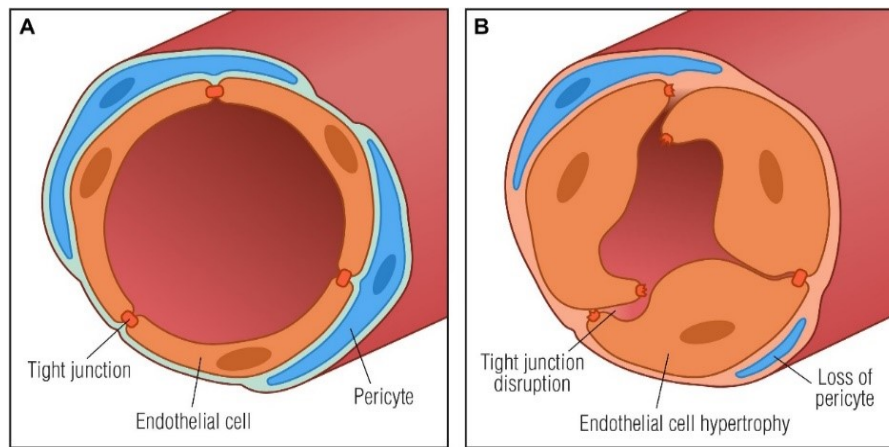


Figure 10: Schematic of cerebrovasculature.

A) Represents normal blood vessel and B) Represents impaired tight junctions in pathophysiological conditions (Richner et al., 2018).

Vascular endothelial function is important for maintaining the structural and functional integrity of blood vessels. These complications cause impaired angiogenesis and disruption of BBB. VEGF increases BBB leakage and causes haemorrhagic transformation in the early phase of acute stroke and promotes angiogenesis in the ischemic area post-acute phase stroke (48 hours). BBB disruption leads to parenchymal damage (Cai et al., 2017).

Recent preclinical studies have shown that impaired neuroplasticity and neurogenesis maybe involved in poor stroke recovery in diabetic conditions. Neurovascular disruption and white matter damage by increased MMP-9 activation and increased AGE-RAGE interaction contribute to the impaired neurogenesis and neuroplasticity recovery post-stroke. In diabetic rats, an increased resistance to thrombolytic reperfusion, increased haemorrhage and large infarct volumes have been reported (K. A. Kim et al., 2020).

2.3 Therapeutics for diabetic stroke

Many clinical trials have been done and are ongoing to prevent stroke development and its complications in diabetic patients. Most studies are on primary stroke prevention. Lifestyle changes including minimal fat intake, weight control, physical activity and glycemic control may help in controlling the initial risk of stroke. Lipid and glucose control has shown to reduce the risk for atherosclerosis and ischemic stroke (George & Steinberg, 2015). Vanadium lowered the blood glucose in MCAO (middle cerebral artery occlusion) rat model and showed to minimize the damage to brain tissue by reducing the production of oxidants (Ahmadi-Eslamloo, Dehghani, & Moosavi, 2018). Rosiglitazone compound showed neuroprotection by decreasing neutrophil

accumulation and reducing the expression of inflammatory cytokines in the rat brain (Luo et al., 2006). Pioglitazone is also shown to protect against hypertension induced cerebrovascular injury and stroke by reducing oxidative stress, vascular endothelial dysfunction and inhibiting brain inflammation (Nakamura et al., 2007). Similarly, rosiglitazone and pioglitazone have been shown to reduce cerebral infarct size in animal models, down regulation of cyclooxygenase-2, reduced oxidative stress and activation of mitogen-activated protein kinases, and nuclear factor-kappa B (Curb et al., 1996; Zhao, Patzer, Herdegen, Gohlke, & Culman, 2006). Thiazolidinedione treatment did not change the cerebral blood flow but reduced the post-ischemic expression of pro-inflammatory genes and increased the expression of antioxidant enzymes (Tureyen et al., 2007).

Although there are a lot of therapeutic strategies available, they are not always optimal in completely limiting the pathophysiological mechanisms of stroke. However, delivering therapeutics to the ischemic brain region has always been challenging. Various physiological, chemical, and pharmacological approaches can be utilized to develop novel drug delivery strategies by using encapsulated bioactive compounds, which could impact ischemic stroke outcome. Here few studies have been mentioned that have shown improved benefits using polyphenols and nanoparticles (Nozohouri, Sifat, Vaidya, & Abbruscato, 2020).

Resveratrol showed its antioxidant effect to relieve brain edema, improve neurological function, and lower cerebral infarct volume by interacting with MMP-2 and MMP-9 (A. K. Pandey, Bhattacharya, Shukla, Paul, & Patnaik, 2015). The drug encapsulated nanoparticles can be promising to cross the BBB by endothelial or transendothelial route (McCarthy, Malhotra, O'Mahony, Cryan, & O'Driscoll, 2015). Despite the developments in nanoparticle research, its use in CNS diseases such as stroke is still under development. Growth factor (bFGF) or caspase-3 peptide inhibitor encapsulated in chitosan nanoparticles were found to accumulate within the brain by crossing the BBB and showed to reduce the blood loss after 2h artery occlusion in the middle cerebral locus (Yemisci et al., 2015).

2.4 Impaired diabetic wound healing

Impaired wound healing is associated with increased mortality in diabetes. Chronic, non-healing wounds, mostly ulcerations of the foot are one of the leading cause of lower extremity amputations in diabetic conditions (Gao, Regier, & Close, 2016). Abnormal cellular responses, immunological and microvascular dysfunction, infection and peripheral neuropathy associated

with diabetes are involved in the pathogenesis of wound healing impairment and progression of diabetic foot ulcer (Feldman, Nave, Jensen, & Bennett, 2017).

Despite extensive research, exact pathogenic mechanisms involved in impaired diabetic wound healing have not been completely elucidated. Yet, It could be the result of both micro and macrovascular diseases (Lim, Ng, & Thomas, 2017). Diabetic neuropathy has been recognized as one of the major cause of delayed wound healing in diabetic foot ulcer patients. Hyperglycemia has been linked to impaired diabetic wound healing by AGE formation. Both *in vitro* and *in vivo* studies have shown that AGE plays a role in the pathogenesis of impaired diabetic wound healing (Armstrong, Lavery, Wu, & Boulton, 2005).

Wound healing is a well-orchestrated process, which is activated during injury or infection. It involves certain events including platelet aggregation, inflammatory infiltration, cellular differentiation, and tissue remodelling (S. L. Yang et al., 2017). The above mentioned cascade of events is divided into 3 main phases, namely inflammation, proliferation, and wound contraction and remodeling which contribute to the renewal of damaged tissue at the affected sites of a wound (Goova et al., 2001).

The inflammatory phase includes the formation of the fibrin clot, which provides the substrate for cell migration of neutrophils into the wound (Albelda, Smith, & Ward, 1994). Neutrophils migration is followed by macrophages migration that phagocytose microorganisms, fragments of the extracellular matrix, neutrophils, erythrocytes, fibrin and other cell debris and secretes a variety of molecules that are considered crucial for effective wound repair (J. Chen et al., 2005).

The proliferation phase includes re-epithelialization and granulation tissue formation. Re-epithelialization involves the differentiation and proliferation of keratinocytes and their migration along the free edge of the wound, which is mediated by tissue hypoxia and various growth factors (O'Toole et al., 1997). Granulation tissue formation involves new blood vessel formation and invasion of the extracellular matrix by fibroblasts emerging from the periwound collagenous matrix. These invading fibroblasts are incorporated into the new extracellular matrix and get differentiated into myofibroblasts that synthesize a more collagenous matrix that facilitates wound contraction and remodelling (Shirakata et al., 2005).

The normal wound healing process is delayed in diabetes. Inflammatory phase seems to be dysregulated in diabetes condition involving diminished Tissue factor expression from keratinocytes, fibroblasts, and smooth muscle cells that negatively affect the formation of initial

hemostatic plug (Boniakowski, Kimball, Jacobs, Kunkel, & Gallagher, 2017). Also, hyperglycemia related impairment of cytokine release, chemotaxis, adherence, and phagocytic activity and increased oxidative stress showed inhibition of cell activation, migration, and chemotaxis (Loots et al., 1998). All these events have shown to prolong the inflammatory response that suppresses rather than proceeding to the next steps of the wound-healing process. Diabetic wounds have been associated with reduced proliferation and migration of mesenchymal cells in the fibrin clot, decreased new blood vessel formation, and low extracellular matrix density (Fadini, Albiro, Bonora, & Avogaro, 2019).

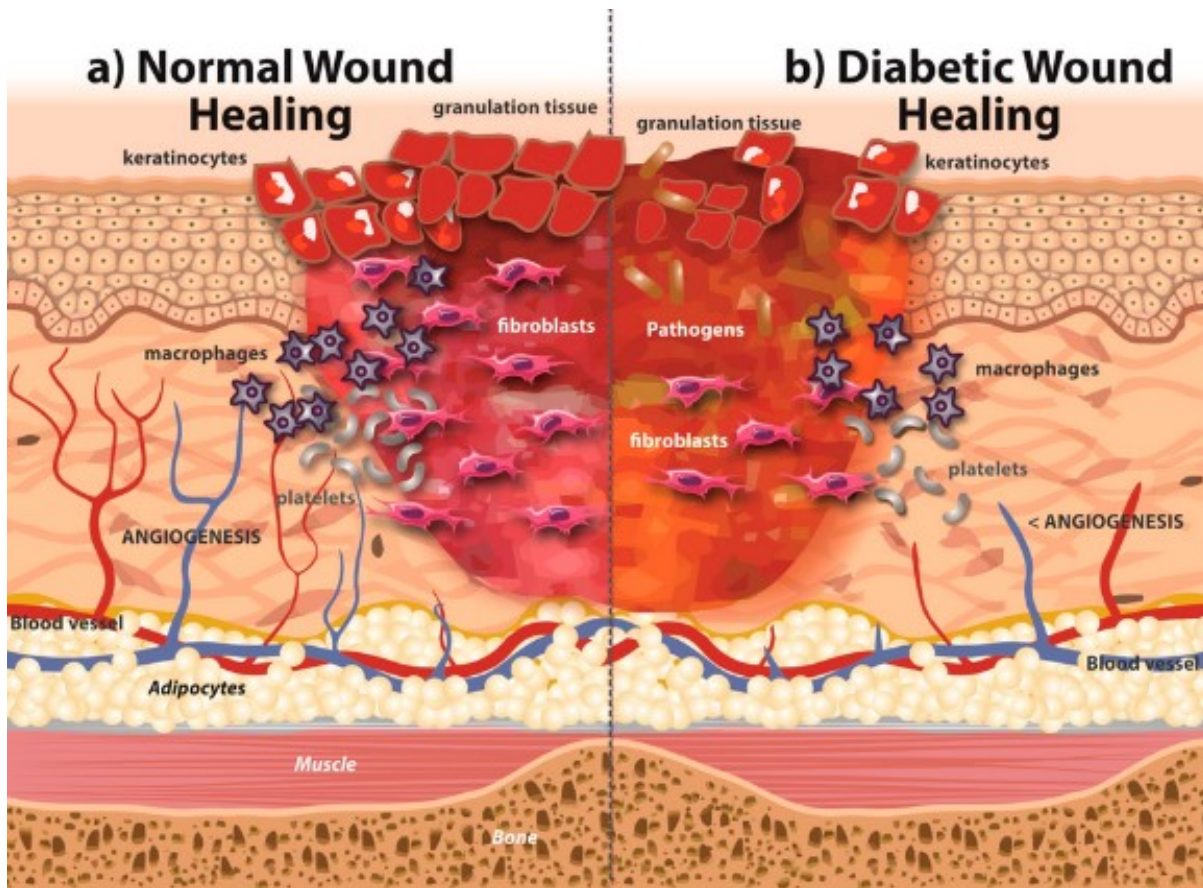


Figure 11: Wound healing process in diabetes.

a) Normal wound healing. In healthy people, wound closure consists of several processes that occur sequentially: the rapid hemostasis that involves platelet aggregation to form the platelet plug; an inflammation phase where neutrophils, macrophages, and mast cells release proinflammatory cytokines; wound contraction when inflammation decreases, angiogenesis occurs, keratinocytes and fibroblasts migrate, and the extracellular matrix forms; and, finally, the remodeling phase, where granulation tissue converts into mature scar tissue. **(b)** Diabetic wound healing. In patients with diabetes mellitus (DM), the wound closure processes are affected, starting with a decrease in fibrinolysis and an imbalance of cytokines, which causes an alteration in wound closure. There is also a decrease in angiogenesis due to hyperglycemia, and the migration of cells such as keratinocytes and fibroblasts is diminished, causing deficient re-epithelialization; in the same

way, the poor production of the extracellular matrix (ECM) by fibroblasts contributes to the problem of a deficient wound closure.

Current treatment options for preventing or healing diabetic ulcers are limited, particularly pathogenesis-based therapeutic approaches. Therefore, new strategies for wound healing is emerging by using polyphenols such as curcumin and resveratrol.

III Curcumin, its therapeutics benefits

3.1 Use of polyphenols in therapeutics

Natural herbal substances are known to have many beneficial effects on human health since ancient times. Plants have always been used in traditional medicine to treat different diseases. Synthetic substances used in food and therapeutics show toxic effects which are being replaced by natural substances as they are less toxic, cost-effective and biodegradable. The biocompatibility, chemical and structural diversity of natural substances makes them suitable for their use in therapeutics. So natural plant-based substances are being mostly used in the development of modern therapeutics.

Polyphenols are bioactive molecules of plants widely used in food, cosmetics and therapeutics. They can be found in tree barks, flowers, seeds, leaves, vegetables, nuts, roots and fruits (Fraga, Croft, Kennedy, & Tomas-Barberan, 2019). Based on the number of phenol rings and components attached to phenol rings polyphenols are categorised into flavonoids and non-flavonoids containing more than 8000 distinctive bioactive molecules. Non-flavonoids include stilbenes, phenolic acids, lignans and other polyphenols. Natural polyphenols contain numerous hydroxyl groups on aromatic rings and occur as conjugated forms with one or more sugar residues attached to a hydroxyl group or aromatic carbon atom (Luca et al., 2020; Tsao, 2010).

Polyphenols have various beneficial effects on human health. Resveratrol is a polyphenol found in grapes, berries and peanuts (Rasines-Perea & Teissedre, 2017). *Limonium algarvense* flower decoction and infusion showed antioxidant and anti-inflammatory properties. Many phenolic molecules like curcumin, caffeic acid, quercetin and rutin were used to study diabetic vascular complications.

Polyphenols are metabolized in the liver and intestines and are rapidly eliminated from the physiological system limiting their biological benefits (Marin, Miguelez, Villar, & Lombo, 2015). A wide range of nanoformulations are developed to overcome this limitation and improve the polyphenol therapeutic benefits.

Curcumin is a well-known polyphenol molecule that can improve pathophysiological events of diabetes and alleviates its complications including atherosclerosis, stroke, diabetic wound healing and coronary heart diseases. It shows wound healing properties by scavenging the free

radicals and reducing oxidative stress. Curcumin also showed a reduction in arterial stiffness in type 2 diabetes patients. By the antioxidant capacity and anti-inflammatory action, curcumin can be a potential polyphenol molecule for limiting endothelial dysfunction associated with diabetic stroke and reducing chronic inflammation and lesions in diabetes condition (Marton et al., 2021).

3.2 Curcumin

Curcumin is a natural polyphenol molecule isolated from *Curcuma longa* Linn (family Zingiberaceae). It is a low molecular weight hydrophobic molecule. It is widely used in food as a spice and colouring agent, cosmetics, textile and herbal medicine as antiseptic (Ipar, Dsouza, & Devarajan, 2019). Chemically name of curcumin is 1, 7-bis-(4-hydroxy-3-methoxyphenyl)-hepta-1, 6- diene-3, 5- dione. Turmeric consists of two other curcuminoids (77 wt. %), demethoxy curcumin (17 wt. %) and bis-demethoxy curcumin along with curcumin (Fig 11) (Lestari & Indrayanto, 2014). Curcumin is the major curcuminoid of turmeric (Nelson et al., 2017). The hydrophobicity of curcumin makes it less soluble in aqueous solutions but is readily soluble in dimethyl sulfoxide (DMSO), methanol, ethanol and acetone. The maximum absorption wavelength (λ max) of curcumin occurs at 430 nm. It is a bis- α , β - unsaturated β - diketone that has keto-enol tautomerism and it occurs in keto form in acidic and neutral PH whereas in enol form in alkaline medium (Nelson et al., 2017).

Curcumin doses of 4000 to 8000 mg/day and up to 12000 mg/day have been reported to be safe in the clinical trials approved by US food and drug administration (FDA) (Basnet & Skalko-Basnet, 2011). Curcumin is being used in different formulations including tablets, ointments, soaps, capsules and health drinks (Gupta, Patchva, & Aggarwal, 2013).

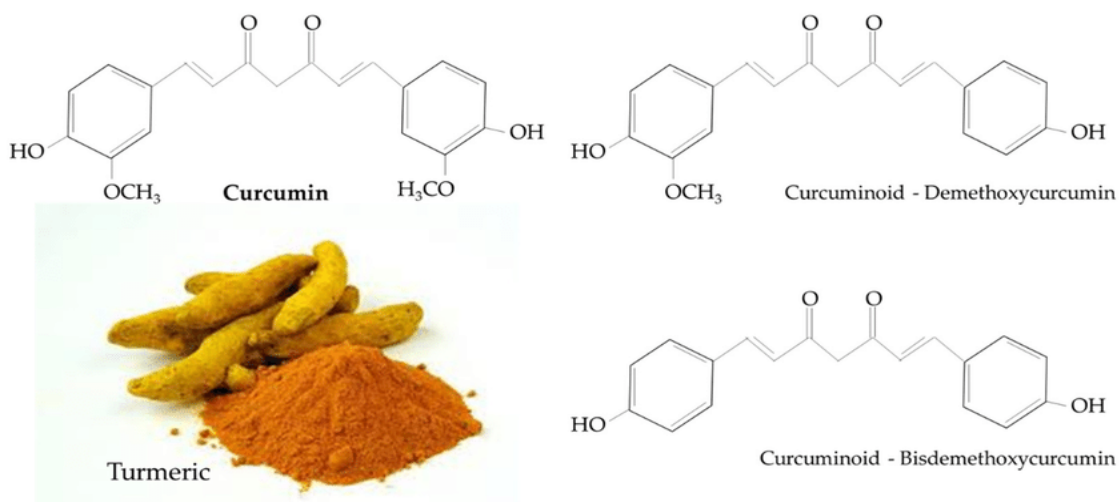


Figure 12: Chemical structure of curcuminoids of turmeric (Den Hartogh, Gabriel, & Tsiani, 2020).

3.3 Bioactive properties of curcumin

Although the medicinal properties of curcumin have been known for thousands of years, the bioactive compounds and their mechanism of action have only been recently investigated (Kotha & Luthria, 2019). Curcumin has many therapeutic properties including anti-oxidant, anti-cancer, anti-inflammatory, anti-microbial, hepatoprotective, neuroprotective, anti-diabetic, anti-atherosclerotic and wound healing properties (Fig 12) (Pulido-Moran, Moreno-Fernandez, Ramirez-Tortosa, & Ramirez-Tortosa, 2016).

Curcumin is being used for the treatment of various diseases such as cancer, cardiovascular diseases, degenerative eye disease, Alzheimer’s disease, neurological diseases, hepatic diseases, stomach disorders, diabetic complications, stroke and inflammatory diseases (Patel et al., 2020).

Curcumin is rapidly metabolised and cleared from the physiological system resulting in its poor absorption. Due to its poor bioavailability and solubility therapeutic use of curcumin is limited. Various nanoformulations have been investigated to improve the bioavailability and therapeutic potential of curcumin by overcoming the limitations (Jin, Song, Weng, & Fantus, 2018). Curcumin has been an important therapeutic molecule in biomedical research as thirty seven clinical trials of curcumin and two FDA phase 4 trials have been completed by December 2017.

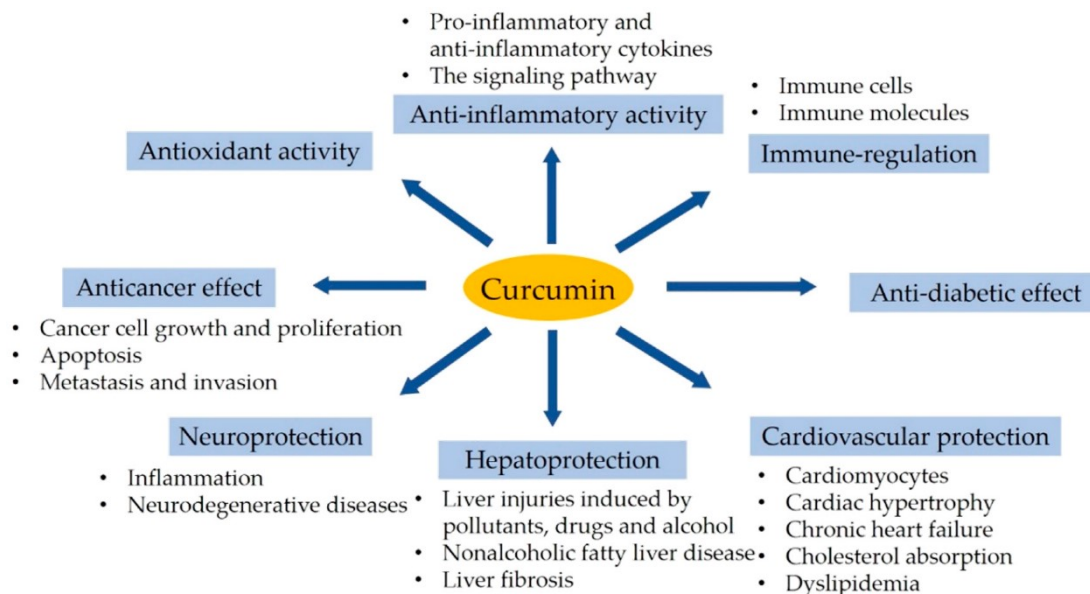


Figure 13: Therapeutic properties of curcumin (X. Y. Xu et al., 2018).

3.3.1 Anti-inflammatory activity of curcumin

Till date various anti-inflammatory mediators, effectors have been explored for their use in inflammatory diseases but curcumin is known to be a powerful anti-inflammatory molecule. Curcumin exhibits anti-inflammatory properties by inhibiting the production of inflammatory mediators and regulating the inflammatory signalling pathways (He et al., 2015).

Curcumin regulates various signalling pathways including MAPK, nuclear factor kappa- B (NFκB) and activator protein -1, JAK/STAT and other signalling pathways by interacting with TLRs, PPAR-γ, and NOD-like receptor pyrin containing 3 (NLRP3) inflammasome (Mohammadian Haftcheshmeh et al., 2020). Anti-inflammatory mechanisms of curcumin involve the down-regulates NFκB by interacting with PPAR-γ and inhibition of inflammasomes activation and assembly via NOD-like receptors. Curcumin also regulates T helper17 cells differentiation which produces pro-inflammatory cytokines including IL-17, IL-22 and IL-23 that promote inflammatory responses. Curcumin is known to promote the Th17/Treg signalling pathway that maintains immune homeostasis by inhibiting IL-23/Th17 pathway (Chainani-Wu, 2003).

Anti-inflammatory properties of curcumin are being studied and used in the pre-clinical and clinical trials on inflammatory diseases including arthritis, atherosclerosis, depression, psoriasis and inflammatory bowel disease. Inflammation plays a major role in the formation and development of atherosclerotic plaques. Curcumin is known to inhibit TNFα, IL-1β and NF-κB pathways in aorta and serum. It inhibits the vascular smooth muscle cell migration, vascular inflammation and alleviated hypertension by inhibiting NFκB regulated NLRP3 inflammasome formation and expression.

3.3.2 Antioxidant activity of curcumin

Antioxidant and anti-inflammatory properties of curcumin are the two major mechanisms of action involved in its therapeutic benefits (Lin et al., 2007). Curcumin is a natural substance that shows antioxidant properties. It is a potential lipid-soluble antioxidant (Menon & Sudheer, 2007). Oxidative stress is associated with many pathological diseases like metabolic disorders (diabetes, atherosclerosis) (Banach et al., 2014) and neurodegenerative diseases (Alzheimer's and Parkinson's disease) (Alizadeh & Kheirouri, 2019). The free radical scavenging property of curcumin is due to its CH₂ group of β-diketone moiety or OH group. Studies on the antioxidant activity of curcumin and its derivatives showed that hydrogenated curcumin derivatives exhibited strong antioxidant activity compared to the original curcumin molecule.

Tetrahydrocurcumin (THC) showed more antioxidant activity compared to dihydrocurcumin (DHC) and unmodified curcumin.

Curcumin is known to reduce oxidative stress by increasing the levels of antioxidants like catalase, lipid peroxidases, glutathione peroxidase and superoxide dismutase. It is reported to scavenge the free radical species including ROS and RNS (Panahi, Alishiri, Parvin, & Sahebkar, 2016).

3.3.3 Antimicrobial activity of curcumin

Curcumin is also known to have antimicrobial activity and is used as an antimicrobial agent for many fatal bacterial and viral infections (Trigo-Gutierrez, Vega-Chacon, Soares, & Mima, 2021). It shows antibacterial, antiviral and antifungal activities. There is also research on curcumin anti-influenza activity (Moghadamtousi et al., 2014).

Curcumin leaves essential oil is used against fungal infections. Curcumin along with epigallocatechin gallate was used against *Acinetobacter baumannii* multi- drug resistance (S. Lee, Razqan, & Kwon, 2017). Curcumin mouthwash resulted in microbial growth reduction that could be used to prevent microbial plaque formation and gingivitis (Anusha et al., 2019). It is also known to hinder the growth of *Bacillus subtilis* bacteria (Kaur, Modi, Panda, & Roy, 2010). It showed antiviral activity by inhibiting HIV-1 integrase. Anti-influenza activity of curcumin against the influenza-A virus was by inhibiting its adsorption and replication and also by inhibiting NF- κ B pathway reduces the inflammatory responses in IAV (Ou et al., 2013).

3.3.4 Anti-cancer mechanism

Curcumin and its analogues show anti-cancer properties that are being widely tested and used for different cancer treatments. Curcumin exhibits anti-cancer properties by inhibiting proliferation, invasion and promoting apoptosis of tumors by suppressing various signalling pathways (Unlu, Nayir, Dogukan Kalenderoglu, Kirca, & Ozdogan, 2016). The anti-tumor property of curcumin is due to the chelating effect of diketone moiety which suppresses the NF- κ B pathway in cancer cells (Kunnumakkara et al., 2017).

Curcumin showed anti-tumor activity on lung cancer, prostate cancer, brain tumor, breast cancer and head and neck squamous cell carcinoma. Metallo-curcumin conjugated DNA complexes made with metal ions including $Zn^{2+}/Ni^{2+}/Cu^{2+}$ showed significant toxicity in prostate cancer cell lines (Vellampatti, Chandrasekaran, Mitta, Lakshmanan, & Park, 2018).

3.3.5 Role of curcumin in metabolic disorders and wound healing

Curcumin has been shown to reduce triglycerides, high blood pressure, inflammation, oxidative stress and insulin resistance that lead to various metabolic disorders including diabetes and obesity (Mohammadi et al., 2021).

Curcumin has been widely used and explored as a wound-healing agent due to its varied therapeutic properties. Many polymeric nanoparticles and scaffolds combined with curcumin are being developed for wound healing and wound dressing studies (Akbik, Ghadiri, Chrzanowski, & Rohanizadeh, 2014).

3.4 Metabolism of curcumin

Curcumin metabolites contribute to the therapeutic activities of curcumin, which makes it important to study and explore them (Metzler, Pfeiffer, Schulz, & Dempe, 2013). Curcumin is metabolized by various reactions including oxidation, reduction, cleavage and conjugation (Fig 13) (Tsuda, 2018). Studies have shown that curcumin gets metabolized rapidly in *in vitro* and *in vivo* (Prasad, Tyagi, & Aggarwal, 2014). Curcumin is mostly metabolized in the liver and intestines (A. Pandey et al., 2020).

There are two phases of curcumin metabolism, phase I and phase II. Phase I involves reduction of the curcumin and phase II involves conjugation of curcumin and its hydrogenated curcumin. Curcumin is also metabolised by an alternative metabolism by intestinal microbiota of *E.coli*

3.4.1 Phase I curcumin metabolism

Phase I curcumin metabolism involves the reduction of double bonds of curcumin to form dihydrocurcumin, tetrahydrocurcumin, hexahydrocurcumin (HHC) and octahydrocurcumin (OHC) metabolites by reductase enzyme. Tetrahydrocurcumin is the major reductive metabolite of curcumin. Dihydrocurcumin and tetrahydrocurcumin were detected in the liver and kidney. Ferulic acid and dihydroferulic acid are some minor metabolites of curcumin reduction (Aggarwal, Deb, & Prasad, 2014).

The reductive curcumin metabolites show more bioactivity and are associated with various diseases with possible molecular targets. DHC is known to reduce oxidative stress by Nrf2 upregulation and may overcome insulin resistance by regulating PI3K/AKT pathway. DHC also inhibited lipid oxidation and lipid biosynthesis in both L02 and HepG2 cells. THC showed anti-cancer, antioxidant, anti-neurodegeneration and anti-aging properties. About 400mg/kg of THC was regarded as safe in rats in pre-clinical safety studies. It showed neuroprotective effects in

traumatic brain injury by activating autophagy and inhibiting antioxidant and mitochondrial apoptotic pathways. THC also improved arterial stiffness, vascular dysfunction and hypertension in cadmium exposed mice (Holder, Plummer, & Ryan, 1978). THC suppressed hyperglycemia induced oxidative stress by upregulation of SIRT1 and inhibit ROS, TGF β 1 and exhibited anti-diabetic, anti-fibrotic cardiomyopathy effects (A. Pandey et al., 2020).

HHC is known to have anticancer, cardioprotective, antioxidant and anti-inflammatory activities. OHC is the final reduced metabolite of curcumin. It is known to have more anti-tumor activity than curcumin (Pan, Huang, & Lin, 1999).

Curcumin and its reduced hydrocurcumins of phase I metabolism are further conjugated in phase II metabolism on its phenol-OH site.

3.4.2 Phase II curcumin metabolism

Phase II curcumin metabolism involves the conjugation of curcumin by glucuronidation and sulfation. The Higher levels of curcumin conjugation is one of the reasons for its poor bioavailability. Glucuronidation involves glucuronidases enzymes and sulfation involves sulfotransferase enzymes (SULT1A1 and SULT1A3). The enzymes for glucuronidation and sulfation were found in liver, kidney and intestinal mucosa. Curcumin conjugates were detected to be much higher in human intestinal fractions than rats and much lower in human hepatic fractions than in rats (Ireson et al., 2002).

3.4.3 Alternative curcumin metabolism

Alternative metabolism of curcumin involves the metabolism of curcumin by intestinal microbiota of *E.coli* (Hassaninasab, Hashimoto, Tomita-Yokotani, & Kobayashi, 2011). The CurA, a NADPH dependent enzyme of *E.coli* metabolizes curcumin into dihydrocurcumin and tetrahydrocurcumin by reduction reaction (Park et al., 2018).

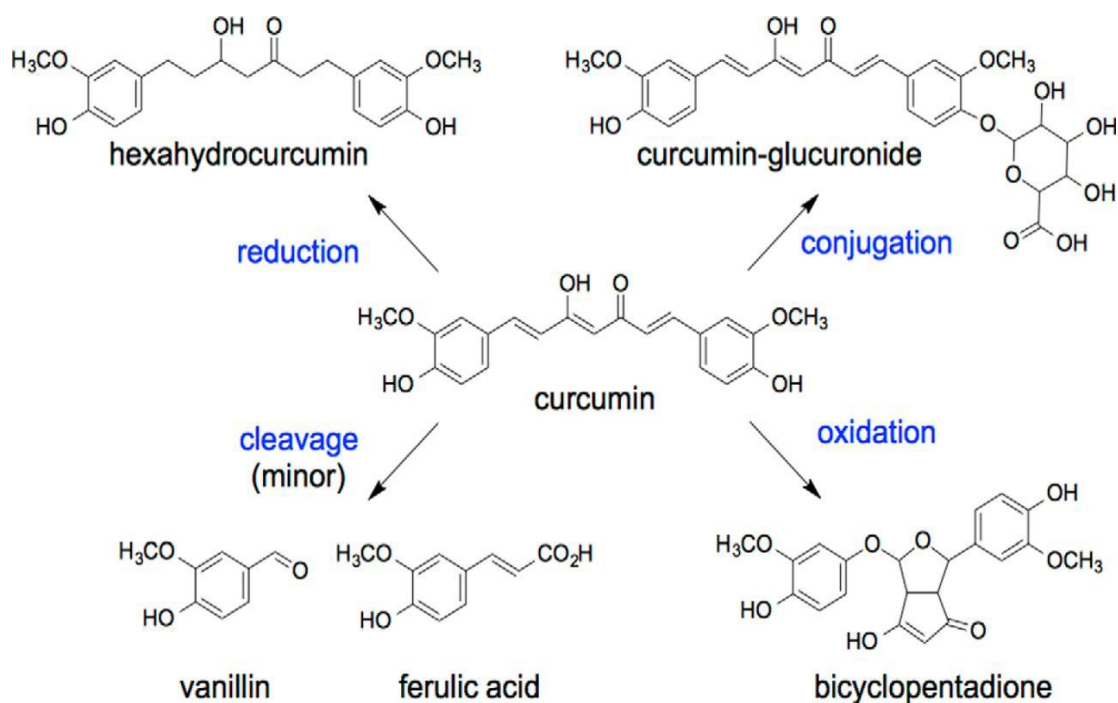


Figure 14: Different metabolites of curcumin (Gordon, Luis, Sintim, & Schneider, 2015).

3.5 Bioavailability and Biodistribution of curcumin

The poor bioavailability of curcumin limits its therapeutic benefits. Thereby understanding the bio-distribution of curcumin is critical for therapeutic research studies (Sohn et al., 2021). To understand the *in vivo* bio-distribution of curcumin (Fig 14) and its metabolism various methods of administration of curcumin have been used including oral, subcutaneous, intraperitoneal (IP), intravenous (IV) topical and nasal routes (Prasad et al., 2014).

3.5.1 Oral administration

Oral administration involves the uptake of a substance through mouth. Many studies have been done on oral administration of curcumin. With the oral administration, half of the curcumin remained in the lower part of the gut after absorption (W. Liu et al., 2016). In the gut curcumin is known to be metabolized and modified as glucuronide and sulfate derivatives and 40% remain unchanged that were detected in the urinary excretion. Orally administered curcumin gets modified in the gut and enters the portal blood as glucuronide and sulphate metabolites and so does not reach the liver in its free form. *In vivo* study of oral administration of curcumin showed that a very less amount of curcumin was detected in liver, kidney and portal blood (Ipar et al., 2019).

3.5.2 Intravenous (IV) administration

Intravenous administration is the injection of a substance directly into the blood vessels. This route of administration helps the substances to bypass physiological barriers and improves their absorption and bioavailability. Curcumin was reported to bypass the physiological barriers when given by IV. By IV administration of curcumin, glucuronide conjugates of THC and HHC were found in bile excretion (Homayun, Lin, & Choi, 2019).

3.5.3 Intraperitoneal administration (IP)

In this route of administration, the drug is directly injected into the peritoneum (body cavity). IP route of administration is used mostly for animal models than humans. The bioavailability of curcumin was shown to be better by IP than oral. Curcumin IP administration has shown to reduce intracerebral haemorrhage by reducing matrix metalloproteinase induced BBB damage (Prasad et al., 2014).

3.5.4 Subcutaneous administration

Subcutaneous injection involves the application of a substance under the skin. Subcutaneous administration of curcumin showed a sustained effective tissue concentration. Formulated curcumin showed an improved sustained release than unformulated curcumin by subcutaneous administration. Subcutaneous administration of curcumin formulated microparticles showed a sustained release of curcumin for almost a month in mouse models (Karabasz et al., 2019).

3.5.5 Topical and nasal administration

In topical administration, a substance is applied to the surface of skin or mucous membranes. It is used mostly to study wound healing, skin cancer and inflammation on target organ (Lopez-Jornet, Camacho-Alonso, Jimenez-Torres, Orduna-Domingo, & Gomez-Garcia, 2011).

The nasal route of administration of substances has gained interest as it is a direct way to transport drug substances to the brain (Zhuang et al., 2011). To increase the curcumin bioavailability and direct transport to the brain nasal route can be used. Biodistribution of curcumin in the brain was found to be more by intranasal administration than by intravenous route (Agrawal et al., 2018).

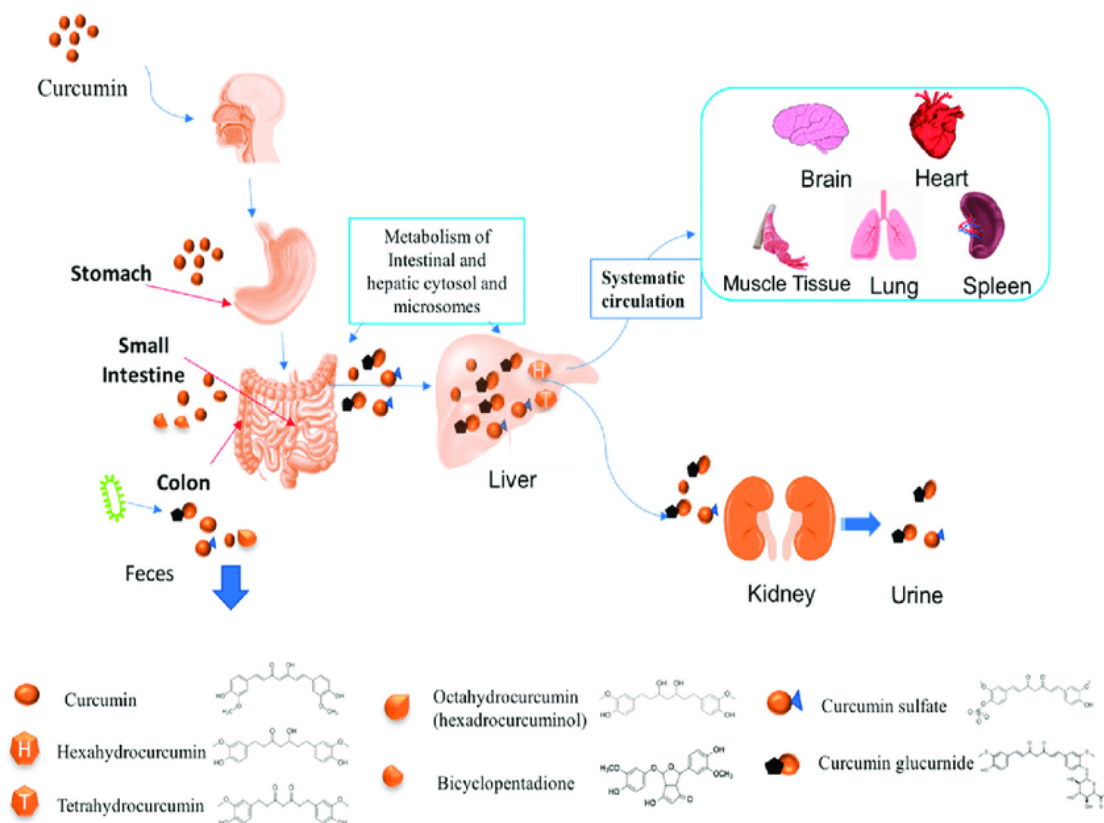


Figure 15: Biodistribution of curcumin and its metabolites (B. Zheng & McClements, 2020). Curcumin undergoes chemical degradation due to metabolism as it passes through the human gut and body. The metabolites formed have different bioactivities to the parent molecule.

3.6 Therapeutic formulations of curcumin

Although curcumin has many therapeutic properties, they are greatly limited by its hydrophobic nature, its rapid metabolism contribute to its low bioavailability. To overcome these limitations various nanoformulations drug delivery systems have been tested to encapsulated curcumin to enhance its bioavailability and bio-efficacy. Till date, the reported delivery systems for curcumin include micelles, liposomes, phospholipid complexes, micro-emulsions, nano-emulsions, emulsions, solid lipid nanoparticles, nanostructured lipid carriers, biopolymer nanoparticles and micro-gels. (Wong et al., 2019).

Few studies reporting curcumin nanoformulations with improved bioavailability of curcumin and their use in diabetic wound healing have been mentioned:

A study on antioxidant activity of curcumin on cochlear fibroblasts in STZ-induced rats showed that dietary curcumin controlled oxidative stress effectively by increasing the expression of superoxide dismutase, an antioxidant enzyme (Courret et al., 2021). Newly developed curcumin-

based formulations have shown to be an excellent wound healing agents. Encapsulated curcumin nanoparticles improved the skin wound healing efficiently and safely for diabetics. Chitosan nanoparticles loaded with curcumin could attenuate inflammation mediated by macrophages and enhance angiogenesis both *in vitro* and *in vivo* thereby accelerating the wound healing in diabetic rats (Akbar et al., 2018).

Intravenous administration of poly-d, l-lactic-*co*-glycolic acid (PLGA) encapsulated curcumin showed higher serum concentrations than native curcumin which improved the bioavailability and half-life of curcumin (Tsai, Chang-Liao, Chien, Lin, & Tsai, 2012). The oral delivery of these curcumin formulations improved their bioavailability by 15.6 folds (PLGA-curcumin) and 55.4 folds (PLGA-PEG-curcumin) (Yallapu, Gupta, Jaggi, & Chauhan, 2010).

Liposomes and micelles are potential drug carriers of hydrophobic drug molecules for solubilisation. Liposome encapsulated curcumin showed higher bioavailability and faster absorption rate by oral administration in rats. Silica coated liposomes loaded with curcumin showed 7.76 fold higher curcumin bioavailability than other curcumin suspensions (Peng et al., 2014). Propylene glycol and N-trimethyl chitosan chloride coated liposomes were also prepared to encapsulate curcumin that improved the bioavailability and release profiles compared to native curcumin. Cyclodextrin polysaccharide was also used to formulate curcumin which showed greater cellular uptake and longer half-life compared to native curcumin.

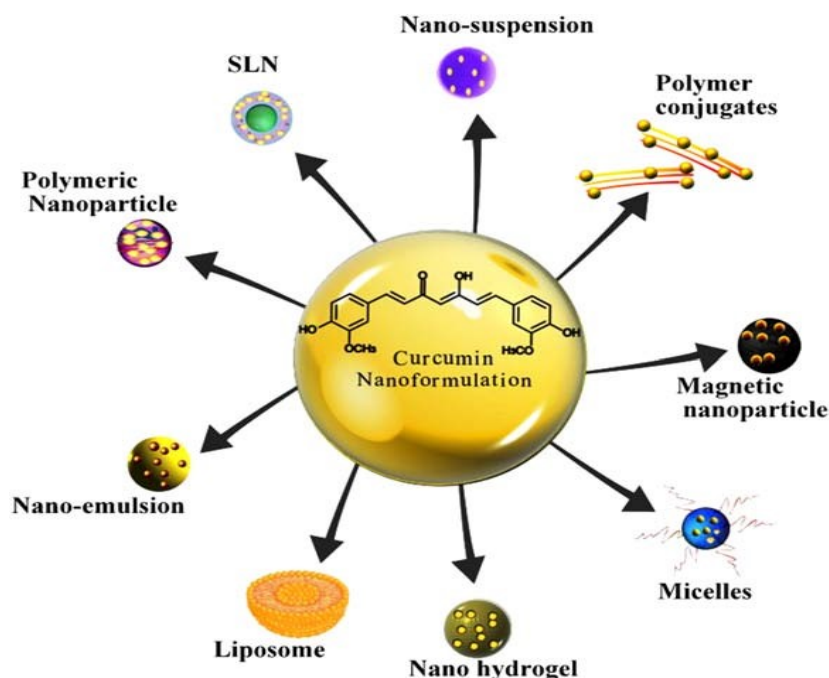


Figure 16: Different nanoformulations of curcumin (Ahmad et al., 2014).

Among different drug delivery vectors, in this work HDL lipoprotein and micelles have been chosen to encapsulate curcumin. HDL has beneficial effects on diabetes and its vascular complications. It shows protective effect on atherosclerosis by mediating cholesterol efflux from lipid rich macrophages in arterial walls of atherosclerotic plaques (Rye & Barter, 2014). HDL also showed protective effect on endothelial cells by stimulating NO production which mediates vascular relaxation, prevents monocyte-endothelial interactions by inhibits downstream inflammatory pathways (Tran-Dinh et al., 2013) and prevents apoptosis by reducing ER stress and ROS production (Petremand et al., 2012; White, Datta, & Giordano, 2017). HDL has also shown to promote angiogenesis in hypoxia condition, where impaired ischemia induced-neovascularization are associated with diabetic vascular complications (Tan, Ng, & Bursill, 2015). It also reduced ischemic stroke infarct volume in mice model (Courret et al., 2021; Tran-Dinh et al., 2020). Curcumin has been previously encapsulated into carrageenan nanomicelles. They have been shown to improve the cellular uptake of curcumin and promoted anti-inflammatory effect by decreasing the levels of inflammatory factors IL-6 and MCP-1 in TNF- α -induced inflammation *in vitro* in EA-hy926 endothelial cell line. *In vivo* studies showed that drug-loaded hyaluronic acid/ κ -carrageenan injectable hydrogels accelerated 90% wound closure in rats. The β -Cyclodextrin/Curcumin loaded carrageenan hydrogel has been developed as a wound dressing material due to its free radical scavenging activity (Youssof et al., 2019). Therefore, the choice of HDL and carrageenan nanomicelles to encapsulate curcumin for evaluating their potential on endothelial dysfunction associated with diabetic stroke and regenerative wound healing for improving diabetic lesions can be a good choice.

IV. HDL and its therapeutic properties in vascular complications

High density lipoproteins are small protein-rich complexes. They contain apolipoprotein, phospholipids, cholesterol, enzymes and acute-phase proteins. Apolipoprotein is the main HDL protein component. HDL has a diverse chemical, structural and biological properties. HDL has various functions but its main function is lipid transport and metabolism. It plays a major role in reverse cholesterol transport where they collect cholesterol from peripheral tissues and transport it to the liver for elimination. Other functions HDLs natural cargo includes lipids, proteins and microRNAs.

Natural nanostructure size and flexible of physiochemical properties make HDL particles suitable for treating many diseases. HDLs are biocompatible and biodegradable protein-lipid complexes that are interesting diagnostic and therapeutic agents. HDL shows cardioprotective and antiatherogenic properties. Increased HDL cholesterol levels were associated with reduced risk of cardiovascular diseases while lower HDL-C levels are a risk factor. HDLs showed arterial protection by the removal of cholesterol from the arterial walls by ABC G1 (ATP-binding cassette) and ABC A1 transporters. Focus on using HDL as a drug delivery vector and scaffold preparations are emerging.

4.1 Structure of HDL

HDL is a nanosized protein-lipid complex that is 8-10 nm in size and 1.063-1.21 g/ml in density. Among other lipoproteins HDLs have high density due to their high protein content which accounts for 30% to 60% by weight. Apolipoprotein A-I and Apolipoprotein A-II are the most abundant HDL proteins. Apolipoprotein A-I is the major structural and functional part of HDL which accounts for 70% of HDL proteins. HDL lipids include phospholipids (phosphatidylcholine, Phosphatidylglycerol, phosphotidylserine, phosphatidylinositol, phosphatidic acid, phosphotidyl ethanolamine and cardiolipin), sphingolipids (sphingomyelin, ceramide), neutral lipids (unesterified (free) sterols), cholesteryl esters and triglycerides (Kontush et al., 2015). Phosphatidylcholine is the major phospholipid that accounts for 32- 35 mol % of total HDL lipids. Phosphatidylglycerol, phosphotidylserine, phosphatidylinositol, phosphatidic acid, and cardiolipin are negatively charged phospholipids. Sphingomyelin enhances the surface lipid rigidity of HDL particles. Cholesterol is the major unesterified sterol component located in the surface lipid monolayer of HDL particles and regulates the fluidity.

Cholesteryl esters are formed during the reverse cholesterol transport by esterification of cholesterol and phospholipids by LCAT (lecithin cholesterol acyltransferase) enzyme.

HDL particles are nascent discoidal in the early stage and form spherical particles in a matured stage. Apolipoproteins are actively involved with HDL in the exchange process between HDL-bound state and lipid-free state (Lund-Katz, Liu, Thuahnai, & Phillips, 2003).

Nascent Discoidal HDL

This discoidal HDL serves as a substrate for LCAT, so are short-lived in the blood plasma with more LCAT activity can be detected more in peripheral lymph and interstitial fluid as they have less LCAT activity. Discoidal HDL consisting of two Apo A-I molecules ($\sim 47\text{\AA}$ and $\sim 96\text{\AA}$ diameter) are the most studied. Based on the double belt molecular model Discoidal HDL contains two ring-shaped Apo A-I molecules that encapsulate a lipid membrane leaflet in an antiparallel orientation.

Spherical HDL

These are the most circulating HDL particles and contain phospholipids, apolipoproteins on the surface with a neutral lipid core of cholesteryl ester and triglycerides (Lund-Katz & Phillips, 2010) (Fig 17).

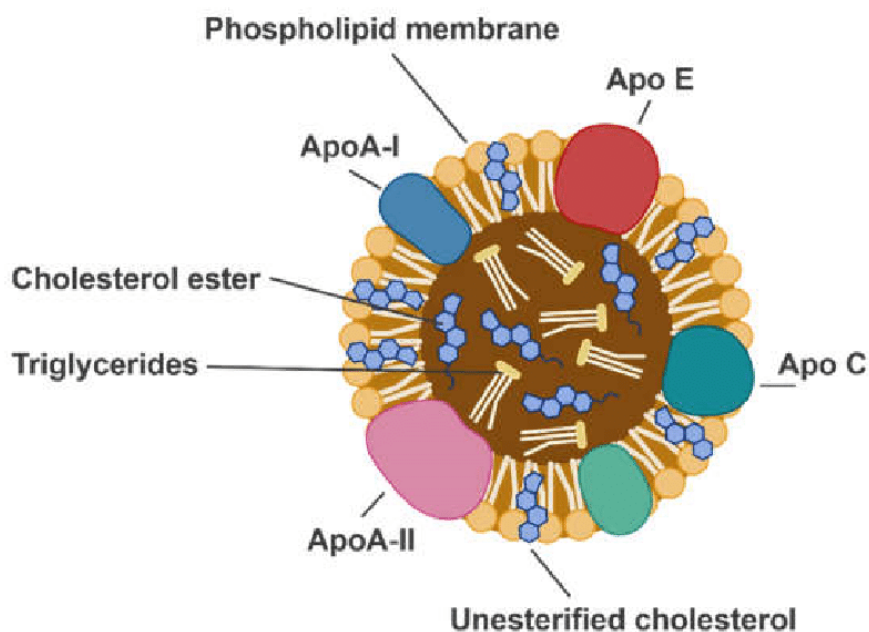


Figure 17: Structure of HDL (Primer, Psaltis, Tan, & Bursill, 2020).

4.2 HDL sub types

As HDL particles interact with different enzymes, cells and cargo molecules they tend to form heterogeneous complexes including quasi-spherical or discoid, plurimolecular and pseudomicellar complexes. These complexes are mainly composed of polar lipids solubilized by apolipoproteins. Different analytical techniques including separation, migration and density like ultracentrifugation and electrophoresis are used to identify HDL sub-types based on presence or absence of protein component, size, density, surface charge and shape (Rainwater, Blangero, Moore, Shelledy, & Dyer, 1995).

HDL subtype based on size and density

Using analytical ultracentrifugation and based on density two HDL subclasses were identified as HDL2 and HDL3 molecules. HDL2 are lipid-rich less dense molecules (1.063 – 1.125 g/mL) and HDL3 are protein-rich denser molecules (1.125 – 1.21g/mL). Further, by using single vertical spin ultracentrifugation and rate-zonal ultracentrifugation and based on particle size three subclasses of HDL 2 and two subclasses of HDL3 were identified. They include HDL 2a (8.2 – 8.3 nm diameter), HDL2b (7.8-8.2 nm), HDL3a (7.2- 7.88 nm), HDL 3b (8.8-9.7 nm) and HDL 3c (9.7 – 12.0 nm) (Fig 18).

HDL subtype based on surface charge and shape

Using agarose gel electrophoresis and based on the charge, shape and electrophoretic mobility of two HDL subclasses are identified as α -migrating particles and pre β -migrating particles. Circulating spherical HDL particles are included in the α -migrating particles and pre β -migrating particles include poorly lipidated HDL and nascent discoidal particles (Fig 18).

HDL subtype based on the protein component

An Electroimmunodiffusion technique in agarose gel was used and based on the presence or absence of Apo A-I/ Apo A-II two HDL subclasses were identified as HDL particles with Apo A-I and Apo A-II known as LpA-I: LpA-II and HDL particles with only Apo A-I and without Apo A-II known as LpA-I (Fig 18).

HDL subtype based on lipid methyl group of lipoprotein particle

NMR was used and based on the lipid methyl group of lipoprotein particle HDL subclasses were identified as large HDL (8.8 – 13.0 nm diameter), medium HDL (8.2 -8.8 nm) and small HDL (7.3-8.2 nm) particles.

In the last few years, HDL heterogeneity in clinical studies has increased the focus on exploring various HDL subclasses using different analytical techniques. Different subpopulations of HDL subclasses can further be explored by using analytical techniques.

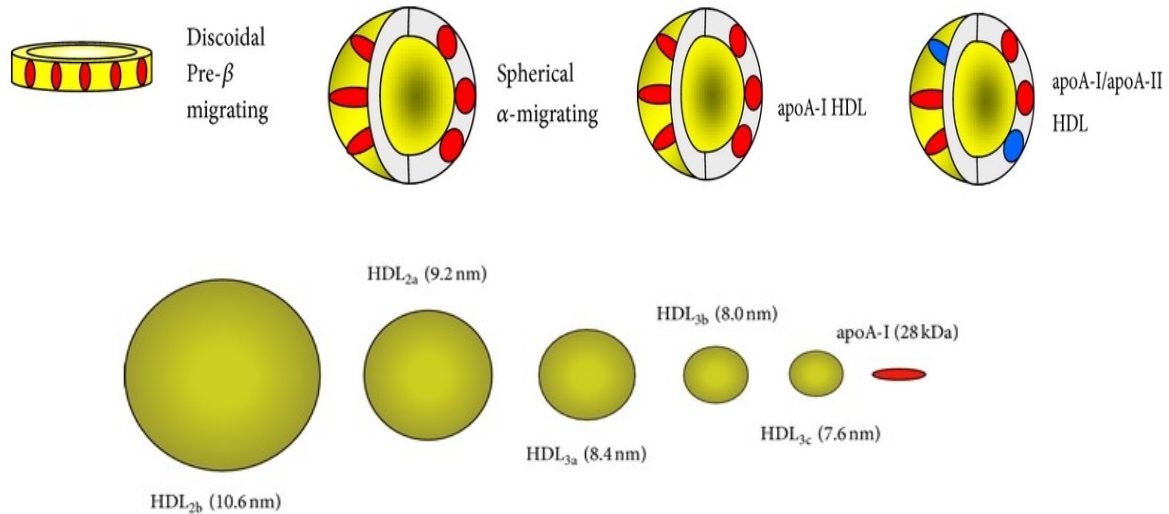


Figure 18: Different sub-types of HDL (Robichaud et al., 2021).

4.3 Biogenesis and function of HDL

HDL biogenesis is initiated by the interaction of Apo A-1 protein with ABCA 1 and occurs on macrophages. It involves the ATP dependent transport of cholesterol and phospholipids to the nascent discoidal HDL. Discoidal HDL are pre- β HDL that contain 2 or 3 Apo A-1 proteins shielding the hydrophobic acyl chains. The pre- β contains 60- 70% proteins, phospholipids and esterified cholesterol (Tsompanidi, Brinkmeier, Fotiadou, Giakoumi, & Kypreos, 2010). When pre- β deposits enough cholesterol they mature into spherical HDL particles through LCAT enzyme. LCAT enzyme transfers an acyl group from a phospholipid to cholesterol to form cholesteryl ester on discoidal HDL. Cholesteryl esters move to the hydrophobic core of the HDL forming spherical particles (Genest, Schwertani, & Choi, 2018).

Spherical HDL further undergo additional maturation by taking more cholesterol and phospholipids from cells through various processes including aqueous diffusion of cholesterol and direct uptake of lipids from cell membrane or associated with ABC G 1 transporters. ABC

G1 transporters enhance the efflux of cholesterol by cholesterol localization on the cell membrane and do not bind to the HDL particle (Yokoyama, 2006). Spherical HDL particles interact with SR-B1 receptors expressed by many cell types. The SR-B1 (scavenger receptor class B type 1) receptors like ABC transporters also selective cholesteryl ester transfer to the target cells. SR-B1 mediated selective lipid uptake does not involve lysosomal degradation and uptake of entire HDL particle. Spherical HDL have high relevance as a drug delivery molecule (Zannis, Chroni, & Krieger, 2006).

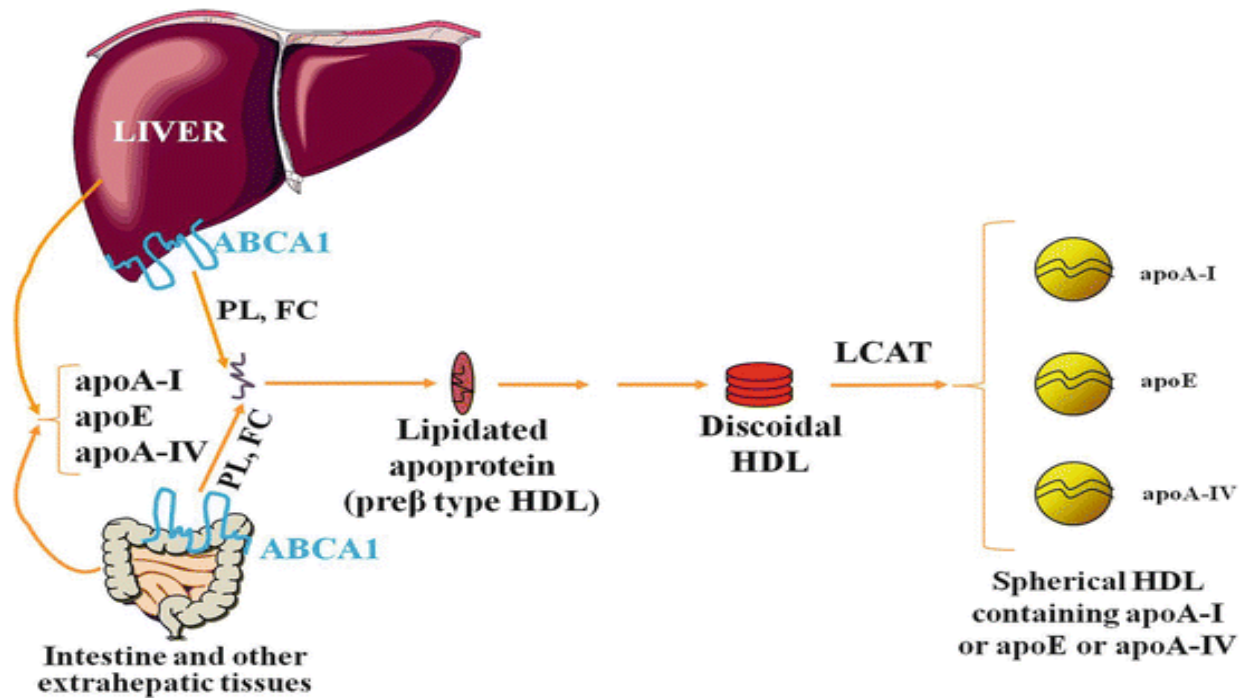


Figure 19: Schematic of HDL biogenesis (Zannis et al., 2015).

The biogenesis of HDL is a complex process and involves several membrane bound and plasma proteins. The first step in HDL biogenesis involves secretion of apoA-I mainly by the liver and the intestine. Secreted apoA-I interacts functionally with ABCA1, and this interaction leads to the transfer of cellular phospholipids and cholesterol to lipid-poor apoA-I. The lipidated apoA-I is gradually converted to discoidal particles enriched in unesterified cholesterol. The esterification of free cholesterol by the enzyme lecithin/cholesterol acyltransferase (LCAT) converts the discoidal to spherical HDL particles. The absence or inactivating mutations in apoA-I, ABCA1, and LCAT prevent the formation of apoA-I-containing HDL. Following a similar pathway, apoE and apoA-IV can also synthesize HDL particles that contain these proteins. The unique properties of apoA-I permit it to acquire lipids via interactions with ABCA1 and LCAT.

4.4 HDL cargo

Proteomics and lipidomic studies have shown that HDL cargo includes proteins, lipids and small RNA.

HDL also has Apo A-II, Apo C-I, Apo C-II and Apo C-III proteins other than Apo A-1. Apo A-II shows pro-inflammatory function by increasing monocyte response to LPS. Apo M inhibited mortality in LPS treated mice and LPS induced acute lung injury.

HDL lipids include cholesterol, sphingolipids, phospholipids and triglycerides. Sphingosine -1-phosphate (S1P) is mostly expressed in endothelial cells and inhibits MCP-1 and activates eNOS in endothelial cells.

Other than proteins, lipids and enzymes HDL particles also carry nucleic acids including miRNA, sRNA, and snRNA. HDL- miRNA association was identified in atherosclerosis and dyslipidemia patients (Ertek, 2018).

4.5 HDL in the pathophysiology of vascular diseases

Other than lipid transport and metabolism, HDL has various functions. HDL serves as a circulating vehicle loaded with many biological activities. They are associated with vascular complication (Femlak, Gluba-Brzozka, Cialkowska-Rysz, & Rysz, 2017).

4.5.1 HDL anti-inflammatory role

HDL exhibits anti-inflammatory functions that are associated with proteome ApoA-1, other proteins including PON1 and clustrin and sphingosine-1-phosphate lipidomic constituents (Holzwirth et al., 2022). HDL exerts anti-inflammatory, anti-atherosclerotic and vascular protective properties by suppressing the inflammation mediated by macrophages, monocytes and neutrophils. Apo A-1 is shown to inhibit cellular adhesion molecules intracellular adhesion molecule-1, vascular cell adhesion molecule-1 and E-selectins and monocyte expression of integrin CD11b induced by inflammatory cytokines. Inhibition of expression of endothelial adhesion molecules decreases the trans-endothelial migration and recruitment of immune cells (monocytes, macrophages and neutrophils) to the vascular arterial walls from blood circulation. Apo A-1 also inhibits the T cell activated production of IL-1 β and TNF- α associated with monocyte or macrophage. HDL is also known to inhibit the NF- κ B pathways by suppressing the activation of monocytes and endothelial cells. It is also known to inhibit LDL induced monocyte

chemoattractant protein-1 (MCP-1), which is a major chemokine that regulates the migration and infiltration of monocyte and macrophages into the arterial walls.

HDL has immunomodulatory properties and has a role in host defence mechanisms by modulating innate and adaptive immune responses (Jia et al., 2021). HDL reduced the lipopolysaccharide (LPS) toxicity and LPS- toll-like receptor TLR 4/CD14 complex-mediated proinflammatory pathways. Innate immune cells such as macrophages, monocytes and dendritic cells express TLR 4 receptors which is activated by LPS. LPS triggers pro-inflammatory cytokine production by TLR 4 induced MyD88 signaling pathway. HDL inhibits TLR signaling by inducing the expression and activation of activating transcription factor 3. By altering cholesterol content in lipid rafts, HDL is known to modulate innate and adaptive immune responses as high cholesterol cell membrane contains many membrane proteins including TLR receptors. Therefore by decreasing cholesterol content in lipid rafts, HDL can inhibit TLR mediated MyD88 signaling, antigen-presenting capacity of macrophages and dendritic cells T cell activation and blocks the transformation of monocytes into migratory dendritic cells by platelet-activating acetylhydrolase enzyme. HDL components including immunoglobulins, Apo A-1, sphingosine-1-phosphate and complement system components directly participate in the immune responses (Saemann et al., 2010).

4.5.2 HDL antioxidant role

HDL also exerts an antioxidant function that prevents lipid oxidation and removes oxidized products. It has many antioxidant enzymes including lipoprotein-associated phospholipase A2, LCAT and PON 1. Lipoprotein-associated phospholipase A2 and LCAT show antioxidant function by hydrolysing the oxidized acyl moieties of oxidized phospholipids. Apo A-1 binds and removes peroxidation products from phosphatidylcholine, LDL and cholesteryl esters. HDL prevents LDL oxidation from lipid peroxidation products of macrophages. HDL3 subclass HDL molecule has shown more potential capacity of LDL protection oxidation than HDL2. Apo A-1 is crucial for PON1 function. PON1 is known to protect HDL and LDL from oxidation and PON-1 knockout mice showed susceptibility to atherosclerosis (Xepapadaki, Zvintzou, Kalogeropoulou, Filou, & Kypreos, 2020). HDL interacts with sphingosine-1-phosphate receptor 3 (S1P3) and SR-B1 receptors and reduces endothelial superoxide production induced by TNF- α associated with an inhibitory effect of HDL lysosphingolipids on NADPH oxidase. HDL plays a role in elimination of hydroxides, hydroperoxides and lipid peroxidation products by

hepatocytes by transporting them to the liver with SR-B1 receptor interaction (Shokri et al., 2020).

4.5.3 HDL anti-apoptotic role

HDL has many biological functions including an anti-apoptotic role. Sphingolipids of HDL regulate cell growth and survival, ceramide and sphingosine sphingolipids induce growth arrest, stress stimuli and apoptosis. SIP is known to regulate apoptosis by binding to Apo M in plasma. SIP regulates many cellular processes including angiogenesis, cell migration cell survival and immune cell trafficking. Inflammation and apoptosis of endothelial cells provoke them to become pro-coagulants and form clots that are associated with atherosclerosis and thrombosis. HDL shows cytoprotective and anti-apoptotic activity on endothelial cells. It protects the endothelial cells from apoptosis and promotes their cell survival. HDL protects the human umbilical vein endothelial cells by inhibition of TNF- α mediated cysteine protease p-32 like protease activity. HDL stimulated the endothelial anti-apoptotic Bcl-xL protein and reduced apoptosis *in vitro* and *in vivo* in apolipoprotein E-deficient mice. HDL also prevents apoptosis of pancreatic beta cells. It protects against growth factor or serum induced cell death in *in vitro* model (Shokri et al., 2020).

HDL also exerts other functions including regulation of glucose metabolism, anti-ischemic and angiogenesis activities. Sphingosine- 1 phosphate of HDL protects from ischemic reperfusion by multiple mechanisms including NO production, inhibition of inflammation and activation of salvage pathway (Ruiz, Okada, & Dahlback, 2017).

4.6 Cellular uptake of HDL

Scavenger receptor class B type -1 is the major HDL receptor. SR-B1 transports HDL cholesterol to liver and regulates reverse cholesterol transport. It is a glycoprotein that mediates selective uptake of cholesterol, cholesteryl ester from HDL molecules to the liver without degradation of HDL (Robert, Osto, & von Eckardstein, 2021). The cellular uptake HDL is mediated by SR-B1 by endocytosis or transcytosis. SR-B1 receptors bind different HDL species with different affinities depending upon the lipid composition and shape of HDL (Fig 20). The cholesterol transfer from HDL makes them smaller particles and thereby decreasing their affinity to the receptors and creates free space for binding of other cholesteryl ester loaded HDL particles. The exchange of cholesterol with the liver is by endocytosis and HDL uptake was reported by

transendocytosis into endosomes by SR-B1 receptors. Retroendocytosis was first reported in rat aortic smooth muscle cells (Rohrer et al., 2009).

The uptake of HDL across BBB is by transcytosis. In transcytosis the lipoprotein is internalized at the luminal surface of endothelium and then finally exocytosed at the base membrane of BBB. This transcytosis of HDL is associated with a neuroprotective effect in neurodegenerative disorders via Apo A-1. Enhanced transcytosis of HDL across BBB has gained importance as a drug delivery tool to the brain. Apo A-1 of HDL transcytosis showed a protective effect against Alzheimer's disease by reducing amyloid β aggregation, deposition and toxicity (Goti et al., 2001).

HDL exerts many beneficial effects on endothelial cells via interaction with the endothelial receptors which include SR-B1, ABCA1 and recently reported ecto-F₁ ATPase receptor. These receptors are involved in HDL cellular internalization and signaling. SR-B1 mediated HDL signaling provides vascular protection by NO, cyclooxygenase and PGI₂ production. PGI₂ is a vasodilator and prevents platelet adhesion.

ABCA1 is involved in the cholesterol efflux from macrophages to Apo A-1 either at plasma membrane or by internalizing apoA1 in late endosomes and released by exocytosis after enrichment with cholesterol. It is known to be expressed in human aortic endothelial cells (HAoECs) and HUVEC. Overexpression of ABC A1 lead to increased cholesterol efflux in HUVECs and HAoECs. It is reported to be a regulator of macrophage cholesterol and phospholipid transport. ABC A1 showed protection of endothelial dysfunction in high-fat diet mice model by reducing the inhibition of NO production.

Ecto-F₁- ATPase was reported as a HDL receptor which is a cell surface enzyme complex associated with mitochondrial F₁ F₀ ATP synthase. It is shown to have a high affinity to Apo A-1 in hepatocytes and mediates endocytosis of HDL. The Apo A-1 binds to β - ecto-F₁- ATPase that stimulates ATP hydrolysis to ADP, ADP then activates P2Y₁₃ receptor that triggers holo HDL uptake. Ecto-F₁- ATPase were shown to be expressed at the surface HUVECs endothelial cells. This receptor was involved in the uptake and transport of lipid-free apoA1 and HDL in bovine aortic endothelial cells. It also inhibited apoptosis of serum deprivation in HUVECs and its α -subunit showed anti-angiogenic effects.

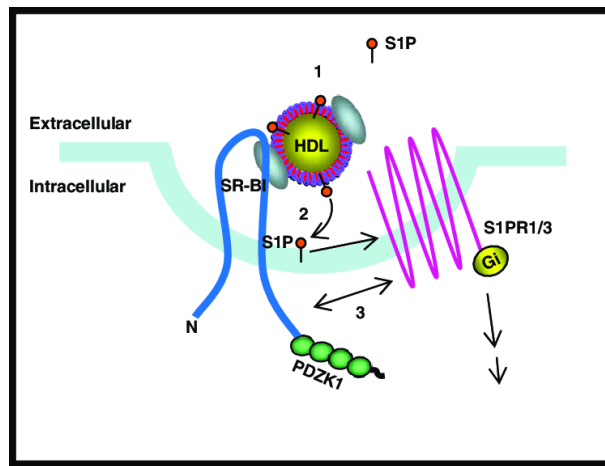


Figure 20: Cellular uptake of HDL by SR-B1 receptors (Al-Jarallah & Trigatti, 2010).

SR-B1 as a mediator of lipid uptake. HDL sequesters S1P, reducing the effective concentration of free S1P and influencing S1P interaction with S1P receptors (1). SR-B1 may mediate the transfer of HDL associated S1P into the cell membrane (2), allowing S1P to access Gi-coupled S1P receptors and initiate signaling. S1P receptors have been shown to physically and functionally associate with growth factor receptors raising the possibility that SR-B1 may also associate directly (or indirectly via adaptor proteins) with one or more S1P receptor to engage in signaling (3).

4.7 HDL molecules in therapeutics

The use of HDL molecules in therapeutics has gained tremendous interest. Nanotechnology-based biomimetic natural HDL molecules are potential platforms for use as drug delivery systems (Ben-Aicha, Badimon, & Vilahur, 2020). It has a lot of advantages as it is highly stable, receptor mediated interactions can potentially be used for specific targeting and smaller particles <13nm in size with higher surface area. Higher HDL blood circulating concentrations (30µM) suggests that biomimetic HDL could be physiologically tolerated. The larger surface area provides enough room for carrying many small molecules at once or alone and the small size makes it easy to penetrate the tissues. Physiological HDL circulation tends to increase its bioavailability to target tissues.

HDL in drug delivery

Endogenous HDL particles have been explored to transport small interfering RNA (siRNA). Studies showed that Apo B1 with siRNA antisense pre-incubated with HDL prior to injection in animals had higher uptake in SR-B1 dependent manner. Cholesterol conjugated siRNA showed that it can be conjugated with HDL or LDL and after injection, they were detected in the vascular compartments in the brain tissue by northern blot analysis. The conjugation of α-tocopherol-

siRNA showed enhanced stability after conjugating with HDL particles by gel shift experiments. Galactose uptake is specific to liver, injection of galactose conjugated HDL promoted its rapid uptake in the liver suggesting this approach for the use to deliver hydrophobic molecules (Fox, Moschetti, & Ryan, 2021).

Reconstituted HDL (Nanodiscs)

Based on the lipophilic components and apolipoprotein of natural HDL particle synthesis nanodiscs termed reconstituted or recombined HDL (rHDL) molecules are being formulated. They range from 9 to 30 nm in size. These rHDLs were first formulated to understand the biochemical and biophysical properties of natural HDL molecules. The interaction between HDL particles and the biological membranes was also explored using rHDLs. Biochemical and biophysical properties of apolipoproteins were used to control the size and assembly of rHDLs. Their similarity with natural HDL molecules makes them biocompatible and their amphiphilic nature makes them suitable for lipophilic drug delivery (Fox et al., 2021). Various drugs have been formulated using nanodiscs. Lipophilic antifungal Amphotericin B loaded nanodiscs showed reduced toxicity compared to unformulated ones in Hep G2 liver cells and red blood cells. This Amphotericin B nanodiscs were also potential against *Candida albicans* infected mice model. Retinoic acid a lipophilic drug prepared by loading into nanodiscs enhanced stable storage at 4 °C and showed a potential effect in lymphoma cell culture models by increasing cell cycle arrest and cell death. Nanodiscs formulated curcumin showed enhanced anti-proliferative effect and increased solubility compared to unformulated curcumin in a cancer cell line. Simvastatin is an HMG-CoA inhibitor, anti-inflammatory and cholesterol lowering properties. Simvastatin formulated with reconstituted HDL was used in Apo E knockout mouse model for atherosclerosis. It reduced macrophage survival *in vitro* which is a major inflammatory cell that mediates atherosclerosis. Also, further developments have been made in nanodiscs formulations such as a fusion protein with Apo A-I combined with a single chain variable antibody vimentin, specifically targeted vimentin (Tsujita, Wolska, Gutmann, & Remaley, 2018).

Spherical HDLs in therapeutics

Spherical HDLs are circulating HDL molecules that are less studied. Synthesis of spherical HDL analogues is more complicated than nanodiscs. The spherical HDL molecules are being developed to use as drug delivery platforms by providing surface loading or hydrophobic core

loading of drugs. They also interact with the SR-B1 receptors and have many distinct functions compared to the discoidal HDLs (Tsujiita et al., 2018).

V Marine Algae and their use in therapeutics

Marine organisms such as marine algae and cyanobacteria have been an interesting source of some bioactive substances with therapeutic activities explored in the last few decades (Blunt, Copp, Keyzers, Munro, & Prinsep, 2016). Marine bioactive compounds include sulphated polysaccharides, carotene, omega-3 fatty acids, β -carotinoids (astaxanthin, carotene and fucoxanthin) and polyphenols (El Gamal, 2010). Marine algae are chlorophyll containing simple marine organism that are either single celled (3 to 10 μm in size) or many cells organised in groups to form kelp (that extends up to 70 m). Algae are found in most of the places of the earth such as rivers, sea, lakes, on the walls (mosses), soil, animals and plants where there is sunlight to prepare their own food by chlorophyll (P. Li, Harding, & Liu, 2001). They are found as micro algae or macroalgae (seaweed) in seas and as phytoplanktons in oceans (Dittami, Heesch, Olsen, & Collen, 2017). Microalgae accounts for 40% of oxygen in the atmosphere and 40,000 species of microalgae have been identified. They are the major source of food and oxygen for the marine life. Based on the chloroplast pigments marine algae are classified into green, brown and red algae.

Marine algae are most interesting source of novel bioactive substances that have diverse chemical structure and biological activities due to which they are being used in the biomedical field. They are also widely being used in cosmetic, food, textile and agriculture fields (C. Song et al., 2021).

5.1 Marine algae and their bioactive properties

The green, brown and red algae have many bioactive properties that are used in biomedical field.

Green algae

Green algae are known as chlorophyta and has green colour chlorophyll pigment. It comprises of 9000 to 12000 species. Their cell wall is made up of cellulose and pectin complexes and starch is the main food storage polysaccharide. Some green algae include *Spirogyra*, *Cladophora*, *Hydrodictyon*. They mostly occur in fresh water either as free-floating or attached to the submerged rocks or wood. Bioactive molecules isolated from green algae showed therapeutic properties such as anti-inflammatory, anti-biotic, anti-viral, anti-mutagenic and anti-fungal activities (Umen, 2014).

Bioactive compounds diphenyl ether 29, 3-O-b-D-glucopyranosyl-stigmasta-5, 25-diene 28 isolated from green algae have shown anti-inflammatory properties. Diphenyl ether 29 molecule showed effective anti-inflammatory effect against toxins injected in a mouse limb study. Cyclooudesmol 59 isolated from *Chondria oppositoclada* showed antibiotic effect against *Staphylococcus aureus* and *Candida albicans* (Lu & Oyler, 2009).

Brown algae

Brown algae belongs to the class phaeophyta and consists of fucoxanthin pigment responsible for its brownish colour. Brown algae is mostly present in the northern hemisphere in the Polar Regions. About 1,500 to 2000 species of brown algae have been identified. It is found in marine water environments. Major storage polysaccharide is laminarin and the cell wall is made up of cellulose and alginic acid (Y. Li et al., 2021). Many bioactive molecules have been isolated from brown algae that have pharmacological properties like anti-tumor, nematocidal activity (used as pesticide for plants), hepatoprotective activity, anti-inflammatory, antiviral, anti-oxidant and anti-diabetic activities (Generalic Mekinic et al., 2019).

Fucoesterol isolated from brown algae *Pellvetia siliquosa* demonstrated anti-diabetic activity. Macrolides and Lophorins isolated from *Lobophora variegata* showed anti-inflammatory properties. Several prenyl toluquinones isolated from *Cystoseira crinite* exhibited free radical scavenging effect (Cock, Peters, & Coelho, 2011).

Red algae

Red algae belong to the class Rhodophyta. The red colour of the algae is due to the presence of phycoerythrin pigment. The cell walls is made up of agars, cellulose and carrageenans. It is the major source of carrageenan polysaccharide compared to other algae. Many red algae are edible such as carrageenan moss *Mastocarpus stellatus*, *Chondrus crispus* and *Palmaria palmate*. *Betaphycus* and *Kappaphycus* red algae species are the important source of carrageenan which are used as food ingredient (Khotimchenko et al., 2020). There are almost 8000 red algae species which live in marine environments. They also have bioactive metabolites that show pharmacological activities.

Aminoacid, kainic acid isolated from *Digenea simplex* showed neurophysiological activity. Bromothenols isolated from *Polysiphonia urceolata* showed free radical scavenging activity. Trans, trans-ceratospongamide isolated from *Ceratodictyon spongiosum* showed anti-inflammatory activity (Blunt et al., 2018).

5.2 Composition of marine algae

5.2.1 Polysaccharides of marine algae

Algal polysaccharides are known as phycocolloids which are abundant source of polysaccharides (4% - 76%). Polysaccharides as the structural component of algal cell wall. Polysaccharides have various biological activities that depend on the type of glycosidic linkage, molecular weight and monosaccharide composition of the polysaccharides (S. Y. Xu, Huang, & Cheong, 2017). Polysaccharides are classified based on their chemical structure including galactans, sulphated xylans and sulphuric acid polysaccharide from green algae, laminarin, fucoidan, sargassan and alginate from brown algae and carrageenans, xylans, agar and floridean from red algae. Carrageenan account for about 50% of dry weight of algal biomass and is considered the most abundant polysaccharide found in red algae such as *Euchema denticulatum*, *Kappaphycus alvarezii* and *Kappaphycus cottoni* species (Baumgen, Dutschei, & Bornscheuer, 2021). Polysaccharides are biodegradable and biocompatible natural material where alginate, collagen, chitosan polysaccharides are being used in nanoparticle preparations to reduce the toxicity and improve the therapeutic properties of the drugs molecules (Y. E. Lee et al., 2017; Y. Sun, Ma, & Hu, 2021).

5.2.1.1 Carrageenan

Carrageenan is an anionic sulphated polysaccharide which is hydrophilic colloid (water soluble gum) and has gel forming property. It is formed by D- galactose and 3, 6 – anhydro- galactose monomer units linked by α -1-3 and β -1-4 glycosidic linkages. They are classified into different types mainly lambda (λ), Kappa (κ), iota (ι), ϵ , μ based on the position and number of sulphated groups (Fig 21). Kappa carrageenan has one, iota has two and lambda has three sulphated groups respectively. The number of sulphated groups and their location effects the gel strength and solubility of carrageenans. Kappa and iota carrageenans form gels in the presence of calcium and potassium ions but lambda carrageenan does not form gels (Prajapati, Maheriya, Jani, & Solanki, 2014).

Among all kappa, iota and lambda carrageenans are widely used in the food and the pharmaceutical industries. Kappa (κ) - carrageenase gel beads and κ - carrageenase immobilized *Acetobacter suboxydans* were successfully used in acetic acid production and vinegar production respectively. Lambda (λ) carrageenan was reported to have highest free-radical scavenging

activity and anti-oxidant activity among all the carrageenans (Pangestuti & Kim, 2014). Kappa or lambda carrageenan isolated from *G. radula* showed a cholesterol lowering effect. Carrageenans have also shown anti-coagulant properties (Rahmati, Alipanahi, & Mozafari, 2019).

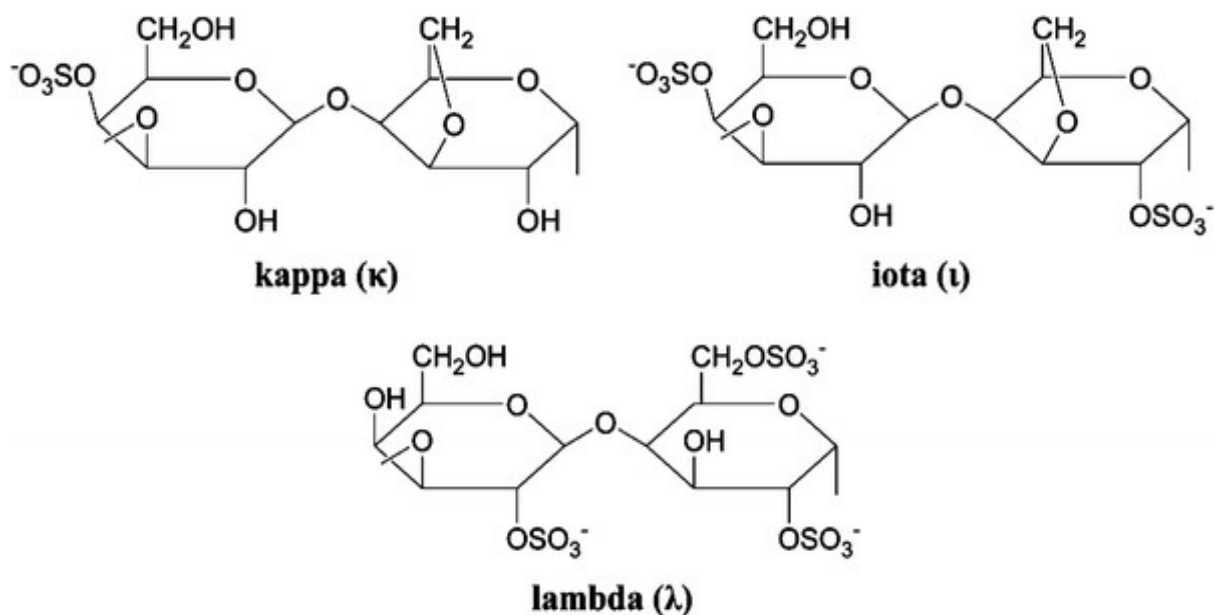


Figure 21: Structure of kappa, iota and lambda carrageenans (Chauhan & Saxena, 2016).

Carrageenans have a wide range of applications in biomedical, cosmetic, textile industries waste water remediation and biodiesel production. The gel forming and binding property of carrageenans is used in food industry. Alginate is used in the textile industry in preparing textile dyes. Kappa carrageenan and polyethylene based solvent films are formulated as drug delivery vehicles. Kappa carrageenan is contributed by the south East Asian countries and among them Philippines contributes the most, around 55% (L. Li, Ni, Shao, & Mao, 2014).

5.3 Marine algae use in nutraceuticals

Marine algae are known to contain many nutrients which include carbohydrates, proteins, lipids, antioxidants, vitamins and minerals. The health benefits of algae are discovered way back in 1500 BC. Algal nutrients have many health benefits and are used as a natural source of nutritional supplement. Due to a wide range of nutritive value algae are gaining tremendous importance as a beneficial and profitable nutritional source in animal and human diet (Liang, Wang, Wang, Zhu, & Jiang, 2019). Algae mainly microalgae are being used in the nutraceutical and food

industries. *Chlorella*, *Nostoc*, *Anabaena* and *Chlamydomonas* are few microalgae that are commonly used as nutrient source (Nicoletti, 2016).

Edible microalgae are rich source of minerals. They are rich in major minerals such as sodium, sulphur, magnesium, nitrogen and calcium, minor minerals and trace elements like copper iodine, manganese, zinc, cobalt, selenium and molybdenum (Panahi, Darvishi, Jowzi, Beiraghdar, & Sahebkar, 2016).

Algal lipids including omega fatty acids and polyunsaturated fatty acids have gained commercial importance as nutraceuticals. Algal lipids are source of essential fatty acids such as omega 3 fatty acids such as eicosapentaenoic acid, docosahexaenoic acid and omega 6 fatty acids that include arachidonic acid (R. Liu, Li, Tu, Hao, & Qiu, 2022). Algal Fatty acids are of high commercial value in the market. They have also shown beneficial effects against cardiovascular diseases and inflammation. Omega 3 and 6 fatty acids are known to reduce atherosclerosis, protect from cardiovascular diseases. Algae also provide a good source of protein and essential aminoacids that mammals cannot produce. They are known to be a well-balanced protein source similar to soy or egg albumin. Microalgae species *Chlorella vulgaris* is reported to have high protein content of 58% (Fernandes & Cordeiro, 2021).

Microalgal carotenoid pigments such as astaxanthin and β - carotene have gained commercial importance as nutraceutical for the use of humans (Pereira et al., 2021).

Algae are being used as nutraceuticals for improving nutrient deficiencies being faced around the world. Also consumption of algae improves the functioning of major systems in the body (Lordan, Ross, & Stanton, 2011).

5.4 Pharmacological use of marine algae in cosmetic industry

Marine algae have gained importance in the cosmetic industry as it is natural biodegradable and less toxic compared to the synthetic material and chemicals. Many algal pigments and metabolites are used in cosmetics such as moisturizing agents, sunscreens, lotions, skin sensitizers and antioxidants. The algal bioactive molecules like polysaccharides, polyphenols, lipids, pigments have cosmetic applications (J. H. Kim, Lee, Kim, & Kang, 2018).

Microalgal extracts have shown skin protection by inhibiting the upregulation of ultraviolet radiation (UVR) induced genes. Micro algae like *Arthrospira*, *Chlorella* increased collagen synthesis and improved vascular imperfections of epidermis that could possibly reduce the wrinkle formation (Ahmed, Adel, Karimi, & Peidayesh, 2014).

Algal polysaccharides are reported to prevent skin dehydration by forming a protective membrane. Sulphated algal polysaccharide like fucoidan protected elastic fibers of skin from enzymatic proteolysis and enhanced the skin healing. Another sulphated polysaccharide Porphyridium is used as biolubricant which showed antioxidant property. Alginate and laminarin polysaccharide also have been reported for the use of reducing skin aging (Ruocco, Costantini, Guariniello, & Costantini, 2016).

Macroalgae contains MAA pigments which are UV absorbing pigments. MAA pigments are potentially used in the cosmetics as they improve the human skin fibroblast regeneration and have anti-photoaging property. MAAs have been reported for their protection on UV damage in both in vitro and in vivo studies (Thomas & Kim, 2013).

Algal phenolic and pigment molecules also have antioxidant properties that are used in cosmetics. Astaxanthin, Fucoxanthin and β -carotene pigments have shown skin protection from UV damage. Studies have shown that astaxanthin pigment showed more protection on UV induced photooxidation compared to β -carotene. Fucoxanthin pigment is shown to enhance the antioxidant defence system in human keratinocytes. Liposomal formulation of astaxanthin pigment showed protective effect on the UV induced skin damage. Phenolic molecule phlorotannin from brown algae are known to be used for skin diseases (H. D. Wang, Chen, Huynh, & Chang, 2015).

5.5 Use of marine algae in food and agricultural industry

Marine algae are extensively used in the food industry. Algae is a low caloric food, packed with vitamins, minerals, polysaccharides, lipids and proteins. In the form of extracts or powder they are reported to enhance the texture and nutritional value of the food products. Algal polysaccharides are the mostly used components in the food industry (Scieszka & Klewicka, 2019). Compared to green (5%), red (33%) and algae brown algae (66%) are consumed more. High fibre content of microalga adds to the health benefits of humans. These dietary fibres promotes the growth of useful gut bacteria and has the capacity to absorb cholesterol and glucose that can protect from the risk of hypercholesterolemia, obesity and diabetes (Gibbs, Kermasha, Alli, & Mulligan, 1999).

Bioactive properties of omega 3 and 6 fatty acids used in infant food formulations showed an improved cognitive function of the infants. In ice-creams, algal oil was used to enhance their omega 3 fatty acid content. Ethanol extract form *Fucus vesiculosus* algae was used to improve the shelf life of yogurt and milk. Algal antioxidants are reported to substitute synthetic

antioxidants to avoid the side effects for better human health. Algal powders are being used in the preparation of bread, cheese and pasta that improved their texture and nutritional value (H. Yang et al., 2020).

Marine polysaccharides are used in food products as binders, texture modifiers and thickening agents. They are used in the meat products, dairy products and also as stabilizers and gelling agents. Agar is mostly used as thickening agent in food products as a gelatin substitute. Alginate is used as an emulsifier and thickening agent (Gateau, Solymosi, Marchand, & Schoefs, 2017).

Algae is also used in the agricultural industry since the historical time. For many centuries the coastal people have used algae as a natural manure for their plants. It has been reported that algae were used as fertilizers by Greeks and as a natural manure for plants by Romans (C. Song et al., 2021).

Laminarine algal polysaccharide has reported to improve defence mechanisms in plants. Algal have improved the plant growth and yield of apple, grape and watermelon vegetation (Stewart et al., 2021).

5.6 Use of marine algae in biomedical field

Besides being widely used in the food, nutraceuticals and cosmetic industries algal biomaterials are gaining importance in the biomedical and pharmacological field (Y. E. Lee et al., 2017).

Biomedical applications of algae in biosensing and bioimaging have been reported. Bioprobes like antibodies, fluorophores attached to the surface of microalgae are used as optical sensors. Thiophenebenzothiadiazole-thiophene based flurophore staining the microalgae *Thalassiosira weissflogii* provided photoluminescence and is applied in bioimaging. Modified frustule (cell wall) of *Coscinodiscus wailesii* microalgae was reported to monitor the interaction of antibody ligand by fluorescence measurements (Rahmati et al., 2019).

As microalgal source provides oxygen via photosynthesis, algal material has been chosen as a source of oxygen for preparing scaffolds in tissue engineering. *Chlamydomonas reinhardtii* a photosynthetic microalgae has been used in scaffolds for tissue repair. In vitro and in vivo studies have shown microalgal scaffold transplantation in the mouse skin had survived for 5 day. *C. reinhardtii* was genetically engineering to produce human VEGF for wound healing *in vivo* studies (Mena et al., 2021). Algal polysaccharides are used as polymer binding material in bone tissue engineering to improve the bone tissue growth and proliferation. Biomimetic scaffolds

made of gelatin and conjugated fucoidan polysaccharide has been used for bone tissue regeneration (Manlusoc et al., 2019).

Algal material have potential therapeutic use as drug delivery vectors for the incorporation of various bioactive molecules (L. Li et al., 2014). Sulphated polysaccharides such as carrageenan, chitosan, and dextran with many hydroxyl groups that can be functionalized are being used in the polymeric micelle preparations (Pangestuti & Kim, 2011).

Purpose of the work: Aim and objectives

Hyperglycemia associated with chronic inflammation, oxidative stress, ER stress are involved in the diabetic pathology, affects the structure and function of numerous macromolecules. Indeed, the formation of various highly reactive compounds by glycation or oxidation mechanisms favors the oxidative stress and contributes to the damage of vascularized tissues and organs. Therefore, through these stress responses, diabetes exacerbates the development of vascular complications associated with stroke, particularly by endothelial dysfunction. Also the hyperglycemia mediated oxidative stress and impaired inflammatory responses are also involved in delayed wound healing in diabetic condition that can lead to chronic lesions and amputations.

Therefore, the objective of this thesis work was to study the impact of curcumin vectorization on cellular stress mediated endothelial dysfunction and regenerative wound healing, to improve curcumin bioavailability and therapeutic properties. Hypothesis of the work is that curcumin's antioxidant, anti-inflammatory and anti-apoptotic properties are improved by vectorization and can be helpful in developing a potential therapeutic strategy for diabetic stroke and diabetic lesions.

To meet this objective, I first focused my research on the impact of curcumin encapsulated in HDL drug delivery vector on the endothelial protection in *in vitro* b.END3 cerebrovascular endothelial cell model.

In the second part of my work, I evaluated the impact of curcumin encapsulated in carrageenan nanomicelles drug delivery vector on the regenerative wound healing in *in vivo* zebrafish tail injury model.

Experimental results

Part 1: Impact of curcumin loaded rHDL nanoparticles on methylglyoxal mediated cytotoxicity and stress in cerebral endothelial cells

I. Introduction

Diabetes is associated with many complications including vascular complications. Methylglyoxal (MGO) is a highly reactive metabolite of glycolytic pathway detected in increased levels in diabetes condition mainly in type 2 diabetic patients (Beisswenger, 2014; Schumacher et al., 2018). It is the main precursor of AGE (advanced glycation end product) formation and induce cellular oxidative stress, inflammation, impaired hyperpermeability of endothelial barrier and ER stress that play a key role in endothelial dysfunction which may lead to vascular complications (Bourajjaj, Stehouwer, van Hinsbergh, & Schalkwijk, 2003; Schalkwijk & Stehouwer, 2020).

Many antioxidant molecules including resveratrol, proanthocyanidins, isorhamnetin and curcumin have been reported to limit MGO induced cellular stress in endothelial cells (HUVECs, HAoEC) (J. H. Lee et al., 2020). But therapeutic benefits of these antioxidant molecules are compromised due their rapid metabolism and clearance in the physiological system. Therefore various nanoparticles have been developed in recently to improve the bioavailability and therapeutic properties of the drug molecules (Nasr & Abdel Rahman, 2019).

HDL is a lipoprotein that has anti-oxidative and anti-inflammatory properties (Rader & Hovingh, 2014). Use of HDL particles as a drug delivery system is newly emerging as it is biocompatible, biodegradable and non-cytotoxic (Q. Song et al., 2016). Curcumin is a well-known and widely used polyphenol molecule in therapeutics (Menon & Sudheer, 2007). Many nanoformulations of curcumin have been developed to enhance its therapeutic properties and bioavailability (Khezri, Saeedi, Mohammadamini, & Zakaryaei, 2021).

Hypothesis of the study was first to test whether nanoencapsulated curcumin HDL nanoparticle preparation can enhance the cellular uptake and therapeutic potential of curcumin. Next, to investigate if nanoencapsulated curcumin HDL nanoparticles showed a more protective synergistic effect in combination compared to HDL or curcumin alone. In this study we used curcumin HDL nanoparticles to test their cellular uptake by cerebral endothelial cells (b.End.3) and potential cytoprotective effect on MGO induced cytotoxicity and cellular stress in cerebral

endothelial cells. We investigated MGO induced cellular stress including oxidative stress, ER stress, impaired endothelial membrane integrity, chromatin condensation.

II. Methods

Preparation of nanoencapsulated curcumin rHDL (Cur-rHDLs) nanoparticles

Reconstituted HDLs (rHDLs) – CSL111 was used in the preparation of Cur-rHDL nanoparticles, which is a nascent discoidal HDL molecule with Apo A1 and phospholipids shell surface with a hydrophobic core that can be loaded with hydrophobic drug molecules.

To prepare Cur-rHDL nanoparticles firstly 3 ml of 2 mg/ml of rHDLs was gently mixed with 5 μ M of curcumin and incubated in dark for 16 hours at 37°C (agitation at 50 rpm). Secondly the rHDL-curcumin sample mixture was prepared for ultracentrifugation by briefly adjusting the density of rHDL-curcumin sample mixture to $d = 1.22$ with KBr (potassium bromide) salt and overlaid with KBr saline solution ($d = 1.21$). Ultracentrifugation was performed at $100,000\times g$ for 24 h at 10 °C. Finally the top yellow colored fraction corresponding to Cur-rHDLs was recovered and centrifuged with 1 X PBS 5 times, 20 minutes each at $12,000\times g$ using a centricon with 10 kDa cutoff to remove the excess of KBr salt (desalting) and the sample was concentrated (Fig 22). Protein concentration of Cur-rHDLs was determined using Bicinchoninic Acid protein (BCA) assay.

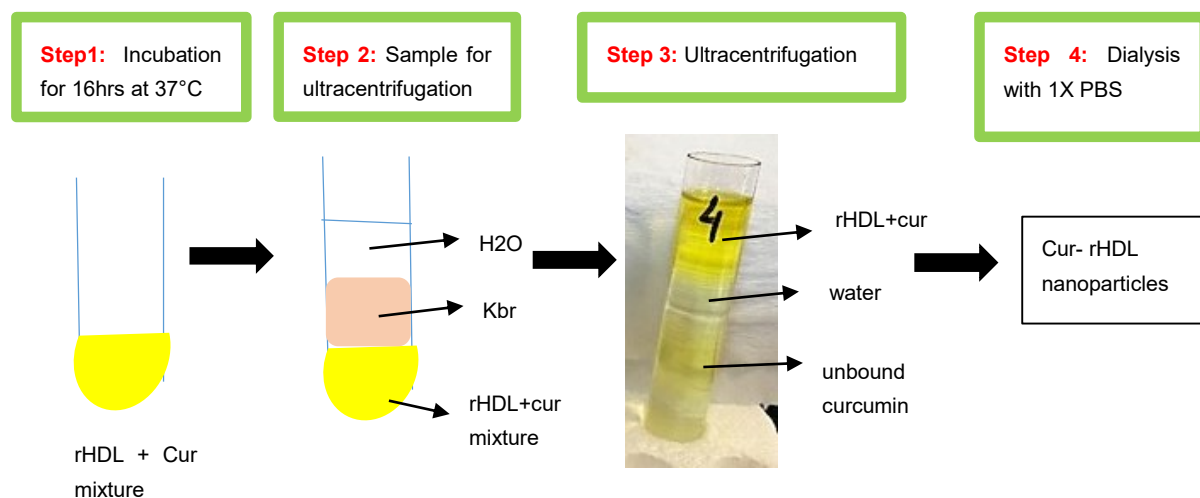


Figure 22: Curcumin loaded rHDL (Cur-rHDLs) preparation method.

Quantification of curcumin in Cur-rHDLs nanoparticles

Curcumin in Cur-rHDLs nanoparticles was quantified using spectrophotometric analysis and ultra-high-performance liquid chromatography coupled with an HESI-Orbitrap mass spectrometer (UHPLC) analysis.

Cellular model: murine cerebral endothelial cell line – bEnd.3

The bEnd.3 endothelial cell line was used as a cell model for this study. MGO induced cytotoxicity, oxidative stress, chromatin condensation and integrity were evaluated.

III. Results

Results of this study are assembled into an article titled “Apo-A1 nanoparticles as curcumin carriers for cerebral endothelial cells: improved cytoprotective effects against methylglyoxal”.
Pharmaceutics MDPI (Published on March 13 2022.)

Article

ApoA-I Nanoparticles as Curcumin Carriers for Cerebral Endothelial Cells: Improved Cytoprotective Effects against Methylglyoxal

Sai Sandhya Narra ¹, Sarah Rosanaly ¹, Philippe Rondeau ¹, Jessica Patche ¹, Bryan Veeren ¹, Marie-Paule Gonthier ¹, Wildriss Viranaicken ², Nicolas Diotel ¹, Palaniyandi Ramanan ³, Christian Lefebvre d' Hellencourt ¹ and Olivier Meilhac ^{1,4,*}

- ¹ INSERM UMR 1188, Diabète athérombose Réunion Océan Indien (DéTROI), Université de La Réunion, 97490 Saint-Denis, La Réunion, France; narra.sai-sandhya@univ-reunion.fr (S.S.N.); sarah.rosanaly@univ-reunion.fr (S.R.); philippe.rondeau@univ-reunion.fr (P.R.); jessica.patche@univ-reunion.fr (J.P.); bryan.veeren@univ-reunion.fr (B.V.); marie-paule.gonthier@univ-reunion.fr (M.-P.G.); nicolas.diotel@univ-reunion.fr (N.D.); christian.lefebvre-d-hellencourt@univ-reunion.fr (C.L.d.H.)
- ² Unité Mixte Processus Infectieux en Milieu Insulaire Tropical (PIMIT), Université de La Réunion, INSERM UMR 1187, CNRS UMR 9192, IRD UMR 249, Plateforme Technologique CYROI, 94791 Sainte Clotilde, La Réunion, France; wildriss.viranaicken@univ-reunion.fr
- ³ Department of Microbiology, School of Life Sciences, Central University of Tamil Nadu, Thiruvavur 610005, India; ramanan@cutn.ac.in
- ⁴ Centre Hospitalier Universitaire (CHU) de La Réunion, CIC 1410, 97410 Saint-Pierre, La Réunion, France
- * Correspondence: olivier.meilhac@inserm.fr; Tel.: +33-262-693406545



Citation: Narra, S.S.; Rosanaly, S.; Rondeau, P.; Patche, J.; Veeren, B.; Gonthier, M.-P.; Viranaicken, W.; Diotel, N.; Ramanan, P.; Hellencourt, C.L.d.; et al. ApoA-I Nanoparticles as Curcumin Carriers for Cerebral Endothelial Cells: Improved Cytoprotective Effects against Methylglyoxal. *Pharmaceuticals* **2022**, *15*, 347. <https://doi.org/10.3390/ph15030347>

Academic Editor: Alfredo Berzal-Herranz

Received: 10 February 2022

Accepted: 9 March 2022

Published: 13 March 2022

Publisher's Note: MDPI stays neutral with regard to jurisdictional claims in published maps and institutional affiliations.



Copyright: © 2022 by the authors. Licensee MDPI, Basel, Switzerland. This article is an open access article distributed under the terms and conditions of the Creative Commons Attribution (CC BY) license (<https://creativecommons.org/licenses/by/4.0/>).

Abstract: Methylglyoxal (MGO) is a highly reactive metabolite of glucose present at elevated levels in diabetic patients. Its cytotoxicity is associated with endothelial dysfunction, which plays a role in cardiovascular and cerebrovascular complications. Although curcumin has many therapeutic benefits, these are limited due to its low bioavailability. We aimed to improve the bioavailability of curcumin and evaluate a potential synergistic effect of curcumin and reconstituted high-density lipoprotein (rHDL) nanoparticles (Cur-rHDLs) on MGO-induced cytotoxicity and oxidative stress in murine cerebrovascular endothelial cells (bEnd.3). Cur-rHDL nanoparticles (14.02 ± 0.95 nm) prepared by ultracentrifugation and containing curcumin were quantified by LC–MS/MS. The synergistic effect of cur-rHDL nanoparticles was tested on bEnd.3 cytotoxicity, reactive oxygen species (ROS) production, chromatin condensation, endoplasmic reticulum (ER) stress, and endothelial barrier integrity by impedancemetry. The uptake of curcumin, alone or associated with HDLs, was also assessed by mass spectrometry. Pretreatment with Cur-rHDLs followed by incubation with MGO showed a protective effect on MGO-induced cytotoxicity and chromatin condensation, as well as a strong protective effect on ROS production, endothelial cell barrier integrity, and ER stress. These results suggest that Cur-rHDLs could be used as a potential therapeutic agent to limit MGO-induced dysfunction in cerebrovascular endothelial cells by enhancing the bioavailability and protective effects of curcumin.

Keywords: nanoparticle; curcumin; HDL; methylglyoxal; cerebral endothelial cells; endothelial dysfunction

1. Introduction

Type 2 diabetes (T2D) is a global health issue that increases the risk of cardiovascular and cerebrovascular diseases, including ischemic stroke and its hemorrhagic complications. Prolonged hyperglycemia leads to various biochemical modifications, such as oxidative stress, apoptosis, and glycation, particularly mediated by methylglyoxal (MGO), a physiological reactive carbonyl compound derived from glucose metabolism. High concentrations of MGO and MGO-derived products are found in the plasma of diabetic patients and are

associated with diabetic complications [1–3]. Increased plasma MGO levels have been shown to be associated with cardiovascular disease and mortality in T2D patients [4]. MGO induces massive intracellular oxidative stress, particularly in endothelial cells (ECs) at the interface between blood and different tissues. This reactive compound is a precursor of advanced glycation products (AGEs) but has a greater potential than AGEs or glucose itself to induce vascular damage [5]. MGO has been shown to be cytotoxic to different types of ECs, including human umbilical vein ECs (HUVECs) and cerebral ECs [6,7]. It was shown to induce endoplasmic reticulum stress (ER stress) that may lead to apoptosis [5]. To prevent MGO- or high-glucose-induced oxidative stress and resulting cytotoxicity, various antioxidants have been used, such as proanthocyanidins [8], isorhamnetin [7], resveratrol [9], and pterostilbene, a natural derivative of resveratrol [10]. Curcumin, a potent but hydrophobic antioxidant, anti-inflammatory, and anti-apoptotic compound, has been used to limit MGO-induced cytotoxicity in different cell types such as mouse embryonic stem cells [11] and human hepatoma cells [12] but not in ECs. In the present study, we sought to test the protective effect of curcumin on MGO-induced intracellular oxidative stress and cytotoxicity in cerebral ECs. We also tested the capacity of curcumin to limit the increase in endothelial permeability induced by MGO by monitoring real-time cell impedance. Despite its numerous neuroprotective effects, curcumin has limited bioavailability and poor solubility. Our second objective was to improve curcumin bioavailability by loading it into Apolipoprotein A-I phospholipid nanoparticles (also called reconstituted high-density lipoproteins-rHDLs) and test the potential synergistic effect of curcumin and HDLs versus HDLs or curcumin alone. HDL particles themselves have pleiotropic properties similar to those of curcumin (antioxidant, anti-inflammatory, and anti-apoptotic effects). In particular, HDL treatment limits infarct volume and mortality in different models of ischemic stroke via endothelial protective effects [13,14]. In the present study, we tested a potential synergistic effect of rHDLs and curcumin on MGO-induced oxidative stress, endothelial permeability, and cytotoxicity in cerebral endothelial cells.

2. Results

2.1. Particle Size Distribution of rHDL and Cur-rHDLs by DLS Analysis

Dynamic light scattering was used to determine the particle size distribution of rHDLs and Cur-rHDLs. The particle average size was determined to be 12.55 ± 0.21 nm for rHDLs and 14.02 ± 0.95 nm for Cur-rHDLs, as shown in Figure 1a,b respectively. A polydispersity index (PDI) near to zero implies homogeneity of dispersions, and a PDI greater than 0.3 indicates heterogeneity [15]. The PDI of our Cur-rHDL nanoparticles was around 0.25. The incorporation of curcumin did not significantly affect the size of the rHDL particles ($p > 0.05$, comparing Cur-rHDL to rHDL particle size).

2.2. Effect of HDL and Curcumin on Cerebrovascular Endothelial Cell Cytotoxicity Induced by MGO

MGO is known to be cytotoxic to endothelial cells, but MGO cytotoxicity has never been evaluated in bEnd.3 cells [4,7]. Cell viability was determined by the MTT assay after incubation with different concentrations of MGO for 24 h. MGO showed concentration-dependent cytotoxicity with decreased cell viability of approximately 20% and 70% at 1 mM and 2 mM, respectively (Figure 2a). These results are in agreement with previously published results of MGO cytotoxicity [16]. Next, we investigated the effect of rHDLs (H) and curcumin (C) on MGO cytotoxicity in cerebral endothelial cells by pretreating the cells with different concentrations of rHDLs and curcumin for 1 h and then adding 2 mM MGO for 24 h. Reconstituted HDLs were not cytotoxic but showed a cytoprotective effect on MGO-induced cell death in a concentration-dependent manner. While low rHDL concentrations of 5–50 $\mu\text{g}/\text{mL}$ were not cytoprotective, higher concentrations ranging from 100 to 200 $\mu\text{g}/\text{mL}$ were significantly cytoprotective (Figure 2b). On the other hand, curcumin started to be protective at 0.2 and 0.4 μM but was not effective at 0.1 μM and was

potentially cytotoxic at higher doses (0.8, 1m and 2 μM), with a loss of the cytoprotective effect (Figure 2c).

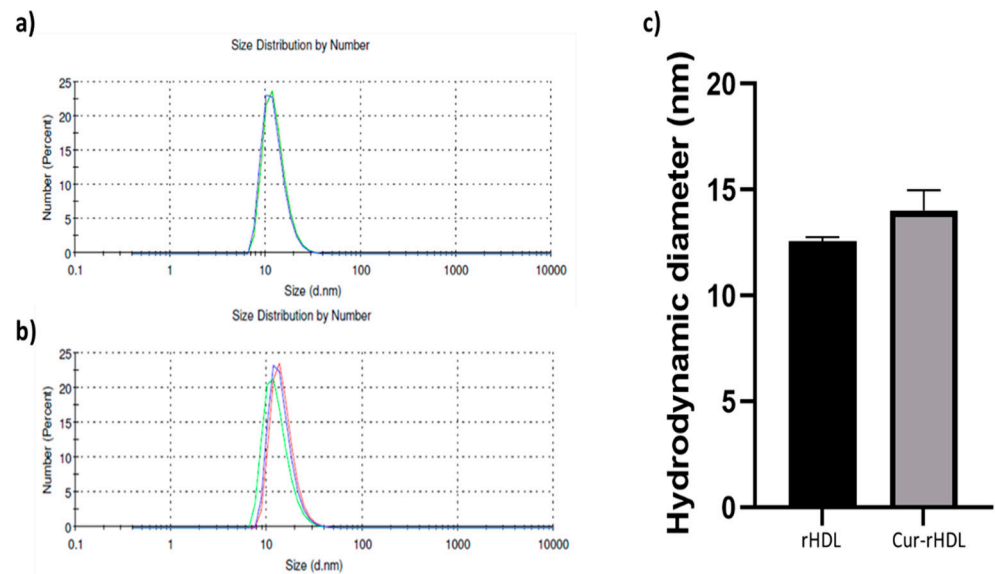


Figure 1. Particle size distribution of rHDLs and Cur-rHDLs determined by DLS analysis. The samples were prepared in PBS at 1 mg/mL. (a) Size distribution of rHDLs and (b) Cur-rHDLs and (c) Histograms representing the hydrodynamic particle diameter of rHDLs and Cur-rHDLs. Data are presented as the mean \pm SD of three independent measurements for each sample.

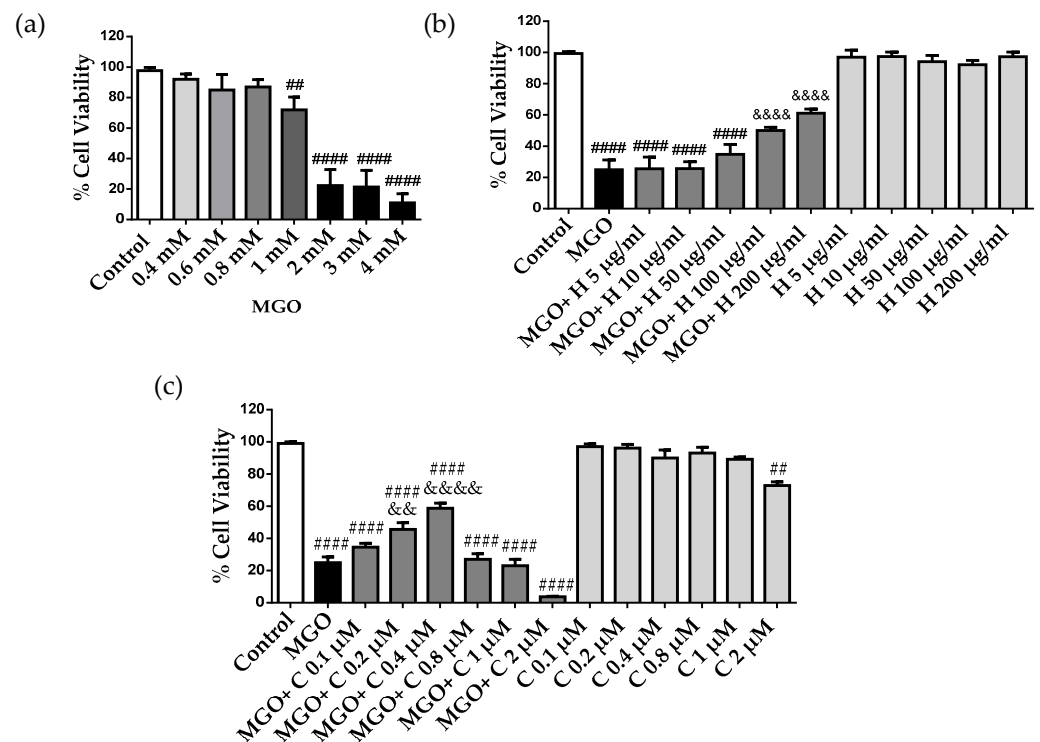


Figure 2. MGO cytotoxicity in bEnd3 cerebral endothelial cells, effect of rHDLs (H) and curcumin (C). (a) The cells were treated with different MGO concentrations (0.4–4 mM) for 24 h. (b) The cells were pre-treated with different concentrations of rHDLs, 5–200 $\mu\text{g}/\text{mL}$, (H) and (c) curcumin (C), 0.1–2 μM , for 1 h, followed by the addition of 2 mM MGO for 24 h. Cell viability was assessed by the MTT assay. Data are presented as mean \pm SD of three independent experiments ($n = 3$). ## $p < 0.01$, #### $p < 0.0001$ as compared to control. && $p < 0.01$, &&&& $p < 0.0001$ as compared to MGO.

2.3. Effect of Curcumin-Enriched rHDLs on MGO Cytotoxicity in Cerebral Endothelial Cells

Given that rHDLs (H) and curcumin (C) alone showed a cytoprotective effect, we tested the synergistic effect of curcumin and rHDLs (Cur-rHDL) on the cytotoxicity of MGO. For this purpose, the cells were pre-treated with rHDLs (H), curcumin (C), or curcumin-enriched rHDLs (Cur-rHDL) for 1 h before the addition of 2 mM MGO. Cur-rHDLs contained 50 to 80 $\mu\text{g}/\text{mL}$ ApoA-I and 0.03 to 0.048 μM curcumin, concentrations that were not protective when rHDLs and curcumin were used alone to prevent MGO cytotoxicity. At these concentrations, Cur-rHDLs were not cytotoxic. The cytoprotective effect was not observed at a concentration of 50 $\mu\text{g}/\text{mL}$ rHDL enriched with 0.03 μM curcumin either alone or in combination (Figure 3a). In contrast, concentrations of 80 $\mu\text{g}/\text{mL}$ rHDL and 0.048 μM curcumin showed a synergistic cytoprotective effect compared to rHDL and curcumin alone in the presence of MGO (Figure 3b). Similarly, 100 $\mu\text{g}/\text{mL}$ of rHDLs enriched with 0.06 μM curcumin and 200 $\mu\text{g}/\text{mL}$ of rHDLs enriched with 0.12 μM curcumin showed an enhanced cytoprotective effect relative to curcumin and rHDLs alone, which were already cytoprotective at these concentrations (Figure 3c,d respectively).

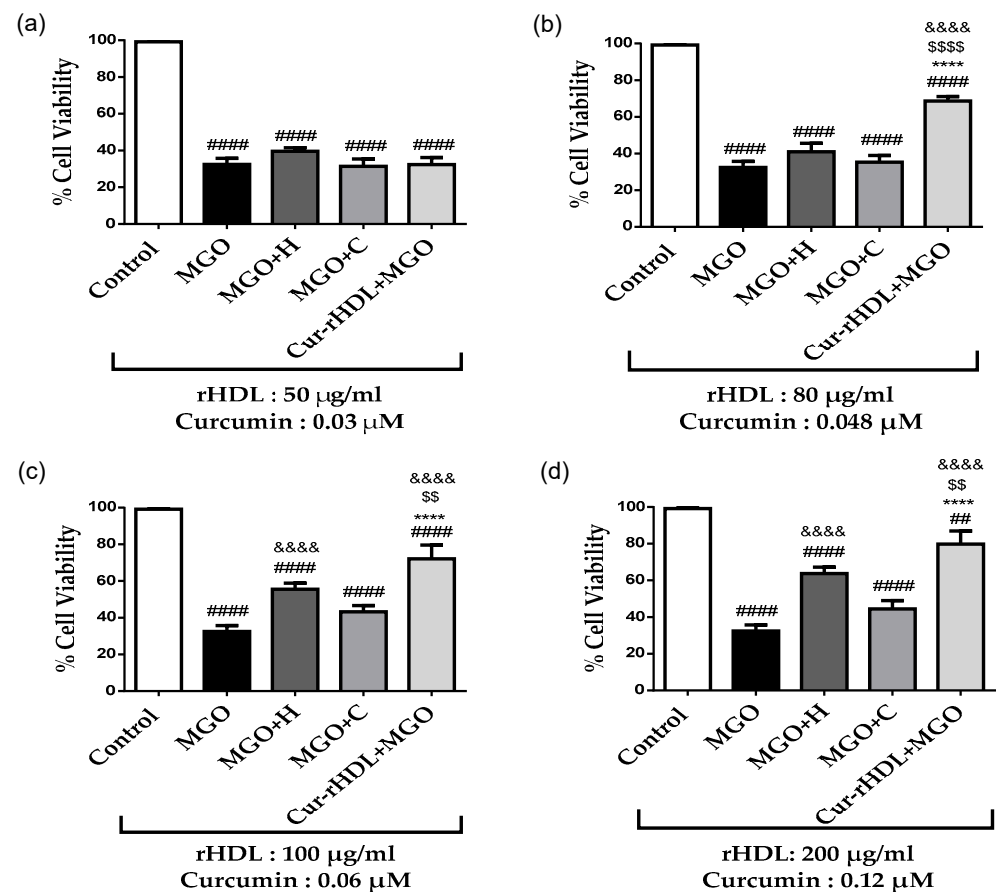


Figure 3. Effect of curcumin-enriched rHDLs on MGO cytotoxicity in cerebral endothelial cells. The cells were pre-treated with different concentrations of rHDLs (H), curcumin (C), and curcumin-enriched rHDLs (Cur-rHDLs) for 1 h before the addition of 2 mM MGO for 24 h. (a) H: 50 $\mu\text{g}/\text{mL}$, C: 0.03 μM and Cur-rHDL: 50 $\mu\text{g}/\text{mL}$ + 0.03 μM . (b) H: 80 $\mu\text{g}/\text{mL}$, C: 0.048 μM and Cur-rHDLs: 80 $\mu\text{g}/\text{mL}$ + 0.048 μM . (c) H: 100 $\mu\text{g}/\text{mL}$, C: 0.06 μM and Cur-rHDLs: 100 $\mu\text{g}/\text{mL}$ + 0.06 μM (d) H: 200 $\mu\text{g}/\text{mL}$, C: 0.12 μM and Cur-rHDLs: 200 $\mu\text{g}/\text{mL}$ + 0.12 μM . Data are presented as mean \pm SD of three independent experiments ($n = 3$). #### $p < 0.0001$, ## $p < 0.01$ as compared to control, \$\$ $p < 0.01$, \$\$\$ $p < 0.0001$ as compared to MGO+H, &&&& $p < 0.0001$ as compared to MGO and **** $p < 0.0001$ as compared to MGO+C.

2.4. Effect of Curcumin-Enriched rHDLs on Cerebral Endothelial Layer Integrity

To investigate the integrity of the endothelial layer, the cells were treated with different concentrations of MGO (0.8, 1, and 2 mM), and the cell real-time electrical impedance was measured using the xCELLigence system. Cerebral endothelial cell integrity was not affected by MGO at 0.8 mM and 1 mM but was altered at 2 mM, resulting in a decreased impedance compared to the control (Figure 4a). This is consistent with the cytotoxic effect of MGO at 2 mM observed by the MTT assay (Figure 2a). We further tested the effect of curcumin-enriched rHDLs on MGO-induced reduction of impedance. These results showed a synergistic protective effect on the integrity of the cerebral endothelial cell monolayer impaired by MGO, whereas individually, rHDLs and curcumin were not protective (Figure 4b). This suggests that curcumin-enriched rHDLs contribute to protecting the integrity of cerebral endothelial cells from the cytotoxic effects of MGO.

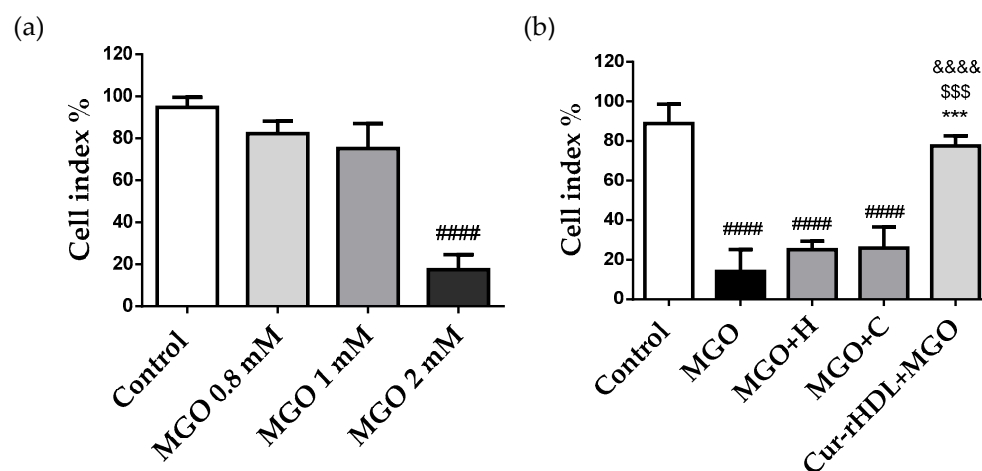


Figure 4. Effect of curcumin-enriched rHDLs on the cerebral endothelial cell monolayer integrity assessed by the measurement of electrical impedance. (a) The cells were treated with different MGO concentrations (0.8–2 mM). (b) The cells were pre-treated with HDL (80 $\mu\text{g}/\text{mL}$), curcumin (0.048 μM), curcumin-enriched rHDLs (Cur-rHDLs-80 $\mu\text{g}/\text{mL}$ + 0.048 μM) for 1 h before the addition of 2 mM MGO. The cell index was measured as electrical impedance generated by cell attachment and proliferation detected by electrodes present at the bottom of the plate. Data are presented as mean \pm SD of three independent experiments ($n = 3$). #### $p < 0.0001$ as compared to control, \$\$\$ $p < 0.001$ as compared to MGO+H, *** $p < 0.001$ as compared to MGO+C and &&&& $p < 0.0001$ as compared to MGO.

2.5. Effect of Curcumin-Enriched rHDLs on Intracellular ROS Production Induced by MGO in Cerebral Endothelial Cells

We then evaluated the effect of curcumin-enriched rHDLs on intracellular reactive oxygen species (ROS) production in the presence of MGO by DCFH-DA fluorimetry. The cells were pretreated with rHDLs, curcumin, and Cur-rHDLs for 1 h before the addition of 2 mM MGO from 1 to 6 h. MGO increased the intracellular ROS production as early as 2 h, which peaked at 3 h and started to decrease slightly at 4–6 h, while remaining above that in the control. Curcumin-enriched rHDLs limited significantly MGO-induced ROS production compared to rHDLs and curcumin alone (except for rHDL at 5 h that showed a significant ROS reduction) (Figure 5).

2.6. Effect of Curcumin-Enriched rHDLs on MGO-Induced Chromatin Condensation in Cerebral Endothelial Cells

We then investigated the effect of curcumin-enriched rHDLs on MGO-induced chromatin condensation in cerebral endothelial cells by DAPI staining. MGO induced chromatin condensation that was significantly reduced by pre-treatment with curcumin-enriched

rHDLs, whereas rHDLs and curcumin alone showed no significant protective effect (Figure 6a,b).

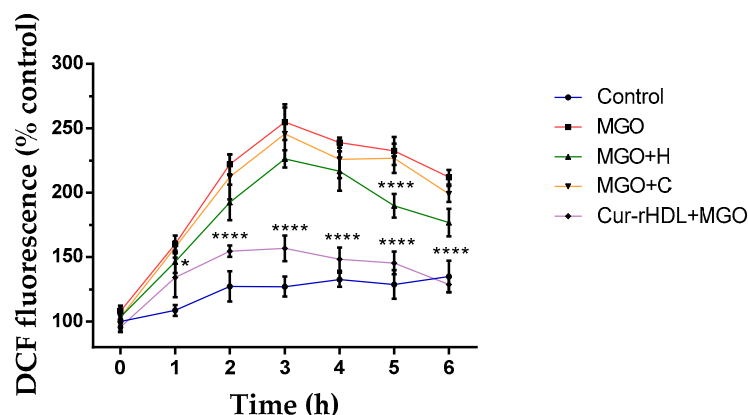


Figure 5. Effect of curcumin-enriched rHDLs on intracellular ROS production induced by MGO in cerebral endothelial cells evaluated by the DCFH-DA assay. The cells were pretreated with rHDLs (H-80 $\mu\text{g}/\text{mL}$), curcumin (C-0.048 μM), and curcumin-enriched rHDLs (H+C-80 $\mu\text{g}/\text{mL}$ + 0.048 μM) for 1 h before the addition of 2 mM MGO for 1–6 h. Intracellular ROS were quantified by the measurement of DCFH-DA fluorescence. Data are represented as mean \pm SD of three independent experiments ($n = 3$). * $p < 0.05$, **** $p < 0.0001$ as compared to MGO.

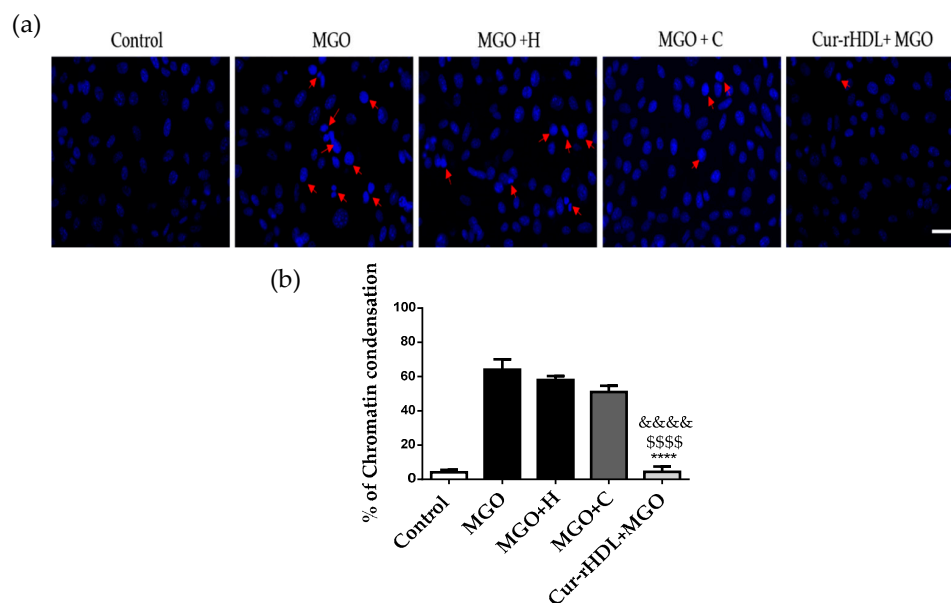


Figure 6. Effect of curcumin-enriched rHDLs on chromatin condensation induced by MGO in cerebral endothelial cells by DAPI staining. (a) DAPI staining images; the cells were treated with rHDLs (H-80 $\mu\text{g}/\text{mL}$), curcumin (C-0.048 μM), and curcumin-enriched rHDLs (Cur-rHDL-80 $\mu\text{g}/\text{mL}$ + 0.048 μM) before the addition of 2 mM MGO for 24 h. Red arrows indicate a typical example of chromatin condensation. (b) The results were obtained by counting the number of cells with condensed chromatin. Scale bar: 60 μm . Data are presented as mean \pm SD of three independent experiments ($n = 3$). &&&& $p < 0.0001$ as compared to MGO+H, **** $p < 0.0001$ as compared to MGO+C and &&&& $p < 0.0001$ as compared to MGO.

2.7. Effect of Curcumin-Enriched rHDLs on MGO-Induced ER Stress in Cerebral Endothelial Cells

The effect of curcumin-enriched rHDLs on MGO-induced ER stress was assessed by immunofluorescence. During ER stress, Xbp-1 and ATF-4 are translocated into the nucleus, whereas GRP-78 levels increase. Nuclear translocation of Xbp-1 and ATF-4, as well as

increased levels of GRP-78, were observed upon MGO exposure, similar to what seen in the presence of thapsigargin, which is a well know ER stress inducer. Pre-treatment with rHDLs or curcumin alone did not have a significant effect on these ER stress markers, whereas curcumin-enriched rHDLs prevented the nuclear translocation of Xbp-1 (Figure 7a) and ATF-4 (Figure 7b) and decreased the levels of GRP-78 (Figure 7c). This suggests that curcumin-enriched rHDLs have a protective effect on MGO-induced ER stress.

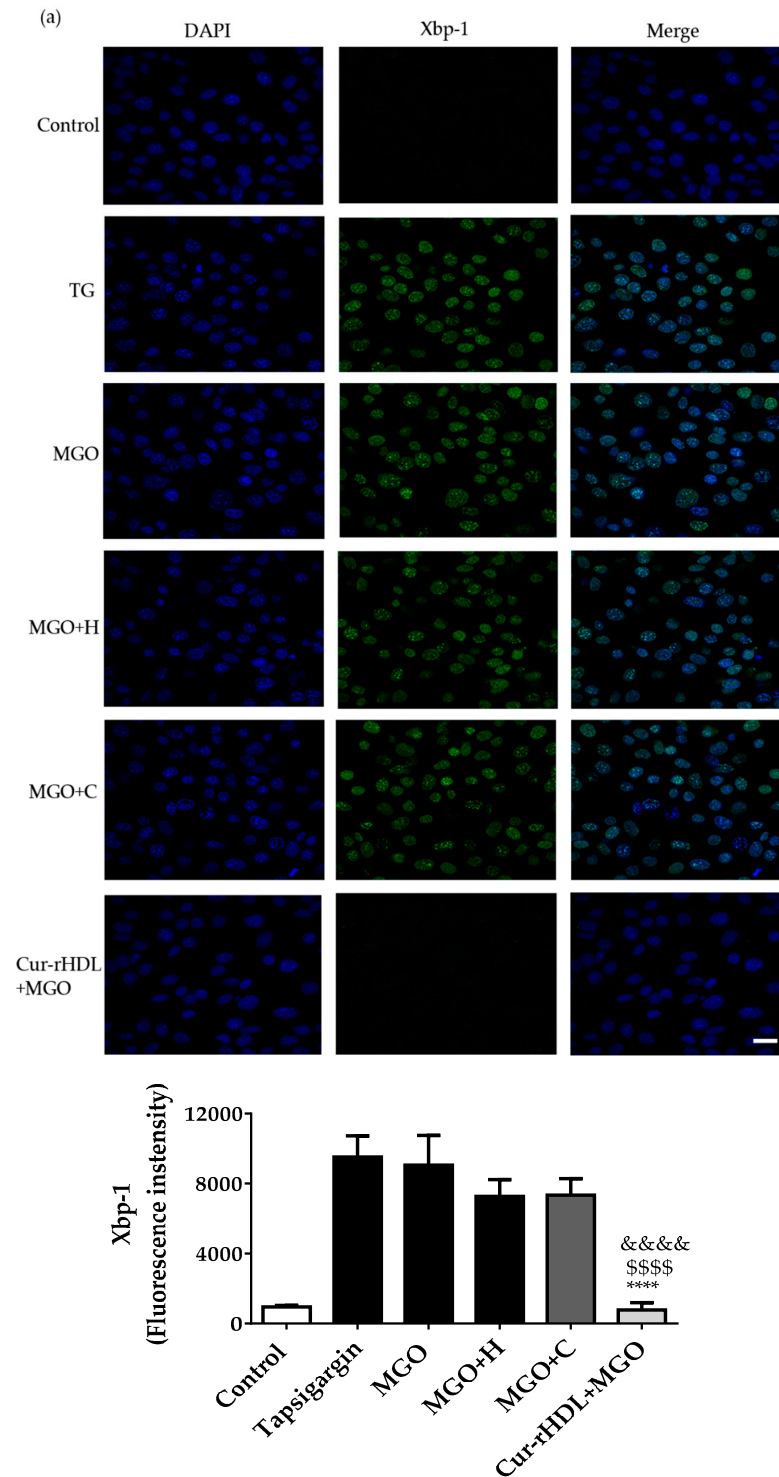


Figure 7. Cont.

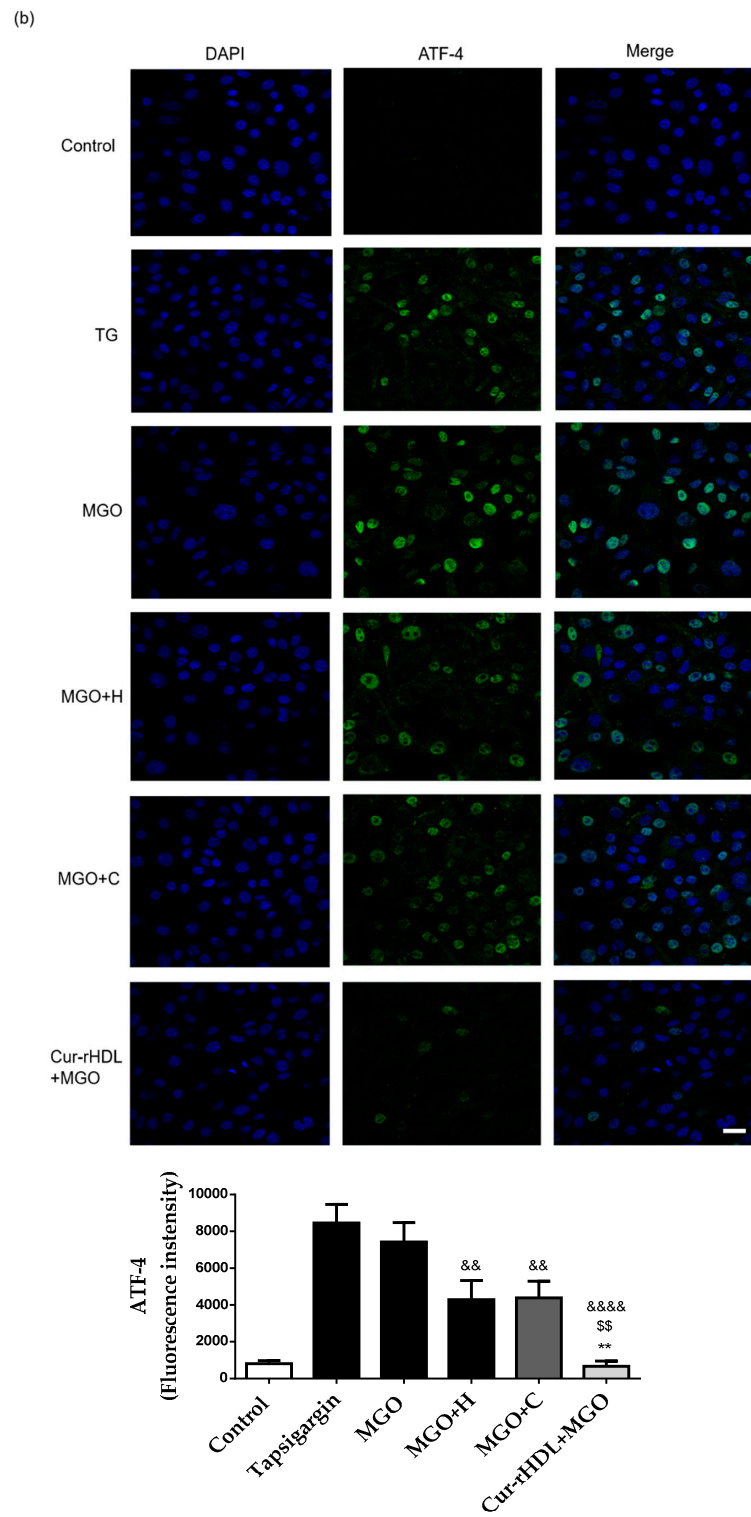


Figure 7. Cont.

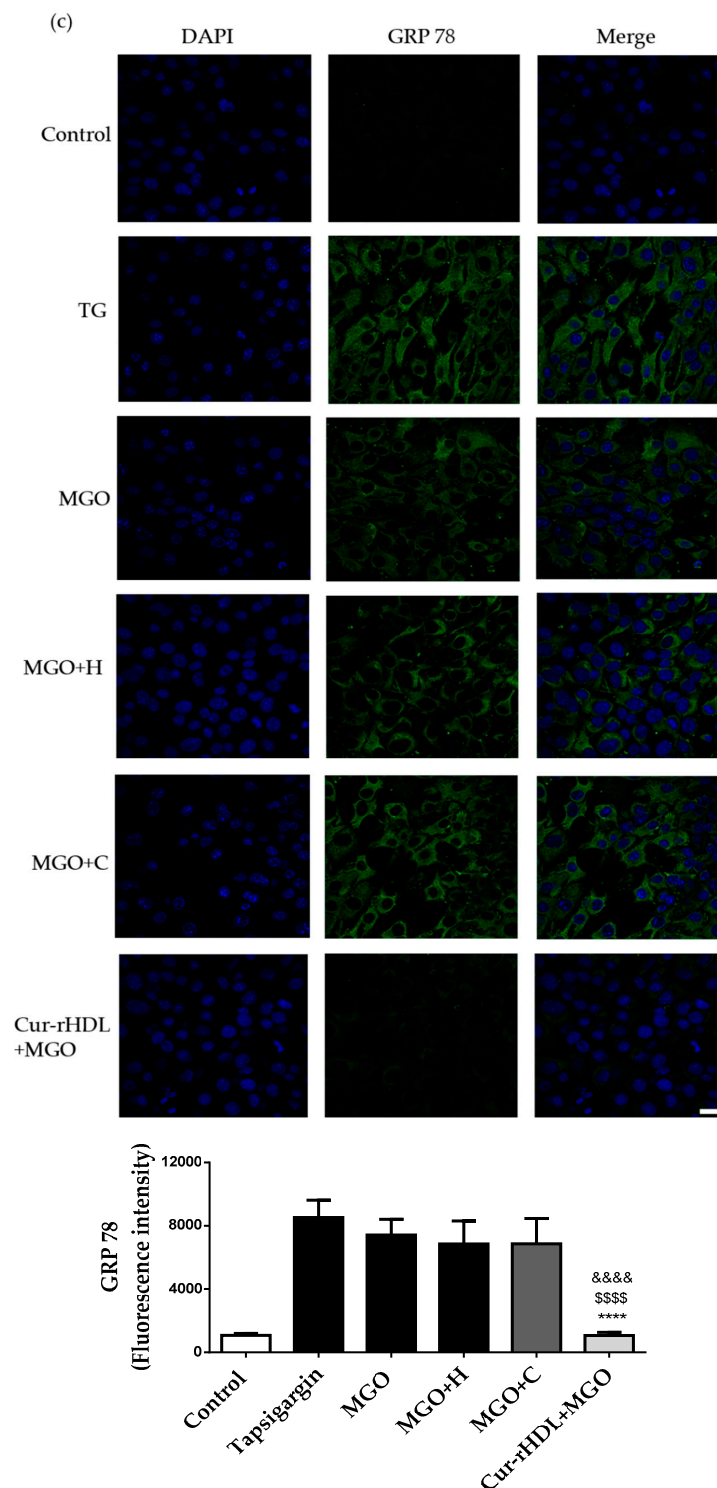


Figure 7. Effect of curcumin-enriched rHDLs on ER stress induced by MGO in cerebral endothelial cells assessed by immunohistochemistry analysis. (a) Confocal microscopy images of the nuclear translocation of Xbp-1, (b) ATF-4, and (c) GRP 78 markers. The cells were treated with 1 $\mu\text{g}/\text{mL}$ of thapsigargin, used as positive control for ER stress (TG), 2 mM methylglyoxal (MGO), pretreated with rHDLs (H, 80 $\mu\text{g}/\text{mL}$), curcumin (C, 0.048 μM), or curcumin-enriched rHDLs (Cur-rHDL, 80 $\mu\text{g}/\text{mL}$ + 0.048 μM) before the addition of 2 mM MGO for 6 h. Scale bar: 24 μm . Data are presented as mean \pm SD of three independent experiments ($n = 3$). \$\$ $p < 0.01$, \$\$\$\$ $p < 0.0001$ as compared to MGO+H, ** $p < 0.01$, **** $p < 0.0001$ as compared to MGO+C and && $p < 0.01$, &&&& $p < 0.0001$ as compared to MGO.

2.8. Quantification of Cellular Curcumin after Incubation of bEnd 3 Cells with Curcumin-Enriched rHDLs or Curcumin Alone

We evaluated the cellular uptake of free curcumin compared to that of Cur-rHDLs by bEnd 3 cells to understand the impact of encapsulation on curcumin uptake. The uptake of curcumin was assessed by mass spectrometry. bEnd.3 cells were incubated with free curcumin or curcumin-enriched rHDLs for 3 and 6 h. The intracellular uptake of free curcumin was faster and higher than that of curcumin-enriched rHDLs at both 3 and 6 h. The uptake of free curcumin was similar at 3 and 6 h, whereas curcumin-enriched rHDL uptake was greater at 3 h and decreased at 6 h, suggesting saturation of the HDL uptake process (Figure 8).

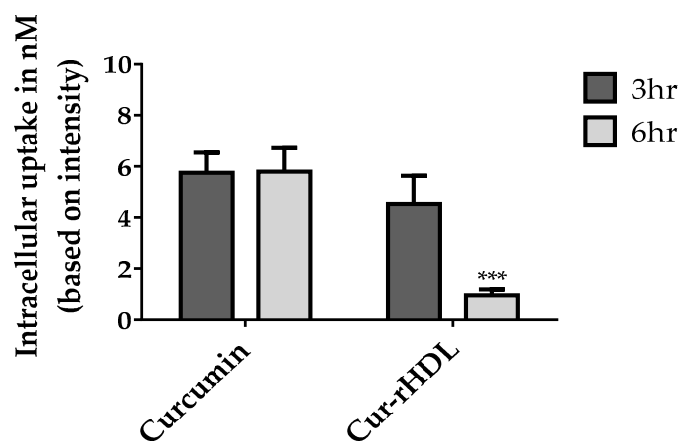


Figure 8. LC–MS/MS analysis of curcumin uptake in cerebral endothelial cells after incubation (3–6 h) with curcumin-enriched rHDLs or curcumin alone. The samples were prepared and analyzed by LC–MS/MS as described in the materials and methods. Data are presented as \pm SD of three independent experiments ($n = 3$). *** $p < 0.001$ as compared to curcumin.

3. Discussion

Most diseases involve an imbalance between free radical and antioxidant responses leading to oxidative stress. This is notably the case in diabetes and its cardiovascular and cerebrovascular complications. Methylglyoxal (MGO) is a highly reactive metabolite of glucose metabolism whose levels are increased in type II diabetic patients. It has been shown to accumulate in the brain of mice deficient for glyoxalase 1/vitamin B6 (MGO detoxification system), suggesting that this imbalance is particularly critical for MGO accumulation in the brain [17]. Studies have shown that the dysfunction of the glyoxalase system is related to several diabetic complications, including macrovascular diseases in humans [18]. As vascular dysfunction plays an important role in diabetes-associated vascular complications, several studies have been conducted to understand the effect of MGO on endothelial dysfunction [19,20]. Many antioxidants are used to reduce MGO cytotoxicity, such as resveratrol, curcumin, and luteolin, but their use is limited by their poor solubility and bioavailability. Improving the bioavailability of antioxidant molecules to reach the cells or tissues of interest and their therapeutic benefits in the body remains a topic of intense research.

The present study aimed to test the ability of curcumin and rHDLs to limit MGO-induced oxidative stress, cytotoxicity, and endoplasmic reticulum (ER) stress in murine cerebral endothelial cells (bEnd 3). In a second step, the potential synergistic effect of curcumin- and rHDLs, which could improve curcumin bioavailability, was also evaluated on the same processes. For this purpose, rHDLs were enriched with curcumin and then re-isolated by ultracentrifugation to remove unincorporated free curcumin. The average particle size of Cur-rHDLs was determined to be 14.02 ± 0.95 nm. MGO was cytotoxic (2 mM) in our cerebral endothelial cell model and, previously, was also shown to be cytotoxic in different cell lines including neuroglial cells, HUVECs, and human brain endothelial cells [7,21,22].

MGO also induced reactive oxygen species (ROS) formation [23,24], blood–brain barrier (BBB) hyperpermeability [25,26], chromatin condensation, and ER stress [27,28], as shown in previous studies.

MGO damage and cytotoxicity in endothelial cells (ECs) is mediated by oxidative stress and reactive oxygen species (ROS) formation [24]. Previous studies have shown that many compounds reduce MGO cytotoxicity in endothelial cells via reducing ROS formation. MGO is known to increase ROS production, associated with the weakening of barrier integrity. MGO was shown to promote oxidative stress in brain endothelial cells [16].

Previous studies have shown that MGO leads to increased permeability of brain endothelial cells. This study reported that the decrease of transendothelial electrical resistance by MGO was associated with alterations in tight junction proteins, such as glycation of occludin and redistribution of zonula occludens-1 (ZO-1). MGO treatment also induced the redistribution of claudin-5 and of the adherens junction protein β -catenin in brain endothelial cells [25]. Claudin-5 is the major regulatory protein of BBB permeability [29]. MGO induced the activation of UPR signaling and apoptosis in HUVECs via AMPK, PI3K–AKT, and CHOP induction pathways [30,31]. The mechanism of ER stress inhibition by curcumin is not well known but it has been shown to reduce ER stress responses by increasing peroxiredoxin 6 (prdx 6), decreasing NF- κ B signaling, and reducing oxidative stress [32,33].

The curcumin metabolites, glucuronides and di-tetra- and hexahydrocurcumins were detected in the liver, kidney, and intestines after oral, intraperitoneal (IP), and intravenous (IV) administrations. The oral administration of curcumin showed reduced bioavailability and poor absorption compared to IV or IP administrations [34]. The IP administration of curcumin allowed a wide biodistribution including to the brain, lungs, liver, and kidney. Nanoemulsions of curcumin are reported to improve the bioavailability and therapeutic effects of this molecule compared to free curcumin in both in vitro and in vivo studies [35].

Interestingly, our curcumin-enriched rHDL (Cur-rHDLs) nanoparticles showed an improved synergistic protective effect on MGO-induced cytotoxicity, ROS production, cerebral endothelial cell integrity, chromatin condensation, and ER stress compared to rHDLs or curcumin alone. Anti-apoptotic effects of curcumin in MGO-stimulated endothelial cells have been previously reported. The authors suggested potential direct scavenging of MGO by curcumin and one of its analogues, dimethoxy curcumin [36]. However, the protection by HDLs from MGO-induced endothelial cell death had never been reported before. Here, we provide the first evidence that reconstituted HDL particles exhibit sufficient antioxidant and anti-inflammatory effects to prevent MGO-induced cell death in endothelial cells.

Recently, the bioavailability of curcumin was improved using nanoemulsions administered intraperitoneally in a mouse model of Parkinson's disease [36]. Poloxamer nanoparticles (nonionic triblock copolymers) displayed better penetration of the blood–brain barrier and better accumulation in the brain than non-encapsulated curcumin in subjects with Alzheimer's disease [37]. Previous studies on curcumin encapsulated in low-density lipoprotein (LDL) and HDL particles showed that LDLs were more prone to accumulate curcumin than HDL particles and highlighted their potential to treat cancer, due to the avidity of cancer cells for LDLs [38].

A previous study showed that HDLs reconstituted with soy phosphatidylcholine and Apolipoprotein A-I isolated from the plasma of healthy volunteers significantly reduced the infarct area in two rat models of stroke and had an antioxidant effect in human endothelial and neuroblastoma cell lines [39]. The HDL drug delivery system facilitates the cellular uptake of drugs via interaction with scavenging receptors (SR-BI) by bypassing the endosomal/lysosomal pathway, independently of HDL uptake by transcytosis. Cerebral endothelial cells (including bEnd.3) contain SR-BI class B type I receptors in their membranes. rHDLs injected intraperitoneally were detected in the liver and kidney in in vivo mouse and zebrafish models [40]. rHDLs were also shown to be taken up by endothelial cells and astrocytes in the brain of mice subjected to experimental ischemic stroke. We

recently demonstrated that HDLs isolated from plasma had a neuroprotective effect via SR-BI (scavenger receptor type BI) in a mouse model of MCAO [13]. Improvement of HDL potential to prevent the deleterious effects of stroke in diabetic conditions is of major importance, since our preliminary results tend to demonstrate that HDLs alone are not sufficient to limit infarct volume and hemorrhagic complications in a mouse model of stroke under hyperglycemic conditions [41]. Curcumin-enriched HDLs could then represent a therapeutic option for brain pathologies involving oxidative stress and BBB dysfunction. Nano-curcumin administered orally was shown to have a good brain biodistribution in a mouse model of experimental cerebral malaria [13].

4. Materials and Methods

Methylglyoxal (MGO), curcumin (Cat. Number: C7727), propidium iodide (PI), thiazolyl blue tetrazolium bromide (MTT), and other chemicals were purchased from Sigma Aldrich (St. Louis, MO, USA).

4.1. Cell Culture

The murine cerebral endothelial cell line bEnd.3 was obtained from the American Type Culture Collections (ATCC® CRL™-2299™, Manassas, VA, USA). The cells were cultured in Dulbecco's Modified Eagle Medium (DMEM) containing 25 mM glucose, 10% heat-inactivated Fetal Bovine Serum (FBS), 5 mM L-glutamine, 2 µg/mL streptomycin, and 50 µU/mL penicillin (Pan Biotech, Dutscher, and Brumath, France). The cells were kept in a humidified atmosphere with 5% CO₂, at 37 °C. All the treatments were carried out in serum-free medium.

4.2. Preparation of Curcumin-Enriched rHDLs (Cur-HDLs)

Reconstituted HDLs (rHDLs) were obtained from CSL Behring AG (CSL111, Bern, Switzerland). rHDLs enriched with curcumin were prepared by gently mixing 3 mL of 2 mg/mL rHDLs with 5 µM curcumin followed by incubation in the dark for 16 h at 37 °C (50 rpm). Curcumin-enriched rHDLs (Cur-rHDLs) were isolated by ultracentrifugation as described previously [13] to eliminate free curcumin. Briefly, the rHDL curcumin mixture was adjusted to a density $d = 1.22$ with KBr and overlaid with a KBr saline solution ($d = 1.21$). Ultracentrifugation was performed at $100,000 \times g$ for 24 h at 10 °C. The curcumin-enriched rHDL yellow fraction (top layer) was recovered. The curcumin-enriched rHDL fraction was desalted by centrifugation with PBS 5 times, 20 min each, at $12,000 \times g$ using a Centricon filter (cutoff 10 kDa; Vivascience, Stonehouse, UK) to remove the excess of KBr and concentrate the sample. Protein concentration was determined using the Bicinchoninic Acid (BCA) method (BCA Protein Assay Kit, Thermo Scientific Pierce, and Waltham, MA, USA).

4.3. Quantification of Curcumin by LC-MS Analysis

4.3.1. Extraction of Curcumin from HDL-Curcumin

Curcumin was extracted from Cur-HDLs by precipitation of ApoA-I with acetonitrile (ACN). In brief, 54 µL of ACN was added to 27 µL of the Cur-HDL solution (2:1, *v/v*), vortexed a few seconds, and centrifuged at $20,000 \times g$ for 15 min. The resulting supernatant was collected and directly analyzed by mass spectrometry.

4.3.2. Identification and Quantification of HDL-Curcumin by LC-MS/MS

Curcumin from Cur-HDLs was identified by ultra-high-performance liquid chromatography coupled with a HESI-Orbitrap mass spectrometer (Q Exactive™ Plus, Thermo Fisher). Briefly, 10 µL of sample was injected in a UHPLC system equipped with a Thermo Fisher Ultimate 3000 series WPS-3000 RS autosampler and then separated on a PFP column (2.6 µm, 100 mm × 2.1 mm, Phenomenex, Torrance, CA, USA). Elution was performed using a binary gradient of water and ACN, both acidified with 0.1% formic acid (B). A flow rate of 450 µL/min was used. The following elution was setup: 0.0–3.0 min, from 20 to 50%

B; continue with 50% B for 8 min. Then, the column was washed with 95% B for 3 min and equilibrated with 20% B for 2 min. The column oven was thermostated at 30 °C.

For mass spectrometry conditions, the Heated Electrospray Ionization source II was set at 3.9 kV, the capillary temperature at 320 °C, the sheath gas flow rate at 65 units, the auxiliary gas flow rate at 20 units, and the S-lens RF at 50%. Mass spectra were registered in full scan data-dependent acquisition from m/z 100 to 500 in positive ion mode at a resolving power of 70,000 FWHM (at m/z 400). The automatic gain control (AGC) was set at $1e6$, and the injection time (IT) at 200 ms. The MS/MS spectra were acquired at a resolving power of 17,500 FWHM (at m/z 200) with an AGC set to $2e5$ and an IT of 50 ms. A relative higher energy collisional dissociation (HCD) energy of 40% was applied. Identification and quantification of curcumin were based on its retention time, accurate mass, elemental composition, MS fragmentation pattern, and comparisons with a commercial standard. Data were acquired by XCalibur 4.2.47 software (Thermo Fisher Scientific Inc. Waltham, MA, USA) and processed by Skyline 21.1.0.146 software (MacCoss Lab.). The performance of the Orbitrap was evaluated weekly, and external calibration of the mass spectrometer was performed before analysis with an LTQ ESI positive ion calibration solution (Pierce™).

4.3.3. Preparation of Standard Solution and Calibration Curve

The standard stock solution of curcumin was dissolved in DMSO at a concentration of 100 μ M. Calibration standard solutions were prepared by dilution of the stock solution in 20% ACN acidified with 0.1% formic acid to obtain the desired calibration curves ranging from 0.0156 to 2 μ M. The calibration curves were constructed by plotting the peak area of the analytes against the corresponding analyte concentrations with linear regression (1/x weighting, linear through zero) using standard samples at six concentrations. The obtained calibration curve had a correlation coefficient (R^2) of 0.989. The concentration of curcumin from the Cur-HDLs was 2.8 ± 0.4 μ M (Figure 9).

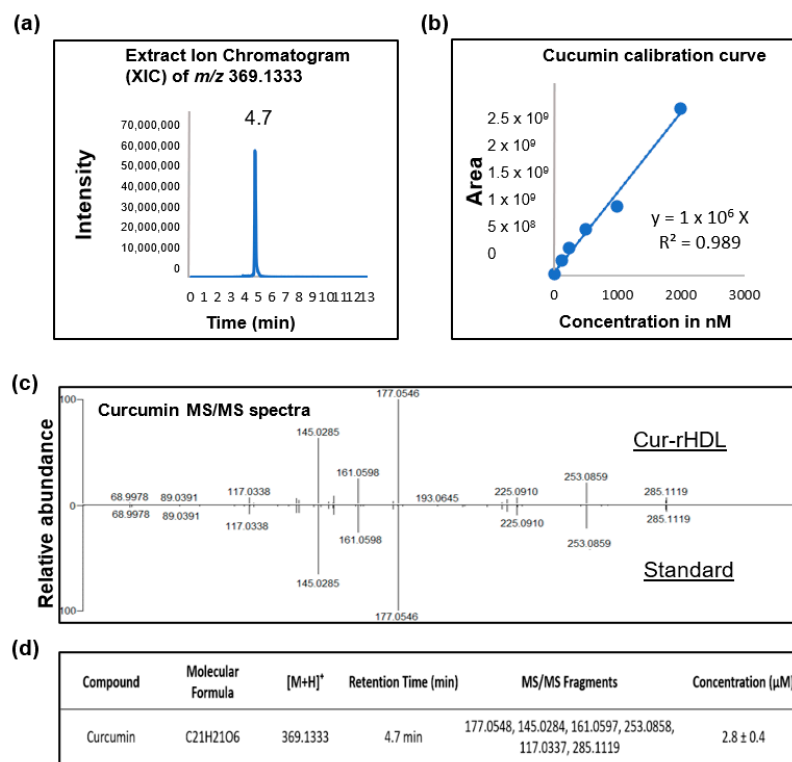


Figure 9. Quantification of curcumin in curcumin-enriched rHDLs by LC-MS/MS analysis. (a) Representative ion chromatogram of curcumin, (b) Calibration curve used to quantify curcumin, (c) LC-MS/MS analysis spectrum of curcumin in the Cur-rHDL sample vs. the curcumin standard and (d) Combined LC-MS/MS analysis details of curcumin quantification.

4.4. Determination of Particle Size

The particle size of rHDLs and Cur-rHDLs was determined using a dynamic light scattering (DLS) particle size analyzer (Zetasizer Nano, Malvern Instruments, UK), which measures the hydrodynamic diameter and polydispersity index (PDI) of the nanoparticles. The analysis was performed at 25 °C with a scattering angle of 173°. The rHDL and Cur-rHDL samples were prepared at a concentration of 1 mg/mL in PBS and filtered through a 0.22 µm-pore size PTFE syringe filter (to remove any aggregates).

4.5. Evaluation of Cell Viability

Cell viability was evaluated by assessment of mitochondrial metabolic activity via the MTT assay (3-(4, 5-dimethylthiazol-2-yl)-2, 5-diphenyltetrazolium bromide) as previously described [42]. The cells were seeded in 96-well plates at a density of 5×10^3 cells per well and grown for 24 h. The culture medium was removed, and the cells were washed once with PBS. The cells were then incubated with HDLs (H), curcumin (C), curcumin-enriched rHDLs (Cur-rHDLs) for 1 h before the addition of 2 mM MGO for 24 h. After 24 h, 20 µL of 5 mg/mL MTT reagent prepared in PBS was added to each well, and the cells were incubated in the dark at 37 °C for 2 h. Then, the medium was removed, the formed formazan crystals were dissolved in 100 µL DMSO, and the absorbance was measured at 570 nm (TECAN, Männedorf, Switzerland).

4.6. Evaluation of Intracellular ROS

The levels of intracellular reactive oxygen species (ROS) were measured using the fluorescent probe 2',7'-dichlorodihydrofluorescein-diacetate (DCFH-DA) as described previously [42]. The cells were seeded in a black 96-well plate with a transparent bottom at a cell density of 5×10^3 cells for 24 h. The medium was removed, and 100 µL of a 10 µM DCFH-DA solution in PBS was added to each well after washing the cells with PBS. After 40 min of incubation in the dark at 37 °C, the probe was removed and the cells were pre-treated with rHDLs (H), curcumin (C), curcumin-enriched rHDLs (Cur-rHDLs) for 1 h, before addition of 2 mM MGO for 1–6 h. ROS levels were measured by fluorescence analysis at an excitation wavelength of 492 nm and an emission wavelength of 520 nm (FLUOstar Optima, Bmg Labtech, and Cambridge, UK).

4.7. Assessment of Endothelial Layer Integrity by Real-Time Electrical Impedance

The cellular integrity was analyzed by impedance measurement using the xCELLigence system (Acea Biosciences, San Diego, CA, USA). The cells were seeded in a 16-well xCELLigence plate specifically designed for monitoring the impedance, at a cell density of 4×10^3 cells per well. After the cells reached confluency, they were pre-treated with rHDLs (H), curcumin (C), and curcumin-enriched rHDLs (Cur-rHDLs) for 1 h before the addition of 2 mM MGO. The impedance was monitored for 4 days.

4.8. Evaluation of Chromatin Condensation

Chromatin condensation was evaluated using the fluorescent dye DAPI (4'-6-diamidino-2-phenylindole). The cells were seeded on sterile 14 mm coverslips placed in a 24-well plate at a density of 5×10^3 per well for 24 h. The culture medium was removed 24 h after the different treatment, and the cells were washed with PBS and fixed in 4% PFA for 10 min. The cells were then stained with DAPI (1 µg/mL) for 5 min and washed twice with PBS, and the coverslips were mounted on slides. The number of cells with condensed chromatin was determined using a fluorescent microscope (Eclipse 80i Nikon microscope equipped with a Hamamatsu digital camera, Life Sciences, Tokyo, Japan). The results are expressed as percentage of cells with condensed chromatin.

4.9. Immunocytochemistry

Cells were seeded in a 24-well plate containing 14 mm-diameter coverslips at a density of 5×10^3 per well for 24 h. After treatment, the cells were washed and fixed

in 4% PFA (for ATF-4 primary antibody staining) for 5 min at room temperature or 100% ice-cold ($-20\text{ }^{\circ}\text{C}$) methanol (for XBP-1 and GRP 78 primary antibodies staining) for 10 min and then incubated with the primary antibodies ATF-4 (Cell signaling technology-11815S, Danvers, MA; dilution 1:200–500 ng/mL), XBP-1 (Abcam-ab37152, Cambridge, UK; dilution 1:200–500 ng/mL), and GRP 78 (Abcam-ab21685, Cambridge, UK; dilution 1:500–200 ng/mL) prepared in blocking buffer (PBS containing 1% BSA) overnight at $4\text{ }^{\circ}\text{C}$. The primary antibody was removed, and the cells were washed 3 times with PBS. Secondary antibody and DAPI prepared in blocking buffer were added to the cells, which were incubated in the dark for 1 h at room temperature. The cells were washed with PBS, and the coverslips were mounted on slides that were examined under a confocal microscope (Nikon Eclipse Ti2 with a C2si confocal system, Tokyo, Japan).

4.10. Intracellular Uptake of Curcumin-Enriched rHDLs

The cells were seeded in a 6-well plate at a density of 2×10^5 for 24 h. The culture medium was removed, and cells were washed with PBS, incubated with rHDL (H), curcumin (C), and curcumin-enriched rHDLs (Cur-rHDLs) for 3 and 6 h. The medium was removed, and the cells were washed with 500 μL of PBS and then with 500 μL of 0.4% PBS-BSA/well to remove traces of polyphenols from the cell membrane. Then, 500 μL of methanol containing 200 mM HCl/well was added to collect the intracellular polyphenol moiety by cell scraping and transfer of the medium into Eppendorf tubes. After 45 min at $4\text{ }^{\circ}\text{C}$, the tubes were centrifuged at $14,000 \times g$ at $4\text{ }^{\circ}\text{C}$ for 5 min, and the supernatant was collected for subsequent analysis by LC-MS/MS. For quantitation, chromatographic conditions and mass spectrometer parameters were the same as described above. A calibration curve ranging from 1.953 nM to 1000 nM was used. A quality control sample was analyzed within each batch, with two blank samples containing 20% ACN in water and 0.1% formic acid.

4.11. Statistical Analysis

Data are expressed as mean \pm SD of three independent experiments. Statistical analyses were performed by one-way analysis of variance (ANOVA) followed by Bonferroni's multiple comparison test using Graph-Pad Prism 6 (Graph Pad Software, Inc., San Diego, CA, USA). Statistical significance was considered for a p -value < 0.05 .

5. Conclusions

We demonstrated for the first time an improved protective effect of curcumin-enriched rHDL nanoparticles on MGO-induced cerebral endothelial dysfunction linked to oxidative stress and endoplasmic reticulum stress mechanisms, that need to be further investigated *in vivo*. These cur-rHDL nanoparticles are stable and biocompatible and have therapeutic potential as an emerging drug delivery system for pathologies involving endothelial dysfunction and oxidative stress, such as stroke under diabetic conditions.

Author Contributions: Conceptualization, O.M., P.R. (Palaniyandi Ramanan) and M.-P.G.; methodology, P.R. (Philippe Rondeau), B.V. and P.R. (Palaniyandi Ramanan); validation, O.M.; investigation, S.S.N., S.R. and W.V.; data curation, S.S.N., S.R., P.R. (Philippe Rondeau), J.P., B.V., M.-P.G., N.D. and O.M.; writing—original draft preparation, S.S.N. and O.M.; writing—review and editing, P.R. (Philippe Rondeau), N.D., C.L.d.H. and O.M.; supervision, P.R. (Palaniyandi Ramanan), C.L.d.H. and O.M.; funding acquisition, O.M. All authors have read and agreed to the published version of the manuscript.

Funding: This research was funded by the Ministère de l'Enseignement Supérieur et de la Recherche, the Université de La Réunion, the "Structure fédérative de recherche biosécurité en milieu tropical (BIOST)" and by the European Regional Development Funds RE0001897 (EU- Région Réunion -French State national counterpart). SSN is recipient of a fellowship grant from Région Réunion.

Institutional Review Board Statement: Not applicable.

Informed Consent Statement: Not applicable.

Data Availability Statement: Data is contained within the article.

Conflicts of Interest: The authors declare no conflict of interest.

References

1. McLellan, A.C.; Thornalley, P.J.; Benn, J.; Sonksen, P.H. Glyoxalase system in clinical diabetes mellitus and correlation with diabetic complications. *Clin. Sci.* **1994**, *87*, 21–29. [[CrossRef](#)] [[PubMed](#)]
2. Van Eupen, M.G.A.; Schram, M.T.; Colhoun, H.M.; Hanssen, N.M.J.; Niessen, H.W.M.; Tarnow, L.; Parving, H.H.; Rossing, P.; Stehouwer, C.D.A.; Schalkwijk, C.G. The methylglyoxal-derived AGE tetrahydropyrimidine is increased in plasma of individuals with type 1 diabetes mellitus and in atherosclerotic lesions and is associated with sVCAM-1. *Diabetologia* **2013**, *56*, 1845–1855. [[CrossRef](#)] [[PubMed](#)]
3. Kilhovd, B.K.; Giardino, I.; Torjesen, P.; Birkeland, K.; Berg, T.; Thornalley, P.; Brownlee, M.; Hanssen, K. Increased serum levels of the specific AGE-compound methylglyoxal-derived hydroimidazolone in patients with type 2 diabetes. *Metabolism* **2003**, *52*, 163–167. [[CrossRef](#)] [[PubMed](#)]
4. Hanssen, N.M.J.; Westerink, J.; Scheijen, J.L.; van der Graaf, Y.; Stehouwer, C.D.; Schalkwijk, C.G.; Algra, A.; Grobbee, R.D.; Rutten, G.E.; Visseren, F.L.; et al. Higher Plasma Methylglyoxal Levels Are Associated With Incident Cardiovascular Disease and Mortality in Individuals with Type 2 Diabetes. *Diabetes Care* **2018**, *41*, 1689–1695. [[CrossRef](#)] [[PubMed](#)]
5. Bourajaj, M.; Stehouwer, C.; Van Hinsbergh, V.; Schalkwijk, C. Role of methylglyoxal adducts in the development of vascular complications in diabetes mellitus. *Biochem. Soc. Trans.* **2003**, *31*, 1400–1402. [[CrossRef](#)] [[PubMed](#)]
6. Yamawaki, H.; Saito, K.; Okada, M.; Hara, Y. Methylglyoxal mediates vascular inflammation via JNK and p38 in human endothelial cells. *Am. J. Physiol. Physiol.* **2008**, *295*, 1510–1517. [[CrossRef](#)] [[PubMed](#)]
7. Li, W.; Chen, Z.; Yan, M.; He, P.; Chen, Z.; Dai, H. The protective role of isorhamnetin on human brain microvascular endothelial cells from cytotoxicity induced by methylglyoxal and oxygen-glucose deprivation. *J. Neurochem.* **2016**, *136*, 651–659. [[CrossRef](#)] [[PubMed](#)]
8. Navarro, V. The Arguments against a National Health Program: Science or Ideology? *Int. J. Heal. Serv.* **1988**, *18*, 179–189. [[CrossRef](#)] [[PubMed](#)]
9. Santini, S.J.; Cordone, V.; Mijit, M.; Bignotti, V.; Aimola, P.; Dolo, V.; Falone, S.; Amicarelli, F. SIRT1-Dependent Upregulation of Antigliycative Defense in HUVECs Is Essential for Resveratrol Protection against High Glucose Stress. *Antioxidants* **2019**, *8*, 346. [[CrossRef](#)]
10. Tang, D.; Xiao, W.; Gu, W.-T.; Zhang, Z.-T.; Xu, S.-H.; Chen, Z.-Q.; Xu, Y.-H.; Zhang, L.-Y.; Wang, S.-M.; Nie, H. Pterostilbene prevents methylglyoxal-induced cytotoxicity in endothelial cells by regulating glyoxalase, oxidative stress and apoptosis. *Food Chem. Toxicol.* **2021**, *153*, 112244. [[CrossRef](#)]
11. Hsuuw, Y.D.; Chang, C.-K.; Chan, W.-H.; Yu, J.-S. Curcumin prevents methylglyoxal-induced oxidative stress and apoptosis in mouse embryonic stem cells and blastocysts. *J. Cell. Physiol.* **2005**, *205*, 379–386. [[CrossRef](#)]
12. Chan, W.H.; Wu, H.J.; Hsuuw, Y.D. Curcumin Inhibits ROS Formation and Apoptosis in Methylglyoxal-Treated Human Hepatoma G2 Cells. *Ann. NY Acad. Sci.* **2005**, *1042*, 372–378. [[CrossRef](#)]
13. Tran-Dinh, A.; Levoye, A.; Couret, D.; Galle-Treger, L.; Moreau, M.; Delbosc, S.; Hoteit, C.; Montravers, P.; Amarenco, P.; Huby, T.; et al. High-Density Lipoprotein Therapy in Stroke: Evaluation of Endothelial SR-BI-Dependent Neuroprotective Effects. *Int. J. Mol. Sci.* **2021**, *22*, 106. [[CrossRef](#)]
14. Tran-Dinh, A.; Diallo, D.; Delbosc, S.; Varela-Perez, L.M.; Dang, Q.B.; Lapergue, B.; Burillo, E.; Michel, J.B.; Levoye, A.; Martin-Ventura, J.L.; et al. HDL and endothelial protection. *Br. J. Pharmacol.* **2013**, *169*, 493–511. [[CrossRef](#)]
15. Gonzales, C.M.; Dalmolin, L.F.; da Silva, K.A.; Slade, N.B.L.; Lopez, R.F.V.; Moreto, J.A.; Schwarz, K. New Insights of Turmeric Extract-Loaded PLGA Nanoparticles: Development, Characterization and In Vitro Evaluation of Antioxidant Activity. *Mater. Veg.* **2021**, *76*, 507–515. [[CrossRef](#)]
16. Kim, D.; Kim, K.-A.; Kim, J.-H.; Kim, E.-H.; Bae, O.-N. Methylglyoxal-Induced Dysfunction in Brain Endothelial Cells via the Suppression of Akt/HIF-1 α Pathway and Activation of Mitophagy Associated with Increased Reactive Oxygen Species. *Antioxidants* **2020**, *9*, 820. [[CrossRef](#)] [[PubMed](#)]
17. Koike, S.; Toriumi, K.; Kasahara, S.; Kibune, Y.; Ishida, Y.-I.; Dan, T.; Miyata, T.; Arai, M.; Ogasawara, Y. Accumulation of Carbonyl Proteins in the Brain of Mouse Model for Methylglyoxal Detoxification Deficits. *Antioxidants* **2021**, *10*, 574. [[CrossRef](#)]
18. Rabbani, N.; Thornalley, P.J. Glyoxalase in diabetes, obesity and related disorders. *Semin. Cell Dev. Biol.* **2011**, *22*, 309–317. [[CrossRef](#)]
19. Kim, J.H.; Kim, K.A.; Shin, Y.J.; Kim, H.; Majid, A.; Bae, O.N. Methylglyoxal induced advanced glycation end products (AGE)/receptor for AGE (RAGE)-mediated angiogenic impairment in bone marrow-derived endothelial progenitor cells. *J. Toxicol. Environ. Health Part A* **2018**, *81*, 266–277. [[CrossRef](#)]
20. Vulesevic, B.; McNeill, B.; Giacco, F.; Maeda, K.; Blackburn, N.J.R.; Brownlee, M.; Milne, R.W.; Suuronen, E.J. Methylglyoxal-Induced Endothelial Cell Loss and Inflammation Contribute to the Development of Diabetic Cardiomyopathy. *Diabetes* **2016**, *65*, 1699–1713. [[CrossRef](#)] [[PubMed](#)]
21. Chan, W.H.; Wu, H.J. Methylglyoxal and high glucose co-treatment induces apoptosis or necrosis in human umbilical vein endothelial cells. *J. Cell. Biochem.* **2008**, *103*, 1144–1157. [[CrossRef](#)] [[PubMed](#)]

22. Choudhary, D.; Chandra, D.; Kale, R.K. Influence of methylglyoxal on antioxidant enzymes and oxidative damage. *Toxicol. Lett.* **1997**, *93*, 141–152. [[CrossRef](#)]
23. Weber, V.; Olzscha, H.; Längrich, T.; Hartmann, C.; Jung, M.; Hofmann, B.; Horstkorte, R.; Bork, K. Glycation Increases the Risk of Microbial Traversal through an Endothelial Model of the Human Blood-Brain Barrier after Use of Anesthetics. *J. Clin. Med.* **2020**, *9*, 3672. [[CrossRef](#)]
24. Miyazawa, N.; Abe, M.; Souma, T.; Tanemoto, M.; Abe, T.; Nakayama, M.; Ito, S. Methylglyoxal augments intracellular oxidative stress in human aortic endothelial cells. *Free Radic. Res.* **2009**, *44*, 101–107. [[CrossRef](#)] [[PubMed](#)]
25. Li, W.; Maloney, R.E.; Circu, M.L.; Alexander, J.S.; Aw, T.Y. Acute carbonyl stress induces occludin glycation and brain microvascular endothelial barrier dysfunction: Role for glutathione-dependent metabolism of methylglyoxal. *Free Radic. Biol. Med.* **2012**, *54*, 51–61. [[CrossRef](#)] [[PubMed](#)]
26. Zannis, V.I.; Fotakis, P.; Koukos, G.; Kardassis, D.; Ehnholm, C.; Jauhiainen, M.; Chroni, A. HDL Biogenesis, Remodeling, and Catabolism. *Anxiety Anxiolytic Drugs* **2014**, *224*, 53–111.
27. Kim, S.; Kim, S.; Hwang, A.R.; Choi, H.C.; Lee, J.Y.; Woo, C.H. Apelin-13 inhibits methylglyoxal-induced unfolded protein responses and endothelial dysfunction via regulating AMPK pathway. *Int. J. Mol. Sci.* **2020**, *21*, 4069. [[CrossRef](#)] [[PubMed](#)]
28. Chan, C.M.; Huang, D.-Y.; Huang, Y.-P.; Hsu, S.-H.; Kang, L.-Y.; Shen, C.-M.; Lin, W.W. Methylglyoxal induces cell death through endoplasmic reticulum stress-associated ROS production and mitochondrial dysfunction. *J. Cell. Mol. Med.* **2016**, *20*, 1749–1760. [[CrossRef](#)] [[PubMed](#)]
29. Liebner, S.; Plate, K.H. Differentiation of the brain vasculature: The answer came blowing by the Wnt. *J. Angiogenesis Res.* **2010**, *2*, 1. [[CrossRef](#)]
30. Japp, A.G.; Newby, D.E. The apelin–APJ system in heart failure: Pathophysiologic relevance and therapeutic potential. *Biochem. Pharmacol.* **2008**, *75*, 1882–1892. [[CrossRef](#)] [[PubMed](#)]
31. Yang, X.; Zhu, W.; Zhang, P.; Chen, K.; Zhao, L.; Li, J.; Wei, M.; Liu, M. Apelin-13 stimulates angiogenesis by promoting cross-talk between AMP-activated protein kinase and Akt signaling in myocardial microvascular endothelial cells. *Mol. Med. Rep.* **2014**, *9*, 1590–1596. [[CrossRef](#)] [[PubMed](#)]
32. Jutooru, I.; Chadalapaka, G.; Lei, P.; Safe, S. Inhibition of NFκB and pancreatic cancer cell and tumor growth by curcumin is dependent on specificity protein down-regulation. *J. Biol. Chem.* **2010**, *285*, 25332–25344. [[CrossRef](#)]
33. Chhunchha, B.; Fatma, N.; Kubo, E.; Rai, P.; Singh, S.P.; Singh, D.P. Curcumin abates hypoxia-induced oxidative stress based-ER stress-mediated cell death in mouse hippocampal cells (HT22) by controlling Prdx6 and NF-κB regulation. *Am. J. Physiol. Cell Physiol.* **2013**, *304*, 636–655. [[CrossRef](#)]
34. Holder, G.M.; Plummer, J.L.; Ryan, A.J. The Metabolism and Excretion of Curcumin (1,7-Bis-(4-hydroxy-3-methoxyphenyl)-1,6-heptadiene-3,5-dione) in the Rat. *Xenobiotica* **1978**, *8*, 761–768. [[CrossRef](#)] [[PubMed](#)]
35. Pan, M.H.; Huang, T.M.; Lin, J.K. Biotransformation of curcumin through reduction and glucuronidation in mice. *Drug Metab. Dispos.* **1999**, *27*, 486–494.
36. Júnior, O.V.R.; Alves, B.D.S.; Barros, P.A.B.; Rodrigues, J.L.; Ferreira, S.P.; Monteiro, L.K.S.; Araújo, G.D.M.S.; Fernandes, S.S.; Vaz, G.R.; Dora, C.L.; et al. Nanoemulsion Improves the Neuroprotective Effects of Curcumin in an Experimental Model of Parkinson’s Disease. *Neurotox. Res.* **2021**, *39*, 787–799. [[CrossRef](#)] [[PubMed](#)]
37. Singh, A.; Mahajan, S.D.; Kutscher, H.L.; Kim, S.; Prasad, P.N. Curcumin-Pluronic Nanoparticles: A Theranostic Nanoformulation for Alzheimer’s Disease. *Crit. Rev. Biomed. Eng.* **2020**, *48*, 153–168. [[CrossRef](#)]
38. Jutkova, A.; Chorvat, D.; Miskovsky, P.; Jancura, D.; Datta, S. Encapsulation of anticancer drug curcumin and co-loading with photosensitizer hypericin into lipoproteins investigated by fluorescence resonance energy transfer. *Int. J. Pharm.* **2019**, *564*, 369–378. [[CrossRef](#)] [[PubMed](#)]
39. Paternò, R.; Ruocco, A.; Postiglione, A.; Hubsch, A.; Andresen, I.; Lang, M.G. Reconstituted High-Density Lipoprotein Exhibits Neuroprotection in Two Rat Models of Stroke. *Cerebrovasc. Dis.* **2003**, *17*, 204–211. [[CrossRef](#)]
40. Sulliman, N.C.; Ghaddar, B.; Gence, L.; Patche, J.; Rastegar, S.; Meilhac, O.; Diotel, N. HDL biodistribution and brain receptors in zebrafish, using HDLs as vectors for targeting endothelial cells and neural progenitors. *Sci. Rep.* **2021**, *11*, 1–18. [[CrossRef](#)] [[PubMed](#)]
41. Couret, D.; Planesse, C.; Patche, J.; Diotel, N.; Nativel, B.; Bourane, S.; Meilhac, O. Lack of Neuroprotective Effects of High-Density Lipoprotein Therapy in Stroke under Acute Hyperglycemic Conditions. *Molecules* **2021**, *26*, 6365. [[CrossRef](#)]
42. Hatia, S.; Septembre-Malaterre, A.; Le Sage, F.; Badiou-Bénéteau, A.; Baret, P.; Payet, B.; D’Hellencourt, C.L.; Gonthier, M.-P. Evaluation of antioxidant properties of major dietary polyphenols and their protective effect on 3T3-L1 preadipocytes and red blood cells exposed to oxidative stress. *Free Radic. Res.* **2014**, *48*, 387–401. [[CrossRef](#)] [[PubMed](#)]

IV. Discussion

Methylglyoxal (MGO) is a reactive metabolite that accumulated during diabetes due to hyperglycemia and impaired glyoxalase enzyme system (detoxifies MGO) (Oya et al., 1999). Tissue MGO levels are maintained at a low levels where slight increase at the physiological range is beneficial for modulating physiology but high levels of MGO triggers stress responses (Moraru et al., 2018). High glucose concentrations in diabetes condition result in the formation of MGO (Schalkwijk et al., 2006; Shinohara et al., 1998). Overexpression of glyoxalase I prevented the hyperglycemia induced MGO-AGE formation, demonstrating the importance of MGO in AGE formation (Brouwers et al., 2011). Extracellular MGO adducts and intracellular accumulation of MGO interacts with macromolecules including proteins, lipids and nucleic acids and alters their cellular functions including endothelial cell dysfunction which contribute to the diabetic vascular complications. MGO modified proteins result in an increased oxidative stress (Wu & Juurlink, 2002).

Endothelial cells line the blood vessels and maintains the vascular homeostasis by the secretion of vasodilators and vasoconstrictors. Endothelial dysfunction shifts the endothelial function to vasoconstriction, increased permeability, proinflammatory and prothrombotic states (Schalkwijk & Stehouwer, 2005). Exposure of endothelial cells to high concentrations of MGO induced oxidative stress and apoptosis (Chan & Wu, 2008). Diabetes associated endothelial dysfunction involves impaired vasoregulation, barrier function, increased oxidative stress and inflammation that contribute to the diabetic vascular complications (Eringa et al., 2013). Exogenous administration of MGO in rats induced diabetes-like vascular changes including degenerative changes of microvessels with loss of endothelial cells, vasodilation and increased oxidative stress (Brouwers et al., 2010; Brouwers et al., 2014).

Studies have shown the protective effects of many polyphenol antioxidants in diabetic vascular complications (Habauzit & Morand, 2012). Dietary phytochemicals such as curcumin exhibits anti-oxidative, anti-inflammatory and anti-diabetic properties that can regulate the hyperglycemia mediated oxidative damage, inflammation and endothelial dysfunction in diabetic complications. HDL lipoproteins have antioxidant and anti-inflammatory properties that are emerging as drug delivery systems for various drug molecules including hydrophobic drugs.

In this study we have found that curcumin loaded rHDL nanoparticles showed cytoprotective effect by reducing the reactive oxygen species production, ER stress, chromatin condensation

and impaired membrane integrity induced by MGO in cerebral endothelial cells. It was also interesting to find that curcumin loaded rHDLs showed an improved endothelial protection in combination compared to curcumin alone.

V. Conclusion

These findings suggest that the HDL encapsulation can improve the endothelial protective effects of curcumin antioxidant to attenuate the MGO induced endothelial dysfunction in the progression of diabetic vascular complications. Further *in vivo* studies are required to understand the complete mechanism of action to develop the therapeutics for diabetic vascular complications.

Part 2. Impact of curcumin nanomicelles on zebrafish tail regeneration

I. Introduction

Impaired diabetic wound healing increases the risk of amputation (Alavi et al., 2014). Wound healing and regeneration studies are emerging to understanding the mechanisms and to develop therapeutics for diabetic amputations (Andrews, Houdek, & Kiemele, 2015; Davis, Kimball, Boniakowski, & Gallagher, 2018).

Curcumin has been used widely in wound healing and regeneration studies which has antioxidant, anti-inflammatory properties (Menon & Sudheer, 2007). Many nanoparticles are being developed for drug delivery of curcumin to improve its bioavailability, therapeutic properties and specific targeting. Polymeric micelles are being widely used as drug delivery nanoparticles as they are biodegradable, less toxic and have a flexible physiochemical properties that can be modified and functionalized to achieve improved drug delivery for various pathophysiological conditions (Akbar et al., 2018).

Zebrafish is a simple and easily available model organism that is emerging for wound healing and regenerative studies. Zebrafish shares many common molecular and genetic features with humans which makes it a more potential model for studying various human pathophysiological conditions including wound healing and regeneration studies (Marques, Lupi, & Mercader, 2019). Adult zebrafish is mostly used for the regenerative studies while the use of larvae is emerging as a quick model that can be used in large scale compared to adult zebrafish (Pourghadamyari et al., 2019).

In our study we used carrageenan polysaccharide nanomicelles loaded with curcumin, 3 day post fertilized (3dpf) zebrafish larvae tail amputation model. First we tested curcumin loaded nanomicelles cytotoxicity on the 3dpf zebrafish larvae and then we proceeded to investigate the potential of curcumin loaded nanomicelles to enhance the recruitment of neutrophils and macrophages to the site of tail injury and promote the tail regenerative area post tail amputation

II. Methods

Carrageenan extraction and digestion

Carrageenans were extracted from red algae *Kappaphycus alvarezii*. The algae were pre-treated with 80% ethanol solution and agitated overnight at room temperature to remove salts and debris.

Carrageenans were then hot extracted in water at 90°C, pH 7 along with ultrasound. They were filtered, jellified at 4°C, frozen at -80°C and lyophilized.

The κ -carrageenase enzyme is isolated from *Pseudoaltermonas carrageenovora*. The bacteria were cultured in 1litre marine broth at 21°C under agitation and was stimulated with a 0.15% (M/v) of a κ -carrageenan solution prepared in Tris-HCl 100mM pH=8.5 after the OD reached 0.6. After 24h enzyme was filtered (0.45 μ m Millipore filter and 300kDa cut off membrane filter) and concentrated (10kDa centrifugal filter) which was finally desalted (3 KDa centrifugal filter) and its protein content was determined by Bradford assay.

The κ -carrageenase enzyme was used to digest the κ -carrageenan which is later use for the micelle preparation. κ -carrageenase (75.3 μ g in 1 ml) was used to digest the carrageenans (150mg) dissolved in a Tris-HCl solution (100 mM, pH 8.5) incubated for 6h, 8h and 10h respectively. Non- hydrolysed κ -carrageenan and λ -carrageenan were eliminated by ultracentrifugation using 10kDa centricon. Oligocarrageenans were isolated by precipitation with methanol, freeze-dried, lyophilized.

Carrageenan micelle preparation and characterization

The carrageenan micelles preparation (Fig 23) was done in three steps as follows:

(i) Partial acetylation of oligocarrageenan

500mg of oligocarrageenan was mixed with 644ul of acetic anhydride and 4 ml of pyridine and agitated for 3hrs at room temperature. The reaction was stopped by adding ice and the partially acetylated oligocarrageenan was isolated by precipitation with cold methanol. It was freeze-dried, lyophilized.

(ii) Grafting of caprolactone on partially acetylated oligocarrageenan

To graft hydrophobic caprolactone, 2ml of toluene and 20ul tin (II) ethyl hexanoate catalyst was added to 200 mg of partially acetylated-oligocarrageenan and stirred at 40 °C for 2hrs under argon atmosphere. After 2hrs slowly 330 mg of ϵ -caprolactone was added and allowed to polymerize for 20 h at 110 °C. The resulting caprolactone grafted oligocarrageenan was precipitated using cold methanol.

(iii) Deprotection of partially acetylated oligocarrageenan grafted caprolactone

The acetyl groups were removed by adding THF/methanol (v/v=1/1) solution to the partially acetylated oligocarrageenan grafted caprolactone. This mixture was stirred for 4hr at room temperature by adding sodium methoxide (NaOCH₃) solution drop wise until the pH reached 8. After it was neutralized by 1 M HCL and evaporated under vacuum. This resulted in the formation of amphiphilic copolymer that was lyophilized.

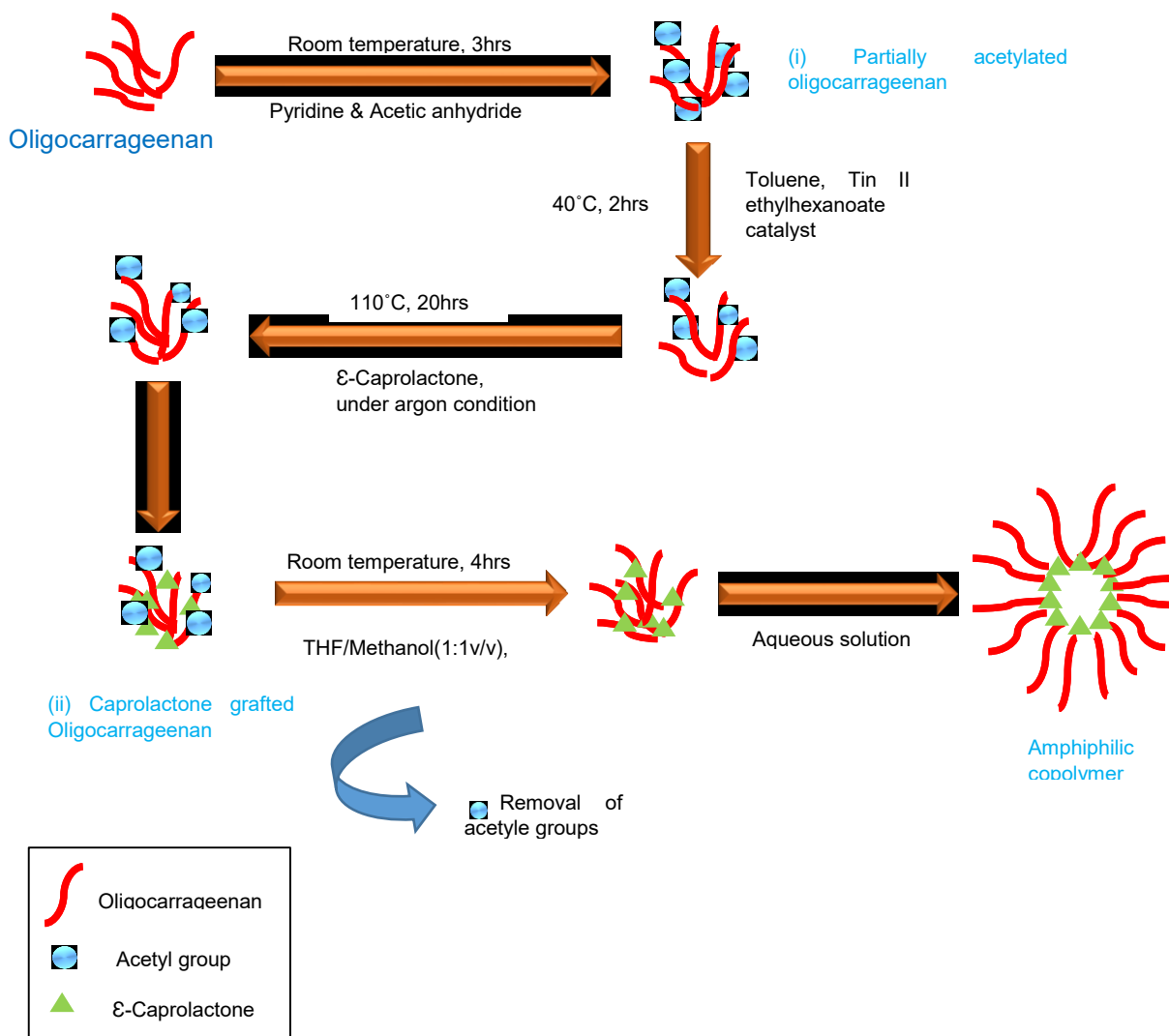


Figure 23: Mechanism of formation of copolymer caprolactone grafted carrageenan micelles.

Characterization of carrageenan micelles

Digested oligocarrageenan, partially acetylated oligocarrageenan and amphiphilic copolymer oligocarrageenan grafted caprolactone were analysed by NMR and the particle size distribution of carrageenan micelles was analysed by DLS

Drug loading

Curcumin encapsulation was done using the acetone volatilization method as previously described. About 500mg of carrageenan micelles were mixed with 50 mg of curcumin and dissolved in 10 ml of acetone. This mixture was slowly agitated overnight at room temperature by addition of deionized water (250 ml) drop wise. Acetone was evaporated at 30 °C and the non-encapsulated curcumin was eliminated by a 0.22 μm filter (stericup GP Millipore) (Fig 24).

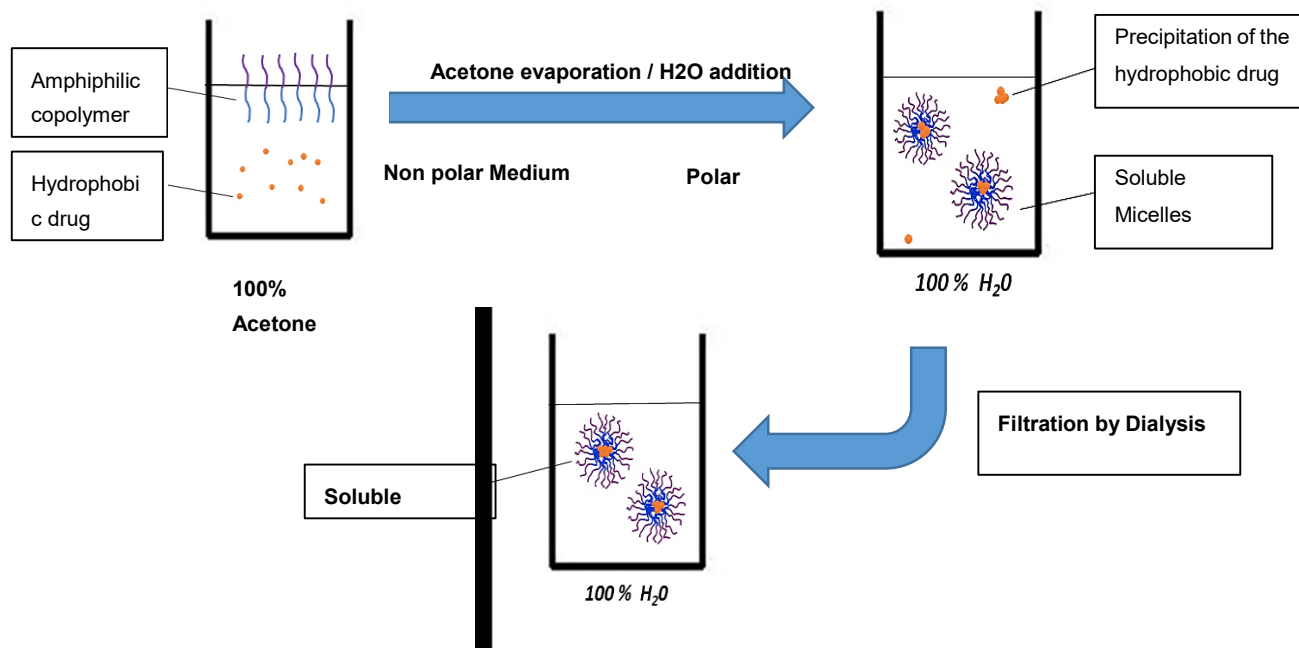


Figure 24: Schematics of curcumin drug loading method.

In vivo model: Zebrafish tail amputation model

Zebrafish (*Danio rerio*) 3dpf larvae were used for this study. Female and male adult zebrafish were kept separately 1 week before crossing and then crossed for obtaining the embryos. Embryos were maintained in fish water for normal development until 3 days and used for the regeneration studies.

Tail amputation

The 3 dpf zebrafish larvae were first anaesthetized by 0.2% tricaine for about 20-40 seconds. Then, the larvae were placed on the slide and the caudal fin (tail) was amputated just close to the notochord using a blade. Then, larvae were immediately placed back in fish water or respective treatments (Fig 25).

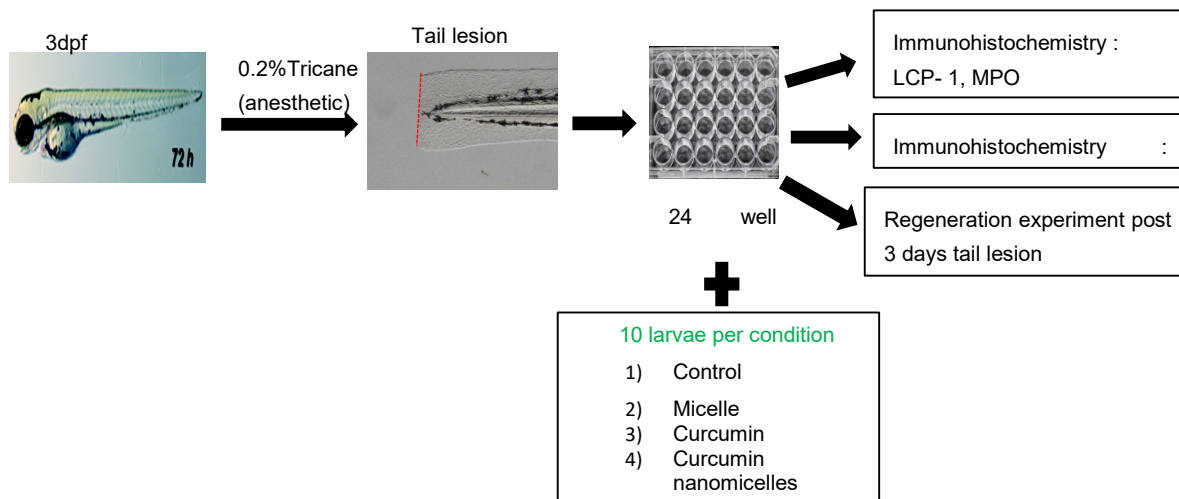


Figure 25: *In vivo* zebrafish tail amputation model.

III. Results

Results of this study are assembled into an article titled “**Protective effect of Curcumin encapsulated micelles on tail regeneration of zebrafish larvae**”. It is in the process of submission to Zebrafish journal.

Curcumin-encapsulated nanomicelles promote tissue regeneration in zebrafish larvae

Sai Sandhya Narra ¹, Laura Gence ¹, Latufa Youssouf ¹ Joël Couprie ¹, Pierre Giraud ¹,
Nicolas Diotel ^{1,2*#}, Christian Lefebvre D'Hellencourt ^{1,2*#}

¹ Université de La Réunion, INSERM UMR 1188, Diabète athérombose Réunion Océan Indien (DéTROI), Saint-Denis de La Réunion, France. narra.sai-sandhya@univ-reunion.fr; latufa.youssouf@gmail.com; pierre.giraud@univ-reunion.fr

#These 2 authors contribute equally to the paper

* Correspondence: christian.lefebvre-d-hellencourt@univ-reunion.fr; nicolas.diotel@univ-reunion.fr

Abstract

Regenerative medicine is an emerging field to understand mechanistics and to develop therapeutic strategies for pathological conditions including neurodegenerative diseases and diabetic microvascular complications. Nanocarriers are used to improve drug bioavailability, solubility and therapeutic abilities. In this study, we used for the first time curcumin loaded κ -carrageenan-graft-polycaprolactone (KC-g-PCL) nanomicelles to investigate their regenerative potential using a model of tail amputation in zebrafish larvae. First, we showed that curcumin encapsulated KC-g-PCL spherical micelles had a mean size of 92 ± 32 nm and that micelles were successfully loaded with curcumin. These micelles showed a slow and controlled drug release over 72h. The toxicity of curcumin nanomicelles was then tested on zebrafish larvae based on the survival rate after 24h. Next, the non-toxic dose of curcumin nanomicelles was used in physiopathological models of zebrafish tail injury. At this non-toxic concentration, curcumin nanomicelles increased the recruitment of neutrophils and macrophages 6 hours post-lesion as shown by Mpo and Lcp1 immunohistochemistry, respectively. Furthermore, we demonstrated that curcumin nanomicelles improve tail regeneration within 3 days post-amputation, compared with empty micelles or curcumin alone. Therefore, our study demonstrates that curcumin nanomicelles can modulate inflammatory processes *in vivo* and promote regeneration. Further investigation can give a better understanding of the mechanisms and new therapeutics sustaining regeneration.

Keywords: Zebrafish, curcumin; nanomicelles; regeneration; tail amputation; carrageenan

Introduction

Wound healing is a natural process that involves restoration of the damaged cells, tissues and organs. The wound environment is associated with high levels of inflammation and oxidative stress that involves the recruitment of immune cells [1]. Diabetes associated with hyperglycemia, chronic inflammation can lead to several disorders including foot amputations, which are highly prevalent and are an issue of mortality. Indeed, impaired wound healing may result in chronic wound development which is observed in

diabetic foot ulcers. [2]. A better understanding of the cellular basis of wound pathology is needed to effectively manage the wounds and develop therapeutic strategies [3]. Therefore, exploring and understanding the mechanisms of self-renewal provides insight into the regeneration processes and help for the development of new regenerative therapeutic strategies [4].

The use of zebrafish (*Danio rerio*) allows to study various pathophysiological processes and has gained the attention of researchers worldwide [5-7]. Indeed, zebrafish shares a strong genomic homology as well as common

physiological processes with mammals [8]. Due to their ability to regenerate, zebrafish has emerged as a model to study wound healing and regeneration [9-12]. Many zebrafish models have been developed in adult fish and larvae for studying regeneration of liver, pancreas, spinal cord, heart, brain [13, 14], retina and tail [15, 16]. The zebrafish tail is relatively accessible for amputation and has simple cellular organization. The tail regeneration process involves 1) epidermal cell migration that covers the wound and epidermal apical cap signaling centre, 2) cell dedifferentiation into mesenchymal blastema structure, 3) proliferation of blastema and replacement of amputated tissue [17]. Many signaling molecules including sonic hedgehog ligands [18], Wnts [19], bone morphogenic proteins (BMPs) [20, 21], fibroblast growth factors (FGFs) [22], insulin-like growth factors (IGFs) [23], and retinoic acids (RAs) [24] are involved in the fin regeneration process. As most organs start to function within 5 days post fertilization, it is reliable to use larvae for large sample size screening and shorter time frames.

Curcumin is a hydrophobic polyphenol molecule present in turmeric isolated from *Curcuma longa* that is widely used as a curry spice. It is the major curcuminoid of turmeric displaying many therapeutic properties including anti-inflammatory, antioxidant, anti-proliferative, anti-angiogenic, anti-diabetic and wound healing [25]. However, the hydrophobic nature, poor bioavailability, low solubility, as well as rapid degradation and clearance of curcumin limits its therapeutic benefits [26]. To overcome these limitations and enhance the therapeutic benefits of curcumin many nanoformulations including liposomes, polymeric micelles and polymer-curcumin conjugates have been developed [27].

Polymeric micelles made of sulphated marine polysaccharides including alginin, carrageenan, chitosan, and dextran copolymerized with different polymers are newly emerging in wound healing research and therapeutics [28-30]. Marine sulphated polysaccharides have many bioactivities such as anti-oxidative, anti-microbial, wound healing, anti-cancer anti-inflammatory and anti-viral properties [31]. Curcumin has

previously been encapsulated into carrageenan nanomicelles that were non-cytotoxic *in vitro* in EA-hy926 endothelial cells and *in vivo* in adult zebrafish. In this study, the nanomicelles have been shown to improve the cellular uptake of curcumin and to promote the anti-inflammatory effect of curcumin at 15 μ M by decreasing the levels of inflammatory factors IL-6 and MCP-1 in TNF-alpha-induced inflammation *in vitro* compared to empty micelles and curcumin alone [32].

In our work, we used curcumin encapsulated carrageenan nanomicelles that were prepared and characterized by NMR and DLS analyses and we also studied the curcumin drug release. In the present study, we first tested the curcumin nanomicelles toxicity in 3 days post fertilization (dpf) larvae for 24h by monitoring the survival rate. Next, we performed a tail injury on 3-dpf larvae to investigate the effect of curcumin nanomicelles on the recruitment of neutrophils and macrophages at the damaged site. We further studied its impact on tail regeneration using the same model.

Materials and methods

Extraction and digestion of carrageenan

Carrageenans were extracted from red algae *Kappaphycus alvarezii* obtained from Ibis Algaculture (Madagascar) as previously described [33]. The algae were treated with 80% ethanol solution and agitated overnight at room temperature to remove all the salts and debris. The next day, the carrageenans were hot extracted in water (90°C, pH 7) along with ultrasound. They were then filtered, jellified at 4°C, frozen at -80°C and lyophilized. The carrageenans extracted were composed of κ -carrageenan (68%) and λ -carrageenan (32%) as analysed previously by NMR [33].

The κ -carrageenase enzyme was used to digest the κ -carrageenan to use for the micelle preparation. This enzyme was isolated from *Pseudoaltermonas carrageenovora* (DSMZ, Germany). The bacteria were stimulated with a 0.15% (M/v) κ -carrageenan solution as previously described [32]. Briefly the bacteria were cultured in 1litre of marine broth at 21°C under agitation. When the OD reached 0.6, the bacteria were stimulated with a 0.15% (M/v) of

a κ -carrageenan solution prepared in Tris-HCl 100mM pH=8.5. After 24h the enzyme was filtered 0.45 μ m filter (Millipore) and 300kDa cut off membrane filter and concentrated by 10kDa centrifugal filter. It was finally desalted by a 3 KDa centrifugal filter and the protein content was determined by Bradford assay.

Enzymatic digestion of κ -carrageenan was done using a κ -carrageenase enzyme which hydrolyses β -(1 \rightarrow 4) the linkage of carrageenan as previously described [32]. κ -carrageenase (75.3 μ g in 1 ml) was used to digest the carrageenans (150mg) dissolved in a Tris-HCl solution (100 mM, pH 8.5) incubated for 6h, 8h and 10h respectively. Non- hydrolysed κ -carrageenan and λ -carrageenan were eliminated by ultracentrifugation using 10kDa centricon. The oligocarrageenans were isolated by precipitation with methanol, freeze-dried, lyophilized and analysed by Size Exclusion Chromatography (SEC) and Nuclear magnetic resonance (NMR). The enzymatic activity was measured as previously described [32]. Digested oligocarrageenan octamers obtained after 8hrs of carrageenan digestion similar to previous studies [32], were used to synthesise carrageenan micelles grafted with polycaprolactone (PCL) after removing the enzyme by ultracentrifugation.

Preparation of carrageenan micelles

The carrageenan micelles were synthesised as previously described [32]. The preparation involved three steps (i) partial acetylation of oligocarrageenan (digested carrageenan) hydroxyl groups (ii) Grafting of hydrophobic caprolactone on partially acetylated oligocarrageenan (iii) deprotection of the partially acetylated hydroxyl groups.

(i) Partial acetylation of oligocarrageenan

Five hundred mg of oligocarrageenan was mixed with 644ul of acetic anhydride and 4 ml of pyridine and agitated for 3h at room temperature. The reaction was stopped by adding ice and the partially acetylated oligocarrageenan was isolated by precipitation with cold methanol. It was then freeze-dried, lyophilized and characterized by NMR.

(ii) Grafting of caprolactone on partially acetylated oligocarrageenan

To graft, the hydrophobic caprolactone, 2ml of toluene and 20ul tin (II) ethyl hexanoate catalyst was added to 200 mg of partially acetylated-oligocarrageenan. The mixture was stirred at 40 °C for 2h under argon atmosphere after 330 mg of ϵ -caprolactone was added and was allowed to polymerize for 20 h at 110 °C. The resulting caprolactone grafted oligocarrageenan was precipitated using cold methanol. It was then freeze-dried, lyophilized and characterized by NMR.

(iii) Deprotection of the partially acetylated oligocarrageenan grafted caprolactone

The acetyl groups are removed by adding THF/methanol (v/v=1/1) solution to the partially acetylated oligocarrageenan grafted caprolactone. This mixture was stirred for 4hr at room temperature by adding sodium methoxide (NaOCH₃) solution dropwise until the pH reached 8. After it was neutralized by 1 M HCL and evaporated under vacuum. This resulted in the formation of amphiphilic copolymers which were lyophilized and analysed by NMR.

Drug loading

Curcumin encapsulation was done using the acetone volatilization method as previously described [32]. About 500mg of carrageenan micelles were mixed with 50 mg of curcumin and dissolved in 10 ml of acetone. This mixture was slowly agitated overnight at room temperature by dropwise addition of deionized water (250 ml). Acetone was evaporated at 30 °C followed by the non-encapsulated curcumin was eliminated by a 0.22 μ m filter (stericup GP Millipore).

Characterization of carrageenan micelles

NMR analysis

NMR analysis was performed on a 600 MHz Avance III Bruker NMR spectrometer equipped with a ¹H/¹⁹F, ¹³C and ¹⁵N cryoprobe. 1D ¹H and 1D ¹³C spectra were recorded in 100%

D₂O or CDCl₃ (Eurisotop, France) at room temperature and tetramethylsilane (TMS, Sigma-Aldrich, Germany) was used as a reference as described previously. ¹H NMR spectra were recorded with 128 scans using a sweep width of 10 ppm. 2D spectra were obtained with 32 scans and a sweep width of 10 ppm for ¹H and 120 ppm for ¹³C. In all spectra, the carrier was placed at 4.7 ppm for ¹H and 50 ppm for ¹³C as performed previously [32].

Determination of particle size

The particle size distribution of carrageenan micelles was analysed using Dynamic Light Scattering (DLS) particle size analyser (Zetasizer Nano (Malvern Instruments) as previously described. 1ml of an aqueous solution of amphiphilic micelles prepared in PBS filtered through a 0.22 µm pore size PTFE syringe filter (to remove any aggregates. The CMC (Critical Micelle concentration) was determined at concentrations of 1 & 2 mg/ml. CMC was obtained by plotting the logarithm of the intensity of the scattered light as a function of oligocarrageenan-graft-PCL concentration as previously described [32].

Drug release

The drug release was done by dialysis method using a dialysis membrane as previously described. 20 mg of curcumin-loaded micelles were dissolved in 10 ml of PBS and were subjected to dialysis using a Cellu-Sep H1 dialysis membrane (MWCO = 2000 Da) immersed in 200 ml of PBS at 37°C. The amount of curcumin released in the PBS was measured by absorbance at 420 nm over 3 days.

Zebrafish husbandry

Zebrafish (*Danio rerio*) were housed in the facility at the CYROI/DéTROU (La Réunion). Adult fish (AB strain) were maintained under standard conditions of temperature (28.5°C for adult fish and 26.5°C for larvae), photoperiod (14h dark and 10h light), pH (7.4) and conductivity (400 µS). Fish were fed 3 times a day with Gemma Micro 300 (Planktovie). All the animal experiments were conducted in

accordance with the French and European Community Guidelines for the Use of Animals in Research (86/609/EEC and 2010/63/EU).

Larva acute toxicity test

To determine a maximum non-toxic concentration (MNTC), we evaluated the toxicity of micelles, curcumin, and curcumin-encapsulated micelles on 3-days post-fertilization (dpf) larvae. Newly fertilized eggs were maintained in fish water for normal development at 26.5°C. At 3-dpf, zebrafish larvae (10 per group) were treated with different concentrations (5 µM, 10 µM and 30 µM) of empty micelles, curcumin and curcumin encapsulated micelles for 24h. As 15µM of curcumin encapsulated micelles showed anti-inflammatory activity *in vitro*, we first decided to test the toxicity of some concentrations of curcumin-encapsulated micelles ranged from 5 to 30 µM it was on zebrafish larvae. After 24h of treatment, larvae survival was analysed. The MNTC was then determined, which corresponds to the highest concentration that did not induce any death.

Tail amputation and treatment

Amputation and treatments were performed on the 3-dpf zebrafish larvae as previously described [34]. Briefly, larvae were first anaesthetized with 0.02% tricaine (MS-222). They were then placed on a microscopic slide and the caudal fin was amputated just close to the notochord using a blade, under a stereomicroscope. After the amputation, larvae were immediately placed back in E3 medium (Control) or the respective treatments namely micelles, curcumin and curcumin encapsulated micelles at the MNTC (10 µM).

Analyses of immune cell recruitment and tail regeneration

The recruitment of macrophages (Lcp1+ cells) and neutrophils (Mpo+ cells) was performed on 3-dpf larvae exposed to the above-mentioned treatments for 6h after the tail amputation. Briefly, the amputated larvae were placed in micelles, free curcumin and curcumin

encapsulated micelles at the MNTC (10 μ M) for 6h, before being fixed in 4% paraformaldehyde overnight at 4°C and processing for immunohistochemistry experiments.

For tail regeneration assay, the amputated larvae were placed in the above mentioned treatments for 3 days with daily renewal of the treatments. Pictures were taken using a stereomicroscope after anaesthetizing the larvae, at 0 and 3-days post-lesion. The regeneration area was then analysed by Image J software.

Tissue preparation & Immunohistochemistry

For Lcp1 staining, fixed larvae were washed 4 times with 1X PBS containing 0.1% tween-20 (PTW) for permeabilization. Then, larvae were washed 3 times in distilled water for 5 min and further permeabilized with cold acetone (-20 °C) for 10 min at room temperature. Larvae were next washed with distilled water and PTW. Then, the blocking of nonspecific sites was performed using a blocking buffer (PTW with 2ml BSA 10%, 0.1ml DMSO) for 1h at room temperature. Larvae were then treated with primary rabbit anti-Lcp1 antibody (GeneTex, reference: GTX124420, dilution: 1/200 in blocking buffer) and incubated overnight at 4°C.

For Mpo staining, fixed larvae were dehydrated with 25, 50, 75 and 100% methanol (MeOH) series and stored at -20°C overnight. Larvae were next gradually rehydrated and washed 4 times in PTW for 5 min. After 1h in blocking buffer, larvae were treated with primary antibody rabbit anti-Mpo (Abcam, ref: ab210563, dilution: 1/200 in blocking buffer) and incubated overnight at 4°C.

The next day, after washes with PTW, larvae were incubated with fluorescent secondary antibody Alexa Fluor® 594 donkey anti-rabbit antibody (1:500 dilution, Abcam, Reference: ab150064) and DAPI (4',6'-diamidino-2-phenylindole, Dihydrochloride) (1 ng/ml, ThermoFisher, Reference: D1306) counterstaining (4',6'-diamidino-2-phenylindole, Dihydrochloride) (1 ng/ml, ThermoFisher, Reference: D1306) for 2h at room temperature. Finally, larvae were washed 3 times with PTW and visualized by fluorescence microscopy.

Statistical analysis and microscopy

Data were expressed as mean \pm SD (standard deviation) of three independent experiments. Statistical analysis was performed by one-way analysis of variance (ANOVA) followed by Bonferroni's multiple comparison test using Graph-Pad Prism 6 (Graph Pad Software, Inc., San Diego, CA, USA). Statistical significance was considered for a p-value < 0.05.

Images were acquired using a Nikon eclipse 80i equipped with a Hamamatsu camera, a Nikon SMZ18 stereomicroscope equipped with a Nikon DS-Fi3 Camera and the respective NIS elements software.

Images were analysed using Image J software. Quantification of regenerated fin area, fluorescence intensity and cell numbers were performed and then the results were averaged.

Results

Characterization of carrageenan micelles by nuclear magnetic resonance (NMR) analysis

OligoKC-g-PCL (oligo kappa-carrageenan-grafted-polycaprolactone) was synthesized using previously described method [32]. Briefly, hydroxyl groups of digested carrageenan (oligocarrageenan) (Figure 1a) were partially acetylated and then copolymerized with hydrophobic ϵ -caprolactone (PCL). Self-assembled amphiphilic carrageenan micelles in an aqueous solution were obtained by removing acetyl groups.

The ^1H NMR analysis of digested and undigested carrageenan is represented in Figure 1a. Partially acetylated oligoKC-g-PC was analysed using ^1H NMR. The peak at 2.13 ppm corresponds to acetyl functional groups (Figure 1b). The ^1H NMR spectra of partially acetylated oligoKC-g-PC indicated 60 % of acetylation based on integration values of protons at 5.04 ppm and 4.6 ppm (corresponding to anomeric H in oligocarrageenan) and at 2.13 ppm (acetyl groups).

Oligocarrageenan-graft-caprolactone analysed by ^1H NMR spectrum (Figure 1c) showed both PCL signals between 1.3 and 4 ppm,

oligocarrageenan signals from 3 to 5.5 ppm and acetyl protons which detected in the above step at 2.09 ppm is not detected in this spectrum confirming the removal of partial acetyl groups in the last step.

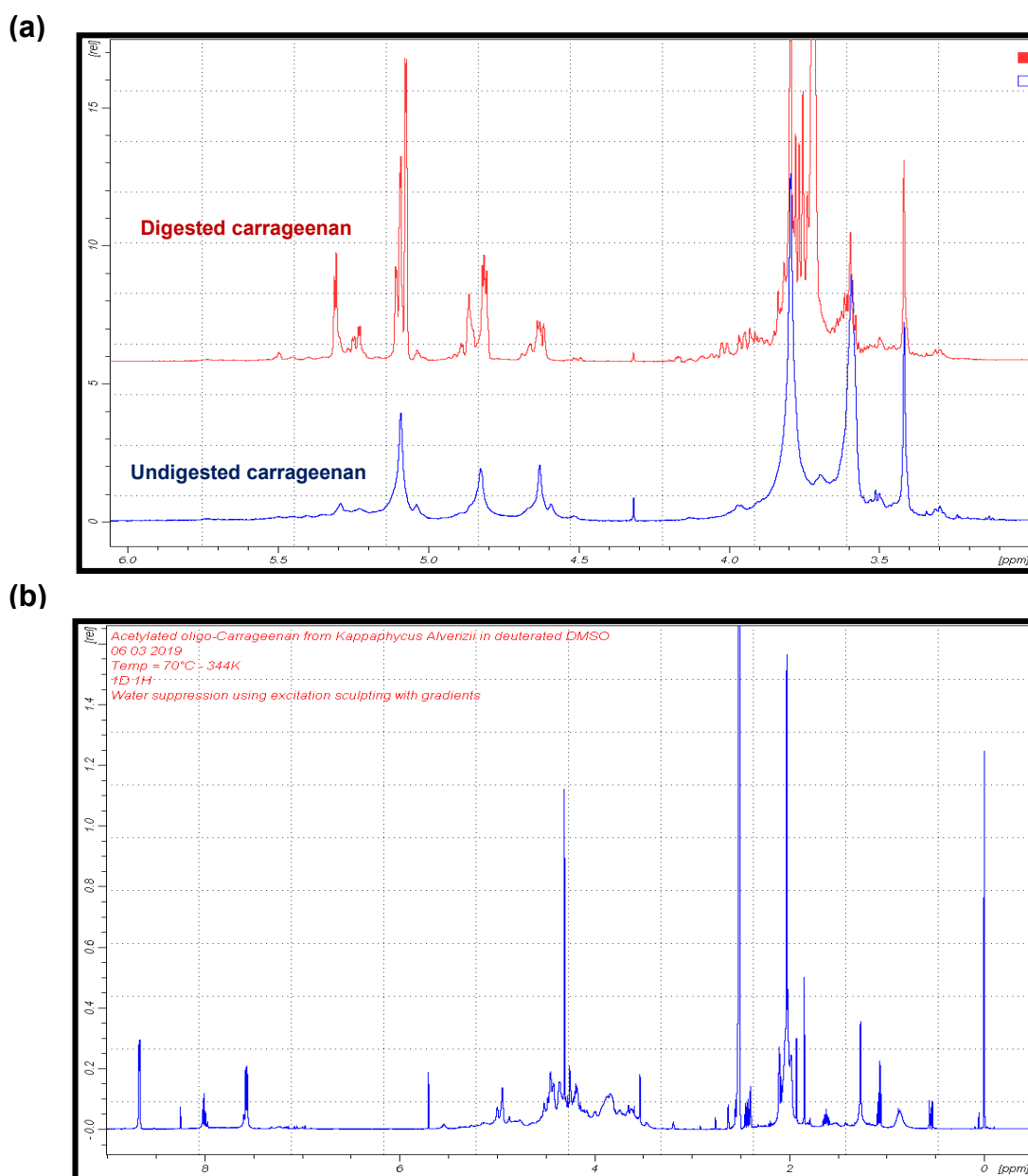
Drug loading and release studies

Hydrophobic curcumin was encapsulated into carrageenan micelles using acetone volatilisation method and drug release studies were done using dialysis method [32]. The amount of drug encapsulated was determined by UV absorption and calibration curve. The drug release studies of Curcumin encapsulated micelles were done using 1X

The results of carrageenan micelles (oligoKC-g-PCL) characterization were in agreement with the previous results.

PBS and dialysis method at 37°C (Figure 2). The drug release of Curcumin was determined to be 60 % after 72 h.

The drug release rate and amount of curcumin encapsulated in nanomicelles were similar to the previously developed micelles [32]. As demonstrated previously, the drug release rate can vary depending on the interaction between the drug and micelle core.



(c)

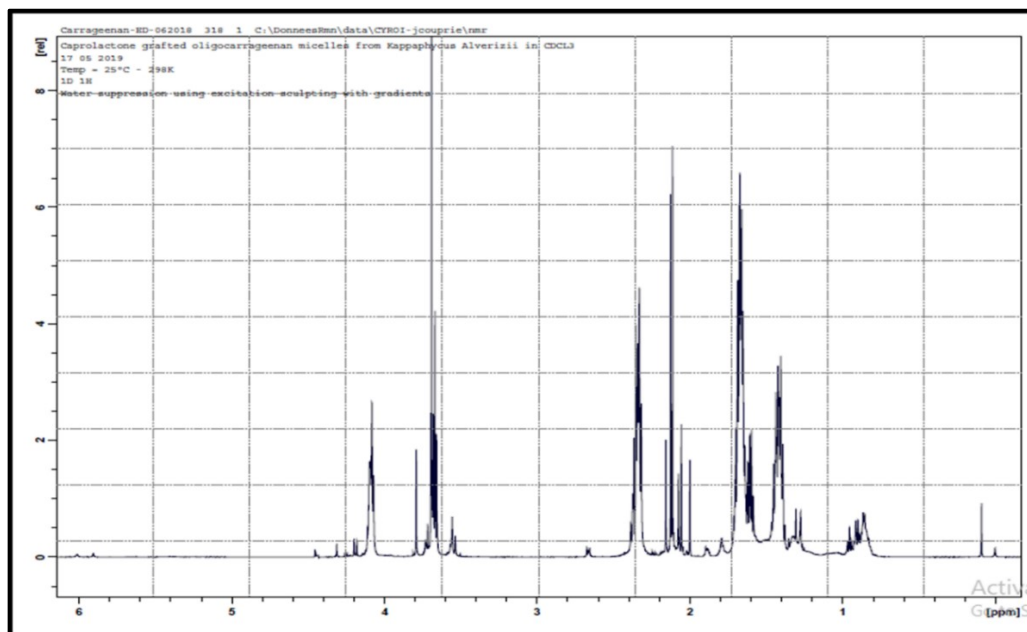


Figure 1: Characterization of carrageenan nanomicelles by NMR analysis. **a)** ¹H NMR spectra of digested oligo-carrageenan (red spectrum) and undigested-oligocarrageenan (blue spectrum) prepared in D₂O. **b)** ¹H NMR spectrum of acetylated oligo-carrageenan with acetyl-group protons detected at 2.13 ppm prepared in CDCl₃. **c)** ¹H NMR spectrum of acetylated-oligocarrageen-graft-PCL sample prepared in CDCl₃. ¹H NMR spectrum of oligocarrageen-graft-PCL sample prepared in D₂O, oligocarrageenan signals were detected between 3ppm and 5.5ppm and caprolactone between 1.3 ppm and 4 ppm.

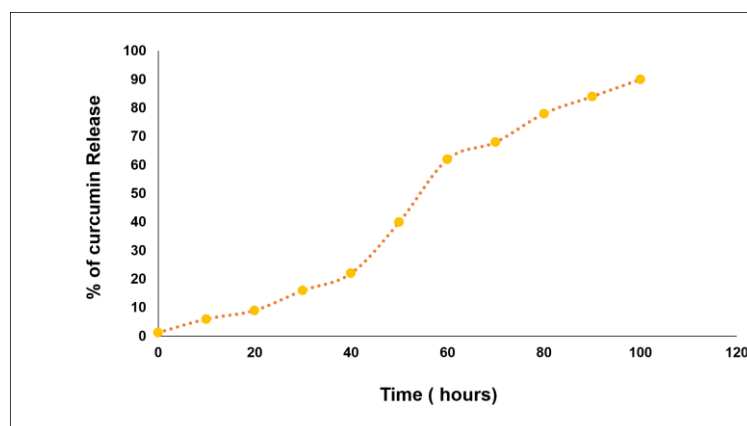


Figure 2: Kinetic studies of curcumin release from carrageenan nanomicelles. Drug released into the PBS medium was measured by absorbance at 420 nm.

Particle size determination of carrageenan micelles (oligoKC-g-PCL) and curcumin encapsulated micelles by dynamic light scattering (DLS) analysis

The average particle size of empty micelles was determined to be 142±93 nm and curcumin encapsulated micelles was 92±32 nm as shown in Figure 3a and 3b respectively. The CMC estimated by DLS was 4.10⁻⁵ M. A

polydispersity index (PDI) near to zero implies homogeneity of dispersions, and a PDI greater than 0.3 indicates heterogeneity. The PDI of our Cur-nanomicelles nanoparticles was around 0.2. The particle size of curcumin encapsulated micelles is smaller than the empty micelles due to the strong interaction of curcumin with the hydrophobic PCL core of micelles which may cause the shrinkage of the micelles. As well, the particle size of empty micelles was interestingly

smaller compared to the previously developed micelles, suggesting a higher surface area for

functionalization and then a better uptake by the cells.

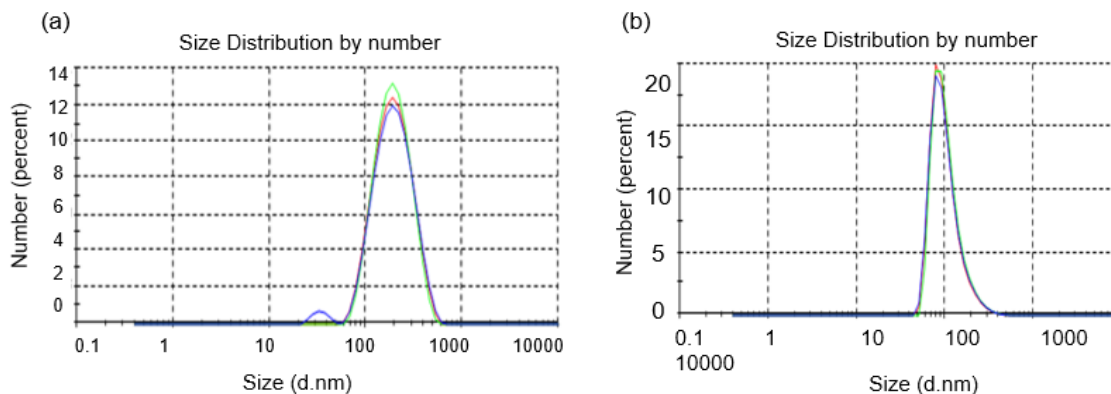


Figure 3: Particle size distribution of carrageenan nanomicelles determined by DLS analysis. Samples were prepared in PBS at 1 μ g/ml. Size distribution of empty micelles (a) and curcumin encapsulated micelles (b). Data is presented as three independent measurements for each sample.

Acute toxicity of curcumin nanomicelles in 3-dpf zebrafish larvae

To study the toxicity of micelles, curcumin and curcumin encapsulated micelles, 3-dpf were treated with different concentrations of the above-mentioned conditions for 24h. Micelles alone did not show a toxic effect on the survival rate at 5, 10 and 30 μ M (Figure 4). In contrast, a

significant mortality was observed for curcumin alone and curcumin-encapsulated micelles at 30 μ M. At lower concentrations (5 and 10 μ M), we did not observe any death. Based on these results, we decided to use the concentration of 10 μ M of empty micelles and curcumin-encapsulated micelles for assessing their biological properties.

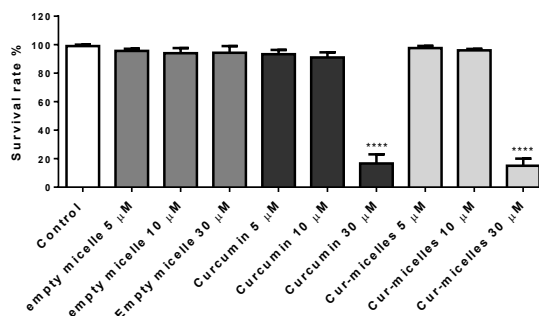


Fig 4: Toxicity of curcumin nanomicelles on 3-dpf zebrafish larvae. The toxicity was determined by measuring the survival rate of larvae after 24 hours of exposure with E3 medium (control), empty micelles, curcumin and Cur-micelles (5 μ M, 10 μ M and 30 μ M). Survival rate percentage was calculated by counting the number of alive and dead larvae after the different treatments for 24h. Curcumin and curcumin nanomicelles were both toxic at 30 μ M concentration. Data are represented as mean \pm SD of three independent experiments, n=60 larvae per condition. **** p <0.0001 as compared to control.

Effect of curcumin nanomicelles on regeneration and immune cell recruitment in a model of tail injury

After determining the MNTC of curcumin, empty and curcumin loaded micelles, we

decided to further investigate their potential effects on regeneration and immune cell recruitment in a model of tail amputation on 3-dpf larvae as used recently [34]. To this aim, we monitored the effect of curcumin encapsulated

micelles on the regenerative area and recruitment of neutrophils and macrophages by Mpo and Lcp1 immunostainings, respectively.

For that, 3-dpf larvae were amputated and treated with E3 medium, micelles, curcumin and curcumin encapsulated micelles. Three days after the transection, the tail regeneration was significantly increased with curcumin-encapsulated micelles compared to control, micelle or curcumin alone (Figure 7), demonstrated pro-regenerative properties of curcumin on this tail injury model.

Given that the inflammatory cells recruited at the site of injury play a role in tail regeneration [35] we decided to further investigate the effect

of curcumin encapsulated micelles on immune cell recruitment.

As shown in Figure 5, the recruitment of Lcp1-positive cells labelling macrophages was significantly higher in larvae treated with curcumin encapsulated micelle compared to control, empty micelles or curcumin alone. Similar results were obtained for Mpo-positive cells corresponding to neutrophils (Figure 6). Indeed a higher number of neutrophils was observed at the site of injury in the larvae treated with curcumin encapsulated micelles exposure compared to control, micelles or curcumin alone.

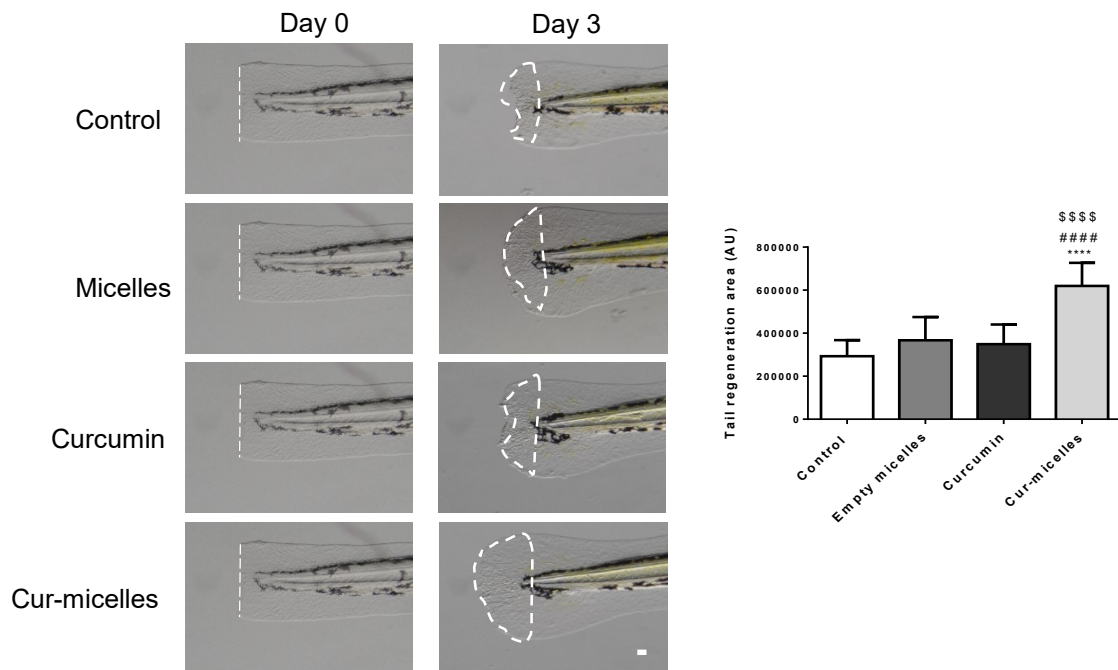


Figure 7: Curcumin nanomicelles promote the regeneration of the zebrafish tail after amputation.

A) Representative images of larval tail amputation and regeneration after the different treatments (control, micelles, curcumin, cur-micelles at 10 μ M) as previously mentioned. B) Quantification of the regenerative area of zebrafish tail 3 days post-amputation. Curcumin nanomicelles treated larvae showed an increased tail regeneration compared to the ones treated with empty micelles and curcumin alone. Data are represented as mean \pm SD of three independent experiments, N=30 larvae per condition. Bar = 0.07mm. **** $p < 0.0001$ as compared to control, #### $p < 0.0001$ as compared to empty micelles and \$\$\$\$ $p < 0.0001$ as compared to curcumin (One-way ANOVA).

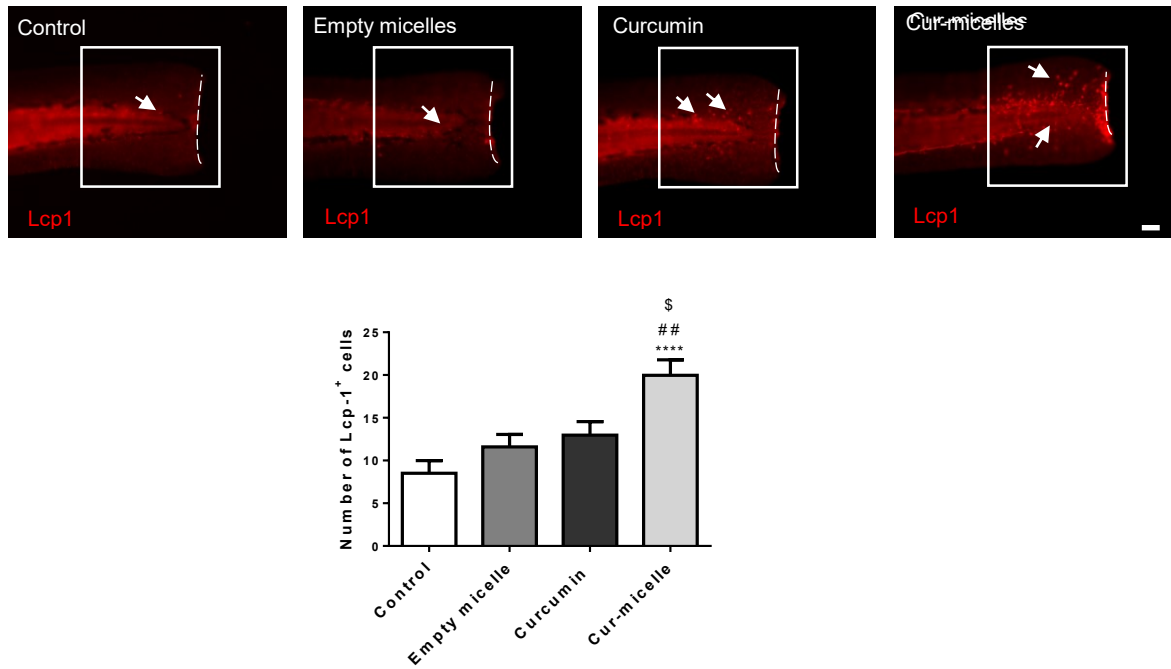


Figure 5: Curcumin nanomicelles increase the recruitment of macrophages at the tail injury site.

A) Representative images of Lcp1-positive cell recruitment at the site of tail amputation in the different conditions 6 hours post injury. B) Quantification of Lcp1-positive cells at the site of tail amputation in different conditions (10 μ M each). White arrows indicate the Lcp1-positive cells and the white dotted line indicates the level of tail amputation. Curcumin nanomicelles treated larvae showed an increased recruitment of Lcp1 cells compared to larvae treated with empty micelles and curcumin alone. Data are represented as mean \pm SD of three independent experiments, n=30 per condition. Bar = 0.1mm. **** $p < 0.0001$ as compared to control, ### $p < 0.0001$ as compared to empty micelles and \$\$\$\$ $p < 0.0001$ as compared to curcumin (One-way ANOVA).

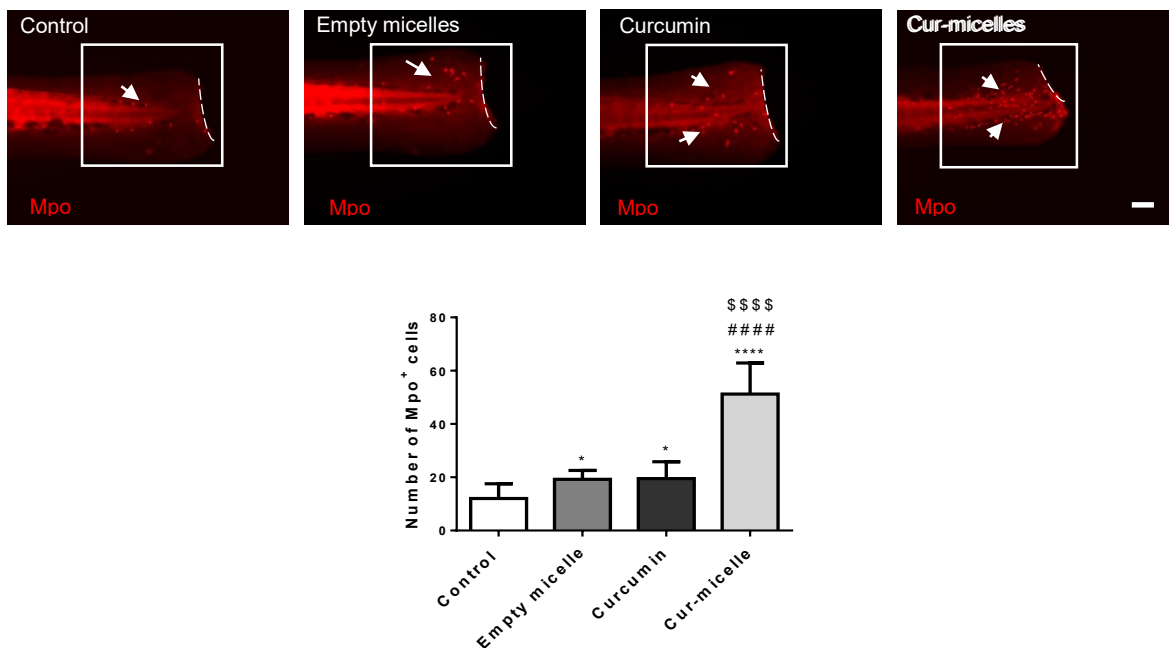


Figure 6: Curcumin nanomicelles increases the recruitment of neutrophils at the tail injury site.

A) Representative images of Mpo-positive cell recruitment at the site of tail amputation in the different conditions (10 μ M) 6 hours post tail amputation. B) Quantification of Mpo-positive cells at the site of tail amputation in different conditions (10 μ M). White arrows indicate the Mpo-positive cells and the white dotted line indicates the tail amputation. Curcumin nanomicelles treated larvae showed an increased MPO cell recruitment compared to the larvae treated with empty micelles and curcumin alone. Data are represented as mean \pm SD of three independent experiments, N=30 per condition. Bar = 0.1mm. **** $p < 0.0001$ as compared to control, #### $p < 0.0001$ as compared to empty micelles and \$\$\$\$ $p < 0.0001$ as compared to curcumin (One-way ANOVA).

Discussion

Curcumin has been used in regenerative wound healing studies [36, 37]. In our curcumin encapsulated nanomicelles (Cur-micelles) interestingly showed a smaller particle size 142 ± 93 nm compared to the previously developed curcumin nanomicelles which were determined to be 187 ± 21 nm [32]. Curcumin drug release was 60% by 72h indicating a slow and controlled drug release similar to the previous studies. Our *in vivo* studies using zebrafish larvae showed that cur-micelles enhanced tail regeneration and recruitment of neutrophils (Mpo), macrophages (Lcp1) at the site of the tail injury compared to curcumin or micelle alone.

Zebrafish fin amputation causes acute inflammation which triggers a rapid increase in ROS production [38]. Within 24 hours of tail amputation ROS mediated chemokine and cytokine signals from the site of amputation tends to increase the proliferation and migration of epithelial cells to the site of injury and contributes to the formation of new tissue. As neutrophils have limited phagocytic capacity and rapidly undergo apoptosis, macrophages replace the neutrophils that play a crucial role in phagocytosis of the tissue debris and resolves the inflammatory responses and remains until the tissue repair [39]. Macrophages also promote fin regeneration by down regulating the ROS at the site of injury [38]. Macrophage depletion was linked to decreased tissue regeneration [39] while neutrophil depletion did not affect the fin regeneration in adult zebrafish [40]. Caudal fin regeneration also involves cell migration and proliferation of epidermis and mesenchymal cells which contribute to the regenerative tissue. Wound epidermis at the tail injury covers the underlying matured tissue from which the highly proliferative mesenchymal

cells grow and regenerate the lost tissue [7]. FGF receptor fgfr 1 is involved in the signaling of epithelial cap, mesenchymal cells and blastema recruitment needed for proliferation and regeneration of tail tissue [41, 42]. Sonic hedgehog (shh) signaling may also be involved in fin regeneration [43]. Our results were in agreement with previous studies on zebrafish tail regeneration [39] and mice [38] which showed increased neutrophil and macrophage recruitment to the site of amputation.

Curcumin plays a synergistic role in attributing to the healing property. The studies of polyphenol molecules including flavonoids reveal that they promote wound healing by several mechanisms such as scavenging free radicals and reactive oxygen species, suppressing acute inflammation through time-dependent regulation of pro-inflammatory and anti-inflammatory chemokine expression [44]. The anti-microbial property of the polyphenol molecules also contributes to wound healing by avoiding prolonged inflammation by reducing the microbial load at the site of injury [45]. But therapeutic benefits of curcumin are limited by poor bioavailability, solubility due to its hydrophobic nature [46]. Many nano-formulations of curcumin encapsulated nanoparticles have been developed recently to overcome these limitations and enhance its therapeutic properties [47]. The bio-distribution of Cur-micelles in zebrafish and mice showed their accumulation in liver, lungs and brain tissues [32]. Although many beneficial effects of curcumin have been shown in wound healing and regeneration [48], the effect of nano-formulated curcumin on zebrafish tail regeneration has not yet been studied or explored. Our curcumin encapsulated micelles showed regenerative wound healing potential of curcumin encapsulated nanomicelles that could further be developed

as a new therapeutic strategy for impaired diabetic wound healing.

Conclusion

This study demonstrates the regenerative wound healing potential of curcumin nanomicelles by increasing the neutrophil and macrophage recruitment at the damage site which possibly enhances the zebrafish tail regeneration.

Author's Contribution

N.D and L.G designed the experiments. All the authors participated in the analysis of the experiments and/ or in the writing of the article.

Disclosure statement

The authors declare no competing interests.

Funding information

This work was supported by grants from La Reunion University and from FEDER (RE0022527-ZEBRATOX) EU-Region Reunion-French state national counterpart.

References

1. Nelson, G., et al., *The senescent bystander effect is caused by ROS-activated NF-kappaB signalling*. Mech Ageing Dev, 2018. **170**: p. 30-36.
2. Baltzis, D., I. Eleftheriadou, and A. Veves, *Pathogenesis and treatment of impaired wound healing in diabetes mellitus: new insights*. Adv Ther, 2014. **31**(8): p. 817-36.
3. Lindholm, C. and R. Searle, *Wound management for the 21st century: combining effectiveness and efficiency*. Int Wound J, 2016. **13 Suppl 2**: p. 5-15.
4. Sanchez Alvarado, A. and P.A. Tsonis, *Bridging the regeneration gap: genetic insights from diverse animal models*. Nat Rev Genet, 2006. **7**(11): p. 873-84.
5. Kanungo, J., et al., *Zebrafish model in drug safety assessment*. Curr Pharm Des, 2014. **20**(34): p. 5416-29.
6. Bruneel, B., et al., *Imaging the zebrafish dentition: from traditional approaches to emerging technologies*. Zebrafish, 2015. **12**(1): p. 1-10.
7. Gemberling, M., et al., *The zebrafish as a model for complex tissue regeneration*. Trends Genet, 2013. **29**(11): p. 611-20.
8. Howe, K., et al., *The zebrafish reference genome sequence and its relationship to the human genome*. Nature, 2013. **496**(7446): p. 498-503.
9. Pfefferli, C. and A. Jazwinska, *The art of fin regeneration in zebrafish*. Regeneration (Oxf), 2015. **2**(2): p. 72-83.
10. Beffagna, G., *Zebrafish as a Smart Model to Understand Regeneration After Heart Injury: How Fish Could Help Humans*. Front Cardiovasc Med, 2019. **6**: p. 107.
11. Stoick-Cooper, C.L., R.T. Moon, and G. Weidinger, *Advances in signaling in vertebrate regeneration as a prelude to regenerative medicine*. Genes Dev, 2007. **21**(11): p. 1292-315.
12. Marz, M., et al., *Regenerative response following stab injury in the adult zebrafish telencephalon*. Dev Dyn, 2011. **240**(9): p. 2221-31.
13. Ghaddar, B., et al., *Cellular Mechanisms Participating in Brain Repair of Adult Zebrafish and Mammals after Injury*. Cells, 2021. **10**(2).
14. Baumgart, E.V., et al., *Stab wound injury of the zebrafish telencephalon: a model for comparative analysis of reactive gliosis*. Glia, 2012. **60**(3): p. 343-57.
15. Iovine, M.K., *Conserved mechanisms regulate outgrowth in zebrafish fins*. Nat Chem Biol, 2007. **3**(10): p. 613-8.
16. Nakatani, Y., A. Kawakami, and A. Kudo, *Cellular and molecular processes of regeneration, with special emphasis on fish fins*. Dev Growth Differ, 2007. **49**(2): p. 145-54.
17. Tal, T.L., J.A. Franzosa, and R.L. Tanguay, *Molecular signaling networks that choreograph epimorphic fin regeneration in*

- zebrafish - a mini-review.*
Gerontology, 2010. **56**(2): p. 231-40.
18. Braunstein, J.A., et al., *Basal epidermis collective migration and local Sonic hedgehog signaling promote skeletal branching morphogenesis in zebrafish fins.* Dev Biol, 2021. **477**: p. 177-190.
 19. Stoick-Cooper, C.L., et al., *Distinct Wnt signaling pathways have opposing roles in appendage regeneration.* Development, 2007. **134**(3): p. 479-89.
 20. Quint, E., et al., *Bone patterning is altered in the regenerating zebrafish caudal fin after ectopic expression of sonic hedgehog and bmp2b or exposure to cyclopamine.* Proc Natl Acad Sci U S A, 2002. **99**(13): p. 8713-8.
 21. Smith, A., et al., *Inhibition of BMP signaling during zebrafish fin regeneration disrupts fin growth and scleroblasts differentiation and function.* Dev Biol, 2006. **299**(2): p. 438-54.
 22. Poss, K.D., et al., *Roles for Fgf signaling during zebrafish fin regeneration.* Dev Biol, 2000. **222**(2): p. 347-58.
 23. Chablais, F. and A. Jazwinska, *IGF signaling between blastema and wound epidermis is required for fin regeneration.* Development, 2010. **137**(6): p. 871-9.
 24. Blum, N. and G. Begemann, *Retinoic acid signaling controls the formation, proliferation and survival of the blastema during adult zebrafish fin regeneration.* Development, 2012. **139**(1): p. 107-16.
 25. Topman, G., F.H. Lin, and A. Gefen, *The natural medications for wound healing - Curcumin, Aloe-Vera and Ginger - do not induce a significant effect on the migration kinematics of cultured fibroblasts.* J Biomech, 2013. **46**(1): p. 170-4.
 26. Jurenka, J.S., *Anti-inflammatory properties of curcumin, a major constituent of Curcuma longa: a review of preclinical and clinical research.* Altern Med Rev, 2009. **14**(2): p. 141-53.
 27. Araya-Sibaja, A.M., et al., *Use of nanosystems to improve the anticancer effects of curcumin.* Beilstein J Nanotechnol, 2021. **12**: p. 1047-1062.
 28. Ni, J., et al., *Curcumin-carboxymethyl chitosan (CNC) conjugate and CNC/LHR mixed polymeric micelles as new approaches to improve the oral absorption of P-gp substrate drugs.* Drug Deliv, 2016. **23**(9): p. 3424-3435.
 29. Akbar, M.U., et al., *In-vivo anti-diabetic and wound healing potential of chitosan/alginate/maltodextrin/pluronic-based mixed polymeric micelles: Curcumin therapeutic potential.* Int J Biol Macromol, 2018. **120**(Pt B): p. 2418-2430.
 30. Mocanu, G., M. Nichifor, and L. Sacarescu, *Dextran based Polymeric Micelles as Carriers for Delivery of Hydrophobic Drugs.* Curr Drug Deliv, 2017. **14**(3): p. 406-415.
 31. Lee, Y.E., et al., *Marine polysaccharides: therapeutic efficacy and biomedical applications.* Arch Pharm Res, 2017. **40**(9): p. 1006-1020.
 32. Youssof, L., et al., *Enhanced effects of curcumin encapsulated in polycaprolactone-grafted oligocarrageenan nanomicelles, a novel nanoparticle drug delivery system.* Carbohydr Polym, 2019. **217**: p. 35-45.
 33. Youssof, L., et al., *Ultrasound-assisted extraction and structural characterization by NMR of alginates and carrageenans from seaweeds.* Carbohydr Polym, 2017. **166**: p. 55-63.
 34. Laura Gence, D.F., Matthieu Bringart , Bryan Veeren,, F.B. Armelle Christophe, Olivier Meilhac, Jean-Loup Bascands and, and N. Diotel, *Hypericum lanceolatum Lam. Medicinal Plant: Potential Toxicity and Therapeutic Effects Based on a*

- Zebrafish Model*. Front in pharmacol, 2022. **13**.
35. Keightley, M.C., et al., *Delineating the roles of neutrophils and macrophages in zebrafish regeneration models*. Int J Biochem Cell Biol, 2014. **56**: p. 92-106.
 36. Sidhu, G.S., et al., *Curcumin enhances wound healing in streptozotocin induced diabetic rats and genetically diabetic mice*. Wound Repair Regen, 1999. **7**(5): p. 362-74.
 37. Jagetia, G.C. and G.K. Rajanikant, *Curcumin treatment enhances the repair and regeneration of wounds in mice exposed to hemibody gamma-irradiation*. Plast Reconstr Surg, 2005. **115**(2): p. 515-28.
 38. Morales, R.A. and M.L. Allende, *Peripheral Macrophages Promote Tissue Regeneration in Zebrafish by Fine-Tuning the Inflammatory Response*. Front Immunol, 2019. **10**: p. 253.
 39. Li, L., et al., *Live imaging reveals differing roles of macrophages and neutrophils during zebrafish tail fin regeneration*. J Biol Chem, 2012. **287**(30): p. 25353-60.
 40. Petrie, T.A., et al., *Macrophages modulate adult zebrafish tail fin regeneration*. Development, 2014. **141**(13): p. 2581-91.
 41. Richardson, R., et al., *Adult zebrafish as a model system for cutaneous wound-healing research*. J Invest Dermatol, 2013. **133**(6): p. 1655-65.
 42. Poss, K.D., J. Shen, and M.T. Keating, *Induction of *lef1* during zebrafish fin regeneration*. Dev Dyn, 2000. **219**(2): p. 282-6.
 43. Laforest, L., et al., *Involvement of the sonic hedgehog, patched 1 and bmp2 genes in patterning of the zebrafish dermal fin rays*. Development, 1998. **125**(21): p. 4175-84.
 44. Pastore, S., et al., *Plant polyphenols regulate chemokine expression and tissue repair in human keratinocytes through interaction with cytoplasmic and nuclear components of epidermal growth factor receptor system*. Antioxid Redox Signal, 2012. **16**(4): p. 314-28.
 45. Shedoeva, A., et al., *Wound Healing and the Use of Medicinal Plants*. Evid Based Complement Alternat Med, 2019. **2019**: p. 2684108.
 46. Guzman-Villanueva, D., et al., *Design and in vitro evaluation of a new nano-microparticulate system for enhanced aqueous-phase solubility of curcumin*. Biomed Res Int, 2013. **2013**: p. 724763.
 47. Stohs, S.J., et al., *Highly Bioavailable Forms of Curcumin and Promising Avenues for Curcumin-Based Research and Application: A Review*. Molecules, 2020. **25**(6).
 48. Tejada, S., et al., *Wound Healing Effects of Curcumin: A Short Review*. Curr Pharm Biotechnol, 2016. **17**(11): p. 1002-7.

IV. Discussion

Diabetic peripheral artery disease including foot ulcers is a major issue of foot amputations that involves failure of wound healing in diabetic conditions. Many studies are emerging to understand the mechanisms of wound healing and regeneration that can be used to develop some new strategies for diabetic peripheral artery disease associated with foot amputations (Alavi et al., 2014). Zebrafish are being widely used for regeneration and wound healing studies as they share many morphological and genetic aspects with humans (J. Y. Kim et al., 2018; Richardson et al., 2013).

Our study has shown that curcumin loaded nanomicelles promote the neutrophil and macrophage recruitment at the site of tail amputation which was in agreement with previous studies on zebrafish tail amputation of both larvae and adults (Morales & Allende, 2019). Macrophages and neutrophils are the main immune cells that migrate to the wound after injury which invade the microorganism and remove cell debris (Petrie, Strand, Yang, Rabinowitz, & Moon, 2014). This helps in promoting regeneration of new tissues at the site of injury. Many inflammatory factors including cytokines and chemokines also produced by macrophages that triggers inflammatory signaling to recruit more immune cells to the site of injury (Morales & Allende, 2019).

Our study has also shown the potential of curcumin loaded nanomicelles in promoting regeneration by increasing the regeneration area post tail amputation compared to both curcumin and micelle alone.

V. Conclusion

The curcumin loaded nanomicelles have shown wound healing and regenerative potential of zebrafish tail amputation. This can be further studied to understand the mechanism involved in the wound healing and regeneration to develop new therapeutics for diabetic amputations.

Perspectives and conclusion

***In vitro* approach of HDL nanoparticles**

Reconstituted HDL (rHDL) loaded with various polyphenols molecules can be interesting prospective to study and understand the mechanism and develop therapeutics for diabetic stroke. In this study we have already used curcumin loaded rHDLs to test its cellular uptake and cytoprotective properties (reduced ER stress, oxidative stress, cell membrane integrity, reduced chromatin condensation) on methylglyoxal induced cytotoxicity and stress (oxidative stress, ER stress, impaired cell membrane integrity) in murine cerebral endothelial cells.

Curcumin loaded rHDLs can be further studied for understanding the mechanistic impact of curcumin loaded rHDLs on methylglyoxal impaired BBB functionality by evaluating the tight junction proteins Zo-1, occludin and claudin 5 gene expression analysis by RT qPCR, distribution by immunocytochemistry and permeability of the cerebral endothelial cells membrane by dextran permeability assay.

Further rHDL can be loaded with resveratrol, which is a well-known polyphenol found in grapes and groundnuts. Resveratrol similar to curcumin shows many biological activities including antioxidant, anti-inflammatory, anti-cancer and cardioprotective properties (A. P. Singh et al., 2019). In humans resveratrol is known to be rapidly absorbed by oral administration and detected in plasma and urine but the potential therapeutic benefits of the pure molecule is still limited (Bano, Ahmed, Khan, Chaudhary, & Samim, 2020). Recent animal studies have shown potential use of resveratrol in treating metabolic disorders such as obesity and diabetes (Breuss, Atanasov, & Uhrin, 2019; A. P. Singh et al., 2019).

We have done some preliminary studies with resveratrol loaded rHDLs nanoparticles (Res-rHDLs). Cerebral endothelial – bEnd.3 cell line was used. Res-rHDLs were prepared and the amount of resveratrol in Res-rHDLs was quantified by LC- MS/MS analysis similar to Cur-rHDLs. We further evaluated the impact of Res-rHDLs on methylglyoxal induced cytotoxicity in cerebral endothelial cells.

Preliminary results

Effect of free resveratrol on MGO cytotoxicity in cerebral endothelial cell viability

The effect of free resveratrol on MGO cytotoxicity in cerebral endothelial cell viability was evaluated by MTT assay. Cells were seeded in a 96 well plates at a cell density of 5×10^3 for

24 h. Culture medium was removed and cells were pre-treatment with different concentrations of resveratrol (0.1 μM to 20 μM) for 1hr before 2 mM MGO treatment for 24h. After 24h 5mg/ml of MTT reagent was added and absorbance was measured at 570 nm.

Resveratrol was not cytotoxic even at higher concentrations up to 20 μM . It showed a cytoprotective effect on MGO cytotoxicity at 10 μM and 20 μM concentrations. The non-protective resveratrol concentration was 0.1 μM (Fig 26).

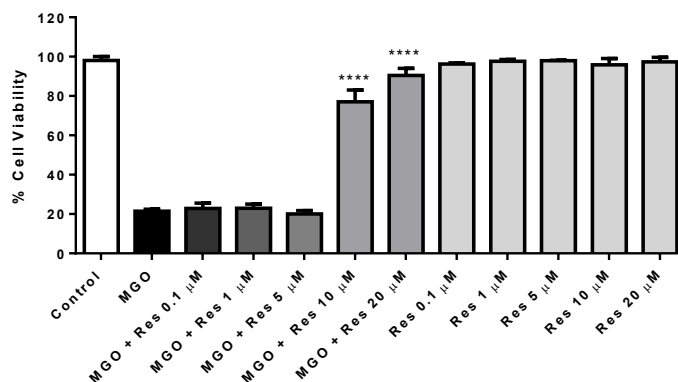


Figure 26: Effect of free resveratrol on bEnd3 cerebral endothelial cells treated with MGO.

Cells were pre-treated with different resveratrol concentrations (0.1 μM – 20 μM) for 1h followed by 2mM MGO treatment for 24 h. Cell viability was assessed by 3-(4, 5-dimethylthiazol-2-yl)-2, 5-diphenyltetrazolium bromide (MTT) assay. Data are represented as mean \pm SD of three independent experiments. ****p<0.0001 as compared to MGO.

Quantification of resveratrol loaded in rHDL by LC-MS analysis

Quantification of resveratrol by LC-MS analysis revealed that about 2.8 mM resveratrol was present in the resveratrol loaded rHDL sample and the recovery of resveratrol was around 75.9% (Table 3).

HDL+R-S1	
INTENSITY	AREA
28,5	26,8
30,0	29,6
29,3	28,2
2898,5	2793,9
Mean [RESV]	2846,2
Expected RESV concentration in μM	3750
Recovery (%)	75,9

Table 3: Quantification of resveratrol by LC-MS analysis.

Effect of res-rHDL nanoparticles on MGO cytotoxicity in cerebral endothelial cell viability

Effect of resveratrol loaded rHDLs on MGO cytotoxicity in cerebral endothelial cell was evaluated by MTT assay. Cells were seeded in a 96 well plates at a cell density of 5×10^3 for 24 h. Culture medium was removed and cells were pre-treatment with different concentrations of resveratrol, rHDL and resveratrol loaded rHDL (Res-rHDLs) before the 2 mM MGO treatment for 24 h. After 24h 5mg/ml of MTT reagent was added and absorbance was measured at 570 nm.

Res-rHDLs did not show a synergistic effect on MGO cytotoxicity even at 0.2 mg/ml rHDL and 4 μ M resveratrol concentrations compared to HDL or resveratrol alone (Fig 27).

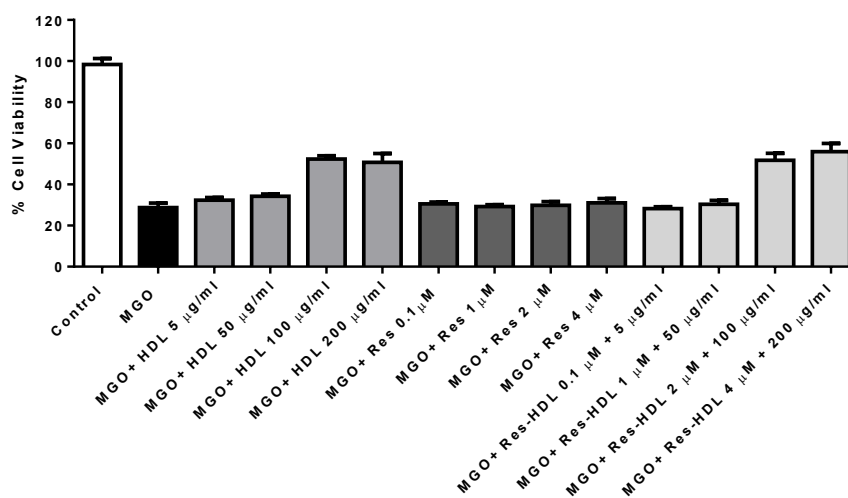


Figure 27: Effect of resveratrol loaded rHDLs on bEnd3 cerebral endothelial cells treated with MGO.

Cells were pre-treated with different concentrations of resveratrol, rHDLs, Res-rHDLs for 1 h followed by 2 mM MGO treatment for 24 h. Cell viability was assessed by 3-(4, 5-dimethylthiazol-2-yl)-2, 5-diphenyltetrazolium bromide (MTT) assay. Data are represented as mean \pm SD of three independent experiments.

Res-rHDLs preparation should be further modified to adjust the resveratrol and rHDL ratio to have a potential synergistic effect. HDL-enriched curcumin or resveratrol could be developed as a new therapeutic approach for diabetic vascular complications concerning stroke that involve

involves oxidative stress, inflammation, ER stress, endothelial dysfunction and BBB dysfunction.

***In vitro* approach of curcumin nanomicelles**

Curcumin nanomicelles have already shown *in vitro* non-cytotoxicity, anti-inflammatory effect, and *in vivo* biodistribution in liver, kidney, intestine and brain of mice.

Further, curcumin nanomicelles impact on oxidative stress, ER stress, and BBB dysfunction can be studied using cerebral endothelial cells (b.End.3) in hyperglycemia condition to understand the mechanism of action and to develop therapeutic strategy for diabetes. Intracellular reactive oxygen species levels can be tested via DCFH-DA fluorescent probe assay, ER stress by RT qPCR gene expression analysis of ER stress markers (XBP-1, ATF-4, Bip, CHOP, ATF-6) and BBB dysfunction by studying tight junction integrity using Xcelligence system (to study real time impedance of membrane integrity), RT qPCR gene expression study of tight junction proteins (ZO-1, Claudin 5 and occluding) and immunocytochemistry (Fig 30).

Along with curcumin, resveratrol loaded nanomicelles can also be evaluated on the above mentioned approach. It would be further interesting to investigate whether curcumin or resveratrol nanomicelles show synergistic effect compared to micelles or curcumin alone if they can enhance the therapeutic potential of the drugs.

Preliminary results

Evaluation of Cur-micelles or Res-micelles cytotoxicity on cerebral endothelial cells

Resveratrol loaded nanomicelles (Res-micelles) were prepared similar to the curcumin loaded nanomicelles (Cur-micelles). Cerebral endothelial – bEnd.3 cell line was used. We have tested both curcumin and resveratrol loaded nanomicelles on bEnd.3 cytotoxicity by MTT assay for 24h. Cells were seeded in a 96 well plates at a cell density of 5×10^3 for 24 h. Culture medium was removed and cells were pre-treated with different concentrations of micelles, curcumin, resveratrol, Cur-micelles and Res-micelles for 24 h. After 24 h 5mg/ml of MTT reagent was added and absorbance was measured at 570nm.

Cur-micelles and Res-micelles were not cytotoxic until 1000mg/ml and 500mg/ml concentrations respectively. Free curcumin was cytotoxic at 10 μ M while Cur-micelles at 100mg/ml corresponding to 21.6 μ M was not cytotoxic. Free resveratrol was cytotoxic at 20 μ M while Res-micelles at 500mg/ml corresponding to 26 μ M was not cytotoxicity (Fig 28).

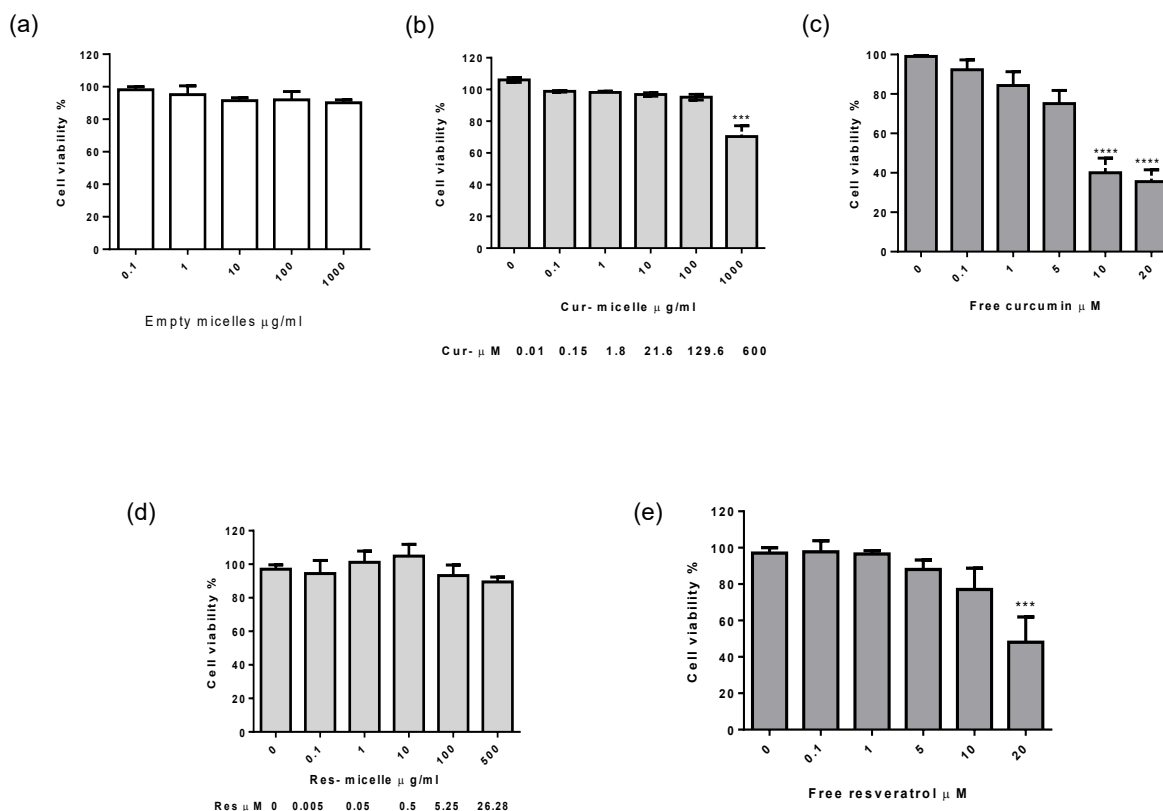


Figure 28: Cytotoxicity of curcumin or resveratrol loaded micelles on bEnd3 cerebral endothelial cells.

Cells were pre-treated with different concentrations of resveratrol empty micelles, free resveratrol and cur-micelles/Res-micelles for 24 h. a) Represents the cell viability was assessed by 3-(4, 5-dimethylthiazol-2-yl)-2, 5-diphenyltetrazolium bromide (MTT) assay. Data are represented as mean \pm SD of three independent experiments. **** p <0.0001, *** p <0.001 as compared to control.

Other *in vitro* studies of curcumin or resveratrol micelles can be done to understand the mechanisms of regeneration and wound healing. RAW 264.7 macrophage cell line can be used to study the impact of curcumin loaded carrageenan micelles on wound healing by performing scratch assay (Fig 30).

Preliminary cytotoxicity studies of curcumin loaded nanomicelles on RAW 246.7 cells were done by MTT assay at 24h. Curcumin nanomicelles did not show any cytotoxicity while free curcumin showed cytotoxicity at 50uM (Fig 29).

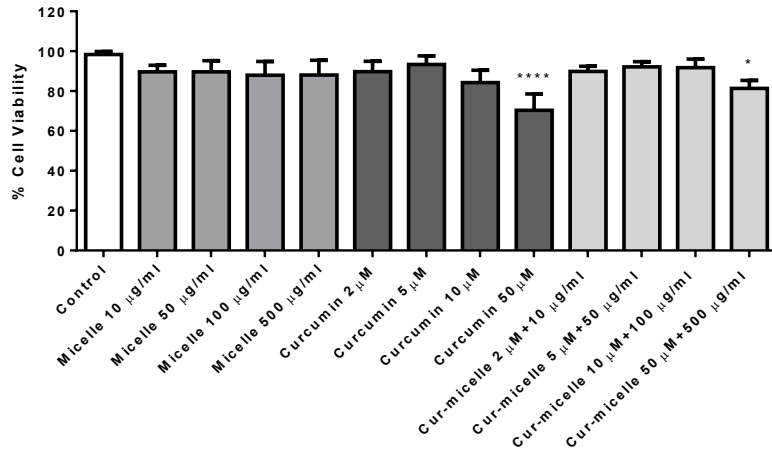


Figure 29: Cytotoxicity of Curcumin loaded micelles on RAW 264.7 macrophage cells.

Cells were pre-treated with different concentrations of resveratrol empty micelles, free resveratrol and cur-micelles/Res-micelles for 24 h. a) Represents the cell viability was assessed by 3-(4, 5-dimethylthiazol-2-yl)-2, 5-diphenyltetrazolium bromide (MTT) assay. Data are represented as mean \pm SD of three independent experiments. **** $p < 0.0001$, * $p < 0.05$ as compared to control.

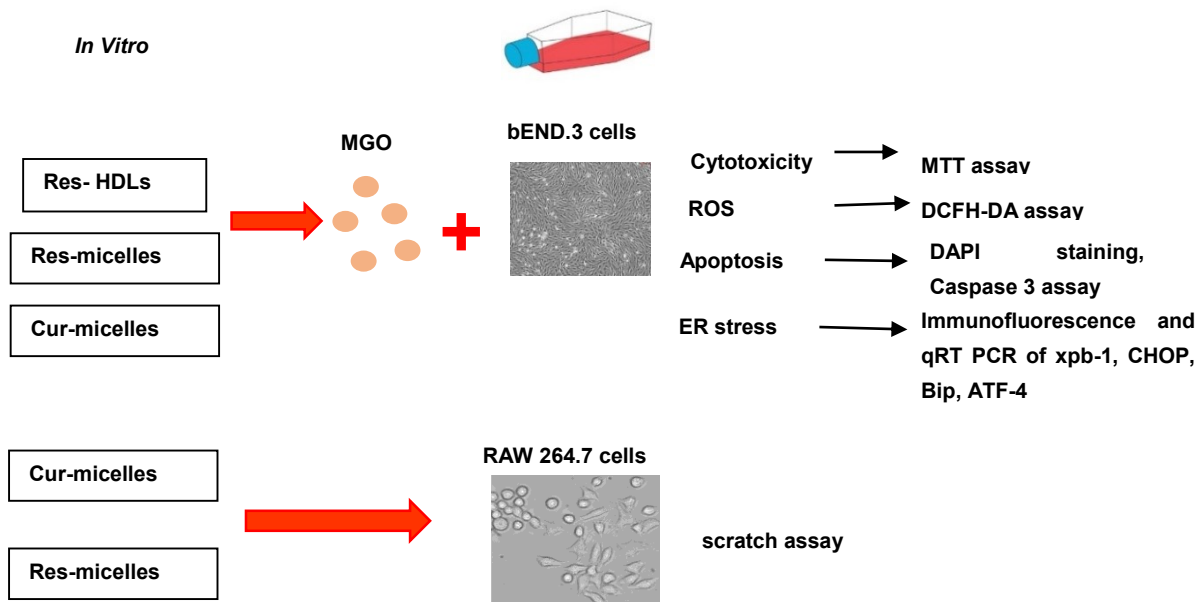


Figure 30: Illustration of *in vitro* approach of using drug encapsulated vectors.

***In vivo* approach of HDL nanoparticles**

Neuroprotective effects of HDL was tested in ischemic stroke condition previously in our lab (Tran-Dinh et al., 2020). The objective of this study was to prevent the deleterious effects of stroke in diabetic conditions is of major focus by using HDL particle as therapeutic strategy. Transient middle cerebral artery occlusion (tMCAO) mouse model was used. Different experimental conditions including Control, tMCAO and endothelial SR-BI deficient mice were injected with HDLs or saline to test the neuroprotective effects of HDLs. HDL showed endothelial protection in MCAO mouse model via SR-BI (scavenger receptor type BI) endothelial receptors. Results of this study revealed that HDLs alone were not enough and only partially limited the infarct volume and hemorrhagic complications in the stroke mouse model under hyperglycemic condition but shows a potential neuro and vasculoprotective properties for acute stroke (Couret et al., 2021).

Further it could be interesting to use HDL particles with improved physiochemical properties and loaded with drug molecules such as curcumin, resveratrol as drug delivery system. Drug loaded HDL particles could enhance the therapeutic properties of drug molecules combined with HDL bioactive properties. Curcumin or resveratrol loaded HDLs or micelles can further be tested and studied to limit the stroke infarct volumes in MCAO stroke mouse model compared to only HDLs or drug alone (curcumin or resveratrol) (Fig 31).

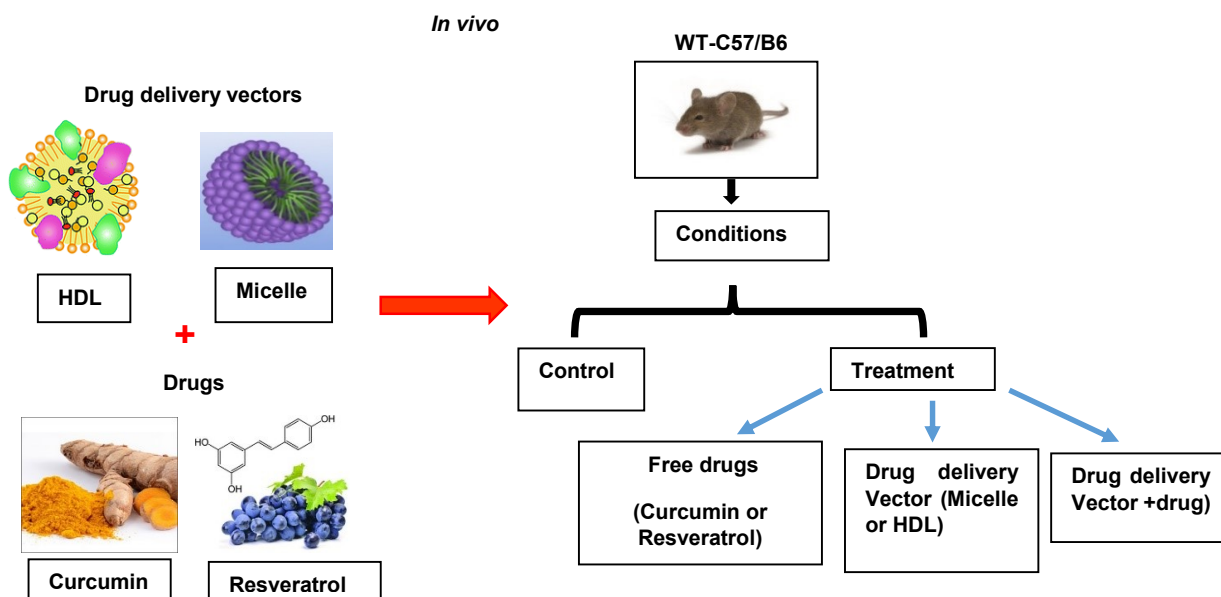


Figure 31: Illustration of *in vivo* approach of using drug encapsulated vectors in MCAO mice model.

Conclusion

This study demonstrated the potential of HDL and micelles nanoparticles that improved the efficiency of curcumin therapeutic benefits. Cur-HDL nanoparticles showed an improved endothelial protection from methylglyoxal endothelial dysfunction and Cur-micelles showed enhanced zebrafish tail regeneration. This study can further be explored to understand the mechanisms of cerebrovascular damage concerning stroke and wound healing mechanisms concerning diabetic amputation. It further opens new perspectives for the nanoencapsulation of other polyphenol molecules like resveratrol to understand and develop new therapeutic strategies for diabetic complications such as stroke and diabetic amputation.

References

- Abdullah, A., & Ravanan, P. (2018). The unknown face of IRE1alpha - Beyond ER stress. *Eur J Cell Biol*, 97(5), 359-368. doi:10.1016/j.ejcb.2018.05.002
- Abdullahi, W., Tripathi, D., & Ronaldson, P. T. (2018). Blood-brain barrier dysfunction in ischemic stroke: targeting tight junctions and transporters for vascular protection. *Am J Physiol Cell Physiol*, 315(3), C343-C356. doi:10.1152/ajpcell.00095.2018
- Aggarwal, B. B., Deb, L., & Prasad, S. (2014). Curcumin differs from tetrahydrocurcumin for molecular targets, signaling pathways and cellular responses. *Molecules*, 20(1), 185-205. doi:10.3390/molecules20010185
- Agrawal, M., Saraf, S., Saraf, S., Antimisariis, S. G., Chougule, M. B., Shoyele, S. A., & Alexander, A. (2018). Nose-to-brain drug delivery: An update on clinical challenges and progress towards approval of anti-Alzheimer drugs. *J Control Release*, 281, 139-177. doi:10.1016/j.jconrel.2018.05.011
- Ahmad, M. Z., Akhter, S., Mohsin, N., Abdel-Wahab, B. A., Ahmad, J., Warsi, M. H., . . . Ahmad, F. J. (2014). Transformation of curcumin from food additive to multifunctional medicine: nanotechnology bridging the gap. *Curr Drug Discov Technol*, 11(3), 197-213. doi:10.2174/1570163811666140616153436
- Ahmadi-Eslamloo, H., Dehghani, G. A., & Moosavi, S. M. S. (2018). Long-term treatment of diabetic rats with vanadyl sulfate or insulin attenuate acute focal cerebral ischemia/reperfusion injury via their antiglycemic effect. *Metab Brain Dis*, 33(1), 225-235. doi:10.1007/s11011-017-0153-7
- Ahmed, A. B., Adel, M., Karimi, P., & Peidayesh, M. (2014). Pharmaceutical, cosmeceutical, and traditional applications of marine carbohydrates. *Adv Food Nutr Res*, 73, 197-220. doi:10.1016/B978-0-12-800268-1.00010-X
- Ajith, T. A., & Vinodkumar, P. (2016). Advanced Glycation End Products: Association with the Pathogenesis of Diseases and the Current Therapeutic Advances. *Curr Clin Pharmacol*, 11(2), 118-127. doi:10.2174/1574884711666160511150028
- Akbar, M. U., Zia, K. M., Akash, M. S. H., Nazir, A., Zuber, M., & Ibrahim, M. (2018). In-vivo anti-diabetic and wound healing potential of chitosan/alginate/maltodextrin/pluronic-based mixed polymeric micelles: Curcumin therapeutic potential. *Int J Biol Macromol*, 120(Pt B), 2418-2430. doi:10.1016/j.ijbiomac.2018.09.010
- Akbik, D., Ghadiri, M., Chrzanowski, W., & Rohanizadeh, R. (2014). Curcumin as a wound healing agent. *Life Sci*, 116(1), 1-7. doi:10.1016/j.lfs.2014.08.016
- Al-Jarallah, A., & Trigatti, B. L. (2010). A role for the scavenger receptor, class B type I in high density lipoprotein dependent activation of cellular signaling pathways. *Biochim Biophys Acta*, 1801(12), 1239-1248. doi:10.1016/j.bbailip.2010.08.006
- Alavi, A., Sibbald, R. G., Mayer, D., Goodman, L., Botros, M., Armstrong, D. G., . . . Kirsner, R. S. (2014). Diabetic foot ulcers: Part I. Pathophysiology and prevention. *J Am Acad Dermatol*, 70(1), 1 e1-18; quiz 19-20. doi:10.1016/j.jaad.2013.06.055
- Albelda, S. M., Smith, C. W., & Ward, P. A. (1994). Adhesion molecules and inflammatory injury. *FASEB J*, 8(8), 504-512.
- Alizadeh, M., & Kheirouri, S. (2019). Curcumin reduces malondialdehyde and improves antioxidants in humans with diseased conditions: a comprehensive meta-analysis of randomized controlled trials. *Biomedicine (Taipei)*, 9(4), 23. doi:10.1051/bmdcn/2019090423
- American Diabetes, A. (2021). 2. Classification and Diagnosis of Diabetes: Standards of Medical Care in Diabetes-2021. *Diabetes Care*, 44(Suppl 1), S15-S33. doi:10.2337/dc21-S002
- Andreone, B. J., Chow, B. W., Tata, A., Lacoste, B., Ben-Zvi, A., Bullock, K., . . . Gu, C. (2017). Blood-Brain Barrier Permeability Is Regulated by Lipid Transport-Dependent Suppression of Caveolae-Mediated Transcytosis. *Neuron*, 94(3), 581-594 e585. doi:10.1016/j.neuron.2017.03.043
- Andrews, K. L., Houdek, M. T., & Kiemele, L. J. (2015). Wound management of chronic diabetic foot ulcers: from the basics to regenerative medicine. *Prosthet Orthot Int*, 39(1), 29-39. doi:10.1177/0309364614534296

- Anusha, D., Chaly, P. E., Junaid, M., Nijesh, J. E., Shivashankar, K., & Sivasamy, S. (2019). Efficacy of a mouthwash containing essential oils and curcumin as an adjunct to nonsurgical periodontal therapy among rheumatoid arthritis patients with chronic periodontitis: A randomized controlled trial. *Indian J Dent Res*, *30*(4), 506-511. doi:10.4103/ijdr.IJDR_662_17
- Armstrong, D. G., Lavery, L. A., Wu, S., & Boulton, A. J. (2005). Evaluation of removable and irremovable cast walkers in the healing of diabetic foot wounds: a randomized controlled trial. *Diabetes Care*, *28*(3), 551-554. doi:10.2337/diacare.28.3.551
- Babon, J. A., DeNicola, M. E., Blodgett, D. M., Crevecoeur, I., Buttrick, T. S., Maehr, R., . . . Kent, S. C. (2016). Analysis of self-antigen specificity of islet-infiltrating T cells from human donors with type 1 diabetes. *Nat Med*, *22*(12), 1482-1487. doi:10.1038/nm.4203
- Baliga, B. S., & Weinberger, J. (2006). Diabetes and stroke: part one--risk factors and pathophysiology. *Curr Cardiol Rep*, *8*(1), 23-28. doi:10.1007/s11886-006-0006-1
- Banach, M., Serban, C., Aronow, W. S., Rysz, J., Dragan, S., Lerma, E. V., . . . Covic, A. (2014). Lipid, blood pressure and kidney update 2013. *Int Urol Nephrol*, *46*(5), 947-961. doi:10.1007/s11255-014-0657-6
- Banarjee, R., Sharma, A., Bai, S., Deshmukh, A., & Kulkarni, M. (2018). Proteomic study of endothelial dysfunction induced by AGEs and its possible role in diabetic cardiovascular complications. *J Proteomics*, *187*, 69-79. doi:10.1016/j.jprot.2018.06.009
- Bano, S., Ahmed, F., Khan, F., Chaudhary, S. C., & Samim, M. (2020). Enhancement of the cancer inhibitory effect of the bioactive food component resveratrol by nanoparticle based delivery. *Food Funct*, *11*(4), 3213-3226. doi:10.1039/c9fo02445j
- Barbosa, J. H., Oliveira, S. L., & Seara, L. T. (2008). [The role of advanced glycation end-products (AGEs) in the development of vascular diabetic complications]. *Arq Bras Endocrinol Metabol*, *52*(6), 940-950. doi:10.1590/s0004-27302008000600005
- Barnes, J. A., Eid, M. A., Creager, M. A., & Goodney, P. P. (2020). Epidemiology and Risk of Amputation in Patients With Diabetes Mellitus and Peripheral Artery Disease. *Arterioscler Thromb Vasc Biol*, *40*(8), 1808-1817. doi:10.1161/ATVBAHA.120.314595
- Basnet, P., & Skalko-Basnet, N. (2011). Curcumin: an anti-inflammatory molecule from a curry spice on the path to cancer treatment. *Molecules*, *16*(6), 4567-4598. doi:10.3390/molecules16064567
- Baumgen, M., Dutschei, T., & Bornscheuer, U. T. (2021). Marine Polysaccharides: Occurrence, Enzymatic Degradation and Utilization. *ChemBiochem*, *22*(13), 2247-2256. doi:10.1002/cbic.202100078
- Beisswenger, P. J. (2014). Methylglyoxal in diabetes: link to treatment, glycaemic control and biomarkers of complications. *Biochem Soc Trans*, *42*(2), 450-456. doi:10.1042/BST20130275
- Ben-Aicha, S., Badimon, L., & Vilahur, G. (2020). Advances in HDL: Much More than Lipid Transporters. *Int J Mol Sci*, *21*(3). doi:10.3390/ijms21030732
- Betteridge, D. J. (2000). What is oxidative stress? *Metabolism*, *49*(2 Suppl 1), 3-8. doi:10.1016/s0026-0495(00)80077-3
- Blunt, J. W., Carroll, A. R., Copp, B. R., Davis, R. A., Keyzers, R. A., & Prinsep, M. R. (2018). Marine natural products. *Nat Prod Rep*, *35*(1), 8-53. doi:10.1039/c7np00052a
- Blunt, J. W., Copp, B. R., Keyzers, R. A., Munro, M. H., & Prinsep, M. R. (2016). Marine natural products. *Nat Prod Rep*, *33*(3), 382-431. doi:10.1039/c5np00156k
- Boniakowski, A. E., Kimball, A. S., Jacobs, B. N., Kunkel, S. L., & Gallagher, K. A. (2017). Macrophage-Mediated Inflammation in Normal and Diabetic Wound Healing. *J Immunol*, *199*(1), 17-24. doi:10.4049/jimmunol.1700223
- Botero, D., & Wolfsdorf, J. I. (2005). Diabetes mellitus in children and adolescents. *Arch Med Res*, *36*(3), 281-290. doi:10.1016/j.arcmed.2004.12.002
- Bourajjaj, M., Stehouwer, C. D., van Hinsbergh, V. W., & Schalkwijk, C. G. (2003). Role of methylglyoxal adducts in the development of vascular complications in diabetes mellitus. *Biochem Soc Trans*, *31*(Pt 6), 1400-1402. doi:10.1042/bst0311400
- Bragg, F., Holmes, M. V., Iona, A., Guo, Y., Du, H., Chen, Y., . . . China Kadoorie Biobank Collaborative, G. (2017). Association Between Diabetes and Cause-Specific Mortality in Rural and Urban Areas of China. *JAMA*, *317*(3), 280-289. doi:10.1001/jama.2016.19720

- Breuss, J. M., Atanasov, A. G., & Uhrin, P. (2019). Resveratrol and Its Effects on the Vascular System. *Int J Mol Sci*, 20(7). doi:10.3390/ijms20071523
- Brouwers, O., Niessen, P. M., Ferreira, I., Miyata, T., Scheffer, P. G., Teerlink, T., . . . Schalkwijk, C. G. (2011). Overexpression of glyoxalase-I reduces hyperglycemia-induced levels of advanced glycation end products and oxidative stress in diabetic rats. *J Biol Chem*, 286(2), 1374-1380. doi:10.1074/jbc.M110.144097
- Brouwers, O., Niessen, P. M., Haenen, G., Miyata, T., Brownlee, M., Stehouwer, C. D., . . . Schalkwijk, C. G. (2010). Hyperglycaemia-induced impairment of endothelium-dependent vasorelaxation in rat mesenteric arteries is mediated by intracellular methylglyoxal levels in a pathway dependent on oxidative stress. *Diabetologia*, 53(5), 989-1000. doi:10.1007/s00125-010-1677-0
- Brouwers, O., Niessen, P. M., Miyata, T., Ostergaard, J. A., Flyvbjerg, A., Peutz-Kootstra, C. J., . . . Schalkwijk, C. G. (2014). Glyoxalase-1 overexpression reduces endothelial dysfunction and attenuates early renal impairment in a rat model of diabetes. *Diabetologia*, 57(1), 224-235. doi:10.1007/s00125-013-3088-5
- Burgos-Moron, E., Abad-Jimenez, Z., Maranon, A. M., Iannantuoni, F., Escribano-Lopez, I., Lopez-Domenech, S., . . . Victor, V. M. (2019). Relationship Between Oxidative Stress, ER Stress, and Inflammation in Type 2 Diabetes: The Battle Continues. *J Clin Med*, 8(9). doi:10.3390/jcm8091385
- Cadenas, E., & Davies, K. J. (2000). Mitochondrial free radical generation, oxidative stress, and aging. *Free Radic Biol Med*, 29(3-4), 222-230. doi:10.1016/s0891-5849(00)00317-8
- Cai, W., Zhang, K., Li, P., Zhu, L., Xu, J., Yang, B., . . . Chen, J. (2017). Dysfunction of the neurovascular unit in ischemic stroke and neurodegenerative diseases: An aging effect. *Ageing Res Rev*, 34, 77-87. doi:10.1016/j.arr.2016.09.006
- Campbell, J. E., & Drucker, D. J. (2015). Islet alpha cells and glucagon--critical regulators of energy homeostasis. *Nat Rev Endocrinol*, 11(6), 329-338. doi:10.1038/nrendo.2015.51
- Cerqueira, M. T., da Silva, L. P., Santos, T. C., Pirraco, R. P., Correlo, V. M., Reis, R. L., & Marques, A. P. (2014). Gellan gum-hyaluronic acid spongy-like hydrogels and cells from adipose tissue synergize promoting neoskin vascularization. *ACS Appl Mater Interfaces*, 6(22), 19668-19679. doi:10.1021/am504520j
- Chainani-Wu, N. (2003). Safety and anti-inflammatory activity of curcumin: a component of tumeric (*Curcuma longa*). *J Altern Complement Med*, 9(1), 161-168. doi:10.1089/107555303321223035
- Chan, W. H., & Wu, H. J. (2008). Methylglyoxal and high glucose co-treatment induces apoptosis or necrosis in human umbilical vein endothelial cells. *J Cell Biochem*, 103(4), 1144-1157. doi:10.1002/jcb.21489
- Chauhan, P. S., & Saxena, A. (2016). Bacterial carrageenases: an overview of production and biotechnological applications. *3 Biotech*, 6(2), 146. doi:10.1007/s13205-016-0461-3
- Chavda, V., Vashi, R., & Patel, S. (2021). Cerebrovascular Complications of Diabetes: SGLT-2 Inhibitors as a Promising Future Therapeutics. *Curr Drug Targets*, 22(14), 1629-1636. doi:10.2174/1389450121666201020163454
- Cheeseman, K. H., & Slater, T. F. (1993). An introduction to free radical biochemistry. *Br Med Bull*, 49(3), 481-493. doi:10.1093/oxfordjournals.bmb.a072625
- Chen, J., Kasper, M., Heck, T., Nakagawa, K., Humpert, P. M., Bai, L., . . . Bierhaus, A. (2005). Tissue factor as a link between wounding and tissue repair. *Diabetes*, 54(7), 2143-2154. doi:10.2337/diabetes.54.7.2143
- Chen, R., Ovbiagele, B., & Feng, W. (2016). Diabetes and Stroke: Epidemiology, Pathophysiology, Pharmaceuticals and Outcomes. *Am J Med Sci*, 351(4), 380-386. doi:10.1016/j.amjms.2016.01.011
- Cheung, N., Mitchell, P., & Wong, T. Y. (2010). Diabetic retinopathy. *Lancet*, 376(9735), 124-136. doi:10.1016/S0140-6736(09)62124-3
- Cock, J. M., Peters, A. F., & Coelho, S. M. (2011). Brown algae. *Curr Biol*, 21(15), R573-575. doi:10.1016/j.cub.2011.05.006
- Cohen, J. A., Jeffers, B. W., Faldut, D., Marcoux, M., & Schrier, R. W. (1998). Risks for sensorimotor peripheral neuropathy and autonomic neuropathy in non-insulin-dependent diabetes mellitus (NIDDM). *Muscle Nerve*, 21(1), 72-80. doi:10.1002/(sici)1097-4598(199801)21:1<72::aid-mus10>3.0.co;2-2
- Cohen, R. A. (2005). Role of nitric oxide in diabetic complications. *Am J Ther*, 12(6), 499-502. doi:10.1097/01.mjt.0000178776.77267.19
- Couret, D., Planesse, C., Patche, J., Diotel, N., Nativel, B., Bourane, S., & Meilhac, O. (2021). Lack of Neuroprotective Effects of High-Density Lipoprotein Therapy in Stroke under Acute Hyperglycemic Conditions. *Molecules*, 26(21). doi:10.3390/molecules26216365

- Cowin, S. C. (2004). Tissue growth and remodeling. *Annu Rev Biomed Eng*, 6, 77-107. doi:10.1146/annurev.bioeng.6.040803.140250
- Crecil Dias, C., Kamath, S., & Vidyasagar, S. (2020). Blood glucose regulation and control of insulin and glucagon infusion using single model predictive control for type 1 diabetes mellitus. *IET Syst Biol*, 14(3), 133-146. doi:10.1049/iet-syb.2019.0101
- Cryer, P. E. (2012). Minireview: Glucagon in the pathogenesis of hypoglycemia and hyperglycemia in diabetes. *Endocrinology*, 153(3), 1039-1048. doi:10.1210/en.2011-1499
- Cullinan, S. B., & Diehl, J. A. (2006). Coordination of ER and oxidative stress signaling: the PERK/Nrf2 signaling pathway. *Int J Biochem Cell Biol*, 38(3), 317-332. doi:10.1016/j.biocel.2005.09.018
- Curb, J. D., Pressel, S. L., Cutler, J. A., Savage, P. J., Applegate, W. B., Black, H., . . . Stamler, J. (1996). Effect of diuretic-based antihypertensive treatment on cardiovascular disease risk in older diabetic patients with isolated systolic hypertension. Systolic Hypertension in the Elderly Program Cooperative Research Group. *JAMA*, 276(23), 1886-1892.
- Daneman, R., & Prat, A. (2015). The blood-brain barrier. *Cold Spring Harb Perspect Biol*, 7(1), a020412. doi:10.1101/cshperspect.a020412
- Davis, F. M., Kimball, A., Boniakowski, A., & Gallagher, K. (2018). Dysfunctional Wound Healing in Diabetic Foot Ulcers: New Crossroads. *Curr Diab Rep*, 18(1), 2. doi:10.1007/s11892-018-0970-z
- Deedwania, P. C., & Fonseca, V. A. (2005). Diabetes, prediabetes, and cardiovascular risk: shifting the paradigm. *Am J Med*, 118(9), 939-947. doi:10.1016/j.amjmed.2005.05.018
- Den Hartogh, D. J., Gabriel, A., & Tsiani, E. (2020). Antidiabetic Properties of Curcumin I: Evidence from In Vitro Studies. *Nutrients*, 12(1). doi:10.3390/nu12010118
- Dittami, S. M., Heesch, S., Olsen, J. L., & Collen, J. (2017). Transitions between marine and freshwater environments provide new clues about the origins of multicellular plants and algae. *J Phycol*, 53(4), 731-745. doi:10.1111/jpy.12547
- Domingueti, C. P., Dusse, L. M., Carvalho, M., de Sousa, L. P., Gomes, K. B., & Fernandes, A. P. (2016). Diabetes mellitus: The linkage between oxidative stress, inflammation, hypercoagulability and vascular complications. *J Diabetes Complications*, 30(4), 738-745. doi:10.1016/j.jdiacomp.2015.12.018
- Dwyer-Lindgren, L., Mackenbach, J. P., van Lenthe, F. J., Flaxman, A. D., & Mokdad, A. H. (2016). Diagnosed and Undiagnosed Diabetes Prevalence by County in the U.S., 1999-2012. *Diabetes Care*, 39(9), 1556-1562. doi:10.2337/dc16-0678
- Eid, S., Sas, K. M., Abcouwer, S. F., Feldman, E. L., Gardner, T. W., Pennathur, S., & Fort, P. E. (2019). New insights into the mechanisms of diabetic complications: role of lipids and lipid metabolism. *Diabetologia*, 62(9), 1539-1549. doi:10.1007/s00125-019-4959-1
- El Gamal, A. A. (2010). Biological importance of marine algae. *Saudi Pharm J*, 18(1), 1-25. doi:10.1016/j.jsps.2009.12.001
- Eringa, E. C., Serne, E. H., Meijer, R. I., Schalkwijk, C. G., Houben, A. J., Stehouwer, C. D., . . . van Hinsbergh, V. W. (2013). Endothelial dysfunction in (pre)diabetes: characteristics, causative mechanisms and pathogenic role in type 2 diabetes. *Rev Endocr Metab Disord*, 14(1), 39-48. doi:10.1007/s11154-013-9239-7
- Ertek, S. (2018). High-density Lipoprotein (HDL) Dysfunction and the Future of HDL. *Curr Vasc Pharmacol*, 16(5), 490-498. doi:10.2174/1570161115666171116164612
- Erusalimsky, J. D. (2021). The use of the soluble receptor for advanced glycation-end products (sRAGE) as a potential biomarker of disease risk and adverse outcomes. *Redox Biol*, 42, 101958. doi:10.1016/j.redox.2021.101958
- Expert Committee on the, D., & Classification of Diabetes, M. (2000). Report of the Expert Committee on the Diagnosis and Classification of Diabetes Mellitus. *Diabetes Care*, 23 Suppl 1, S4-19.
- Fadini, G. P., Albiero, M., Bonora, B. M., & Avogaro, A. (2019). Angiogenic Abnormalities in Diabetes Mellitus: Mechanistic and Clinical Aspects. *J Clin Endocrinol Metab*, 104(11), 5431-5444. doi:10.1210/jc.2019-00980
- Farber, A., & Eberhardt, R. T. (2016). The Current State of Critical Limb Ischemia: A Systematic Review. *JAMA Surg*, 151(11), 1070-1077. doi:10.1001/jamasurg.2016.2018
- Feldman, E. L., Nave, K. A., Jensen, T. S., & Bennett, D. L. H. (2017). New Horizons in Diabetic Neuropathy: Mechanisms, Bioenergetics, and Pain. *Neuron*, 93(6), 1296-1313. doi:10.1016/j.neuron.2017.02.005

- Feltbower, R. G., Bodansky, H. J., Patterson, C. C., Parslow, R. C., Stephenson, C. R., Reynolds, C., & McKinney, P. A. (2008). Acute complications and drug misuse are important causes of death for children and young adults with type 1 diabetes: results from the Yorkshire Register of diabetes in children and young adults. *Diabetes Care*, *31*(5), 922-926. doi:10.2337/dc07-2029
- Femlak, M., Gluba-Brzozka, A., Cialkowska-Rysz, A., & Rysz, J. (2017). The role and function of HDL in patients with diabetes mellitus and the related cardiovascular risk. *Lipids Health Dis*, *16*(1), 207. doi:10.1186/s12944-017-0594-3
- Fernandes, T., Barauna, V. G., Negrao, C. E., Phillips, M. I., & Oliveira, E. M. (2015). Aerobic exercise training promotes physiological cardiac remodeling involving a set of microRNAs. *Am J Physiol Heart Circ Physiol*, *309*(4), H543-552. doi:10.1152/ajpheart.00899.2014
- Fernandes, T., & Cordeiro, N. (2021). Microalgae as Sustainable Biofactories to Produce High-Value Lipids: Biodiversity, Exploitation, and Biotechnological Applications. *Mar Drugs*, *19*(10). doi:10.3390/md19100573
- Feske, S. K. (2021). Ischemic Stroke. *Am J Med*, *134*(12), 1457-1464. doi:10.1016/j.amjmed.2021.07.027
- Fiorentino, T. V., Prioletta, A., Zuo, P., & Folli, F. (2013). Hyperglycemia-induced oxidative stress and its role in diabetes mellitus related cardiovascular diseases. *Curr Pharm Des*, *19*(32), 5695-5703. doi:10.2174/1381612811319320005
- Fox, C. A., Moschetti, A., & Ryan, R. O. (2021). Reconstituted HDL as a therapeutic delivery device. *Biochim Biophys Acta Mol Cell Biol Lipids*, *1866*(11), 159025. doi:10.1016/j.bbalip.2021.159025
- Fraga, C. G., Croft, K. D., Kennedy, D. O., & Tomas-Barberan, F. A. (2019). The effects of polyphenols and other bioactives on human health. *Food Funct*, *10*(2), 514-528. doi:10.1039/c8fo01997e
- Frey, T., & Antonetti, D. A. (2011). Alterations to the blood-retinal barrier in diabetes: cytokines and reactive oxygen species. *Antioxid Redox Signal*, *15*(5), 1271-1284. doi:10.1089/ars.2011.3906
- Gao, H. X., Regier, E. E., & Close, K. L. (2016). Prevalence of and trends in diabetes among adults in the United States, 1988-2012. *J Diabetes*, *8*(1), 8-9.
- Gateau, H., Solymosi, K., Marchand, J., & Schoefs, B. (2017). Carotenoids of Microalgae Used in Food Industry and Medicine. *Mini Rev Med Chem*, *17*(13), 1140-1172. doi:10.2174/1389557516666160808123841
- Gelfand, J. M., & Wan, M. T. (2018). Psoriasis: a novel risk factor for type 2 diabetes. *Lancet Diabetes Endocrinol*, *6*(12), 919-921. doi:10.1016/S2213-8587(18)30127-X
- Generalic Mekinic, I., Skroza, D., Simat, V., Hamed, I., Cagalj, M., & Popovic Perkovic, Z. (2019). Phenolic Content of Brown Algae (Pheophyceae) Species: Extraction, Identification, and Quantification. *Biomolecules*, *9*(6). doi:10.3390/biom9060244
- Genest, J., Schwertani, A., & Choi, H. Y. (2018). Membrane microdomains and the regulation of HDL biogenesis. *Curr Opin Lipidol*, *29*(1), 36-41. doi:10.1097/MOL.0000000000000470
- George, P. M., & Steinberg, G. K. (2015). Novel Stroke Therapeutics: Unraveling Stroke Pathophysiology and Its Impact on Clinical Treatments. *Neuron*, *87*(2), 297-309. doi:10.1016/j.neuron.2015.05.041
- Ghayempour, S., Montazer, M., & Mahmoudi Rad, M. (2016). Encapsulation of Aloe Vera extract into natural Tragacanth Gum as a novel green wound healing product. *Int J Biol Macromol*, *93*(Pt A), 344-349. doi:10.1016/j.ijbiomac.2016.08.076
- Giacco, F., & Brownlee, M. (2010). Oxidative stress and diabetic complications. *Circ Res*, *107*(9), 1058-1070. doi:10.1161/CIRCRESAHA.110.223545
- Gibbs, B. F., Kermasha, S., Alli, I., & Mulligan, C. N. (1999). Encapsulation in the food industry: a review. *Int J Food Sci Nutr*, *50*(3), 213-224. doi:10.1080/096374899101256
- Gillett, M. J. (2009). International Expert Committee report on the role of the A1c assay in the diagnosis of diabetes: Diabetes Care 2009; *32*(7): 1327-1334. *Clin Biochem Rev*, *30*(4), 197-200.
- Glass, C. K., Saijo, K., Winner, B., Marchetto, M. C., & Gage, F. H. (2010). Mechanisms underlying inflammation in neurodegeneration. *Cell*, *140*(6), 918-934. doi:10.1016/j.cell.2010.02.016
- Godo, S., & Shimokawa, H. (2017). Endothelial Functions. *Arterioscler Thromb Vasc Biol*, *37*(9), e108-e114. doi:10.1161/ATVBAHA.117.309813
- Goova, M. T., Li, J., Kislinger, T., Qu, W., Lu, Y., Bucciarelli, L. G., . . . Schmidt, A. M. (2001). Blockade of receptor for advanced glycation end-products restores effective wound healing in diabetic mice. *Am J Pathol*, *159*(2), 513-525. doi:10.1016/S0002-9440(10)61723-3

- Gordon, O. N., Luis, P. B., Sintim, H. O., & Schneider, C. (2015). Unraveling curcumin degradation: autoxidation proceeds through spiroepoxide and vinyl ether intermediates en route to the main bicyclopentadione. *J Biol Chem*, *290*(8), 4817-4828. doi:10.1074/jbc.M114.618785
- Gorman, A. M., Healy, S. J., Jager, R., & Samali, A. (2012). Stress management at the ER: regulators of ER stress-induced apoptosis. *Pharmacol Ther*, *134*(3), 306-316. doi:10.1016/j.pharmthera.2012.02.003
- Goti, D., Hrzenjak, A., Levak-Frank, S., Frank, S., van der Westhuyzen, D. R., Malle, E., & Sattler, W. (2001). Scavenger receptor class B, type I is expressed in porcine brain capillary endothelial cells and contributes to selective uptake of HDL-associated vitamin E. *J Neurochem*, *76*(2), 498-508. doi:10.1046/j.1471-4159.2001.00100.x
- Greenbaum, C. J., Anderson, A. M., Dolan, L. M., Mayer-Davis, E. J., Dabelea, D., Imperatore, G., . . . Group, S. S. (2009). Preservation of beta-cell function in autoantibody-positive youth with diabetes. *Diabetes Care*, *32*(10), 1839-1844. doi:10.2337/dc08-2326
- Gupta, S. C., Patchva, S., & Aggarwal, B. B. (2013). Therapeutic roles of curcumin: lessons learned from clinical trials. *AAPS J*, *15*(1), 195-218. doi:10.1208/s12248-012-9432-8
- Habauzit, V., & Morand, C. (2012). Evidence for a protective effect of polyphenols-containing foods on cardiovascular health: an update for clinicians. *Ther Adv Chronic Dis*, *3*(2), 87-106. doi:10.1177/2040622311430006
- Haik, G. M., Jr., Lo, T. W., & Thornalley, P. J. (1994). Methylglyoxal concentration and glyoxalase activities in the human lens. *Exp Eye Res*, *59*(4), 497-500. doi:10.1006/exer.1994.1135
- Hassaninasab, A., Hashimoto, Y., Tomita-Yokotani, K., & Kobayashi, M. (2011). Discovery of the curcumin metabolic pathway involving a unique enzyme in an intestinal microorganism. *Proc Natl Acad Sci U S A*, *108*(16), 6615-6620. doi:10.1073/pnas.1016217108
- He, Y., Yue, Y., Zheng, X., Zhang, K., Chen, S., & Du, Z. (2015). Curcumin, inflammation, and chronic diseases: how are they linked? *Molecules*, *20*(5), 9183-9213. doi:10.3390/molecules20059183
- Hetz, C. (2012). The unfolded protein response: controlling cell fate decisions under ER stress and beyond. *Nat Rev Mol Cell Biol*, *13*(2), 89-102. doi:10.1038/nrm3270
- Hetz, C., Zhang, K., & Kaufman, R. J. (2020). Mechanisms, regulation and functions of the unfolded protein response. *Nat Rev Mol Cell Biol*, *21*(8), 421-438. doi:10.1038/s41580-020-0250-z
- Holder, G. M., Plummer, J. L., & Ryan, A. J. (1978). The metabolism and excretion of curcumin (1,7-bis-(4-hydroxy-3-methoxyphenyl)-1,6-heptadiene-3,5-dione) in the rat. *Xenobiotica*, *8*(12), 761-768. doi:10.3109/00498257809069589
- Holzwirth, E., Fischer-Schaepmann, T., Obradovic, D., von Lucadou, M., Schwedhelm, E., Daum, G., . . . Buttner, P. (2022). Anti-inflammatory HDL effects are impaired in atrial fibrillation. *Heart Vessels*, *37*(1), 161-171. doi:10.1007/s00380-021-01908-w
- Homayun, B., Lin, X., & Choi, H. J. (2019). Challenges and Recent Progress in Oral Drug Delivery Systems for Biopharmaceuticals. *Pharmaceutics*, *11*(3). doi:10.3390/pharmaceutics11030129
- Hudson, B. I., & Lippman, M. E. (2018). Targeting RAGE Signaling in Inflammatory Disease. *Annu Rev Med*, *69*, 349-364. doi:10.1146/annurev-med-041316-085215
- Hull, C. M., Peakman, M., & Tree, T. I. M. (2017). Regulatory T cell dysfunction in type 1 diabetes: what's broken and how can we fix it? *Diabetologia*, *60*(10), 1839-1850. doi:10.1007/s00125-017-4377-1
- Hybertson, B. M., Gao, B., Bose, S. K., & McCord, J. M. (2011). Oxidative stress in health and disease: the therapeutic potential of Nrf2 activation. *Mol Aspects Med*, *32*(4-6), 234-246. doi:10.1016/j.mam.2011.10.006
- Ighodaro, O. M. (2018). Molecular pathways associated with oxidative stress in diabetes mellitus. *Biomed Pharmacother*, *108*, 656-662. doi:10.1016/j.biopha.2018.09.058
- Illsley, N. P. (2000). Glucose transporters in the human placenta. *Placenta*, *21*(1), 14-22. doi:10.1053/plac.1999.0448
- Indyk, D., Bronowicka-Szydelko, A., Gamian, A., & Kuzan, A. (2021). Advanced glycation end products and their receptors in serum of patients with type 2 diabetes. *Sci Rep*, *11*(1), 13264. doi:10.1038/s41598-021-92630-0
- Ipar, V. S., Dsouza, A., & Devarajan, P. V. (2019). Enhancing Curcumin Oral Bioavailability Through Nanoformulations. *Eur J Drug Metab Pharmacokinet*, *44*(4), 459-480. doi:10.1007/s13318-019-00545-z
- Ireson, C. R., Jones, D. J., Orr, S., Coughtrie, M. W., Boocock, D. J., Williams, M. L., . . . Gescher, A. J. (2002). Metabolism of the cancer chemopreventive agent curcumin in human and rat intestine. *Cancer Epidemiol Biomarkers Prev*, *11*(1), 105-111.

- Jia, C., Anderson, J. L. C., Gruppen, E. G., Lei, Y., Bakker, S. J. L., Dullaart, R. P. F., & Tietge, U. J. F. (2021). High-Density Lipoprotein Anti-Inflammatory Capacity and Incident Cardiovascular Events. *Circulation*, *143*(20), 1935-1945. doi:10.1161/CIRCULATIONAHA.120.050808
- Jin, T., Song, Z., Weng, J., & Fantus, I. G. (2018). Curcumin and other dietary polyphenols: potential mechanisms of metabolic actions and therapy for diabetes and obesity. *Am J Physiol Endocrinol Metab*, *314*(3), E201-E205. doi:10.1152/ajpendo.00285.2017
- Jones, D. P. (2008). Radical-free biology of oxidative stress. *Am J Physiol Cell Physiol*, *295*(4), C849-868. doi:10.1152/ajpcell.00283.2008
- Jude, E. B., Anderson, S. G., Cruickshank, J. K., Srivatsa, A., Tentolouris, N., Chandrasekaran, R., . . . Boulton, A. J. (2002). Natural history and prognostic factors of diabetic nephropathy in type 2 diabetes. *QJM*, *95*(6), 371-377. doi:10.1093/qjmed/95.6.371
- Kalaria, R. N., Akinyemi, R., & Ihara, M. (2016). Stroke injury, cognitive impairment and vascular dementia. *Biochim Biophys Acta*, *1862*(5), 915-925. doi:10.1016/j.bbadis.2016.01.015
- Karabasz, A., Lachowicz, D., Karewicz, A., Mezyk-Kopec, R., Stalinska, K., Werner, E., . . . Bzowska, M. (2019). Analysis of toxicity and anticancer activity of micelles of sodium alginate-curcumin. *Int J Nanomedicine*, *14*, 7249-7262. doi:10.2147/IJN.S213942
- Kaur, S., Modi, N. H., Panda, D., & Roy, N. (2010). Probing the binding site of curcumin in Escherichia coli and Bacillus subtilis FtsZ--a structural insight to unveil antibacterial activity of curcumin. *Eur J Med Chem*, *45*(9), 4209-4214. doi:10.1016/j.ejmech.2010.06.015
- Khezri, K., Saeedi, M., Mohammadamini, H., & Zakaryaei, A. S. (2021). A comprehensive review of the therapeutic potential of curcumin nanoformulations. *Phytother Res*, *35*(10), 5527-5563. doi:10.1002/ptr.7190
- Khotimchenko, M., Tiasto, V., Kalitnik, A., Begun, M., Khotimchenko, R., Leonteva, E., . . . Khotimchenko, Y. (2020). Antitumor potential of carrageenans from marine red algae. *Carbohydr Polym*, *246*, 116568. doi:10.1016/j.carbpol.2020.116568
- Kim, J. H., Lee, J. E., Kim, K. H., & Kang, N. J. (2018). Beneficial Effects of Marine Algae-Derived Carbohydrates for Skin Health. *Mar Drugs*, *16*(11). doi:10.3390/md16110459
- Kim, J. Y., Lee, S. Y., Kim, H., Park, J. W., Lim, D. K., & Moon, D. W. (2018). Biomolecular Imaging of Regeneration of Zebrafish Caudal Fins Using High Spatial Resolution Ambient Mass Spectrometry. *Anal Chem*, *90*(21), 12723-12730. doi:10.1021/acs.analchem.8b03066
- Kim, K. A., Kim, D., Kim, J. H., Shin, Y. J., Kim, E. S., Akram, M., . . . Bae, O. N. (2020). Autophagy-mediated occludin degradation contributes to blood-brain barrier disruption during ischemia in bEnd.3 brain endothelial cells and rat ischemic stroke models. *Fluids Barriers CNS*, *17*(1), 21. doi:10.1186/s12987-020-00182-8
- Kontush, A., Lindahl, M., Lhomme, M., Calabresi, L., Chapman, M. J., & Davidson, W. S. (2015). Structure of HDL: particle subclasses and molecular components. *Handb Exp Pharmacol*, *224*, 3-51. doi:10.1007/978-3-319-09665-0_1
- Kotha, R. R., & Luthria, D. L. (2019). Curcumin: Biological, Pharmaceutical, Nutraceutical, and Analytical Aspects. *Molecules*, *24*(16). doi:10.3390/molecules24162930
- Kunnumakkara, A. B., Bordoloi, D., Padmavathi, G., Monisha, J., Roy, N. K., Prasad, S., & Aggarwal, B. B. (2017). Curcumin, the golden nutraceutical: multitargeting for multiple chronic diseases. *Br J Pharmacol*, *174*(11), 1325-1348. doi:10.1111/bph.13621
- Kuprash, D. V., & Nedospasov, S. A. (2016). Molecular and Cellular Mechanisms of Inflammation. *Biochemistry (Mosc)*, *81*(11), 1237-1239. doi:10.1134/S0006297916110018
- Kuriakose, D., & Xiao, Z. (2020). Pathophysiology and Treatment of Stroke: Present Status and Future Perspectives. *Int J Mol Sci*, *21*(20). doi:10.3390/ijms21207609
- Kuzan, A. (2021). Toxicity of advanced glycation end products (Review). *Biomed Rep*, *14*(5), 46. doi:10.3892/br.2021.1422
- Langen, U. H., Ayloo, S., & Gu, C. (2019). Development and Cell Biology of the Blood-Brain Barrier. *Annu Rev Cell Dev Biol*, *35*, 591-613. doi:10.1146/annurev-cellbio-100617-062608
- Lau, L. H., Lew, J., Borschmann, K., Thijs, V., & Ekinci, E. I. (2019). Prevalence of diabetes and its effects on stroke outcomes: A meta-analysis and literature review. *J Diabetes Investig*, *10*(3), 780-792. doi:10.1111/jdi.12932

- Lee, J. H., Parveen, A., Do, M. H., Kang, M. C., Yumnam, S., & Kim, S. Y. (2020). Molecular mechanisms of methylglyoxal-induced aortic endothelial dysfunction in human vascular endothelial cells. *Cell Death Dis*, *11*(5), 403. doi:10.1038/s41419-020-2602-1
- Lee, S., Razqan, G. S., & Kwon, D. H. (2017). Antibacterial activity of epigallocatechin-3-gallate (EGCG) and its synergism with beta-lactam antibiotics sensitizing carbapenem-associated multidrug resistant clinical isolates of *Acinetobacter baumannii*. *Phytomedicine*, *24*, 49-55. doi:10.1016/j.phymed.2016.11.007
- Lee, Y. E., Kim, H., Seo, C., Park, T., Lee, K. B., Yoo, S. Y., . . . Lee, J. (2017). Marine polysaccharides: therapeutic efficacy and biomedical applications. *Arch Pharm Res*, *40*(9), 1006-1020. doi:10.1007/s12272-017-0958-2
- Lestari, M. L., & Indrayanto, G. (2014). Curcumin. *Profiles Drug Subst Excip Relat Methodol*, *39*, 113-204. doi:10.1016/B978-0-12-800173-8.00003-9
- Li, L., Ni, R., Shao, Y., & Mao, S. (2014). Carrageenan and its applications in drug delivery. *Carbohydr Polym*, *103*, 1-11. doi:10.1016/j.carbpol.2013.12.008
- Li, P., Harding, S. E., & Liu, Z. (2001). Cyanobacterial exopolysaccharides: their nature and potential biotechnological applications. *Biotechnol Genet Eng Rev*, *18*, 375-404. doi:10.1080/02648725.2001.10648020
- Li, Y., Zheng, Y., Zhang, Y., Yang, Y., Wang, P., Imre, B., . . . Wang, D. (2021). Brown Algae Carbohydrates: Structures, Pharmaceutical Properties, and Research Challenges. *Mar Drugs*, *19*(11). doi:10.3390/md19110620
- Liang, M. H., Wang, L., Wang, Q., Zhu, J., & Jiang, J. G. (2019). High-value bioproducts from microalgae: Strategies and progress. *Crit Rev Food Sci Nutr*, *59*(15), 2423-2441. doi:10.1080/10408398.2018.1455030
- Liebner, S., Dijkhuizen, R. M., Reiss, Y., Plate, K. H., Agalliu, D., & Constantin, G. (2018). Functional morphology of the blood-brain barrier in health and disease. *Acta Neuropathol*, *135*(3), 311-336. doi:10.1007/s00401-018-1815-1
- Lim, J. Z., Ng, N. S., & Thomas, C. (2017). Prevention and treatment of diabetic foot ulcers. *J R Soc Med*, *110*(3), 104-109. doi:10.1177/0141076816688346
- Lin, Y. G., Kunnumakkara, A. B., Nair, A., Merritt, W. M., Han, L. Y., Armaiz-Pena, G. N., . . . Sood, A. K. (2007). Curcumin inhibits tumor growth and angiogenesis in ovarian carcinoma by targeting the nuclear factor-kappaB pathway. *Clin Cancer Res*, *13*(11), 3423-3430. doi:10.1158/1078-0432.CCR-06-3072
- Liu, R., Li, S., Tu, Y., Hao, X., & Qiu, F. (2022). Recovery of value-added products by mining microalgae. *J Environ Manage*, *307*, 114512. doi:10.1016/j.jenvman.2022.114512
- Liu, W., Zhai, Y., Heng, X., Che, F. Y., Chen, W., Sun, D., & Zhai, G. (2016). Oral bioavailability of curcumin: problems and advancements. *J Drug Target*, *24*(8), 694-702. doi:10.3109/1061186X.2016.1157883
- Liu, X., Xu, H., Zhang, M., & Yu, D. G. (2021). Electrospun Medicated Nanofibers for Wound Healing: Review. *Membranes (Basel)*, *11*(10). doi:10.3390/membranes11100770
- Lizak, B., Szarka, A., Kim, Y., Choi, K. S., Nemeth, C. E., Marcolongo, P., . . . Margittai, E. (2019). Glucose Transport and Transporters in the Endomembranes. *Int J Mol Sci*, *20*(23). doi:10.3390/ijms20235898
- Loots, M. A., Lamme, E. N., Zeegelaar, J., Mekkes, J. R., Bos, J. D., & Middelkoop, E. (1998). Differences in cellular infiltrate and extracellular matrix of chronic diabetic and venous ulcers versus acute wounds. *J Invest Dermatol*, *111*(5), 850-857. doi:10.1046/j.1523-1747.1998.00381.x
- Lopez-Jornet, P., Camacho-Alonso, F., Jimenez-Torres, M. J., Orduna-Domingo, A., & Gomez-Garcia, F. (2011). Topical curcumin for the healing of carbon dioxide laser skin wounds in mice. *Photomed Laser Surg*, *29*(12), 809-814. doi:10.1089/pho.2011.3004
- Lordan, S., Ross, R. P., & Stanton, C. (2011). Marine bioactives as functional food ingredients: potential to reduce the incidence of chronic diseases. *Mar Drugs*, *9*(6), 1056-1100. doi:10.3390/md9061056
- Lu, Y., & Oyler, G. A. (2009). Green algae as a platform to express therapeutic proteins. *Discov Med*, *8*(40), 28-30.
- Luc, K., Schramm-Luc, A., Guzik, T. J., & Mikolajczyk, T. P. (2019). Oxidative stress and inflammatory markers in prediabetes and diabetes. *J Physiol Pharmacol*, *70*(6). doi:10.26402/jpp.2019.6.01
- Luca, S. V., Macovei, I., Bujor, A., Miron, A., Skalicka-Wozniak, K., Aprotosoiaie, A. C., & Trifan, A. (2020). Bioactivity of dietary polyphenols: The role of metabolites. *Crit Rev Food Sci Nutr*, *60*(4), 626-659. doi:10.1080/10408398.2018.1546669
- Lund-Katz, S., Liu, L., Thuahnai, S. T., & Phillips, M. C. (2003). High density lipoprotein structure. *Front Biosci*, *8*, d1044-1054. doi:10.2741/1077

- Lund-Katz, S., & Phillips, M. C. (2010). High density lipoprotein structure-function and role in reverse cholesterol transport. *Subcell Biochem*, *51*, 183-227. doi:10.1007/978-90-481-8622-8_7
- Luo, Y., Yin, W., Signore, A. P., Zhang, F., Hong, Z., Wang, S., . . . Chen, J. (2006). Neuroprotection against focal ischemic brain injury by the peroxisome proliferator-activated receptor-gamma agonist rosiglitazone. *J Neurochem*, *97*(2), 435-448. doi:10.1111/j.1471-4159.2006.03758.x
- Maamoun, H., Benameur, T., Pintus, G., Munusamy, S., & Agouni, A. (2019). Crosstalk Between Oxidative Stress and Endoplasmic Reticulum (ER) Stress in Endothelial Dysfunction and Aberrant Angiogenesis Associated With Diabetes: A Focus on the Protective Roles of Heme Oxygenase (HO)-1. *Front Physiol*, *10*, 70. doi:10.3389/fphys.2019.00070
- Mahler, R. J., & Adler, M. L. (1999). Clinical review 102: Type 2 diabetes mellitus: update on diagnosis, pathophysiology, and treatment. *J Clin Endocrinol Metab*, *84*(4), 1165-1171. doi:10.1210/jcem.84.4.5612
- Manlusoc, J. K. T., Hsieh, C. L., Hsieh, C. Y., Salac, E. S. N., Lee, Y. T., & Tsai, P. W. (2019). Pharmacologic Application Potentials of Sulfated Polysaccharide from Marine Algae. *Polymers (Basel)*, *11*(7). doi:10.3390/polym11071163
- Marin, L., Miguelez, E. M., Villar, C. J., & Lombo, F. (2015). Bioavailability of dietary polyphenols and gut microbiota metabolism: antimicrobial properties. *Biomed Res Int*, *2015*, 905215. doi:10.1155/2015/905215
- Marques, I. J., Lupi, E., & Mercader, N. (2019). Model systems for regeneration: zebrafish. *Development*, *146*(18). doi:10.1242/dev.167692
- Marton, L. T., Pescinini, E. S. L. M., Camargo, M. E. C., Barbalho, S. M., Haber, J., Sinatora, R. V., . . . Cincotto Dos Santos Bueno, P. (2021). The Effects of Curcumin on Diabetes Mellitus: A Systematic Review. *Front Endocrinol (Lausanne)*, *12*, 669448. doi:10.3389/fendo.2021.669448
- McCarthy, D. J., Malhotra, M., O'Mahony, A. M., Cryan, J. F., & O'Driscoll, C. M. (2015). Nanoparticles and the blood-brain barrier: advancing from in-vitro models towards therapeutic significance. *Pharm Res*, *32*(4), 1161-1185. doi:10.1007/s11095-014-1545-6
- McCrimmon, R. J., Ryan, C. M., & Frier, B. M. (2012). Diabetes and cognitive dysfunction. *Lancet*, *379*(9833), 2291-2299. doi:10.1016/S0140-6736(12)60360-2
- Medzhitov, R. (2008). Origin and physiological roles of inflammation. *Nature*, *454*(7203), 428-435. doi:10.1038/nature07201
- Menaa, F., Wijesinghe, U., Thiripuranathar, G., Althobaiti, N. A., Albalawi, A. E., Khan, B. A., & Menaa, B. (2021). Marine Algae-Derived Bioactive Compounds: A New Wave of Nanodrugs? *Mar Drugs*, *19*(9). doi:10.3390/md19090484
- Menon, V. P., & Sudheer, A. R. (2007). Antioxidant and anti-inflammatory properties of curcumin. *Adv Exp Med Biol*, *595*, 105-125. doi:10.1007/978-0-387-46401-5_3
- Metzler, M., Pfeiffer, E., Schulz, S. I., & Dempe, J. S. (2013). Curcumin uptake and metabolism. *Biofactors*, *39*(1), 14-20. doi:10.1002/biof.1042
- Michels, A. W., Landry, L. G., McDaniel, K. A., Yu, L., Campbell-Thompson, M., Kwok, W. W., . . . Nakayama, M. (2017). Islet-Derived CD4 T Cells Targeting Proinsulin in Human Autoimmune Diabetes. *Diabetes*, *66*(3), 722-734. doi:10.2337/db16-1025
- Moghadamtousi, S. Z., Kadir, H. A., Hassandarvish, P., Tajik, H., Abubakar, S., & Zandi, K. (2014). A review on antibacterial, antiviral, and antifungal activity of curcumin. *Biomed Res Int*, *2014*, 186864. doi:10.1155/2014/186864
- Mohammadi, E., Behnam, B., Mohammadinejad, R., Guest, P. C., Simental-Mendia, L. E., & Sahebkar, A. (2021). Antidiabetic Properties of Curcumin: Insights on New Mechanisms. *Adv Exp Med Biol*, *1291*, 151-164. doi:10.1007/978-3-030-56153-6_9
- Mohammadian Haftcheshmeh, S., Karimzadeh, M. R., Azhdari, S., Vahedi, P., Abdollahi, E., & Momtazi-Borojeni, A. A. (2020). Modulatory effects of curcumin on the atherogenic activities of inflammatory monocytes: Evidence from in vitro and animal models of human atherosclerosis. *Biofactors*, *46*(3), 341-355. doi:10.1002/biof.1603
- Montano, A., Hanley, D. F., & Hemphill, J. C., 3rd. (2021). Hemorrhagic stroke. *Handb Clin Neurol*, *176*, 229-248. doi:10.1016/B978-0-444-64034-5.00019-5

- Morales, R. A., & Allende, M. L. (2019). Peripheral Macrophages Promote Tissue Regeneration in Zebrafish by Fine-Tuning the Inflammatory Response. *Front Immunol*, *10*, 253. doi:10.3389/fimmu.2019.00253
- Moraru, A., Wiederstein, J., Pfaff, D., Fleming, T., Miller, A. K., Nawroth, P., & Teleman, A. A. (2018). Elevated Levels of the Reactive Metabolite Methylglyoxal Recapitulate Progression of Type 2 Diabetes. *Cell Metab*, *27*(4), 926-934 e928. doi:10.1016/j.cmet.2018.02.003
- Muriach, M., Flores-Bellver, M., Romero, F. J., & Barcia, J. M. (2014). Diabetes and the brain: oxidative stress, inflammation, and autophagy. *Oxid Med Cell Longev*, *2014*, 102158. doi:10.1155/2014/102158
- Nagai, R., Shirakawa, J., Ohno, R., Moroishi, N., & Nagai, M. (2014). Inhibition of AGEs formation by natural products. *Amino Acids*, *46*(2), 261-266. doi:10.1007/s00726-013-1487-z
- Nakamura, T., Yamamoto, E., Kataoka, K., Yamashita, T., Tokutomi, Y., Dong, Y. F., . . . Kim-Mitsuyama, S. (2007). Pioglitazone exerts protective effects against stroke in stroke-prone spontaneously hypertensive rats, independently of blood pressure. *Stroke*, *38*(11), 3016-3022. doi:10.1161/STROKEAHA.107.486522
- Nash, A., Noh, S. Y., Birch, H. L., & de Leeuw, N. H. (2021). Lysine-arginine advanced glycation end-product cross-links and the effect on collagen structure: A molecular dynamics study. *Proteins*, *89*(5), 521-530. doi:10.1002/prot.26036
- Naslafkih, A., & Sestier, F. (2003). Diabetes mellitus related morbidity, risk of hospitalization and disability. *J Insur Med*, *35*(2), 102-113.
- Nasr, M., & Abdel Rahman, M. H. (2019). Simultaneous Determination of Curcumin and Resveratrol in Lipidic Nanoemulsion Formulation and Rat Plasma Using HPLC: Optimization and Application to Real Samples. *J AOAC Int*, *102*(4), 1095-1101. doi:10.5740/jaoacint.18-0269
- Naylor, C. D., Sermer, M., Chen, E., & Sykora, K. (1996). Cesarean delivery in relation to birth weight and gestational glucose tolerance: pathophysiology or practice style? Toronto Trihospital Gestational Diabetes Investigators. *JAMA*, *275*(15), 1165-1170.
- Nelson, K. M., Dahlin, J. L., Bisson, J., Graham, J., Pauli, G. F., & Walters, M. A. (2017). The Essential Medicinal Chemistry of Curcumin. *J Med Chem*, *60*(5), 1620-1637. doi:10.1021/acs.jmedchem.6b00975
- Nian, K., Harding, I. C., Herman, I. M., & Ebong, E. E. (2020). Blood-Brain Barrier Damage in Ischemic Stroke and Its Regulation by Endothelial Mechanotransduction. *Front Physiol*, *11*, 605398. doi:10.3389/fphys.2020.605398
- Nicoletti, M. (2016). Microalgae Nutraceuticals. *Foods*, *5*(3). doi:10.3390/foods5030054
- Nilsson, J., Bengtsson, E., Fredrikson, G. N., & Bjorkbacka, H. (2008). Inflammation and immunity in diabetic vascular complications. *Curr Opin Lipidol*, *19*(5), 519-524. doi:10.1097/MOL.0b013e32830f47cd
- Nishikawa, T., Edelstein, D., Du, X. L., Yamagishi, S., Matsumura, T., Kaneda, Y., . . . Brownlee, M. (2000). Normalizing mitochondrial superoxide production blocks three pathways of hyperglycaemic damage. *Nature*, *404*(6779), 787-790. doi:10.1038/35008121
- Nishio, Y. (2016). [Epidemiology of coronary heart diseases in the patients with diabetes]. *Nihon Rinsho*, *74 Suppl 2*, 297-301.
- Nour, S., Baheiraei, N., Imani, R., Khodaei, M., Alizadeh, A., Rabiee, N., & Moazzeni, S. M. (2019). A review of accelerated wound healing approaches: biomaterial- assisted tissue remodeling. *J Mater Sci Mater Med*, *30*(10), 120. doi:10.1007/s10856-019-6319-6
- Nozohouri, S., Sifat, A. E., Vaidya, B., & Abbruscato, T. J. (2020). Novel approaches for the delivery of therapeutics in ischemic stroke. *Drug Discov Today*, *25*(3), 535-551. doi:10.1016/j.drudis.2020.01.007
- O'Toole, E. A., Marinkovich, M. P., Peavey, C. L., Amieva, M. R., Furthmayr, H., Mustoe, T. A., & Woodley, D. T. (1997). Hypoxia increases human keratinocyte motility on connective tissue. *J Clin Invest*, *100*(11), 2881-2891. doi:10.1172/JCI119837
- Oakes, S. A., & Papa, F. R. (2015). The role of endoplasmic reticulum stress in human pathology. *Annu Rev Pathol*, *10*, 173-194. doi:10.1146/annurev-pathol-012513-104649
- Obermeier, B., Daneman, R., & Ransohoff, R. M. (2013). Development, maintenance and disruption of the blood-brain barrier. *Nat Med*, *19*(12), 1584-1596. doi:10.1038/nm.3407
- Onat, A., Donmez, I., Karadeniz, Y., Cakir, H., & Kaya, A. (2014). Type-2 diabetes and coronary heart disease: common physiopathology, viewed from autoimmunity. *Expert Rev Cardiovasc Ther*, *12*(6), 667-679. doi:10.1586/14779072.2014.910114

- Orasanu, G., & Plutzky, J. (2009). The pathologic continuum of diabetic vascular disease. *J Am Coll Cardiol*, *53*(5 Suppl), S35-42. doi:10.1016/j.jacc.2008.09.055
- Ou, J. L., Mizushima, Y., Wang, S. Y., Chuang, D. Y., Nadar, M., & Hsu, W. L. (2013). Structure-activity relationship analysis of curcumin analogues on anti-influenza virus activity. *FEBS J*, *280*(22), 5829-5840. doi:10.1111/febs.12503
- Oya, T., Hattori, N., Mizuno, Y., Miyata, S., Maeda, S., Osawa, T., & Uchida, K. (1999). Methylglyoxal modification of protein. Chemical and immunochemical characterization of methylglyoxal-arginine adducts. *J Biol Chem*, *274*(26), 18492-18502. doi:10.1074/jbc.274.26.18492
- Pan, M. H., Huang, T. M., & Lin, J. K. (1999). Biotransformation of curcumin through reduction and glucuronidation in mice. *Drug Metab Dispos*, *27*(4), 486-494.
- Panahi, Y., Alishiri, G. H., Parvin, S., & Sahebkar, A. (2016). Mitigation of Systemic Oxidative Stress by Curcuminoids in Osteoarthritis: Results of a Randomized Controlled Trial. *J Diet Suppl*, *13*(2), 209-220. doi:10.3109/19390211.2015.1008611
- Panahi, Y., Darvishi, B., Jowzi, N., Beiraghdar, F., & Sahebkar, A. (2016). Chlorella vulgaris: A Multifunctional Dietary Supplement with Diverse Medicinal Properties. *Curr Pharm Des*, *22*(2), 164-173. doi:10.2174/1381612822666151112145226
- Pandey, A., Chaturvedi, M., Mishra, S., Kumar, P., Somvanshi, P., & Chaturvedi, R. (2020). Reductive metabolites of curcumin and their therapeutic effects. *Heliyon*, *6*(11), e05469. doi:10.1016/j.heliyon.2020.e05469
- Pandey, A. K., Bhattacharya, P., Shukla, S. C., Paul, S., & Patnaik, R. (2015). Resveratrol inhibits matrix metalloproteinases to attenuate neuronal damage in cerebral ischemia: a molecular docking study exploring possible neuroprotection. *Neural Regen Res*, *10*(4), 568-575. doi:10.4103/1673-5374.155429
- Pandit, R., Chen, L., & Gotz, J. (2020). The blood-brain barrier: Physiology and strategies for drug delivery. *Adv Drug Deliv Rev*, *165-166*, 1-14. doi:10.1016/j.addr.2019.11.009
- Pangestuti, R., & Kim, S. K. (2011). Neuroprotective effects of marine algae. *Mar Drugs*, *9*(5), 803-818. doi:10.3390/md9050803
- Pangestuti, R., & Kim, S. K. (2014). Biological activities of carrageenan. *Adv Food Nutr Res*, *72*, 113-124. doi:10.1016/B978-0-12-800269-8.00007-5
- Papachristoforou, E., Lambadiari, V., Maratou, E., & Makrilakis, K. (2020). Association of Glycemic Indices (Hyperglycemia, Glucose Variability, and Hypoglycemia) with Oxidative Stress and Diabetic Complications. *J Diabetes Res*, *2020*, 7489795. doi:10.1155/2020/7489795
- Park, S. B., Bae, D. W., Clavio, N. A. B., Zhao, L., Jeong, C. S., Choi, B. M., . . . Cha, S. S. (2018). Structural and Biochemical Characterization of the Curcumin-Reducing Activity of CurA from *Vibrio vulnificus*. *J Agric Food Chem*, *66*(40), 10608-10616. doi:10.1021/acs.jafc.8b03647
- Patel, S. S., Acharya, A., Ray, R. S., Agrawal, R., Raghuvanshi, R., & Jain, P. (2020). Cellular and molecular mechanisms of curcumin in prevention and treatment of disease. *Crit Rev Food Sci Nutr*, *60*(6), 887-939. doi:10.1080/10408398.2018.1552244
- Peng, S. F., Lee, C. Y., Hour, M. J., Tsai, S. C., Kuo, D. H., Chen, F. A., . . . Yang, J. S. (2014). Curcumin-loaded nanoparticles enhance apoptotic cell death of U2OS human osteosarcoma cells through the Akt-Bad signaling pathway. *Int J Oncol*, *44*(1), 238-246. doi:10.3892/ijo.2013.2175
- Peppas, M., & Vlassara, H. (2005). Advanced glycation end products and diabetic complications: a general overview. *Hormones (Athens)*, *4*(1), 28-37. doi:10.14310/horm.2002.11140
- Pereira, A. G., Otero, P., Echave, J., Carreira-Casais, A., Chamorro, F., Collazo, N., . . . Prieto, M. A. (2021). Xanthophylls from the Sea: Algae as Source of Bioactive Carotenoids. *Mar Drugs*, *19*(4). doi:10.3390/md19040188
- Petremand, J., Puyal, J., Chatton, J. Y., Duprez, J., Allagnat, F., Frias, M., . . . Widmann, C. (2012). HDLs protect pancreatic beta-cells against ER stress by restoring protein folding and trafficking. *Diabetes*, *61*(5), 1100-1111. doi:10.2337/db11-1221
- Petrie, T. A., Strand, N. S., Yang, C. T., Rabinowitz, J. S., & Moon, R. T. (2014). Macrophages modulate adult zebrafish tail fin regeneration. *Development*, *141*(13), 2581-2591. doi:10.1242/dev.098459
- Phaniendra, A., Jestadi, D. B., & Periyasamy, L. (2015). Free radicals: properties, sources, targets, and their implication in various diseases. *Indian J Clin Biochem*, *30*(1), 11-26. doi:10.1007/s12291-014-0446-0

- Pinet, K., & McLaughlin, K. A. (2019). Mechanisms of physiological tissue remodeling in animals: Manipulating tissue, organ, and organism morphology. *Dev Biol*, *451*(2), 134-145. doi:10.1016/j.ydbio.2019.04.001
- Policardo, L., Seghieri, G., Anichini, R., De Bellis, A., Franconi, F., Francesconi, P., . . . Mannucci, E. (2015). Effect of diabetes on hospitalization for ischemic stroke and related in-hospital mortality: a study in Tuscany, Italy, over years 2004-2011. *Diabetes Metab Res Rev*, *31*(3), 280-286. doi:10.1002/dmrr.2607
- Pourghadamyari, H., Rezaei, M., Ipakchi-Azimi, A., Eisa-Beygi, S., Basiri, M., Tahamtani, Y., & Baharvand, H. (2019). Establishing a new animal model for muscle regeneration studies. *Mol Biol Res Commun*, *8*(4), 171-179. doi:10.22099/mbrc.2019.34611.1433
- Prajapati, V. D., Maheriya, P. M., Jani, G. K., & Solanki, H. K. (2014). Carrageenan: a natural seaweed polysaccharide and its applications. *Carbohydr Polym*, *105*, 97-112. doi:10.1016/j.carbpol.2014.01.067
- Prasad, S., Tyagi, A. K., & Aggarwal, B. B. (2014). Recent developments in delivery, bioavailability, absorption and metabolism of curcumin: the golden pigment from golden spice. *Cancer Res Treat*, *46*(1), 2-18. doi:10.4143/crt.2014.46.1.2
- Primer, K. R., Psaltis, P. J., Tan, J. T. M., & Bursill, C. A. (2020). The Role of High-Density Lipoproteins in Endothelial Cell Metabolism and Diabetes-Impaired Angiogenesis. *Int J Mol Sci*, *21*(10). doi:10.3390/ijms21103633
- Profaci, C. P., Munji, R. N., Pulido, R. S., & Daneman, R. (2020). The blood-brain barrier in health and disease: Important unanswered questions. *J Exp Med*, *217*(4). doi:10.1084/jem.20190062
- Pulido-Moran, M., Moreno-Fernandez, J., Ramirez-Tortosa, C., & Ramirez-Tortosa, M. (2016). Curcumin and Health. *Molecules*, *21*(3), 264. doi:10.3390/molecules21030264
- Putala, J. (2020). Ischemic Stroke in Young Adults. *Continuum (Minneapolis)*, *26*(2), 386-414. doi:10.1212/CON.0000000000000833
- Rader, D. J., & Hovingh, G. K. (2014). HDL and cardiovascular disease. *Lancet*, *384*(9943), 618-625. doi:10.1016/S0140-6736(14)61217-4
- Rahmati, M., Alipanahi, Z., & Mozafari, M. (2019). Emerging Biomedical Applications of Algal Polysaccharides. *Curr Pharm Des*, *25*(11), 1335-1344. doi:10.2174/1381612825666190423160357
- Rainwater, D. L., Blangero, J., Moore, P. H., Jr., Shelledy, W. R., & Dyer, T. D. (1995). Genetic control of apolipoprotein A-I distribution among HDL subclasses. *Atherosclerosis*, *118*(2), 307-317. doi:10.1016/0021-9150(95)05623-8
- Rasines-Perea, Z., & Teissedre, P. L. (2017). Grape Polyphenols' Effects in Human Cardiovascular Diseases and Diabetes. *Molecules*, *22*(1). doi:10.3390/molecules22010068
- Ren, J., Bi, Y., Sowers, J. R., Hetz, C., & Zhang, Y. (2021). Endoplasmic reticulum stress and unfolded protein response in cardiovascular diseases. *Nat Rev Cardiol*, *18*(7), 499-521. doi:10.1038/s41569-021-00511-w
- Richardson, R., Slanchev, K., Kraus, C., Knyphausen, P., Eming, S., & Hammerschmidt, M. (2013). Adult zebrafish as a model system for cutaneous wound-healing research. *J Invest Dermatol*, *133*(6), 1655-1665. doi:10.1038/jid.2013.16
- Richner, M., Ferreira, N., Dudele, A., Jensen, T. S., Vaegter, C. B., & Goncalves, N. P. (2018). Functional and Structural Changes of the Blood-Nerve-Barrier in Diabetic Neuropathy. *Front Neurosci*, *12*, 1038. doi:10.3389/fnins.2018.01038
- Robert, J., Osto, E., & von Eckardstein, A. (2021). The Endothelium Is Both a Target and a Barrier of HDL's Protective Functions. *Cells*, *10*(5). doi:10.3390/cells10051041
- Robichaud, S., Fairman, G., Vijithakumar, V., Mak, E., Cook, D. P., Pelletier, A. R., . . . Ouimet, M. (2021). Identification of novel lipid droplet factors that regulate lipophagy and cholesterol efflux in macrophage foam cells. *Autophagy*, *17*(11), 3671-3689. doi:10.1080/1548627.2021.1886839
- Roe, K. (2021). An inflammation classification system using cytokine parameters. *Scand J Immunol*, *93*(2), e12970. doi:10.1111/sji.12970
- Rohrer, L., Ohnsorg, P. M., Lehner, M., Landolt, F., Rinninger, F., & von Eckardstein, A. (2009). High-density lipoprotein transport through aortic endothelial cells involves scavenger receptor BI and ATP-binding cassette transporter G1. *Circ Res*, *104*(10), 1142-1150. doi:10.1161/CIRCRESAHA.108.190587
- Ruiz, M., Okada, H., & Dahlback, B. (2017). HDL-associated ApoM is anti-apoptotic by delivering sphingosine 1-phosphate to S1P1 & S1P3 receptors on vascular endothelium. *Lipids Health Dis*, *16*(1), 36. doi:10.1186/s12944-017-0429-2

- Ruocco, N., Costantini, S., Guariniello, S., & Costantini, M. (2016). Polysaccharides from the Marine Environment with Pharmacological, Cosmeceutical and Nutraceutical Potential. *Molecules*, 21(5). doi:10.3390/molecules21050551
- Rye, K. A., & Barter, P. J. (2014). Cardioprotective functions of HDLs. *J Lipid Res*, 55(2), 168-179. doi:10.1194/jlr.R039297
- Saemann, M. D., Poglitsch, M., Kopecky, C., Haidinger, M., Horl, W. H., & Weichhart, T. (2010). The versatility of HDL: a crucial anti-inflammatory regulator. *Eur J Clin Invest*, 40(12), 1131-1143. doi:10.1111/j.1365-2362.2010.02361.x
- Sakaguchi, M., Kinoshita, R., Putranto, E. W., Ruma, I. M. W., Sumardika, I. W., Youyi, C., . . . Murata, H. (2017). Signal Diversity of Receptor for Advanced Glycation End Products. *Acta Med Okayama*, 71(6), 459-465. doi:10.18926/AMO/55582
- Sano, R., & Reed, J. C. (2013). ER stress-induced cell death mechanisms. *Biochim Biophys Acta*, 1833(12), 3460-3470. doi:10.1016/j.bbamcr.2013.06.028
- Sarikaya, H., Ferro, J., & Arnold, M. (2015). Stroke prevention--medical and lifestyle measures. *Eur Neurol*, 73(3-4), 150-157. doi:10.1159/000367652
- Schalkwijk, C. G., & Stehouwer, C. D. (2005). Vascular complications in diabetes mellitus: the role of endothelial dysfunction. *Clin Sci (Lond)*, 109(2), 143-159. doi:10.1042/CS20050025
- Schalkwijk, C. G., & Stehouwer, C. D. A. (2020). Methylglyoxal, a Highly Reactive Dicarbonyl Compound, in Diabetes, Its Vascular Complications, and Other Age-Related Diseases. *Physiol Rev*, 100(1), 407-461. doi:10.1152/physrev.00001.2019
- Schalkwijk, C. G., van Bezu, J., van der Schors, R. C., Uchida, K., Stehouwer, C. D., & van Hinsbergh, V. W. (2006). Heat-shock protein 27 is a major methylglyoxal-modified protein in endothelial cells. *FEBS Lett*, 580(6), 1565-1570. doi:10.1016/j.febslet.2006.01.086
- Schmidt, M. I., Duncan, B. B., Reichelt, A. J., Branchtein, L., Matos, M. C., Costa e Forti, A., . . . Brazilian Gestational Diabetes Study, G. (2001). Gestational diabetes mellitus diagnosed with a 2-h 75-g oral glucose tolerance test and adverse pregnancy outcomes. *Diabetes Care*, 24(7), 1151-1155. doi:10.2337/diacare.24.7.1151
- Schroder, M., & Kaufman, R. J. (2005a). ER stress and the unfolded protein response. *Mutat Res*, 569(1-2), 29-63. doi:10.1016/j.mrfmmm.2004.06.056
- Schroder, M., & Kaufman, R. J. (2005b). The mammalian unfolded protein response. *Annu Rev Biochem*, 74, 739-789. doi:10.1146/annurev.biochem.73.011303.074134
- Schumacher, D., Morgenstern, J., Oguchi, Y., Volk, N., Kopf, S., Groener, J. B., . . . Freichel, M. (2018). Compensatory mechanisms for methylglyoxal detoxification in experimental & clinical diabetes. *Mol Metab*, 18, 143-152. doi:10.1016/j.molmet.2018.09.005
- Scieszka, S., & Klewicka, E. (2019). Algae in food: a general review. *Crit Rev Food Sci Nutr*, 59(21), 3538-3547. doi:10.1080/10408398.2018.1496319
- Senoner, T., & Dichtl, W. (2019). Oxidative Stress in Cardiovascular Diseases: Still a Therapeutic Target? *Nutrients*, 11(9). doi:10.3390/nu11092090
- Shinohara, M., Thornalley, P. J., Giardino, I., Beisswenger, P., Thorpe, S. R., Onorato, J., & Brownlee, M. (1998). Overexpression of glyoxalase-I in bovine endothelial cells inhibits intracellular advanced glycation endproduct formation and prevents hyperglycemia-induced increases in macromolecular endocytosis. *J Clin Invest*, 101(5), 1142-1147. doi:10.1172/JCI119885
- Shirakata, Y., Kimura, R., Nanba, D., Iwamoto, R., Tokumaru, S., Morimoto, C., . . . Hashimoto, K. (2005). Heparin-binding EGF-like growth factor accelerates keratinocyte migration and skin wound healing. *J Cell Sci*, 118(Pt 11), 2363-2370. doi:10.1242/jcs.02346
- Shishkova, V. N., & Adasheva, T. V. (2021). [Cerebrovascular disease in patients with type 2 diabetes mellitus]. *Zh Nevrol Psikhiatr Im S S Korsakova*, 121(6), 114-118. doi:10.17116/jnevro2021121061114
- Shokri, Y., Variji, A., Nosrati, M., Khonakdar-Tarsi, A., Kianmehr, A., Kashi, Z., . . . Mahrooz, A. (2020). Importance of paraoxonase 1 (PON1) as an antioxidant and antiatherogenic enzyme in the cardiovascular complications of type 2 diabetes: Genotypic and phenotypic evaluation. *Diabetes Res Clin Pract*, 161, 108067. doi:10.1016/j.diabres.2020.108067

- Singh, A. P., Singh, R., Verma, S. S., Rai, V., Kaschula, C. H., Maiti, P., & Gupta, S. C. (2019). Health benefits of resveratrol: Evidence from clinical studies. *Med Res Rev*, *39*(5), 1851-1891. doi:10.1002/med.21565
- Singh, R., Barden, A., Mori, T., & Beilin, L. (2001). Advanced glycation end-products: a review. *Diabetologia*, *44*(2), 129-146. doi:10.1007/s001250051591
- Skrivarhaug, T., Bangstad, H. J., Stene, L. C., Sandvik, L., Hanssen, K. F., & Joner, G. (2006). Long-term mortality in a nationwide cohort of childhood-onset type 1 diabetic patients in Norway. *Diabetologia*, *49*(2), 298-305. doi:10.1007/s00125-005-0082-6
- Smajlovic, D. (2015). Strokes in young adults: epidemiology and prevention. *Vasc Health Risk Manag*, *11*, 157-164. doi:10.2147/VHRM.S53203
- Snelson, M., & Coughlan, M. T. (2019). Dietary Advanced Glycation End Products: Digestion, Metabolism and Modulation of Gut Microbial Ecology. *Nutrients*, *11*(2). doi:10.3390/nu11020215
- So, J. S. (2018). Roles of Endoplasmic Reticulum Stress in Immune Responses. *Mol Cells*, *41*(8), 705-716. doi:10.14348/molcells.2018.0241
- Sohn, S. I., Priya, A., Balasubramaniam, B., Muthuramalingam, P., Sivasankar, C., Selvaraj, A., . . . Pandian, S. (2021). Biomedical Applications and Bioavailability of Curcumin-An Updated Overview. *Pharmaceutics*, *13*(12). doi:10.3390/pharmaceutics13122102
- Song, C., Yang, J., Zhang, M., Ding, G., Jia, C., Qin, J., & Guo, L. (2021). Marine Natural Products: The Important Resource of Biological Insecticide. *Chem Biodivers*, *18*(5), e2001020. doi:10.1002/cbdv.202001020
- Song, Q., Song, H., Xu, J., Huang, J., Hu, M., Gu, X., . . . Gao, X. (2016). Biomimetic ApoE-Reconstituted High Density Lipoprotein Nanocarrier for Blood-Brain Barrier Penetration and Amyloid Beta-Targeting Drug Delivery. *Mol Pharm*, *13*(11), 3976-3987. doi:10.1021/acs.molpharmaceut.6b00781
- Steenbeke, M., De Bruyne, S., De Buyzere, M., Lapauw, B., Speeckaert, R., Petrovic, M., . . . Speeckaert, M. M. (2021). The role of soluble receptor for advanced glycation end-products (sRAGE) in the general population and patients with diabetes mellitus with a focus on renal function and overall outcome. *Crit Rev Clin Lab Sci*, *58*(2), 113-130. doi:10.1080/10408363.2020.1791045
- Steenkamp, D. W., Alexanian, S. M., & McDonnell, M. E. (2013). Adult hyperglycemic crisis: a review and perspective. *Curr Diab Rep*, *13*(1), 130-137. doi:10.1007/s11892-012-0342-z
- Stewart, A., Rioux, D., Boyer, F., Gielly, L., Pompanon, F., Saillard, A., . . . Coissac, E. (2021). Altitudinal Zonation of Green Algae Biodiversity in the French Alps. *Front Plant Sci*, *12*, 679428. doi:10.3389/fpls.2021.679428
- Stitt, A. W., Curtis, T. M., Chen, M., Medina, R. J., McKay, G. J., Jenkins, A., . . . Lois, N. (2016). The progress in understanding and treatment of diabetic retinopathy. *Prog Retin Eye Res*, *51*, 156-186. doi:10.1016/j.preteyeres.2015.08.001
- Stratton, S., Shelke, N. B., Hoshino, K., Rudraiah, S., & Kumbar, S. G. (2016). Bioactive polymeric scaffolds for tissue engineering. *Bioact Mater*, *1*(2), 93-108. doi:10.1016/j.bioactmat.2016.11.001
- Sturtzel, C. (2017). Endothelial Cells. *Adv Exp Med Biol*, *1003*, 71-91. doi:10.1007/978-3-319-57613-8_4
- Sun, H., Saeedi, P., Karuranga, S., Pinkepank, M., Ogurtsova, K., Duncan, B. B., . . . Magliano, D. J. (2022). IDF Diabetes Atlas: Global, regional and country-level diabetes prevalence estimates for 2021 and projections for 2045. *Diabetes Res Clin Pract*, *183*, 109119. doi:10.1016/j.diabres.2021.109119
- Sun, Y., Ma, X., & Hu, H. (2021). Marine Polysaccharides as a Versatile Biomass for the Construction of Nano Drug Delivery Systems. *Mar Drugs*, *19*(6). doi:10.3390/md19060345
- Sweeney, M. D., Zhao, Z., Montagne, A., Nelson, A. R., & Zlokovic, B. V. (2019). Blood-Brain Barrier: From Physiology to Disease and Back. *Physiol Rev*, *99*(1), 21-78. doi:10.1152/physrev.00050.2017
- Takeuchi, M., & Makita, Z. (2001). Alternative routes for the formation of immunochemically distinct advanced glycation end-products in vivo. *Curr Mol Med*, *1*(3), 305-315. doi:10.2174/1566524013363735
- Tan, J. T., Ng, M. K., & Bursill, C. A. (2015). The role of high-density lipoproteins in the regulation of angiogenesis. *Cardiovasc Res*, *106*(2), 184-193. doi:10.1093/cvr/cvv104
- Tervaert, T. W., Mooyaart, A. L., Amann, K., Cohen, A. H., Cook, H. T., Drachenberg, C. B., . . . Renal Pathology, S. (2010). Pathologic classification of diabetic nephropathy. *J Am Soc Nephrol*, *21*(4), 556-563. doi:10.1681/ASN.2010010010
- Tesfamariam, B., Brown, M. L., & Cohen, R. A. (1991). Elevated glucose impairs endothelium-dependent relaxation by activating protein kinase C. *J Clin Invest*, *87*(5), 1643-1648. doi:10.1172/JCI115179

- Thomas, N. V., & Kim, S. K. (2013). Beneficial effects of marine algal compounds in cosmeceuticals. *Mar Drugs*, *11*(1), 146-164. doi:10.3390/md11010146
- Tran-Dinh, A., Diallo, D., Delbosc, S., Varela-Perez, L. M., Dang, Q. B., Lapergue, B., . . . Meilhac, O. (2013). HDL and endothelial protection. *Br J Pharmacol*, *169*(3), 493-511. doi:10.1111/bph.12174
- Tran-Dinh, A., Levoye, A., Couret, D., Galle-Treger, L., Moreau, M., Delbosc, S., . . . Meilhac, O. (2020). High-Density Lipoprotein Therapy in Stroke: Evaluation of Endothelial SR-BI-Dependent Neuroprotective Effects. *Int J Mol Sci*, *22*(1). doi:10.3390/ijms22010106
- Trigo-Gutierrez, J. K., Vega-Chacon, Y., Soares, A. B., & Mima, E. G. O. (2021). Antimicrobial Activity of Curcumin in Nanoformulations: A Comprehensive Review. *Int J Mol Sci*, *22*(13). doi:10.3390/ijms22137130
- Tsai, Y. M., Chang-Liao, W. L., Chien, C. F., Lin, L. C., & Tsai, T. H. (2012). Effects of polymer molecular weight on relative oral bioavailability of curcumin. *Int J Nanomedicine*, *7*, 2957-2966. doi:10.2147/IJN.S32630
- Tsao, R. (2010). Chemistry and biochemistry of dietary polyphenols. *Nutrients*, *2*(12), 1231-1246. doi:10.3390/nu2121231
- Tsompanidi, E. M., Brinkmeier, M. S., Fotiadou, E. H., Giakoumi, S. M., & Kypreos, K. E. (2010). HDL biogenesis and functions: role of HDL quality and quantity in atherosclerosis. *Atherosclerosis*, *208*(1), 3-9. doi:10.1016/j.atherosclerosis.2009.05.034
- Tsuda, T. (2018). Curcumin as a functional food-derived factor: degradation products, metabolites, bioactivity, and future perspectives. *Food Funct*, *9*(2), 705-714. doi:10.1039/c7fo01242j
- Tsujita, M., Wolska, A., Gutmann, D. A. P., & Remaley, A. T. (2018). Reconstituted Discoidal High-Density Lipoproteins: Bioinspired Nanodiscs with Many Unexpected Applications. *Curr Atheroscler Rep*, *20*(12), 59. doi:10.1007/s11883-018-0759-1
- Tureyen, K., Kapadia, R., Bowen, K. K., Satriotomo, I., Liang, J., Feinstein, D. L., & Vemuganti, R. (2007). Peroxisome proliferator-activated receptor-gamma agonists induce neuroprotection following transient focal ischemia in normotensive, normoglycemic as well as hypertensive and type-2 diabetic rodents. *J Neurochem*, *101*(1), 41-56. doi:10.1111/j.1471-4159.2006.04376.x
- Umen, J. G. (2014). Green algae and the origins of multicellularity in the plant kingdom. *Cold Spring Harb Perspect Biol*, *6*(11), a016170. doi:10.1101/cshperspect.a016170
- Umpierrez, G., & Korytkowski, M. (2016). Diabetic emergencies - ketoacidosis, hyperglycaemic hyperosmolar state and hypoglycaemia. *Nat Rev Endocrinol*, *12*(4), 222-232. doi:10.1038/nrendo.2016.15
- Unlu, A., Nayir, E., Dogukan Kalenderoglu, M., Kirca, O., & Ozdogan, M. (2016). Curcumin (Turmeric) and cancer. *J BUON*, *21*(5), 1050-1060.
- Unnithan, A. K. A., & Mehta, P. (2022). Hemorrhagic Stroke. In *StatPearls*. Treasure Island (FL).
- van Sloten, T. T., Sedaghat, S., Carnethon, M. R., Launer, L. J., & Stehouwer, C. D. A. (2020). Cerebral microvascular complications of type 2 diabetes: stroke, cognitive dysfunction, and depression. *Lancet Diabetes Endocrinol*, *8*(4), 325-336. doi:10.1016/S2213-8587(19)30405-X
- Vellampatti, S., Chandrasekaran, G., Mitta, S. B., Lakshmanan, V. K., & Park, S. H. (2018). Metallo-Curcumin-Conjugated DNA Complexes Induces Preferential Prostate Cancer Cells Cytotoxicity and Pause Growth of Bacterial Cells. *Sci Rep*, *8*(1), 14929. doi:10.1038/s41598-018-33369-z
- Vignola, A. M., Kips, J., & Bousquet, J. (2000). Tissue remodeling as a feature of persistent asthma. *J Allergy Clin Immunol*, *105*(6 Pt 1), 1041-1053. doi:10.1067/mai.2000.107195
- Viigimaa, M., Sachinidis, A., Toumpourleka, M., Koutsampasopoulos, K., Alliksoo, S., & Titma, T. (2020). Macrovascular Complications of Type 2 Diabetes Mellitus. *Curr Vasc Pharmacol*, *18*(2), 110-116. doi:10.2174/1570161117666190405165151
- Villasenor, R., Lampe, J., Schwaninger, M., & Collin, L. (2019). Intracellular transport and regulation of transcytosis across the blood-brain barrier. *Cell Mol Life Sci*, *76*(6), 1081-1092. doi:10.1007/s00018-018-2982-x
- Vincent, A. M., & Feldman, E. L. (2004). New insights into the mechanisms of diabetic neuropathy. *Rev Endocr Metab Disord*, *5*(3), 227-236. doi:10.1023/B:REMD.0000032411.11422.e0
- Vistoli, G., De Maddis, D., Cipak, A., Zarkovic, N., Carini, M., & Aldini, G. (2013). Advanced glycoxidation and lipoxidation end products (AGEs and ALEs): an overview of their mechanisms of formation. *Free Radic Res*, *47 Suppl 1*, 3-27. doi:10.3109/10715762.2013.815348

- Wang, H. D., Chen, C. C., Huynh, P., & Chang, J. S. (2015). Exploring the potential of using algae in cosmetics. *Bioresour Technol*, *184*, 355-362. doi:10.1016/j.biortech.2014.12.001
- Wang, X., Antony, V., Wang, Y., Wu, G., & Liang, G. (2020). Pattern recognition receptor-mediated inflammation in diabetic vascular complications. *Med Res Rev*, *40*(6), 2466-2484. doi:10.1002/med.21711
- Wang, X. Z., Harding, H. P., Zhang, Y., Jolicoeur, E. M., Kuroda, M., & Ron, D. (1998). Cloning of mammalian Ire1 reveals diversity in the ER stress responses. *EMBO J*, *17*(19), 5708-5717. doi:10.1093/emboj/17.19.5708
- Wang, Y., Yu, Q., Fan, D., & Cao, F. (2012). Coronary heart disease in type 2 diabetes: mechanisms and comprehensive prevention strategies. *Expert Rev Cardiovasc Ther*, *10*(8), 1051-1060. doi:10.1586/erc.12.52
- White, C. R., Datta, G., & Giordano, S. (2017). High-Density Lipoprotein Regulation of Mitochondrial Function. *Adv Exp Med Biol*, *982*, 407-429. doi:10.1007/978-3-319-55330-6_22
- Wong, K. E., Ngai, S. C., Chan, K. G., Lee, L. H., Goh, B. H., & Chuah, L. H. (2019). Curcumin Nanoformulations for Colorectal Cancer: A Review. *Front Pharmacol*, *10*, 152. doi:10.3389/fphar.2019.00152
- Wu, L., & Juurlink, B. H. (2002). Increased methylglyoxal and oxidative stress in hypertensive rat vascular smooth muscle cells. *Hypertension*, *39*(3), 809-814. doi:10.1161/hy0302.105207
- Xepapadaki, E., Zvintzou, E., Kalogeropoulou, C., Filou, S., & Kypreos, K. E. (2020). Tauhe Antioxidant Function of HDL in Atherosclerosis. *Angiology*, *71*(2), 112-121. doi:10.1177/0003319719854609
- Xu, S. Y., Huang, X., & Cheong, K. L. (2017). Recent Advances in Marine Algae Polysaccharides: Isolation, Structure, and Activities. *Mar Drugs*, *15*(12). doi:10.3390/md15120388
- Xu, X. Y., Meng, X., Li, S., Gan, R. Y., Li, Y., & Li, H. B. (2018). Bioactivity, Health Benefits, and Related Molecular Mechanisms of Curcumin: Current Progress, Challenges, and Perspectives. *Nutrients*, *10*(10). doi:10.3390/nu10101553
- Yallapu, M. M., Gupta, B. K., Jaggi, M., & Chauhan, S. C. (2010). Fabrication of curcumin encapsulated PLGA nanoparticles for improved therapeutic effects in metastatic cancer cells. *J Colloid Interface Sci*, *351*(1), 19-29. doi:10.1016/j.jcis.2010.05.022
- Yamagishi, S. (2009). Advanced glycation end products and receptor-oxidative stress system in diabetic vascular complications. *Ther Apher Dial*, *13*(6), 534-539. doi:10.1111/j.1744-9987.2009.00775.x
- Yamagishi, S. (2012). Potential clinical utility of advanced glycation end product cross-link breakers in age- and diabetes-associated disorders. *Rejuvenation Res*, *15*(6), 564-572. doi:10.1089/rej.2012.1335
- Yamagishi, S., Fukami, K., & Matsui, T. (2015). Crosstalk between advanced glycation end products (AGEs)-receptor RAGE axis and dipeptidyl peptidase-4-incretin system in diabetic vascular complications. *Cardiovasc Diabetol*, *14*, 2. doi:10.1186/s12933-015-0176-5
- Yang, C., Hawkins, K. E., Dore, S., & Candelario-Jalil, E. (2019). Neuroinflammatory mechanisms of blood-brain barrier damage in ischemic stroke. *Am J Physiol Cell Physiol*, *316*(2), C135-C153. doi:10.1152/ajpcell.00136.2018
- Yang, H., Zhang, Y., Zhou, F., Guo, J., Tang, J., Han, Y., . . . Fu, C. (2020). Preparation, Bioactivities and Applications in Food Industry of Chitosan-Based Maillard Products: A Review. *Molecules*, *26*(1). doi:10.3390/molecules26010166
- Yang, Q., Kaji, R., Takagi, T., Kohara, N., Murase, N., Yamada, Y., . . . Bostock, H. (2001). Abnormal axonal inward rectifier in streptozocin-induced experimental diabetic neuropathy. *Brain*, *124*(Pt 6), 1149-1155. doi:10.1093/brain/124.6.1149
- Yang, S. L., Zhu, L. Y., Han, R., Sun, L. L., Li, J. X., & Dou, J. T. (2017). Pathophysiology of peripheral arterial disease in diabetes mellitus. *J Diabetes*, *9*(2), 133-140. doi:10.1111/1753-0407.12474
- Yemisci, M., Caban, S., GURSOY-OZDEMIR, Y., Lule, S., Novoa-Carballal, R., Riguera, R., . . . Dalkara, T. (2015). Systemically administered brain-targeted nanoparticles transport peptides across the blood-brain barrier and provide neuroprotection. *J Cereb Blood Flow Metab*, *35*(3), 469-475. doi:10.1038/jcbfm.2014.220
- Yeung, Y. T., Aziz, F., Guerrero-Castilla, A., & Arguelles, S. (2018). Signaling Pathways in Inflammation and Anti-inflammatory Therapies. *Curr Pharm Des*, *24*(14), 1449-1484. doi:10.2174/1381612824666180327165604
- Yokoyama, S. (2006). ABCA1 and biogenesis of HDL. *J Atheroscler Thromb*, *13*(1), 1-15. doi:10.5551/jat.13.1
- Youssef, L., Bhaw-Luximon, A., Diotel, N., Catan, A., Giraud, P., Gimie, F., . . . Couprie, J. (2019). Enhanced effects of curcumin encapsulated in polycaprolactone-grafted oligocarrageenan nanomicelles, a novel nanoparticle drug delivery system. *Carbohydr Polym*, *217*, 35-45. doi:10.1016/j.carbpol.2019.04.014

- Zannis, V. I., Chroni, A., & Krieger, M. (2006). Role of apoA-I, ABCA1, LCAT, and SR-BI in the biogenesis of HDL. *J Mol Med (Berl)*, 84(4), 276-294. doi:10.1007/s00109-005-0030-4
- Zannis, V. I., Fotakis, P., Koukos, G., Kardassis, D., Ehnholm, C., Jauhiainen, M., & Chroni, A. (2015). HDL biogenesis, remodeling, and catabolism. *Handb Exp Pharmacol*, 224, 53-111. doi:10.1007/978-3-319-09665-0_2
- Zhang, P., Li, T., Wu, X., Nice, E. C., Huang, C., & Zhang, Y. (2020). Oxidative stress and diabetes: antioxidative strategies. *Front Med*, 14(5), 583-600. doi:10.1007/s11684-019-0729-1
- Zhang, Q., Wang, Y., & Fu, L. (2020). Dietary advanced glycation end-products: Perspectives linking food processing with health implications. *Compr Rev Food Sci Food Saf*, 19(5), 2559-2587. doi:10.1111/1541-4337.12593
- Zhang, X., Zeng, H., Bao, S., Wang, N., & Gillies, M. C. (2014). Diabetic macular edema: new concepts in pathophysiology and treatment. *Cell Biosci*, 4, 27. doi:10.1186/2045-3701-4-27
- Zhao, Y., Patzer, A., Herdegen, T., Gohlke, P., & Culman, J. (2006). Activation of cerebral peroxisome proliferator-activated receptors gamma promotes neuroprotection by attenuation of neuronal cyclooxygenase-2 overexpression after focal cerebral ischemia in rats. *FASEB J*, 20(8), 1162-1175. doi:10.1096/fj.05-5007com
- Zheng, B., & McClements, D. J. (2020). Formulation of More Efficacious Curcumin Delivery Systems Using Colloid Science: Enhanced Solubility, Stability, and Bioavailability. *Molecules*, 25(12). doi:10.3390/molecules25122791
- Zheng, Z., & Zheng, F. (2016). Immune Cells and Inflammation in Diabetic Nephropathy. *J Diabetes Res*, 2016, 1841690. doi:10.1155/2016/1841690
- Zhou, H., Zhang, X., & Lu, J. (2014). Progress on diabetic cerebrovascular diseases. *Bosn J Basic Med Sci*, 14(4), 185-190. doi:10.17305/bjbms.2014.4.203
- Zhuang, X., Xiang, X., Grizzle, W., Sun, D., Zhang, S., Axtell, R. C., . . . Zhang, H. G. (2011). Treatment of brain inflammatory diseases by delivering exosome encapsulated anti-inflammatory drugs from the nasal region to the brain. *Mol Ther*, 19(10), 1769-1779. doi:10.1038/mt.2011.164

Annexe

Microglia distribution in adult zebrafish brain: focus on oxidative stress implication during brain repair

Sai Sandhya Narra*¹, Philippe Rondeau*¹, Danielle Fernezelian¹, Laura Gence¹, Batoul Ghaddar¹, Emmanuel Bourdon¹, Christian Lefebvre d'Hellencourt¹, Sepand Rastegar² and Nicolas Diotel^{#1}

*These authors equally contributed to the work

Corresponding author

¹ Université de La Réunion, INSERM, UMR 1188, Diabète athérombose Thérapies Réunion Océan Indien (DÉTROÏ), Saint-Denis de La Réunion, France

² Institute of Biological and Chemical Systems-Biological Information Processing (IBCS-BIP), Karlsruhe Institute of Technology (KIT), Postfach 3640, 76021 Karlsruhe, Germany.

Abstract

Microglia constitutes a macrophage-like cell exerting determinant roles in neuroinflammatory and oxidative stress processes during brain regeneration. Here, zebrafish animals were used to decipher microglia involvement in brain plasticity and repair mechanisms. Firstly by using immunohistochemistry, the distribution of microglia in the whole brain was analyzed with antibodies directed against Tg (*mpeg1.1:mcherry*) fish and L-plastin (Lcp1) antigens. Specific regional differences were evidenced in terms of microglia density and morphology (elongated, branched, highly branched and amoeboid). Using Tg(*fli:GFP*) and Tg (*GFAP::GFP*) enabling detection of endothelial cells and neural stem cells (NSCs) respectively, interaction of elongated microglia with blood vessels and rounded/amoeboid microglia with NSCs were evidenced. Secondly, in a telencephalic injury model, an abundant microglia presence was observed 5 days post-injury (dpi) and was associated with a high regenerative neurogenesis process. Finally, RNA sequencing analysis from telencephalon at 5 dpi confirmed the up-regulation of microglia markers and highlighted a significant increase of genes involved in oxidative stress, such as *nox2*, *nrf2a* and *gsr*. Interestingly, analysis of antioxidant activities at 5 dpi revealed an upregulation of superoxide dismutase (SOD) and peroxidase activities as well as a persistent H₂O₂ generation. Overall, our data provide a better characterization of microglia in the healthy brain, showing evolutionarily conserved features with mammals. They also highlight the persistence of activated microglia and the disruption of redox balance during brain regeneration. Together, these data raise the question of the role of oxidative stress in regenerative neurogenesis in zebrafish.

Key word: brain injury, microglia, oxidative stress, SOD, teleost

Introduction

Microglia were discovered in the early 1920 by Pío del Río Hortega and are derived from progenitors present in the embryonic yolk sac (Ginhoux et al., 2013; Sierra et al., 2016). They are macrophage-like cells located in the central nervous system, representing about 10 to 20% of glial cells. (Nayak et al., 2014; Var and Byrd-Jacobs, 2020). Microglia cells exhibit a very important plasticity and are capable of major adaptations through structural and functional modifications. Under physiological conditions, microglia remain in a quiescent state with a small cell body and highly branched processes, allowing immediate sensing of the microenvironment. In contrast, under pathological conditions (i.e. degenerative diseases, strokes, brain injuries, infections), cells rapidly adopt a phagocytic, ameboid and mobile phenotype, allowing them to move and reach the damaged area (Stence et al., 2001). During brain injury, microglia participate in the removal of cell debris and constitute key players of neuroinflammatory and oxidative stress processes (Kim and Joh, 2006; Smith et al., 2012; Fischer and Maier, 2015; Simpson and Oliver, 2020).

Due to its strong neurogenic activity and capacity to repair large brain injuries, zebrafish is emerging as an excellent organism model for brain plasticity and regeneration studies (März et al., 2011; Kishimoto et al., 2012; Diotel et al., 2013; Schmidt et al., 2014; Alunni and Bally-Cuif, 2016; Diotel et al., 2020; Zambusi and Ninkovic, 2020; Ghaddar et al., 2021b). As a result, a growing number of studies have begun to examine the role of microglia, neuroinflammation, and oxidative stress in brain injury and neurodegenerative conditions in zebrafish (Kyritsis et al., 2012; Bhattarai et al., 2017; Kanagaraj et al., 2020; Var and Byrd-Jacobs, 2020).

In zebrafish, microglia represent the major neuroinflammatory cells present in the central nervous system and are capable of dynamic phenotype change depending on the physiological context. As observed in mammals, zebrafish microglia are widely activated and recruited to the damaged area (Kroehne et al., 2011; März et al., 2011; Baumgart et al., 2012; Kyritsis et al., 2012; Casano et al., 2016; Silva et al., 2020; Ghaddar et al., 2021b). After telencephalic injury in zebrafish, an acute inflammation occurs associated with abundant pro-inflammatory cytokine releases and intense microglia activation (Kyritsis et al., 2012). This inflammatory state has been shown to be essential for the brain repair process, and its inhibition resulted in decreased regenerative neurogenesis. (Kyritsis et al., 2012). As well, the inhibition of microglia in zebrafish led to impaired

regeneration (Kanagaraj et al., 2020), clearly demonstrating the key role of microglia and inflammation in brain repair mechanisms.

The cellular damage and death that occurs during injury also lead to mitochondrial dysfunction and the excessive production of reactive oxygen species (ROS), including the superoxide anion radical, hydroxyl radical and hydrogen peroxide (H₂O₂). This imbalance between free radicals and antioxidant defenses results in the generation of oxidative stress. In order to maintain homeostasis, several antioxidant defenses are activated. They involve among others the enzymes superoxide dismutase (SOD), catalase and glutathione peroxidase (Gpx). SOD are the first detoxification enzymes and catalyze the dismutation of two superoxide anion molecules into H₂O₂ and molecular oxygen. Then, catalase reduces H₂O₂ to water and molecular oxygen, thus completing the detoxification process initiated by SOD. Similarly, glutathione peroxidase (GPx) breaks down H₂O₂ into water. In parallel, glutathione reductase reduces glutathione disulfide to the sulfhydryl form of glutathione, thus helping to resist oxidative stress. Together, these different enzymatic activities help restore redox balance within the tissue. While the characterization of antioxidant defenses is well described in mammals during injury (Lin et al., 2021; Praveen Kumar et al., 2021), not much is known in zebrafish.

In this study, we set out to provide a better general overview of the distribution of microglia in the adult zebrafish brain, highlighting their intimate links to blood vessels and neurogenic niches. Given the emerging roles of microglia in brain regeneration (Bhattarai et al., 2016; Diaz-Aparicio et al., 2020), we took advantage of a recently published RNAseq dataset on the telencephalon of stab wounded adult zebrafish to reanalyze the expression of microglia markers at 5 days post injury (dpi) (Rodriguez Viales et al., 2015; Gourain et al., 2021). In parallel, we correlate these data with gene expression and activities of oxidative stress mediators at 5 dpi.

Material and Methods

Animals and ethics

Three to six month old adult zebrafish, wild type, Tg(*mpeg1.1:mcherry*), Tg(*mpeg1.1:GFP*), double transgenic Tg(*mpeg1.1:mcherry*) x Tg(*GFAP::GFP*) and Tg(*mpeg1.1:mcherry*) X Tg(*fli:GFP*) were obtained from the CYROI/DeTROI zebrafish facility and

maintained under standard conditions (28.5°C; 14 hours dark/10 hours light, pH 7.4 and conductivity at 400 µS). All experiments were conducted in zebrafish in accordance with the French and European Community guidelines for the use of animals in research (86/609/EEC and 2010/63/EU) and approved by the local CYROI animal experimentation ethics committee and the French government (APAFIS_20191105105351_v10).

Stab wound injury of the telencephalon

To perform the telencephalic brain lesion, fish were deeply anesthetized with 0.02% tricaine (MS-222; REF: A5040, Sigma-Aldrich) and a sterile needle (BD Microlance 3; 30 G ½; 0.3 × 13 mm) was inserted into the right telencephalic hemisphere as previously described (März et al., 2011; Diotel et al., 2013; Rodriguez Viales et al., 2015; Dorsemans et al., 2017b). Fish were allowed to survive for 5 days post-lesion (dpl) before being processed for immunohistochemistry or protein extraction from control and injured hemispheres.

Tissue preparation

Fish were euthanized with tricaine before being fixed overnight at 4°C in 4% PFA (Paraformaldehyde) dissolved in 1X PBS (Phosphate Saline Buffer). The next day, zebrafish were dissected and the brains were extracted and dehydrated in 100% Methanol before being stored at -20°C until use.

Immunohistochemistry (IHC)

For immunohistochemistry, brains were processed as described previously (März et al., 2011; Dorsemans et al., 2017a; Ghaddar et al., 2021a). Briefly, brains were rehydrated and permeabilized with PTw (1X PBS containing 0.1% Tween), embedded in 2% agarose, and sectioned (50 µm thickness) using a vibratome (VT1000S, Leica). After 1 h of blocking buffer (PTw containing 0.2% BSA and 1% DMSO), the sections were incubated with the respective antibodies such as anti-Lcp1/L-plastin (rabbit anti-L-plastin from zebrafish, kindly provided by Dr. Michael Redd; 1/10,000) and anti-PCNA (DAKO, clone PC10; Reference: M087901; 1/500) overnight at 4°C.

The next day, the sections were washed 3 times with PTw and incubated with the respective antibodies: Alexa Fluor® 488 goat anti-mouse antibody (ThermoFisher, Reference: A-11001; 1/500), Alexa Fluor® 594 goat anti-rabbit antibody (ThermoFisher, Reference: A-

11012; 1/500) and/or with Alexa fluor 594-coupled anti-mcherry antibody (ThermoFisher, Reference: M11240; 1/500) or Alexa fluor 488-coupled anti-GFP (ThermoFisher, Reference: A-21311; 1/500) for 2 hours at room temperature. During this time, counterstaining of cell nuclei with DAPI was also performed. Finally, the sections were washed with PTw and mounted on slides with Aqua-Poly/Mount (Polysciences).

Note that each immunohistochemistry experiment was performed on at least 3 different animals in independent experiments. The antibodies are listed in Table 1.

Table 1 Antibodies

Antibodies	Interest	Host	Reference	Dilution
PCNA Proliferative Cell Nuclear Antigen	cell proliferation	Mouse	DAKO, clone PC10; Reference: M087901	1/500
Lcp1 (L-plastin) Lymphocyte Cytosolic Protein 1	microglia	Rabbit	Kindly provided by Dr Michael Redd	1/10 000
Alexa Fluor® 488 goat anti-mouse antibody	PCNA antibody detection	Goat	Thermofischer A-11001	1/500
Alexa Fluor® 594 goat anti-rabbit antibody	LCP1 antibody detection	Goat	Thermofischer A-11012	1/500
Anti-mcherry coupled to Alexa fluor 594	Boost mcherry labelling	Rat	ThermoFisher, M11240	1/500
Anti-GFP coupled to Alexa fluor 488	Boost GFP labelling	Rabbit	ThermoFisher, A-21311	1/500

Protein extraction for cerebral antioxidant activities

At 5dpl, fish were euthanized and the skull was immediately open in order to separate and remove the control and injured telencephalon. Three pools of 5 control telencephala and three pools of 5 injured telencephala were collected and snapped frozen. This experiment was reproduced two times independently.

To determine the SOD and peroxidase activities, protein isolation from 5 dpl control and injured hemispheres was performed as follows. Four to eight mg of zebrafish hemispheres were collected and stored at -80°C before being homogenized with a TissueLyser II (Qiagen) in 100 μL of Tris buffer (Tris (25 mM), EDTA (1 mM), NaCl (50 mM), pH 7.4). After centrifugation (5000 rpm, 4°C for 10 min), the supernatant was used for protein quantification and enzymatic assays. Total proteins of lysate were quantified by the bicinchoninic acid assay (BCA).

Total SOD activity was determined using the cytochrome *c* reduction assay, as previously described (Dobi et al., 2019). Superoxide radicals generated by the xanthine/xanthine oxidase system reduce the ferricytochrome *c* into ferrocyanochrome *c*, thereby leading to an increase in absorbance at 560 nm. A 10 μL aliquot (about 30 μg of protein) of the lysates was combined with 170 μL reaction mixture (xanthine oxidase, xanthine (0.5 mM), cytochrome *c* (0.2 mM), KH_2PO_4 (50 mM, pH 7.8), EDTA (2 mM) and NaCN (1 mM)). The reaction was monitored in a microplate reader (Fluostar OPTIMA, BMG Labtech France) at 560 nm for 1 min, at 25°C . Total SOD activity was calculated using a calibration standard curve of SOD (up to 6 units/mg). Results were expressed as international catalytic units per μg of cell proteins. a Peroxidase activities of telencephalic hemisphere lysates were assessed according to the protocol described by Everse and colleagues (Everse et al., 1994) (A reaction mixture was prepared with 200 μL of 50 mM citrate buffer/0.2% o-dianisidine and 5 μL of lysates (between 15 to 20 μg of protein). The reaction was initiated by adding 20 μL of 200 mM H_2O_2 . Peroxidase activity was determined by measuring the absorbance at 450 nm at 25°C for 3 min. Peroxidase activity was expressed as international catalytic units per μg of proteins.

The determination of extracellular H_2O_2 production was performed by using N-acetyl-3,7-dihydroxyphenoxazine (Amplex Red) reagent. In the presence of horseradish peroxidase (HRP), this highly sensitive and stable probe reacts with H_2O_2 to produce highly fluorescent resorufin (PMID: 20526816, 2010). Lysates (10 μL / 30 μg of protein) were incubated in 96-well plates with the reaction buffer (50 μL) (Amplex Red 100 mM, HRP 1 U/mL in Tris-HCl 50 mM, pH 7.4) for 30 min at RT. The fluorescence intensity was measured with excitation/emission wavelength set at 550/590 nm. Hydrogen peroxide production content was calculated using a calibration standard curve of H_2O_2 (ranged from 4 to 40nM) and was expressed as nM of H_2O_2 per μg of proteins.

RNA sequencing data set analyses

For RNA sequencing analyses, data were reanalyzed from the Rodriguez-Viales et al. and Gourain et al. studies for control and injured telencephalon (5 dpl ; n = 3) (Rodriguez Viales et al., 2015; Gourain et al., 2021).

Microscopy

Micrographs were obtained with an Eclipse confocal (Nikon) and with an AXIO OBSERVER 7 equipped with the Apotome 2 (Zeiss). The brightness and contrast of the images were adjusted in Adobe Photoshop.

Cell counting

To determine the number of microglia and proliferating cells, the total area of mpeg- and PCNA-positive cells was measured on a 50- μ m-thick vibratome cross section through the core of the lesion. Quantification was done using Image J software on a total of 3 fish.

Nomenclature and abbreviations

The nomenclatures correspond to those provided in the zebrafish brain atlas (Wullimann et al., 1996). The schemes were modified and adapted from (Wullimann et al., 1996; Menuet et al., 2005). A, anterior thalamic nucleus; APN, accessory pretectal nucleus; ATN, anterior tuberal nucleus; CCe, corpus cerebelli; Chab, habenular commissure; Chor, horizontal commissure; CM, corpus mamillare; CP, central posterior thalamic nucleus; CPN, central pretectal nucleus; Cpop, postoptic commissure; Cpost, posterior commissure; D, dorsal telencephalic area; Dc, central zone of dorsal telencephalic area; Dl, lateral zone of dorsal telencephalic area; Dm, medial zone of dorsal telencephalic area; DOT, dorsomedial optic tract; Dp, posterior zone of dorsal telencephalic area; DP, dorsal posterior thalamic nucleus; ECL, external cellular layer of olfactory bulb; EG, eminentia granularis; ENv, entopenduncular nucleus, ventral part; FR, fasciculus retroflexus; GL, glomerular layer of olfactory bulb; Had, dorsal habenular nucleus; Hav, ventral habenular nucleus; Hc, caudal zone

of periventricular hypothalamus; Hd, dorsal zone of periventricular hypothalamus; Hv, ventral zone of periventricular hypothalamus; ICL, internal cellular layer of olfactory bulb; IL, inferior lobe; LH, lateral hypothalamic nucleus; LLF: lateral longitudinal fascicle; LR, lateral recess of diencephalic nucleus; MLF, medial longitudinal fascicle; NMLF, nucleus of medial longitudinal fascicle; PG, preglomerular nucleus; PGa, anterior preglomerular nucleus; PGI, lateral preglomerular nucleus; Pit, pituitary; PO, posterior pretectal nucleus; PP, periventricular pretectal nucleus; PPa, parvocellular preoptic nucleus, anterior part; PPp, parvocellular preoptic nucleus, posterior part; PR, posterior recess of diencephalic ventricle; PSp, parvocellular superficial pretectal nucleus; PTN, posterior tuberal nucleus; R, rostromedial nucleus; RF, reticular formation; SC, suprachiasmatic nucleus; SD, saccus dorsalis; SO, secondary octaval population; TeO, tectum opticum; TL, torus longitudinalis; TLa, torus lateralis; TPp, periventricular nucleus of posterior tuberculum; TS, torus semi-circularis; V, ventral telencephalic area; V3, third ventricle; VII, sensory root of the facial nerve; VIII, octaval nerve; VCe, valvula cerebelli; Vd, dorsal nucleus of ventral telencephalic area; VL, ventrolateral thalamic nucleus; VM, ventromedial thalamic nucleus; VOT, ventrolateral optic tract; Vp, postcommissural nucleus of ventral telencephalic area; Vv, ventral nucleus of dorsal telencephalic area; ZL, zona limitans.

Results

Distribution and morphology of microglia in the adult zebrafish brain

We first decided to provide a general overview of the distribution of microglia in the adult zebrafish brain. For this purpose, we used the Tg(*mpeg1.1:mcherry*) transgenic fish line and performed L-plastin (Lcp1) immunohistochemistry. We first demonstrated that both markers (*mpeg1.1* and L-plastin) were co-expressed in microglial cells within different brain regions such as the telencephalon and the midbrain parenchyma (Figure 1). In the healthy

telencephalon, we observed ramified/hyper-ramified, elongated and rounded/amoeboid cells (Figure 1, left panels). Evidently, in the midbrain, microglia appeared much more ramified/hyper-ramified than in the telencephalon, as shown in Figure 1 (right panels). The different morphologies are shown in Suppl. Figure 1.

In the forebrain, we observed by L-plastin immunohistochemistry a few microglial cells in the periphery and interior of the olfactory bulbs (not shown). In the telencephalon, small numbers of microglia were detected in all nuclei and brain regions, including the central (Dc), dorsomedian (Dm), and dorsoposterior (Dp) regions of the pallium as well as the central (Vc), ventral (Vv), and dorsal (Vd) nuclei of the subpallium. Microglia were detected in the brain parenchyma and also in close proximity to the ventricles (Figure 2A).

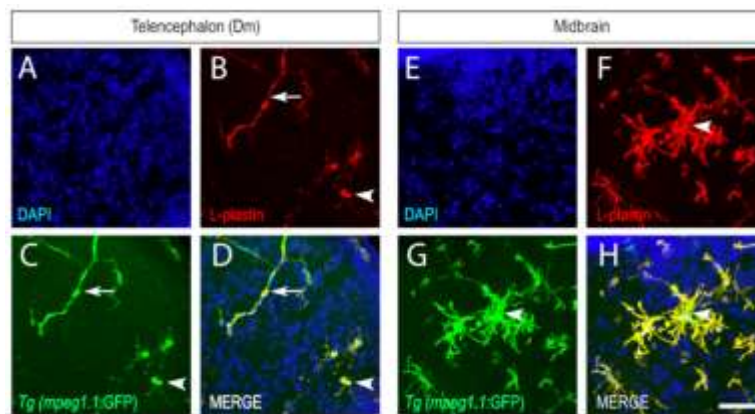


Figure 1: Co-expression of L-plastin and mpeg1.1:GFP in microglia from the telencephalon and midbrain showing different microglia morphologies

A-H: L-plastin immunohistochemistry (red, B and F) on *Tg(mpeg1.1:GFP)* fish (green, C and G) with DAPI counterstaining (blue, A and E) showing co-expression of both markers in the dorsomedian (Dm) telencephalon (left panels) and the midbrain parenchyma (right panels). In the telencephalon, most microglia appeared elongated (arrows) or rounded with a low number of processes (arrowheads). In contrast, in the posterior part of the brain, microglia appeared hyper-ramified (arrowheads). Bar: 70 μ m

More dorsally, microglia were again detected in the pallium, particularly in the dorsolateral telencephalon (DI). They were also reported in the post-commissural nucleus of the ventral telencephalic area (Vp) (Figure 2B). In the diencephalon, a high density of microglia was observed in the anterior (PPa) and posterior (PPp) parts of the preoptic area, in the entopeduncular nucleus (Env), suprachiasmatic nucleus (SC), ventrolateral and ventromedial thalamic nuclei (VL and VM, respectively), and in the habenula (Hav) (Figure 2B and C). Overall, our data showed that in the forebrain, microglia appear to be elongated or rounded but not so hyper-ramified under homeostatic conditions.

More caudally, numerous and abundant microglia were detected in the ventral, medio-basal and caudal hypothalamus (Figure 2D-F) along the ventricular layer but also in the parenchyma. A significant number of microglia was detected along the lateral and posterior recess of the hypothalamus. They were also observed in the optic tectum (TeO), the torus longitudinalis (TLa), the anterior preglomerular nucleus (Pga) and in the cerebellum, especially in the valvula cerebelli (VCe). L-plastin-positive cells were also found in the periventricular nucleus of the posterior tubercle (TPp) and in the zona limitans (ZL). A high density of microglia was also observed below the TeO, near the tectal ventricle and in the region of the torus semi-circularis (Ts). Clearly, microglia density appears to be higher in the hindbrain than in the telencephalon, and hyperbranched microglia are more numerous.

This distribution of microglia in the adult fish brain was also supported by the use of *Tg(mpeg1.1:mcherry)*. Therefore, under homeostatic conditions, we observed (1) elongated microglia (arrowheads) that are notably localized in the telencephalon, (2) rounded/amoeboid microglia (asterisks) detected along the ventricular layer and in the tela choroidea, and (3) ramified/hyper-ramified microglia, the latter being more abundantly observed in the posterior part of the brain.

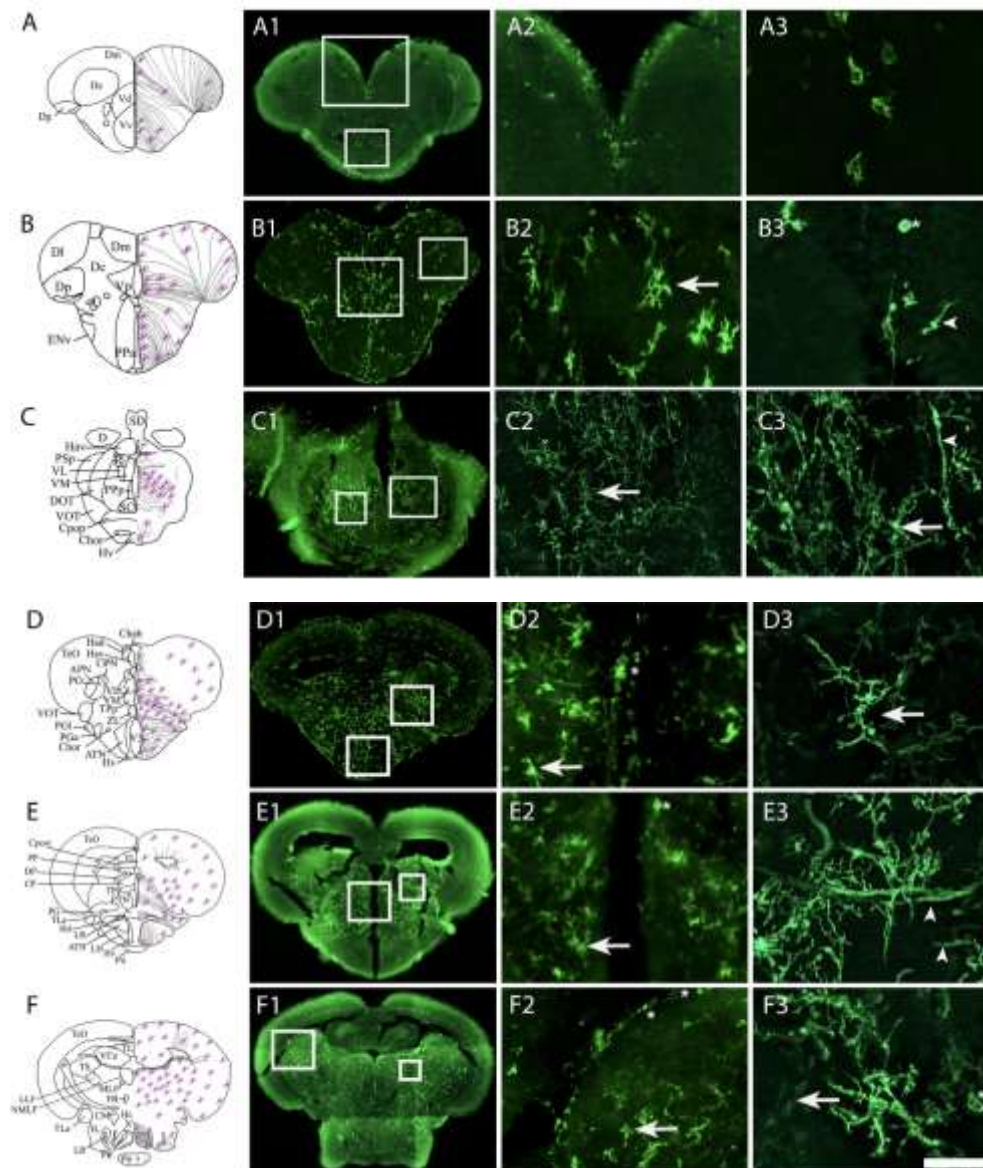


Figure 2 : Mapping of microglia in the brain of adult zebrafish showing heterogeneous distribution of microglia

A-F: The scheme provides the localization of the transversal section performed and purple cells correspond to the schematic distribution of microglia.

A-C: L-plastin immunohistochemistry in the telencephalon (A and B), diencephalon with the anterior (B, PPa) and posterior (C, PpP) parts of the preoptic area. Note that in the telencephalon, ramified, elongated and rounded microglia have been detected.

D-F: L-plastin immunohistochemistry in transversal brain section through the anterior part of the hypothalamus (D, Hv), the mediobasal hypothalamus (E, Hv LR) and the caudal hypothalamus (at the level of LR PR). Note the higher density of microglia in the posterior brain section than in the telencephalon. Microglia were detected in the anterior part of the hypothalamus (D2), the periventricular nucleus of the posterior tuberculum (TPp in D3), the central posterior thalamic nucleus (CP in E2), the torus semi-circularis (TS in F2) and midbrain parenchyma (F3). Note that the higher magnification pictures do not systematically correspond to the same picture of the lower magnification provided in A1 to F1.

Arrows pointed to ramified microglia, arrowheads showed elongated microglia and asterisks to almost ameboid microglia.

Bar: 30 μm (A3, B2, B3; D2, D3, E3, F3); 45 μm (E2); 60 μm (F2); 70 μm (C3); 90 μm (A2, C2); 200 μm (C1); 500 μm (D1, E1, F1); 600 μm (A1, B1)

Microglia is detected in the vicinity of blood vessels and neural stem cells (NSCs).

In our samples, careful observation of elongated microglia suggests that zebrafish microglia may also interact with blood vessels. To confirm this hypothesis in zebrafish, we generated double transgenics by crossing *Tg(mpeg1.1:mcherry)* with *Tg(fli:GFP)* fish, in which GFP is expressed in endothelial cells (Lawson and Weinstein, 2002; Cassam-Sulliman et al., 2021). As clearly demonstrated, many elongated microglial cells were extended along the blood vessels, namely in the dorsolateral and dorsomedial telencephalon and in the preoptic area. In Figure 3C, microglia clearly enveloped a blood vessel (Figure 3C, arrow in high-power view). These neuroanatomical observations strongly suggest a role for microglia in the immune function of the blood-brain barrier.

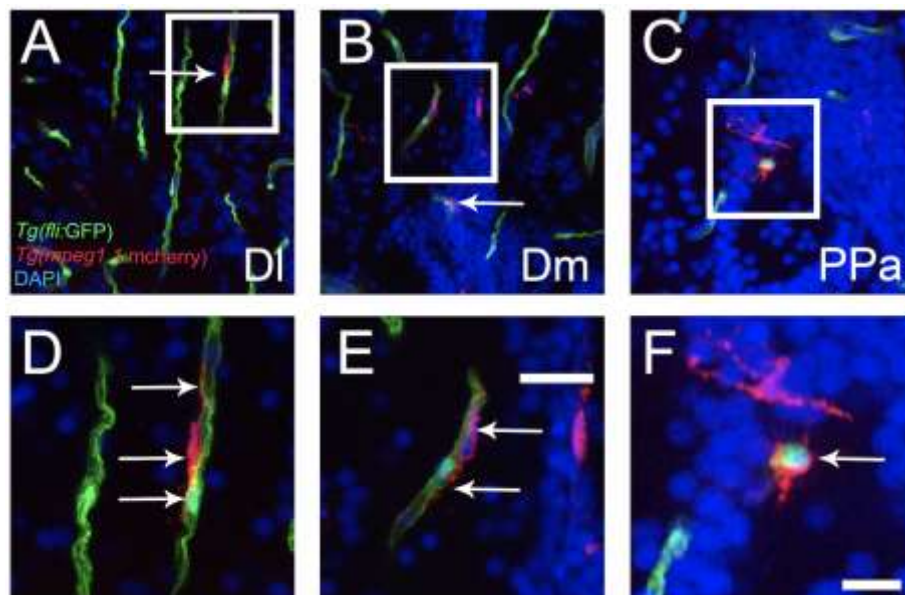


Figure 3: Microglia interact with blood vessels in the brain

A-F: Double transgenic *Tg(mpeg1.1:mcherry)* x *Tg(fli:GFP)* fish showing microglia (red) and endothelial cells (green), respectively. In the dorsolateral (Dl) and dorsomedian (Dm) telencephalon, as well as in the anterior part of the preoptic area (PPa) of the diencephalon, numerous elongated microglia are interacting with blood vessels (arrows). **D-F:** Higher magnifications of the respective white boxes found in A-C. Note that such interactions were observed in the whole brain. Bar: 16 μ m (F), 28 μ m (D and E), 42 μ m (C) and 70 μ m (A and B)

As well, numerous L-plastin and *mpeg1.1:mcherry*-positive cells were also detected in the ventricular/periventricular layer, where neural stem cells (NSCs) are located (Pellegrini et al., 2007; März et al., 2010). To better describe the potential interaction between microglia and NSCs, we generated double transgenic fish by crossing two existing lines and obtained *Tg(mpeg1.1:mcherry)* x *Tg(GFAP::GFP)* fish, allowing the detection of microglia and NSCs in red and green, respectively. In the pallium (Dm), we observed close proximity of rounded/amoeboid microglia with GFAP::GFP-positive NSCs (Figure 4A and D, arrows). Such

interactions were also observed in the Vv/Vd (Figure 4B and E, arrows). In other cases, such as in the posterior part of the preoptic area (PPp), some microglia far from the ventricular zone also appeared to make contact with NSC processes (Figure 4C, see arrows).

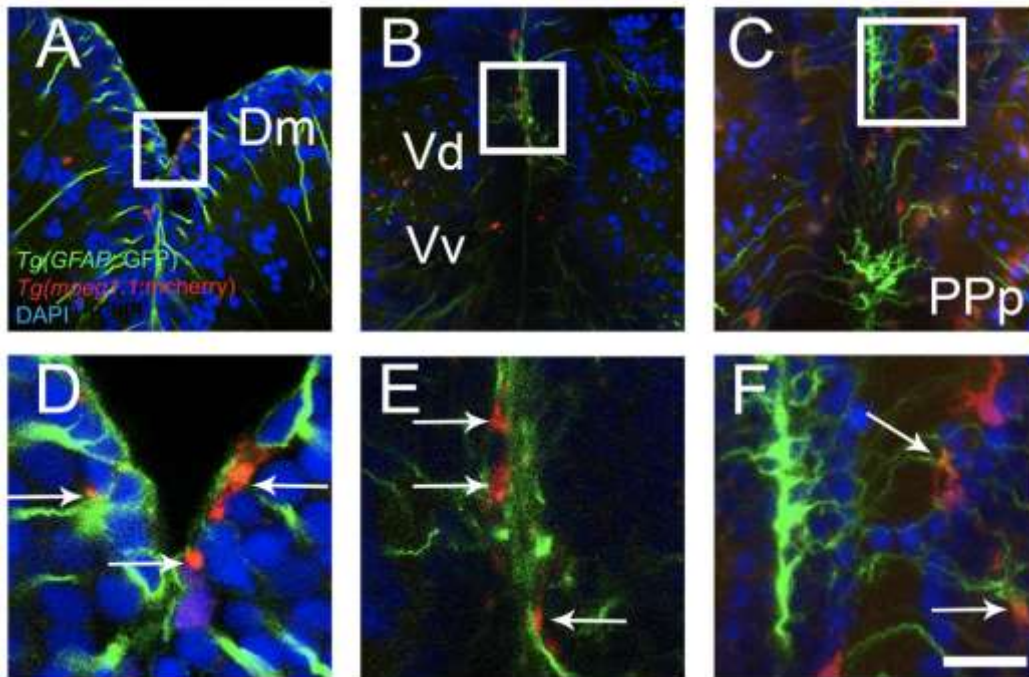


Figure 4: Microglia interact with neural stem cells

A-F: Double transgenic *Tg(mpeg1.1:mcherry) x Tg(GFAP::GFP)* fish showing microglia (red) and radial glial neural stem cells (radial glia in green), respectively. In the ventral (Vv and Vd nuclei) and dorsal (Dm) telencephalon as well as in the posterior part of the preoptic area (PPp) of the diencephalon, numerous rounded microglia are interacting with GFAP::GFP-positive cells known to correspond to radial glia (neural stem cells) (arrows). Most of these interactions were observed at the ventricular surface (D and E) but also at the level of NSC processes in the parenchyma (F). **D-F:** Higher magnifications of the respective white boxes found in A-C. Bar: 14 μ m (D and E), 20 μ m (F), 40 μ m (A) and 60 μ m (B and C).

Recruitment of microglia during telencephalic regeneration and links to oxidative stress

After stab wound injury of the telencephalon, microglia cells are activated, then they proliferate and migrate to the injured site in solely few hours (März et al., 2011; Kyritsis et al., 2012; Ghaddar et al., 2021b). In the injured hemisphere, the number of microglia increases to reach a peak between 2 and 3 days post-lesion according to the different studies, while their number remains constant in the non lesioned hemisphere (März et al., 2011; Kyritsis et al., 2012; Kanagaraj et al., 2020; Ghaddar et al., 2021b).

In our study, we demonstrated using *Tg(mpeg1.1:mcherry)* that the number of microglia was still significantly increased in the injured hemisphere at 5dpl (Figure 5A and B). Similar results were also obtained by L-plastin immunohistochemistry (not shown). In parallel,

a significant ventricular cell proliferation was observed in the lesioned hemisphere (Figure 5A and C), as previously described (Rodriguez Viales et al., 2015).

Reanalysis of the RNA-sequencing datasets reinforced the immunostaining results. Indeed, focusing on the expression of 6 genes (*mpeg1.1*, *spi1a*, *slc7a7*, *irf8a*, *apoeb*, and *lcp1*) that were found to be enriched in zebrafish microglia (Oosterhof et al., 2017), we observed their significant up-regulation 5 days post lesion (Figure 5D-I). Therefore, at 5 dpl, microglia are still activated and abundantly present in the injured hemisphere.

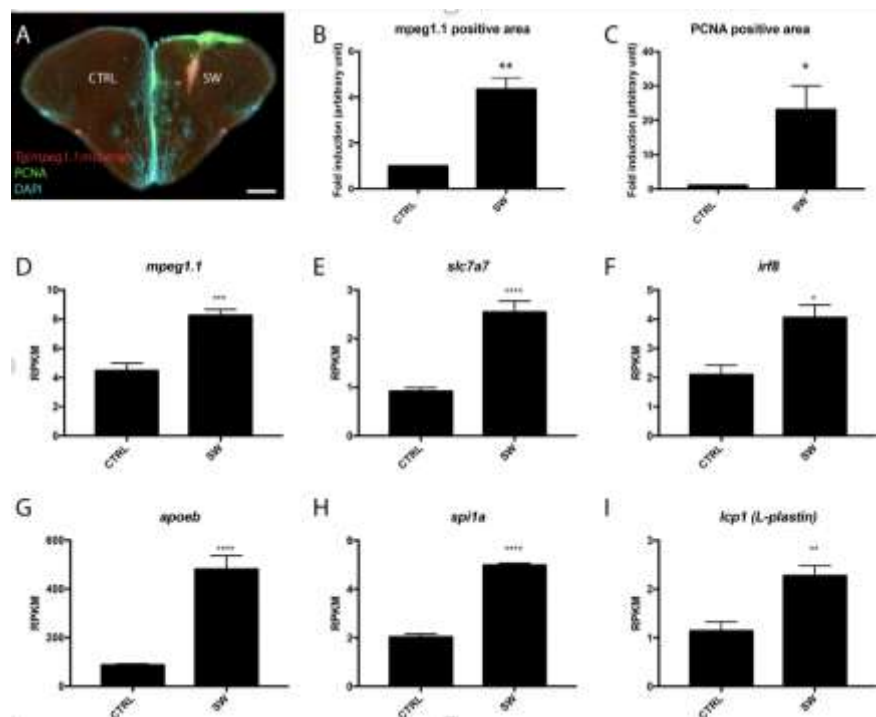


Figure 5: Recruitment of microglia and expression of microglia-enriched gene at 5 days post telencephalic injury

A: PCNA immunohistochemistry (green) on *Tg(mpeg1.1:mcherry)* fish (red) showing a strong ventricular cell proliferation within the telencephalic neurogenic niche and the presence of a higher number of microglia 5 days after brain injury. **B and C:** The quantification of the PCNA- and *mpeg1.1*: *mcherry*-positive area demonstrated their significant increase in the stab wounded hemisphere (SW) compared to control one (CTRL). The quantification corresponds to the mean of 3 different brain fish. **D - I:** Reanalysis of the RNA sequencing data set from injured and uninjured zebrafish telencephalon at 5 dpl from (Rodriguez Viales et al., 2015; Gourain et al., 2021). Enriched microglia genes are upregulated at 5 days post brain injury. * $p < 0.05$; ** $p < 0.01$; **** $p < 0.001$; ***** $p < 0.0001$. Bar: 200 μ m

During brain damage, oxidative stress is an important factor occurring in brain regeneration (Slemmer et al., 2008; Miyamoto et al., 2013; Hameed et al., 2015; Sakai and Shichita, 2019; Eastman et al., 2020). In mammals, ROS are generated by microglia via NADPH oxidase (NOX). Single cell RNA sequencing demonstrated that *Nox2* (*Cybb*) is the most highly expressed *Nox* gene in human and mouse microglia (Zhang et al., 2014; Simpson and Oliver,

2020). In zebrafish, the *nox2* gene was also shown to be enriched in microglia, and Ingenuity Pathway Analysis showed that genes strongly expressed in microglia are notably associated with ROS production (Oosterhof et al., 2017). So far, we decided to monitor *nox2* gene expression by reanalyzing the RNA sequencing data set from (Rodriguez Viales et al., 2015; Gourain et al., 2021). *nox2* expression was significantly upregulated in the injured hemisphere compared to the control one at 5 dpl (Figure 6A). Similarly, the expression of *nrf2a*, a transcription factor activated for combating oxidative stress, was also significantly increased at 5 dpl (Figure 6B).

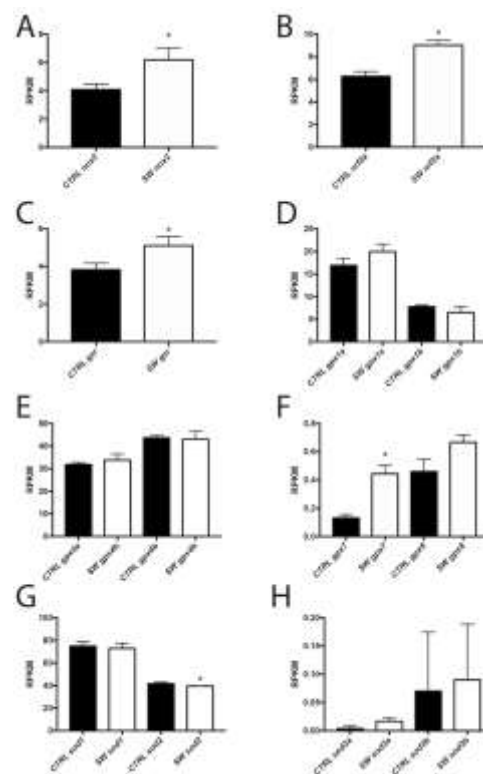


Figure 6: Expression of genes involved in oxidative stress and antioxidant defense during brain injury.

A-G: *nox2*, *nrf2a*, *gsr* (glutathione reductase), *gpx* and *sod* gene expression in the control (CTRL) and stab wounded (SW) telencephalic hemisphere 5 days after brain injury. Reanalysis of the RNA sequencing data set from injured and uninjured zebrafish telencephalon at 5 dpl from (Rodriguez Viales et al., 2015; Gourain et al., 2021). Enriched microglia genes are upregulated at 5 days post brain injury. * $p < 0.05$.

At the same time, by performing the Amplex Red assay, we observed significantly higher fluorescence in the stabbed hemisphere compared with the control. This shows that H_2O_2 levels are still elevated in the injured hemisphere 5 days after injury (Figure 7C). Given the presence of ROS and the upregulation of *nrf2*, known to regulate antioxidant defenses (Miller et al., 2012; Zhao et al., 2013), we then studied the gene expression of the main antioxidant enzymes, glutathione peroxidase (GPx) and superoxide dismutase (SOD). The expression of *gpx1a* and *1b*, *gpx4a* and *4b*, and *gpx8* genes remained unchanged, whereas

gpx7 was significantly increased in the stab wounded hemisphere (Figure 6C-F). The transcript level of *sod1*, *sod3a* and *3b* remained unchanged at 5dpl in the stab wounded telencephalon compared to the control telencephalon, while *sod2* was barely but significantly reduced ($p=0.03$). Interestingly, the *glutathione reductase* gene encoding the enzyme that reduces oxidized glutathione to the sulfhydryl form (reduced form) was significantly upregulated. We also measured the activities of the antioxidant enzymes glutathione peroxidase and SOD. The superoxide dismutase activity was significantly upregulated at 5 dpl. The glutathione peroxidase activity, which remains non-significant, was nevertheless observed to be increased in 2 independent experiments, correlated with a significant increase in Amplex red staining (Figure 7B and C).

Taken together, these data suggest the persistence of a pro-oxidant environment up to 5 dpl and the activation of antioxidant defense, associated with the presence of microglia and the activation of reactive neurogenesis.

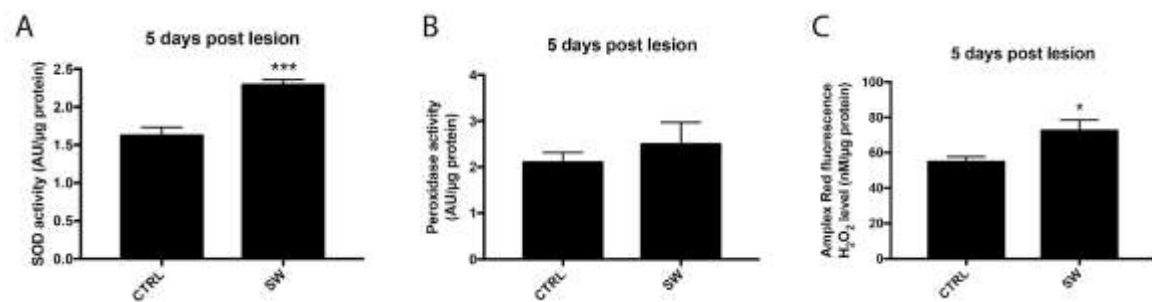


Figure 7 : SOD and Peroxidase activities after telencephalic injury

A: SOD activities from control (CTRL) and stab wounded (SW) telencephalon at 5 dpl from 2 independent experiments showing a significant increased activity of the antioxidant SOD enzyme. **B:** Glutathione Peroxidase activity from control and stab wounded telencephalon. An increasing trend was observed in 2 independent experiments in the injured telencephalon, but remains not significant. **C:** Amplex Red fluorescence showing a significant increase in H₂O₂ levels in the injured telencephalon compared to the respective control at 5dpl. n=3-6 pools of 5 CTRL and SW telencephalon. * $p<0.05$; *** $p<0.001$

DISCUSSION

In this work, we provided a better description of the distribution of microglia in the adult zebrafish brain using immunohistochemistry of L-plastin and Tg(*mpeg1.1:mcherry*) fish. Our results showed that microglia exhibited different distributions and phenotypes throughout the healthy brain. In addition, we also demonstrated a close association between microglia, blood vessels and NSCs, suggesting roles for microglia in the establishment and functions of the blood-brain barrier as well as in neurogenesis in zebrafish. In the context of telencephalic injury, we noted that genes known to be enriched in microglia are still upregulated at 5 dpl (*mpeg1.1*, *slc7a7*, *irf8*, *apoeb*, *spi1a* and *lcp1*). These data were also supported by the increased number of *mpeg1.1:mcherry*- and L-plastin-positive microglia in the injured hemisphere compared with the control hemisphere. Furthermore, we showed that some important regulators of oxidative stress are also upregulated at 5 dpl, such as *nox2*, *nrf2a*, and *glutathione reductase*, while gene expression of antioxidant enzymes (SOD and GPX) remains almost unchanged, except for *gpx7* and *sod2* which were slightly increased and decreased respectively. However, SOD activity was significantly higher in the injured telencephalon, correlated with increased Gpx and H₂O₂ levels. Together, these data highlight the role of microglia in brain homeostasis in constitutive and regenerative conditions and the role of oxidative stress in brain regeneration.

Microglia are widely but heterogeneously distributed in the brain of adult zebrafish

In our study, we provided a detailed mapping of microglia distribution across the different brain nuclei and domains of adult zebrafish based on L-plastin immunohistochemistry and using Tg(*mpeg1.1:mcherry*) fish. This general overview of microglia distribution in the brain of adult zebrafish complete other studies that mainly focused on some brain regions such as the some telencephalic and midbrain areas (März et al., 2011; Baumgart et al., 2012; Oosterhof et al., 2018; Wu et al., 2020; Cassam-Sulliman et al., 2021). We observed microglia in all brain subdivisions studied (tel-, di-, rhombencephalon). Interestingly, we noticed that the density of microglia varies from one brain to another, as well as its morphology. For example, in the telencephalon, the density of microglia under homeostatic conditions is quite low, whereas it is much higher in the midbrain (in the optic tectum and the brain domains below). These data raise the question of the roles and mechanisms that support the correct establishment of microglia density and its correct

migration in the brain. The *csf1r* (Colony-Stimulating Factor 1 Receptor) genes have been shown to play a key role in the density and distribution of microglia in the optic tectum (Oosterhof et al., 2018). However, *csf1r* involvement in other brain regions is largely unknown.

Microglia display different phenotypes in the brain of adult zebrafish

In our study, different types of microglia have been reported in homeostatic condition (i) elongated microglia mainly localized along blood vessels, (ii) rounded/amoeboid microglia mostly localized in the vicinity of cerebral ventricles known to correspond to neurogenic niches), and (iii) ramified and hyper-ramified microglia which were found for a high proportion in the diencephalon and midbrain. The roles of these different microglia subtypes are still not known in the healthy brain.

Elongated microglia were mainly associated with endothelial cells (Figure 3). This could argue for a role of microglia in the maintenance and/or function of the blood-brain barrier (BBB) in zebrafish. In mammals, microglia participate in the establishment and physiology of the BBB, allowing, among other things, its opening to promote leukocyte extravasation and angiogenesis (Dudvarski Stankovic et al., 2016). These blood vessel-associated microglia could also correspond to migratory microglia using the vasculature to reach their destination, as has been shown in mice (Mondo et al., 2020).

The presence of rounded/amoeboid microglia associated with NSCs in the ventricular zone has also been observed. Similar data have also been reported in some ventricular regions in mice, as well as in the subventricular zone of the lateral ventricle, corresponding to a major neurogenic niche in adult mammals (Ribeiro Xavier et al., 2015; Tan et al., 2020). These data suggest a possible role of microglia in the regulation of neurogenic processes in healthy conditions. In mammals, microglia have been described for modulating neural stem cell proliferation, new neuron differentiation and synaptogenesis (Sato, 2015; Diaz-Aparicio et al., 2020; Araki et al., 2021; Perez-Rodriguez et al., 2021). They participate in the clearance and removal of cells, the regulation of neural progenitor differentiation into neuroblasts, their survival, and functional integration (Ribeiro Xavier et al., 2015; Rodriguez-Iglesias et al., 2019; Al-Onaizi et al., 2020; Diaz-Aparicio et al., 2020). So far, in addition to their scavenger roles, microglia are implied in brain remodeling and plasticity of neural circuits (Paolicelli et al., 2011; Paladini et al., 2021). Such features would benefit further investigation in fish.

Regarding ramified microglia, they appear more numerous in the posterior part of the brain where they coexist with amoeboid microglia. In the midbrain, Wu et al (2020) showed that ccl34b.1-negative microglia have branched processes, low mobility and phagocytic characteristics. They also demonstrated that ccl34b.1-positive microglia was the predominant population in the midbrain and exhibited amoeboid, motile and phagocytic properties (Wu et al., 2020).

This diversity in microglia density and phenotype in the adult zebrafish brain is to be compared with the situation in mammals. Indeed, in mice, the number of microglia, their morphology, their molecular signature and their functions differ between brain areas (Tan et al., 2020). This suggests that different phenotypes might also contribute to different microglial functions in fish, as shown by Wu et al. (2020) in the zebrafish midbrain.

Microglia recruitment and oxidative stress after telencephalic injury

After any type of brain injury, inflammatory and oxidative stresses occur , leading to a disruption of brain homeostasis (Rodriguez-Rodriguez et al., 2014). Under such conditions, microglia mediate oxidative and inflammatory processes. In zebrafish, after stab wounding of the telencephalon, microglia are rapidly activated and recruited to the wound site (März et al., 2011; Baumgart et al., 2012; Kyritsis et al., 2012; Diotel et al., 2020; Ghaddar et al., 2021b). The number of microglia recruited to the injured telencephalon increases from 4-6 hours after injury, peaking at around 1-3 days depending on the microglia marker used for tracing these cells, and then slowly decreases. It nevertheless remains significantly elevated at 3-4 dpl in the injured telencephalon compared to the control telencephalon (März et al., 2011; Baumgart et al., 2012; Kyritsis et al., 2012; Kanagaraj et al., 2020; Ghaddar et al., 2021b). At 5 dpl, a key time point for regenerative neurogenesis (März et al., 2011; Rodriguez Viales et al., 2015; Diotel et al., 2020), we demonstrated that the number of mpeg1.1: mcherry-positive microglia remained significantly higher in the injured hemisphere than in the control one (Figure 5). These data were supported by L-plastin immunohistochemistry (data not shown) and by reanalysis of RNA-sequencing datasets, demonstrating the upregulation of genes enriched in microglia (Figure 5).

The inflammatory processes taking place during zebrafish brain damage induce regenerative neurogenesis (Kyritsis et al., 2012), and recent data suggest that this injury-induced neurogenesis was microglia dependent (Kanagaraj et al., 2020). Nevertheless, brain

inflammation appears to be transient with a fast upregulation of pro-inflammatory cytokines that is coming back to basal levels in solely 1 day post injury (Kyritsis et al., 2012). Until recently, only few data were available concerning oxidative stress processes during brain regeneration in fish. The injection of the fluorescent oxidative stress probes DCFH-DA prior to stab wound injury resulted in a strong fluorescence staining 30 minutes after the lesion (Suppl. Figure 2). However, at 5 days after injury, no fluorescence staining was observed (data not shown). We hypothesized that the lack of fluorescence might be due to the inability of the probes to reach the brain tissue once brain repair had begun. For this reason, we analyzed oxidative stress-related genes and performed the Amplex Red assay on the stabbed hemispheres. The *nox2* and *nrf2a* genes were upregulated, showing the persistence of a pro-oxidative environment at 5 days. This was confirmed by the increase in H₂O₂ levels revealed by the Amplex Red assay and by the increased SOD activity, an antioxidant enzyme known to be up-regulated under pro-oxidative conditions. Our results are in agreement with the recent study by Anand and colleagues (2021). These authors showed that stab wounding of the zebrafish telencephalon leads to a significant increase in SOD activity at 1 and 4 dpl, correlated with a significant increase in lipid peroxidation and reduced levels of glutathione (GSH) (Anand et al., 2021). This last point is corroborated by our study showing the significant up-regulation of the *glutathione reductase* gene. Indeed, glutathione reductase catalyzes the reduction of glutathione disulfide (GSSG, the oxidized form of glutathione) to glutathione in the sulfhydryl form (GSH, the reduced form), participating in the resistance to oxidative stress and the maintenance of a reducing environment. Similarly, Anand et al. also demonstrated that catalase activity increased only transiently at 1 dpl before reaching normal levels at 4 dpl. In our series of experiments, we were unfortunately unable to monitor catalase activity.

Overall, these data suggest the persistence of a pro-oxidative environment at 5 dpl, raising the question of the role of oxidative stress and microglia in brain repair mechanisms. Further functional studies would be needed to determine the actual beneficial or detrimental effects of oxidative stress during zebrafish brain regeneration.

Conclusion

In this work, we provided a general mapping of microglia and reported different densities and morphologies of microglia in the adult zebrafish brain. We highlighted the interaction of microglia with endothelial cells and neural stem cells, suggesting a role of

microglia in BBB and neurogenic functions. Finally, we showed that 5 days after brain injury, microglia are still abundantly present at the injury site with persistent oxidative stress as shown by the analysis of different markers such as *nox2* and *nrf2a* and antioxidant defense activities.

Acknowledgements

We thank Matthieu Bringart for excellent technical support with the fish facility, as well as Dr M. Redd for kindly providing the L-plastin antibody.

Author contributions

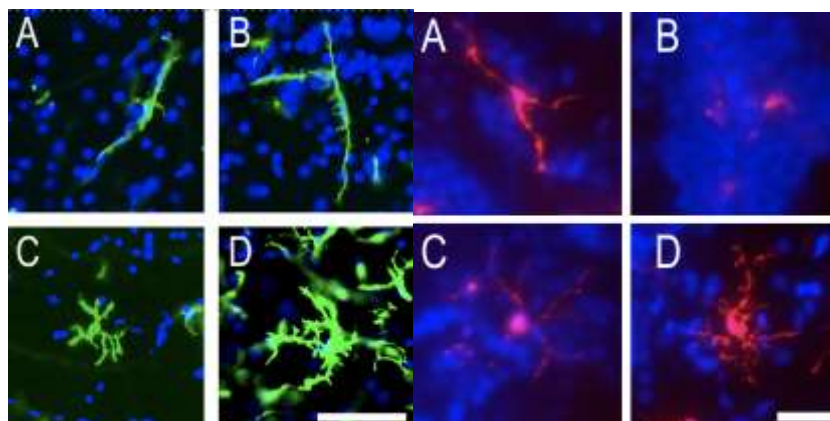
Conceptualization: N.D, P.R, C.L.D.H, E.B. and S.R.; Data curation: N.D. and S.R.; Formal analysis: N.D, P.R, C.L.D.H, E.B., S.S.N, S.R; Funding acquisition: N.D.; Investigation: all authors. Writing original draft: N.D.; Writing-review and editing: all authors. All the authors have read and agreed to the published version of the manuscript.

Funding

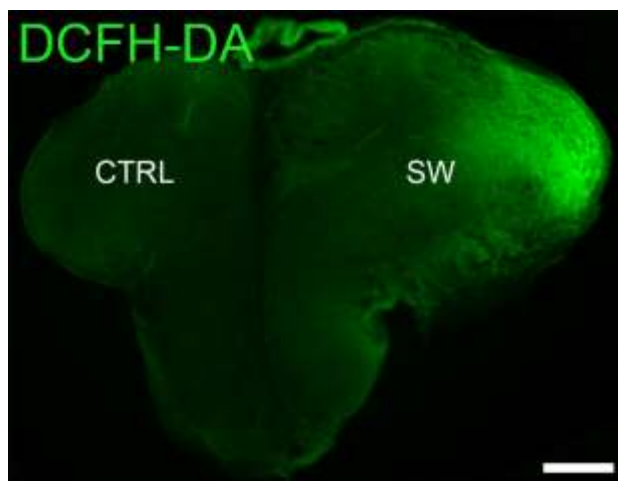
This work was supported by Grants from the University of La Réunion, European Union (EU)-Région Réunion-French State national counterpart: FEDER RE0022527 (ZEBRATOX).

Competing interests

The authors declare no competing interests.



Suppl. Figure 1: Different microglial morphologies observed in the brain of adult zebrafish
A-D: L-plastin immunohistochemistry (green) with DAPI counterstaining (blue) highlighting the different shape of microglia: elongated (A and B), ramified (C) and hyperamified (D) with numerous processes et protrusions.



Suppl. Figure 2: Brain injury leads to oxidative stress

Representative picture of DCFH-DA oxidative stress staining showing increased fluorescence in the stab wounded hemisphere 30 minutes post injury

REFERENCES

- Al-Onaizi M, Al-Khalifah A, Qasem D, ElAli A. 2020. Role of Microglia in Modulating Adult Neurogenesis in Health and Neurodegeneration. *International journal of molecular sciences* 21(18).
- Alunni A, Bally-Cuif L. 2016. A comparative view of regenerative neurogenesis in vertebrates. *Development* 143(5):741-753.
- Anand SK, Sahu MR, Mondal AC. 2021. Induction of oxidative stress and apoptosis in the injured brain: potential relevance to brain regeneration in zebrafish. *Mol Biol Rep* 48(6):5099-5108.
- Araki T, Ikegaya Y, Koyama R. 2021. The effects of microglia- and astrocyte-derived factors on neurogenesis in health and disease. *Eur J Neurosci* 54(5):5880-5901.
- Baumgart EV, Barbosa JS, Bally-Cuif L, Gotz M, Ninkovic J. 2012. Stab wound injury of the zebrafish telencephalon: a model for comparative analysis of reactive gliosis. *Glia* 60(3):343-357.
- Bhattarai P, Thomas AK, Cosacak MI, Papadimitriou C, Mashkaryan V, Froc C, Reinhardt S, Kurth T, Dahl A, Zhang Y, Kizil C. 2016. IL4/STAT6 Signaling Activates Neural Stem Cell Proliferation and Neurogenesis upon Amyloid-beta42 Aggregation in Adult Zebrafish Brain. *Cell reports* 17(4):941-948.
- Bhattarai P, Thomas AK, Zhang Y, Kizil C. 2017. The effects of aging on Amyloid-beta42-induced neurodegeneration and regeneration in adult zebrafish brain. *Neurogenesis (Austin)* 4(1):e1322666.
- Casano AM, Albert M, Peri F. 2016. Developmental Apoptosis Mediates Entry and Positioning of Microglia in the Zebrafish Brain. *Cell reports* 16(4):897-906.
- Cassam-Sulliman N, Ghaddar B, Gence L, Patche J, Rastegar S, Meilhac O, Diotel N. 2021. HDL biodistribution and brain receptors in zebrafish, using HDLs as vectors for targeting endothelial cells and neural progenitors. *Scientific reports* 11(1):6439.

- Diaz-Aparicio I, Paris I, Sierra-Torre V, Plaza-Zabala A, Rodriguez-Iglesias N, Marquez-Ropero M, Beccari S, Huguet P, Abiega O, Alberdi E, Matute C, Bernales I, Schulz A, Otrokocsi L, Sperlagh B, Happonen KE, Lemke G, Maletic-Savatic M, Valero J, Sierra A. 2020. Microglia Actively Remodel Adult Hippocampal Neurogenesis through the Phagocytosis Secretome. *J Neurosci* 40(7):1453-1482.
- Diotel N, Lubke L, Strahle U, Rastegar S. 2020. Common and Distinct Features of Adult Neurogenesis and Regeneration in the Telencephalon of Zebrafish and Mammals. *Front Neurosci* 14:568930.
- Diotel N, Vaillant C, Gabbero C, Mironov S, Fostier A, Gueguen MM, Anglade I, Kah O, Pellegrini E. 2013. Effects of estradiol in adult neurogenesis and brain repair in zebrafish. *Horm Behav* 63(2):193-207.
- Dobi A, Bravo SB, Veeren B, Paradelo-Dobarro B, Alvarez E, Meilhac O, Viranaicken W, Baret P, Devin A, Rondeau P. 2019. Advanced glycation end-products disrupt human endothelial cells redox homeostasis: new insights into reactive oxygen species production. *Free Radic Res* 53(2):150-169.
- Dorsemans AC, Lefebvre d'Hellencourt C, Ait-Arsa I, Jestin E, Meilhac O, Diotel N. 2017a. Acute and Chronic Models of Hyperglycemia in Zebrafish: A Method to Assess the Impact of Hyperglycemia on Neurogenesis and the Biodistribution of Radiolabeled Molecules. *J Vis Exp*(124).
- Dorsemans AC, Soule S, Weger M, Bourdon E, Lefebvre d'Hellencourt C, Meilhac O, Diotel N. 2017b. Impaired constitutive and regenerative neurogenesis in adult hyperglycemic zebrafish. *J Comp Neurol* 525(3):442-458.
- Dudvarski Stankovic N, Teodorczyk M, Ploen R, Zipp F, Schmidt MHH. 2016. Microglia-blood vessel interactions: a double-edged sword in brain pathologies. *Acta neuropathologica* 131(3):347-363.
- Eastman CL, D'Ambrosio R, Ganesh T. 2020. Modulating neuroinflammation and oxidative stress to prevent epilepsy and improve outcomes after traumatic brain injury. *Neuropharmacology* 172:107907.
- Everse J, Johnson MC, Marini MA. 1994. Peroxidative activities of hemoglobin and hemoglobin derivatives. *Methods Enzymol* 231:547-561.
- Fischer R, Maier O. 2015. Interrelation of oxidative stress and inflammation in neurodegenerative disease: role of TNF. *Oxidative medicine and cellular longevity* 2015:610813.
- Ghaddar B, Bringart M, Lefebvre d'Hellencourt C, Meilhac O, Diotel N. 2021a. Deleterious Effects of Overfeeding on Brain Homeostasis and Plasticity in Adult Zebrafish. *Zebrafish* 18(3):190-206.
- Ghaddar B, Lubke L, Couret D, Rastegar S, Diotel N. 2021b. Cellular Mechanisms Participating in Brain Repair of Adult Zebrafish and Mammals after Injury. *Cells* 10(2).
- Ginhoux F, Lim S, Hoeffel G, Low D, Huber T. 2013. Origin and differentiation of microglia. *Front Cell Neurosci* 7:45.
- Gourain V, Armant O, Lubke L, Diotel N, Rastegar S, Strahle U. 2021. Multi-Dimensional Transcriptome Analysis Reveals Modulation of Cholesterol Metabolism as Highly Integrated Response to Brain Injury. *Front Neurosci* 15:671249.
- Hameed LS, Berg DA, Belnoue L, Jensen LD, Cao Y, Simon A. 2015. Environmental changes in oxygen tension reveal ROS-dependent neurogenesis and regeneration in the adult newt brain. *eLife* 4.




- Kanagaraj P, Chen JY, Skaggs K, Qadeer Y, Conner M, Cutler N, Richmond J, Kommidi V, Poles A, Affrunti D, Powell C, Goldman D, Parent J. 2020. Microglia Stimulate Zebrafish Brain Repair Via a Specific Inflammatory Cascade. *BioRxiv* 79(3):268-280.
- Kim YS, Joh TH. 2006. Microglia, major player in the brain inflammation: their roles in the pathogenesis of Parkinson's disease. *Exp Mol Med* 38(4):333-347.
- Kishimoto N, Shimizu K, Sawamoto K. 2012. Neuronal regeneration in a zebrafish model of adult brain injury. *Disease models & mechanisms* 5(2):200-209.
- Kroehne V, Freudenreich D, Hans S, Kaslin J, Brand M. 2011. Regeneration of the adult zebrafish brain from neurogenic radial glia-type progenitors. *Development* 138(22):4831-4841.
- Kyritsis N, Kizil C, Zocher S, Kroehne V, Kaslin J, Freudenreich D, Iltzsche A, Brand M. 2012. Acute inflammation initiates the regenerative response in the adult zebrafish brain. *Science* 338(6112):1353-1356.
- Lawson ND, Weinstein BM. 2002. In vivo imaging of embryonic vascular development using transgenic zebrafish. *Dev Biol* 248(2):307-318.
- Lin MC, Liu CC, Liao CS, Ro JH. 2021. Neuroprotective Effect of Quercetin during Cerebral Ischemic Injury Involves Regulation of Essential Elements, Transition Metals, Cu/Zn Ratio, and Antioxidant Activity. *Molecules* 26(20).
- März M, Chapouton P, Diotel N, Vaillant C, Hesl B, Takamiya M, Lam CS, Kah O, Bally-Cuif L, Strahle U. 2010. Heterogeneity in progenitor cell subtypes in the ventricular zone of the zebrafish adult telencephalon. *Glia* 58(7):870-888.
- März M, Schmidt R, Rastegar S, Strähle U. 2011. Regenerative response following stab injury in the adult zebrafish telencephalon. *Dev Dyn* 240(9):2221-2231.
- Menuet A, Pellegrini E, Brion F, Gueguen MM, Anglade I, Pakdel F, Kah O. 2005. Expression and estrogen-dependent regulation of the zebrafish brain aromatase gene. *J Comp Neurol* 485(4):304-320.
- Miller CJ, Gounder SS, Kannan S, Goutam K, Muthusamy VR, Firpo MA, Symons JD, Paine R, 3rd, Hoidal JR, Rajasekaran NS. 2012. Disruption of Nrf2/ARE signaling impairs antioxidant mechanisms and promotes cell degradation pathways in aged skeletal muscle. *Biochim Biophys Acta* 1822(6):1038-1050.
- Miyamoto N, Maki T, Pham LD, Hayakawa K, Seo JH, Mandeville ET, Mandeville JB, Kim KW, Lo EH, Arai K. 2013. Oxidative stress interferes with white matter renewal after prolonged cerebral hypoperfusion in mice. *Stroke* 44(12):3516-3521.
- Mondo E, Becker SC, Kautzman AG, Schifferer M, Baer CE, Chen J, Huang EJ, Simons M, Schafer DP. 2020. A Developmental Analysis of Juxtavascular Microglia Dynamics and Interactions with the Vasculature. *J Neurosci* 40(34):6503-6521.
- Nayak D, Roth TL, McGavern DB. 2014. Microglia development and function. *Annual review of immunology* 32:367-402.
- Oosterhof N, Holtman IR, Kuil LE, van der Linde HC, Boddeke EW, Eggen BJ, van Ham TJ. 2017. Identification of a conserved and acute neurodegeneration-specific microglial transcriptome in the zebrafish. *Glia* 65(1):138-149.
- Oosterhof N, Kuil LE, van der Linde HC, Burm SM, Berdowski W, van Ijcken WFJ, van Swieten JC, Hol EM, Verheijen MHG, van Ham TJ. 2018. Colony-Stimulating Factor 1 Receptor (CSF1R) Regulates Microglia Density and Distribution, but Not Microglia Differentiation In Vivo. *Cell reports* 24(5):1203-1217 e1206.
- Paladini MS, Feng X, Krukowski K, Rosi S. 2021. Microglia depletion and cognitive functions after brain injury: From trauma to galactic cosmic ray. *Neurosci Lett* 741:135462.

- Paolicelli RC, Bolasco G, Pagani F, Maggi L, Scianni M, Panzanelli P, Giustetto M, Ferreira TA, Guiducci E, Dumas L, Ragozzino D, Gross CT. 2011. Synaptic pruning by microglia is necessary for normal brain development. *Science* 333(6048):1456-1458.
- Pellegrini E, Mouriec K, Anglade I, Menuet A, Le Page Y, Gueguen MM, Marmignon MH, Brion F, Pakdel F, Kah O. 2007. Identification of aromatase-positive radial glial cells as progenitor cells in the ventricular layer of the forebrain in zebrafish. *J Comp Neurol* 501(1):150-167.
- Perez-Rodriguez DR, Blanco-Luquin I, Mendioroz M. 2021. The Participation of Microglia in Neurogenesis: A Review. *Brain Sci* 11(5).
- Praveen Kumar P, D M, Siva Sankar Reddy L, Dastagiri Reddy Y, Somasekhar G, Sirisha NVL, Nagaraju K, Shouib MS, Rizwaan AS. 2021. A new cerebral ischemic injury model in rats, preventive effect of gallic acid and in silico approaches. *Saudi J Biol Sci* 28(9):5204-5213.
- Ribeiro Xavier AL, Kress BT, Goldman SA, Lacerda de Menezes JR, Nedergaard M. 2015. A Distinct Population of Microglia Supports Adult Neurogenesis in the Subventricular Zone. *J Neurosci* 35(34):11848-11861.
- Rodriguez Viales R, Diotel N, Ferg M, Armant O, Eich J, Alunni A, Marz M, Bally-Cuif L, Rastegar S, Strahle U. 2015. The helix-loop-helix protein id1 controls stem cell proliferation during regenerative neurogenesis in the adult zebrafish telencephalon. *Stem Cells* 33(3):892-903.
- Rodriguez-Iglesias N, Sierra A, Valero J. 2019. Rewiring of Memory Circuits: Connecting Adult Newborn Neurons With the Help of Microglia. *Front Cell Dev Biol* 7:24.
- Rodriguez-Rodriguez A, Egea-Guerrero JJ, Murillo-Cabezas F, Carrillo-Vico A. 2014. Oxidative stress in traumatic brain injury. *Current medicinal chemistry* 21(10):1201-1211.
- Sakai S, Shichita T. 2019. Inflammation and neural repair after ischemic brain injury. *Neurochem Int* 130:104316.
- Sato K. 2015. Effects of Microglia on Neurogenesis. *Glia* 63(8):1394-1405.
- Schmidt R, Beil T, Strähle U, Rastegar S. 2014. Stab wound injury of the zebrafish adult telencephalon: a method to investigate vertebrate brain neurogenesis and regeneration. *J Vis Exp*(90):e51753.
- Sierra A, de Castro F, Del Rio-Hortega J, Rafael Iglesias-Rozas J, Garrosa M, Kettenmann H. 2016. The "Big-Bang" for modern glial biology: Translation and comments on Pio del Rio-Hortega 1919 series of papers on microglia. *Glia* 64(11):1801-1840.
- Silva NJ, Nagashima M, Li J, Kakuk-Atkins L, Ashrafzadeh M, Hyde DR, Hitchcock PF. 2020. Inflammation and matrix metalloproteinase 9 (Mmp-9) regulate photoreceptor regeneration in adult zebrafish. *Glia* 68(7):1445-1465.
- Simpson DSA, Oliver PL. 2020. ROS Generation in Microglia: Understanding Oxidative Stress and Inflammation in Neurodegenerative Disease. *Antioxidants (Basel)* 9(8).
- Slemmer JE, Shacka JJ, Sweeney MI, Weber JT. 2008. Antioxidants and free radical scavengers for the treatment of stroke, traumatic brain injury and aging. *Current medicinal chemistry* 15(4):404-414.
- Smith JA, Das A, Ray SK, Banik NL. 2012. Role of pro-inflammatory cytokines released from microglia in neurodegenerative diseases. *Brain Res Bull* 87(1):10-20.
- Stence N, Waite M, Dailey ME. 2001. Dynamics of microglial activation: a confocal time-lapse analysis in hippocampal slices. *Glia* 33(3):256-266.
- Tan YL, Yuan Y, Tian L. 2020. Microglial regional heterogeneity and its role in the brain. *Mol Psychiatry* 25(2):351-367.

- Var SR, Byrd-Jacobs CA. 2020. Role of Macrophages and Microglia in Zebrafish Regeneration. *International journal of molecular sciences* 21(13).
- Wu S, Nguyen LTM, Pan H, Hassan S, Dai Y, Xu J, Wen Z. 2020. Two phenotypically and functionally distinct microglial populations in adult zebrafish. *Sci Adv* 6(47).
- Wullimann MF, Rupp B, Reichert H. 1996. *Neuroanatomy of the zebrafish brain: A topological atlas*. Birhäuser Verlag, Basel, Switzerland:1-144.
- Zambusi A, Ninkovic J. 2020. Regeneration of the central nervous system-principles from brain regeneration in adult zebrafish. *World J Stem Cells* 12(1):8-24.
- Zhang Y, Chen K, Sloan SA, Bennett ML, Scholze AR, O'Keeffe S, Phatnani HP, Guarnieri P, Caneda C, Ruderisch N, Deng S, Liddelow SA, Zhang C, Daneman R, Maniatis T, Barres BA, Wu JQ. 2014. An RNA-sequencing transcriptome and splicing database of glia, neurons, and vascular cells of the cerebral cortex. *J Neurosci* 34(36):11929-11947.
- Zhao S, Zhang L, Xu Z, Chen W. 2013. Neurotoxic effects of iron overload under high glucose concentration. *Neural regeneration research* 8(36):3423-3433.

RESEARCH ARTICLE

Expression of adiponectin receptors in the brain of adult zebrafish and mouse: Links with neurogenic niches and brain repair

Sepand Rastegar^{1*} | Avinash Parimisetty^{2*}  | Nora Cassam Sulliman² |
 Sai Sandhya Narra² | Sabrina Weber¹ | Maryam Rastegar¹ | Wildriss Viranaicken³ |
 David Couret^{2,4} | Cynthia Planesse² | Uwe Strähle¹ | Olivier Meilhac^{2,4}  |
 Christian Lefebvre d'Hellencourt² | Nicolas Diotel² 

¹Institute of Toxicology and Genetics, Karlsruhe Institute of Technology, Eggenstein-Leopoldshafen, Germany

²Université de La Réunion, INSERM, UMR 1188, Diabète athérombose Thérapies Réunion Océan Indien (DÉTRO), Saint-Denis de La Réunion, France

³Université de La Réunion, INSERM, UMR 1187, Processus Infectieux en Milieu Insulaire Tropical (PIMIT), CNRS UMR9192, IRD UMR249, Saint-Denis de La Réunion, France

⁴CHU de La Réunion, Saint-Denis, France

Correspondence

Nicolas Diotel, Université de La Réunion, INSERM, UMR 1188, Diabète athérombose Thérapies Réunion Océan Indien (DÉTRO), Saint-Denis de La Réunion, France.

Email: nicolas.diotel@univ-reunion.fr

Christian Lefebvre d'Hellencourt, Université de La Réunion, INSERM, UMR 1188, Diabète athérombose Thérapies Réunion Océan Indien (DÉTRO), Saint-Denis de La Réunion, France.

Email: christian.lefebvre-d-hellencourt@univ-reunion.fr

Abstract

Adiponectin and its receptors (*adipor*) have been initially characterized for their role in lipid and glucose metabolism. More recently, adiponectin signaling was shown to display anti-inflammatory effects and to participate in brain homeostasis and neuroprotection. In this study, we investigated *adipor* gene expression and its regulation under inflammatory conditions in two complementary models: mouse and zebrafish. We demonstrate that *adipor1a*, *adipor1b*, and *adipor2* are widely distributed throughout the brain of adult fish, in neurons and also in radial glia, behaving as neural stem cells. We also show that telencephalic injury results in a decrease in *adipor* gene expression, inhibited by an anti-inflammatory treatment (Dexamethasone). Interestingly, adiponectin injection after brain injury led to a consistent decrease (a) in the recruitment of microglial cells at the lesioned site and (b) in the proliferation of neural progenitors, arguing for a neuroprotective role of adiponectin. In a comparative approach, we investigate *Adipor1* and *Adipor2* gene distribution in the brain of mice and demonstrated their expression in regions shared with fish including neurogenic regions. We also document *Adipor* gene expression in mice after middle cerebral artery occlusion and lipopolysaccharide injection. In contrast to zebrafish, these inflammatory stimuli do not impact cerebral *adiponectin receptor* gene expression in mouse. This work provides new insights regarding *adipor* expression in the brain of fish, and demonstrates evolutionary conserved distribution of *adipor* with mouse. This is the first report of *adipor* expression in adult neural stem cells of fish, suggesting a potential role of adiponectin signaling during vertebrate neurogenesis. It also suggests a potential contribution of inflammation in the regulation of *adipor* in fish.

KEYWORDS

adipor, brain ischemia, brain repair, neural stem cells, RRID:AB_10013383, RRID:AB_10049650, RRID:AB_141372, RRID:AB_2160651, RRID:AB_221448, RRID:AB_2314535, RRID:AB_2534069, RRID:AB_514497, RRID:AB_514499, RRID:SCR_003070, stab wound

*Sepand Rastegar and Avinash Parimisetty contributed equally to this study.

1 | INTRODUCTION

Adipokines are a group of hormones and cytokines initially described to be secreted by the white adipose tissue (Ouchi, Parker, Lugus, & Walsh, 2011; Tilg & Moschen, 2006). These signaling factors are well known for being involved in several physiological processes such as inflammation, oxidative stress, cardiovascular protection, and contribute to brain homeostasis. Among adipokines, adiponectin is the most abundant in plasma (Matsuzawa, 2005; Thundyil, Pavlovski, Sobey, & Arumugam, 2012). Although adiponectin is mainly synthesized and secreted by the white adipose tissue, other organs such as the liver, the muscles, and also the brain have been described to synthesize adiponectin *de novo* (Kershaw & Flier, 2004; Psilopanagioti, Papadaki, Kranioti, Alexandrides, & Varakis, 2009; Thundyil et al., 2012; Wilkinson, Brown, Imran, & Ur, 2007). Adiponectin controls glucose and lipid homeostasis, increases insulin sensitivity, decreases body-weight, and inhibits tissue inflammation (Berg, Combs, & Scherer, 2002; Okamoto et al., 2002; Stefan & Stumvoll, 2002; Whitehead, Richards, Hickman, Macdonald, & Prins, 2006), and exhibits cardiovascular protective effects (Okamoto, 2011; Spranger et al., 2003). Such effects are mediated by two main receptors called Adiponectin receptor 1 (Adipor1) and Adiponectin receptor 2 (Adipor2).

In rodents, adiponectin is involved in the regulation of the blood-brain barrier physiology, and accumulating data suggest that it could favor brain plasticity, enhance neurogenesis, and neuroprotection (Bloemer et al., 2018; Nishimura et al., 2008; Pan & Kastin, 2007; Parimisetty et al., 2016; Qiu et al., 2011; Song et al., 2015; Song, Choi, Whitcomb, & Kim, 2017; Thundyil et al., 2012; Wan, Mah, Simtchouk, Klegeris, & Little, 2014; Zhang, Wang, & Lu, 2016). Together, these findings suggest that adiponectin plays a role beyond the metabolic sphere. In rats, Adipor1 has been reported to be mainly expressed in neurons and to a lower extent in astrocytes, while Adipor2 was shown to be strongly detected in both neurons and astrocytes, as reported in the olfactory bulbs and the hypothalamus (Guillod-Maximin et al., 2009; Miranda-Martinez, Arriaga-Avila, & Guevara-Guzman, 2017).

Zebrafish has become a well-recognized model for studying metabolic disorders, (Krishnan & Rohner, 2019; Zang, Maddison, & Chen, 2018) as well as brain physiology and brain repair mechanisms (Baumgart, Barbosa, Bally-Cuif, Gotz, & Ninkovic, 2012; Diotel et al., 2010, 2011; Diotel, Beil, Strahle, & Rastegar, 2015; Dorsemans et al., 2017; Kishimoto, Shimizu, & Sawamoto, 2012; Kizil, Kaslin, Kroehne, & Brand, 2012; Rodriguez Viales et al., 2015; Schmidt, Beil, Strähle, & Rastegar, 2014; Zupanc, 2008). In contrast to mammals, zebrafish display a widespread neurogenic activity through the whole encephalon (Lindsey & Tropepe, 2006). This is mainly due to the persistence of neural progenitors, namely (a) radial glial cells and further committed progenitors along the ventricular zones of the tel- and diencephalon and (b) neuroepithelial cells in more posterior regions (Grandel & Brand, 2013; Lindsey, Darabie, & Tropepe, 2012; Marz et al., 2010; Pellegrini et al., 2007, 2013; Rothnagler et al., 2011). Due to a third round of genomic duplication event that occurred ~320–350 million years ago (Ravi & Venkatesh, 2008), the zebrafish genome displays two *adiponectin* genes (*adiponectin a* and *b*) and three *adipor* genes (*adiponectin receptor 1a* [*adipor1a*], *1b* [*adipor1*], and *2* [*adipor2*])

(www.ensembl.org). In adult zebrafish, *adiponectin a* transcripts have been shown to be expressed in the kidney while *adiponectin b* mRNA was detected in the brain, the liver, and also at lower levels in the adipose tissue and muscle (Nishio et al., 2008). In contrast, *adiponectin receptors* appear to be expressed particularly in the brain, the liver, and the adipose tissue in a way similar to mammals.

Given the lack of data concerning *adipor* expression in zebrafish, we first decided to investigate the expression of *adipor* during zebrafish development. In addition, to study a potential involvement of adiponectin and adiponectin receptors in neurogenesis and neuroprotection, we further explore *adipor* gene expression and distribution in the brain of adult zebrafish and compare it with that of mice. In the final part of our work, we also investigated the cerebral expression of *adipor*, following stab wound injury of the zebrafish telencephalon and under inflammatory and brain ischemic conditions, in mice. The effect of adiponectin was also investigated in zebrafish after brain injury suggesting a potential neuroprotective role of adiponectin.

2 | MATERIALS AND METHODS

2.1 | Animals and ethic

Three- to six-month-old male adult wildtype zebrafish (*Danio rerio*) were purchased from commercial suppliers and maintained under standard conditions of photoperiod (14/10 hr light/dark) and temperature (28°C). Zebrafish were fed daily with commercially available dry food (TetraMin). For euthanasia, animals were sacrificed with overdose of tricaine (MS-222; REF: A5040, Sigma-Aldrich). For all surgical procedures and/or injections, fish were deeply anesthetized with 0.02% tricaine.

Male C57BL/6 (10-week old, 25 g) mice were purchased from Janvier Labs (Le Genest-Saint-Isle, France). They were maintained under standard conditions of light, temperature, and humidity and fed a standard diet *ad libitum*.

All animal experiments were done in CYROI (UMR1188) and conducted in accordance with the French and European Community Guidelines for the Use of Animals in Research (86/609/EEC and 2010/63/EU) and approved by the local Ethics Committee for animal experimentation of CYROI (APAFIS #201809252279654_v5, #3209-2015111215451823_v2, #2018040507397248_v2).

2.2 | Stab wound of adult zebrafish telencephalon

Zebrafish were anesthetized with 0.02% tricaine. Stab wound injury of the telencephalon was performed by inserting a sterile needle (BD Microlance 3; 30 G ½"; 0.3 × 13 mm) in the right telencephalic hemisphere as previously described (Diotel et al., 2013; Dorsemans et al., 2017). Fish were then returned to their tanks and maintained for 1, 3, and 5 days post lesion (dpl). At 1 and 5 dpl, brains were extracted and processed for RNA extraction and quantitative real-time polymerase chain reaction (qPCR) experiments to evaluate *adiponectin receptor* expression. At 3 dpl and recombinant adiponectin injection (see below), fish were sacrificed and brains were processed

for immunohistochemistry to quantify microglial recruitment and neural stem cell proliferation.

2.3 | Anti-inflammatory treatment in brain-injured fish

To investigate the impact of inflammation on *adipor* gene expression in brain injury condition, fish were treated with the synthetic anti-inflammatory glucocorticoid dexamethasone (DEX). The final concentration of DEX in the fish water was 15 mg/L. Fish were treated for 7 days with DEX prior to brain injury. On the 6th day, stab wound injury of the telencephalon was performed and fish were allowed to survive for 1 day. For brain RNA extraction, three pools of five telencephali were made. For body/tail RNA extraction, individual extraction was made.

2.4 | Anti-inflammatory treatment in brain-injured fish and anti-inflammatory activity of adiponectin *in vitro* and *in vivo* in zebrafish

To investigate the impact of inflammation on *adipor* gene expression in brain injury condition, fish were treated with the synthetic anti-inflammatory glucocorticoid DEX as previously described (Kyritsis et al., 2012; Rodriguez Viales et al., 2015). In brief, fish were treated with DEX (15 mg/L) for 7 days. On the 6th day, stab wound injury of the left and right telencephalon was performed and fish were allowed to survive for 1 day. Control fish correspond to uninjured brains. For brain RNA extraction, three pools of five telencephali were made, while for body/tail RNA extraction, individual extractions were made for three control and treated fish. RNA extraction was performed using TRIzol™ Reagent (ThermoFisher) according to manufacturer's instruction.

The mouse recombinant adiponectin (Biovision, #4902) was tested for its anti-inflammatory activity, using the RAW-Blue cells, a NF-κB-SEAP Reporter Cell Line, (raw-sp, InvivoGen). Following stimulation with 500 ng/mL of *E. coli* lipopolysaccharide (LPS) (tlrl-eblps, InvivoGen) with increase amount of recombinant adiponectin (from 10 to 100 μg/mL), NF-κB-SEAP activity was quantified after 20 hr using assay (rep-qb1, InvivoGen) according to manufacturer's recommendations (Supporting Information Figure 1).

Zebrafish were anesthetized with 0.02% tricaine, stab wounded in the right telencephalic hemisphere and intraperitoneally injected with 100 μg/g of body weight with recombinant adiponectin (Biovision, #4902). This concentration was selected as 100 μg/mL provides a strong anti-inflammatory effect *in vitro* (Supporting Information Figure 1), assuming that 1 g of fish body weight is close to 1 mL.

Fish were allowed to survive for 3 days, allowing us to study microglial recruitment and neural stem cell proliferation.

2.5 | Lipopolysaccharide injection and middle cerebral artery occlusion

Three mice were intraperitoneally injected with 100 μg/kg of body weight of LPS (LPS-EB standard, REF: O111:B4 tlrl-eblps; InvivoGen)

or with the respective control (vehicle: 1X phosphate buffer saline, PBS). After 6 hr, mice were sacrificed by cervical dislocation, three control and treated brains were quickly removed and dissected for isolation of the hippocampus and the cerebral cortex. These were flash frozen and individually processed for RNA extraction using TRIzol™ Reagent (ThermoFisher) according to manufacturer's instruction.

Middle cerebral artery occlusion (MCAO) was performed to induce brain ischemia. Three mice were anesthetized with Isoflurane (IsoFlo® Centravet France), and body temperature was maintained up to 34°C. MCAO was achieved for 90 min by introducing a 7-0 silicon-coated monofilament (Doccol Corporation, Sharon, MA) through the right common carotid at the bifurcation of the right MCA and the right internal carotid (Courret et al., 2018; Hata et al., 1998). The removal of the monofilament allowed reperfusion and animals were sacrificed at 24 hr post-injury. After sacrifice, three control and treated brains were carefully extracted, cut into 1-mm³ coronal slices using a brain matrix mold. The contralateral and ipsilateral hemispheres ($n = 3$) were separated and processed for RNA extraction using TRIzol™ Reagent (ThermoFisher) according to manufacturer's instruction.

One section was used for the evaluation of the infarct area using 2% 2,3,5-triphenyltetrazolium chloride (TTC, Sigma Aldrich) for 20 min at room temperature. TTC is a colorless water-soluble dye reduced to a deep red, water-insoluble compound (formazan) within the mitochondria of living cells (Sun, Yang, & Kuan, 2012).

2.6 | Gene expression analysis by qPCR and transcriptome studies

PCR experiments were performed with the CFX Connect Real-Time System (Biorad) using the SYBR green master-mix (Eurogentec) and specific mouse and zebrafish primers (see Table 1). Each PCR cycle was conducted for 15 s at 95°C and 1 min at 60°C. PCR efficiency and melting curve analyses were performed to confirm the correct amplification. Results were analyzed using CFX software (Biorad). The relative expression of the *adipor1a*, *adipor1b*, and *adipor2* genes was normalized against the expression level of the *ef1a* gene for fish; the relative expression of the *Adiponectin*, *Adipor1*, *Adipor2*, and *Tnfa* genes was normalized against the expression level of the *Gapdh* gene for mouse.

RNA-Seq/DeTCT database based during zebrafish development was retrieved from expression atlas: [ebi.ac.uk/gxa/](https://www.ebi.ac.uk/gxa/); accession number: E-ERAD-475 (White et al., 2017). The raw count data was normalized by size factor and fragments per kilobase per million (FPKM) and calculated for each gene thanks to DESeq2 (Love, Huber, & Anders, 2014). For each zebrafish development stages, the value corresponds to the mean of 20 biological replicates from 8 to 12 embryos and/or larvae (Hubrecht longfin strain). For RNAseq of adult zebrafish brain, data were extracted from (Wong & Godwin, 2015) for reanalysis.

For mice, the RNA seq data was available on an expression atlas (<https://www.ebi.ac.uk>; E-GEOD-43721). FPKMs were calculated from the raw counts and correspond to the average for each set of technical replicates. They were subsequently quantile normalized within each set of biological replicates and averaged for all biological replicates (C57BL/6, 11 weeks). For RNA seq from mouse cortex, data were available (https://web.stanford.edu/group/barres_lab/brain_

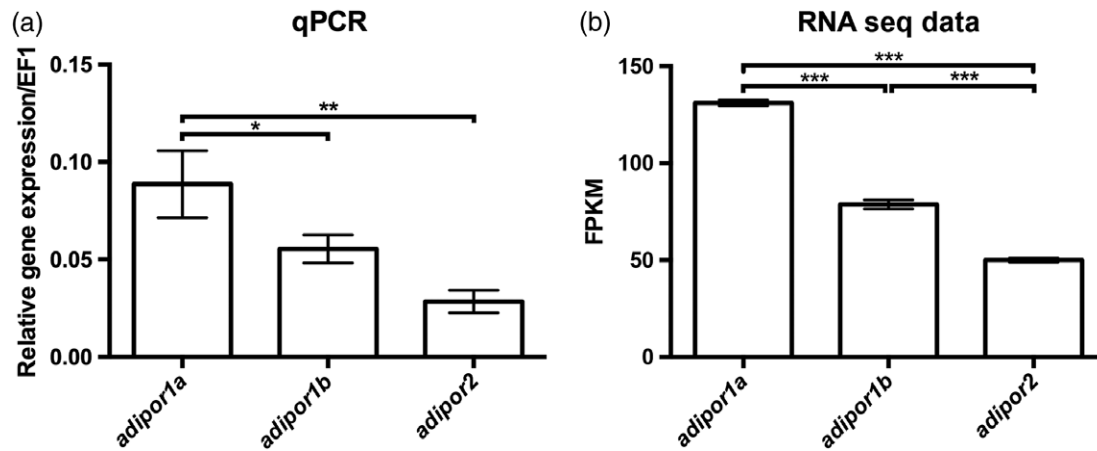


FIGURE 1 Adiponectin receptor mRNA are expressed in the brain of adult zebrafish qPCR analysis (a) and RNA sequencing data (b) showing *adipor1a*, *adipor1b*, and *adipor2* expression in the brain of adult zebrafish. Both techniques indicate that *adipor1a* is the most expressed receptor and *adipor2* the lowest one. Note that the original RNA seq data set from (b) was obtained from Wong and Godwin (2015). For qPCR, the analysis was performed on three pools of three brains. * $p < 0.05$; ** $p < 0.01$; *** $p < 0.0001$

rnaeq.html) (Zhang et al., 2014). The details of the RNA sequencing are described in Zhang et al. (2014).

2.7 | Cloning, tissue preparation, and *in situ* hybridization

A standard PCR using zebrafish/mouse brain cDNA and gene-specific primers (see Table 2 and Supporting Information Figure 2) was performed. The resulting PCR products were subcloned into the pGEMT-Easy vector (Promega) in accordance with the manufacturer's instructions. Plasmids

were sequenced and linearized for the synthesis of digoxigenin (DIG) labeled antisense riboprobes using T7 or SP6 RNA polymerase.

Fish were euthanized before being decapitated. Zebrafish heads were immersed overnight at 4°C in 4% paraformaldehyde (PFA) dissolved in PBS. Brains were next extracted from the skull and stepwise dehydrated in a methanol/PBS concentration series, before being stored at -20°C, as previously described (Adolf et al., 2006).

In situ hybridization (ISH) was performed on vibratome brain slices (50 μm thickness) (Adolf et al., 2006; Schmidt et al., 2014). DIG labeled antisense probes were used for chromogenic and fluorescent

TABLE 1 Zebrafish and mouse qPCR primers

Zebrafish qPCR primers			
Primer name	Sequence	Amplicon size	ensembl ID
qzf <i>adipor1a</i> Fw	GAAAGTGGTGTTCGGGATGT	136	ENSDARG0000002912
qzf <i>adipor1a</i> Rv	CAGAGCAATGCCGAGTAGT		
qzf <i>adipor1b</i> Fw	AAACATCTGGACACACCTGCT	126	ENSDARG00000042717
qzf <i>adipor1b</i> Rv	AGGAAAACACGCCAAACAC		
qzf <i>adipor2</i> Fw	GACCCACCCAAACATCA	102	ENSDARG00000058688
qzf <i>adipor2</i> Rv	CCTCCTCGCATGAAGACAGT		
qzf <i>fkbp5</i> Fw	CAAAGGGGGAATGCTGTT	69	ENSDARG00000028396
qzf <i>fkbp5</i> Rv	TTCTTTTCTGCCCTCTTTC		
qzf <i>ef1</i> Fw	AGCAGCAGCTGAGGAGTGAT	140	ENSDARG00000020850
qzf <i>ef1</i> Rv	CCGCATTTGTAGATCAGATGG		
Mouse qPCR primers			
Primer name	Sequence	Amplicon size	ensembl ID
qmus <i>adipor1</i> Fw	CAGAGAAGCTGACACAGTGGA	109	ENSMUSG00000026457
qmus <i>adipor1</i> Rv	CGGGCATGCTTGATCTTC		
qmus <i>adipor2</i> Fw	CTACCTGATTGTCATCTGTGTGC	113	ENSMUSG00000030168
qmus <i>adipor2</i> Rv	CTAAGCCACGAACACTCCT		
qmus <i>adiponectin</i> Fw	TCAGTGGATCTGACGACACC	165	ENSMUSG00000022878
qmus <i>adiponectin</i> Rv	TGCCATCCAACCTGCACAAG		
qmus <i>tnfa</i> Fw	CTTCTGTCTACTGAACCTCGGG	134	ENSMUSG00000024401
qmus <i>tnfa</i> Rv	CAGGCTTGTCACTCGAATTTTG		
qmus <i>gapdh</i> Fw	CTTTGTCAAGCTCATTTCTGG	243	ENSMUSG00000057666
qmus <i>gapdh</i> Rv	TCTTGCTCAGTGCTCTTGC		

TABLE 2 Zebrafish and mouse cloning primers (the colors refer to the different amplicons highlighted in Supporting Information Figure 2)

Zebrafish cloning primers				
Primer name	Probe	Sequence	Amplicon size	ensembl ID
<i>zf adipor1a Fw</i>	Probe1 (blue in Supporting Information Figure 2)	TGGAAGAAAATGGCCCCA	505	ENS DARG0000002912
<i>zf adipor1a Rv</i>		CGTGAGACTTTCTCAGAAT		
<i>zf adipor1a Fw</i>	Probe2 (yellow in Supporting Information Figure 2)	GTATCCGATGGCTGGAACAT	585	
<i>zf adipor1a Rv</i>		GGATTGCTTGCGACGTAAAT		
<i>zf adipor1b Fw</i>	Probe1 (blue in Supporting Information Figure 2)	GTGGTTACTACTGCCATGC	373	ENS DARG00000042717
<i>zf adipor1b Rv</i>		AAAGCCAGGAGAAGCACAAA		
<i>zf adipor1b Fw</i>	Probe2 (yellow in Supporting Information Figure 2)	GTGGTTACTACTGCCATGC	386	
<i>zf adipor1b Rv</i>		AAAGCCAGGAGAAGCACAAA		
<i>zf adipor2 Fw</i>	Probe1 (blue in Supporting Information Figure 2)	TTCTGCTTCAGGCTCACC	673	ENS DARG00000058688
<i>zf adipor2 Rv</i>		GTCAGGAAGCCCTCAGCAA		
<i>zf adipor2 Fw</i>	Probe2 (yellow in Supporting Information Figure 2)	ACCGAGATGGAGGAGACCTT	414	
<i>zf adipor2 Rv</i>		CGGCTGTGCTCAGAATTACA		
Mouse cloning primers				
Primer name	Probe	Sequence	Amplicon size	ensembl ID
<i>mouse Adipor1 Fw</i>	Probe1	CTTGACGATGCTGAGACCAA	418	ENS MUSG00000026457
<i>mouse Adipor1 Rv</i>		GACAAAGCCCTCAGCGATAG		
<i>mouse Adipor2 Fw</i>	Probe1	CCACTGTTGGGAGTGCTCTT	539	ENS MUSG00000030168
<i>mouse Adipor2 Rv</i>		GCCTTCCACACCTTACAAA		

ISH. Probe synthesis and ISH were performed on whole brain as previously described (Adolf et al., 2006; Diotel, Beil, et al., 2015; Rodriguez Viales et al., 2015). Briefly, brains were rehydrated and washed in 0.1% Tween-PBS buffer (PTw; pH 7.4). They were next incubated with proteinase K (10 mg/mL in PTw) at room temperature (25°C) for 30 min. Brains were postfixed in 4% PFA for 30 min for stopping proteinase K activity, washed in PTw and prehybridized for 3 hr at 65°C. Finally, they were incubated overnight at 65°C in hybridization buffer containing the DIG-labeled probes. Brains were washed, briefly incubated in blocking buffer and embedded in 2% agarose. Brain sections were performed using a Leica vibrating blade microtome VT1000 S at 50 µm thickness. Sections were incubated overnight at 4°C with Anti-DIG Fab fragments conjugated to alkaline phosphatase (1:2,000, Roche, Cat# 11093274910, RRID:AB_514497), washed and stained with NBT/BCIP solution.

Fluorescent ISH was performed using tyramide amplification according to the manufacturer's instructions (TSA Plus Cyanine 3 System, Perkin Elmer, Boston, MA). Endogenous peroxidase activity was first inactivated with 3% H₂O₂ and slices were processed as for chromogenic ISH. After sectioning, brain slices were incubated with anti-DIG-POD (poly) antibody (1:1,000, Roche; RRID:AB_514499) and stained with tyramide Cy3 solution (1:100) in 0.002% H₂O₂ in PBS-Tween 0.1% as previously described (Rodriguez Viales et al., 2015). Each ISH was repeated 3–6 times. Sense probes are not anymore considered as a proper control for all genes, given that they can lead to staining due to antisense transcription at the targeted genomic locus (Katayama et al., 2005; Werner & Berdal, 2005). Consequently, an alternative nonoverlapping antisense probe was generated for each gene to verify the specificity of the staining.

For mouse ISH, fresh brains were extracted from the skull, fixed in 4% PFA dissolved in PBS for 24 hr. The next day, brains were rinsed twice in PBS before being cryoprotected overnight with 30% sucrose-

PBS. Brains were embedded in Tissue-Tek[®] OCT compound and frozen at -80°C before being cut into 12 µm-thick coronal sections using a cryostat (Shandon cryotome FE, Thermo Scientific). ISH was performed on brain sections following the same protocol as for zebrafish brain with minor modifications. Briefly, 12 µm-thick sections were rehydrated, incubated with proteinase K for 15 min and prehybridized before overnight incubation with the respective probes and controls in hybridization buffer. Sections were washed, blocked, and incubated with Anti-DIG-AP Fab fragments (1:2,000, Roche, Cat# 11093274910, RRID:AB_514497), rinsed and stained with NBT/BCIP solution. At the end, sections were washed and processed for immunohistochemistry.

2.8 | Immunohistochemistry

For zebrafish, immunohistochemistry was performed on free-floating 50 µm thickness transverse vibratome sections as previously described (Adolf et al., 2006). For mouse, immunohistochemistry was performed on 12 µm thickness transverse cryostat sections. Briefly, the brain sections were blocked with blocking buffer (BB; PBS containing 0.1% Tween-10, 0.2% bovine serum albumin, 1% dimethyl sulfoxide) and incubated in BB overnight at 4°C with the respective primary antibodies: monoclonal mouse anti-PCNA (1:500; clone PC10, Dako; RRID: AB_2160651), monoclonal mouse anti-HuC/D (1:300, Invitrogen, Cat# A21271, Clone 16A11, RRID:AB_221448), polyclonal rabbit anti-GFAP (1:500; REF: Z033429, Dako; RRID:AB_2314535), polyclonal rabbit anti-S100β (1:400, DAKO, Cat# Z0311, RRID:AB_10013383), and polyclonal rabbit L-Platin antibody (gift from M. Redd-Redd, Kelly, Dunn, Way, & Martin, 2006), to label proliferative cells (PCNA), neuronal cells (HuC/D), astrocyte/neural stem cells (GFAP and anti-S100β), and microglial cells (L-platin). The next day, the sections were washed three times in PTW and incubated for 2 hr at room temperature with 4',6'-diamidino-2-phenylindole (DAPI) for cell nuclei counterstaining and with

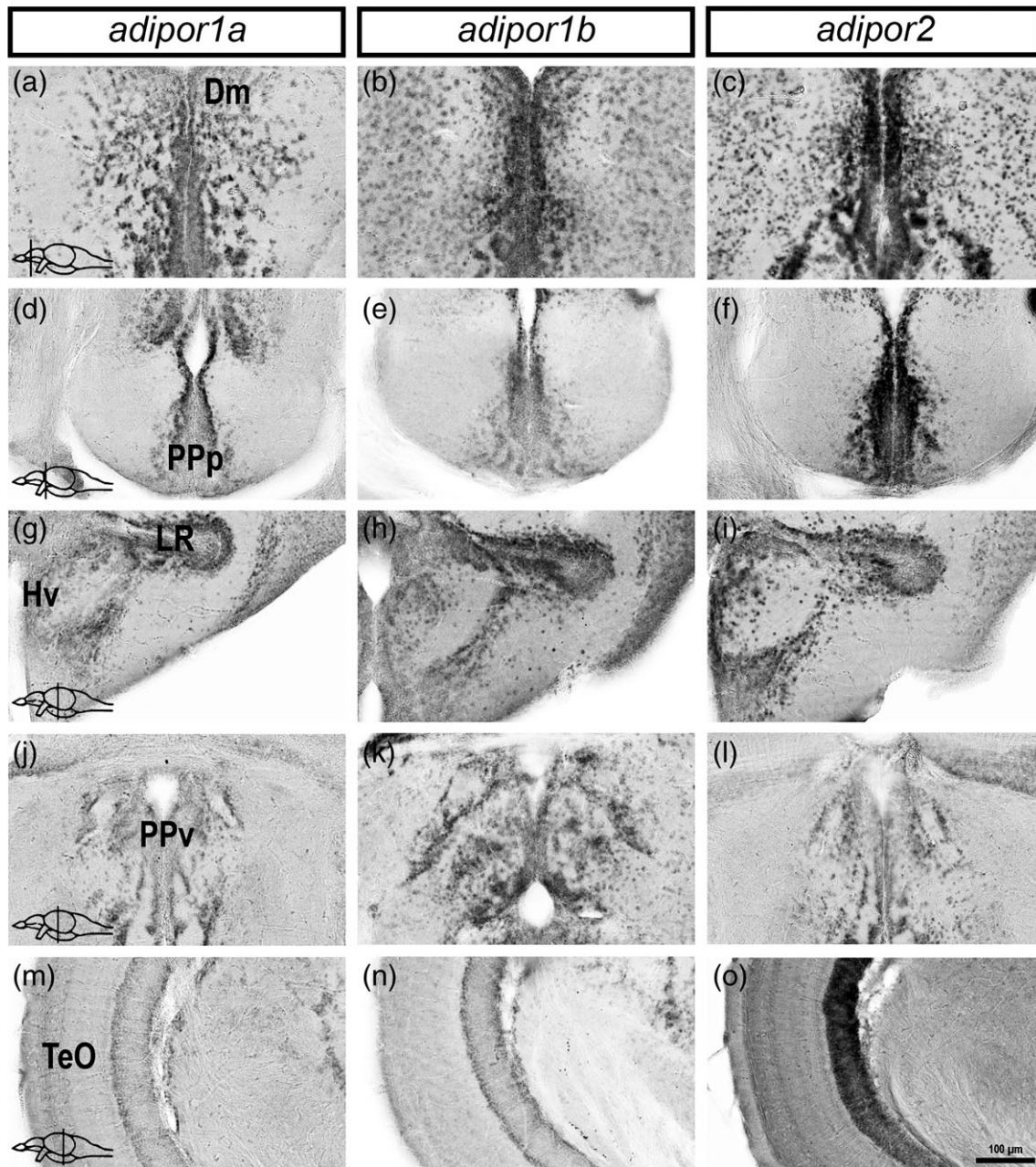


FIGURE 2 Adiponectin receptor expression in the brain of adult fish. Photomicrographs illustrating the expression of *adipor* mRNA in the dorsomedian telencephalon (Dm) (a–c), the posterior part of the preoptic area (PPp) (d–f), the mediobasal hypothalamus along the lateral recess (Hv LR) (g–i), the periventricular pretecal nucleus (PPv) (j–l), and the periglomerular gray zone of the optic tectum (TeO) (m–o). Note that the signal is detected in the brain parenchyma where numerous neurons are localized, as well as in the ventricular/periventricular regions where neural progenitors (radial glial cells and further committed progenitors) are located. Bar: 100 μ m

the respective secondary antibodies: donkey anti-rabbit Alexa Fluor 488 (1:200; REF: A21206; Life Technologies; RRID:AB_10049650) and goat anti-mouse Alexa Fluor 488 and 594 (1:200; REF: A11005; Life Technologies; RRID:AB_141372; 1:200; REF: A11001; Life Technologies; RRID:AB_2534069, respectively). Finally, the sections were washed three times in PBS-T and the slides were mounted with the antifading medium Vectashield (H-1000, Vector Laboratories, Burlingame, CA) or with Aqua Polymount (REF: 18606, Polysciences, Warrington, PA), for mouse and zebrafish sections, respectively. No staining was observed after omission of the primary antibodies or incubation with nonrelevant IgG (data not shown). Table 3 summarizes the antibodies used for immunohistochemistry in this study.

2.9 | Antibodies specificity

PCNA, S100 β , and GFAP antibodies have been previously documented for their use and their specificity in mouse and in zebrafish according to manufacturer's instruction and/or literature (Diotel et al., 2010; Diotel, Beil, et al., 2015; Dorsemans, Soule, et al., 2017; Marz et al., 2010). Consistent with these previous studies, PCNA-labeling was observed in cell nuclei across the neurogenic niches lining the ventricles. In zebrafish, GFAP- and S100 β -positive cells correspond to radial glial cell, as they display a soma localized along the ventricular layer and a long radial process that crosses the brain parenchyma and reaches the pial surface. In mouse, GFAP-staining allows the labeling

TABLE 3 Primary and secondary antibodies used for immunohistochemistry

Primary antibodies			
Antibodies	Reference	RRID	Antigen
Polyclonal rabbit anti glial fibrillary Z033429 acidic protein	Z033429 (Dako)	AB_2314535	GFAP isolated from cow spinal cord
Proliferating cell nuclear antigen M0879 clone PC10	M0879 (Dako)	AB_2160651	Rat PCNA-protein A fusion protein obtained from vector pC2T (Waseem & Lane, 1990)
Mouse monoclonal anti-HuC/D	A21271, Clone 16A11 (Invitrogen)	AB_221448	HuC, HuD, and Hel-N1 neuronal proteins antigens present exclusively in neuronal cells and are thus useful as markers of neuronal cells in tissue
Lymphocyte cytosolic protein 1 (L-plastin)	Gift from M. Redd	Not referenced (Redd et al., 2006)	Fusion protein comprising of glutathione S-transferase fused to the first 111 amino acids of the zebrafish L-plastin protein
Secondary antibodies			
Antibodies	Reference	RRID	
Donkey anti-rabbit Alexa Fluor 488	A21206 (Molecular Probes, Life Technologies)	AB_10049650	
Goat anti-mouse Alexa Fluor 594	A11005 (Molecular Probes, Life Technologies)	AB_141372	
Goat anti-mouse Alexa Fluor 488	A11001 (Molecular Probes, Life Technologies)	AB_2534069	

of star-shaped cells corresponding to astrocyte. The specific L-plastin zebrafish antibodies generated by Redd et al. (2006) labeled ramified microglia in homeostatic conditions and amoeboid/reactive microglia during brain injury in accordance to previously data obtained using the same antibody in zebrafish (Kyritsis et al., 2012). The HuC/D antibodies have been characterized for labeling neurons in mouse and zebrafish (Manufacturer's datasheet and references within).

2.10 | Microscopy

Micrographs were obtained with an Eclipse 80i Nikon microscope equipped with a Hamamatsu digital camera (Life Sciences, Japan), a nanozoomer S60 (Hamamatsu) and with a laser scanning confocal microscope Leica TCS2 SP5 for processing by Leica software. Pictures were adjusted for brightness and contrast in Adobe Photoshop CS7.

2.11 | Cell counting

For analyzing microglia recruitment and injury-induced proliferation in zebrafish, 3–4 vibratome sections of 50 μm thickness were selected in the injured versus uninjured telencephalon. A total of 11–13 brains were counted for control and adiponectin-treated fish in three independent experiments. Images were analyzed for detection of PCNA- and L-plastin-positive cells using ImageJ software (National Institutes of Health; RRID:SCR_003070) by adjusting parameters (threshold, binary, and watershed) and running an analysis on “particles” taking into consideration the area stained (along the ventricular layer for PCNA and in the brain parenchyma for L-plastin). In addition, ImageJ automated selection of PCNA- and L-plastin-positive cells were manually double-checked.

2.12 | Statistical analysis

Comparisons between groups were performed using a statistical Student's *t*-test. If more than two groups were analyzed, multiple testing

was corrected by Benjamini–Hochberg. Error bars correspond to the SEM, and *n* values correspond to the number of animals for all experiments. *p* < 0.05 was considered statistically significant; **p* < 0.05, ***p* < 0.01, and ****p* < 0.001.

3 | NOMENCLATURE

The nomenclature and the schemes of zebrafish brain sections correspond to those provided in the zebrafish brain atlas and other studies (Wullimann, Rupp, & Reichert, 1996; Menuet et al., 2005) and in the Allen Brain Atlas for mouse.

A, anterior thalamic nucleus; APN, accessory pretectal nucleus; ATN, anterior tuberal nucleus; Cc, corpus cerebelli; Chab, habenular commissure; Chor, horizontal commissure; CM, corpus mamillare; CP, central posterior thalamic nucleus; CPN, central pretectal nucleus; Cpop, postoptic commissure; Cpost, posterior commissure; Cx, cortex; D, dorsal telencephalic area; Dc, central zone of dorsal telencephalic area; DG, dentate gyrus of the hippocampus; Dl, lateral zone of dorsal telencephalic area; Dm, medial zone of dorsal telencephalic area; DOT, dorsomedial optic tract; Dp, posterior zone of dorsal telencephalic area; DP, dorsal posterior thalamic nucleus; ECL, external cellular layer of olfactory bulb; EG, eminentia granularis; ENv, entopenduncular nucleus, ventral part; FR, fasciculus retroflexus; GL, glomerular layer of olfactory bulb; Had, dorsal habenular nucleus; Hav, ventral habenular nucleus; Hc, caudal zone of periventricular hypothalamus; Hd, dorsal zone of periventricular hypothalamus; Hv, ventral zone of periventricular hypothalamus; ICL, internal cellular layer of olfactory bulb; IL, inferior lobe; LH, lateral hypothalamic nucleus; LLF: lateral longitudinal fascicle; LR, lateral recess of diencephalic nucleus; MLF, medial longitudinal fascicle; Nd, Not determined; NMLF, nucleus of medial longitudinal fascicle; PG, preglomerular nucleus; PGa, anterior preglomerular nucleus; PGI, lateral preglomerular nucleus; Pit, pituitary; PO, posterior pretectal nucleus; PP, periventricular pretectal nucleus; PPa, parvocellular preoptic nucleus, anterior part; PPp, parvocellular preoptic nucleus, posterior part; PR, posterior recess of diencephalic

ventricle; PSp, parvocellular superficial pretectal nucleus; PTN, posterior tuberal nucleus; R, rostralateral nucleus; RF, reticular formation; SC, suprachiasmatic nucleus; SD, saccus dorsalis; SO, secondary octaval population; SVZ, subventricular zone of the lateral ventricle; TeO, tectum opticum; TL, torus longitudinalis; TLa, torus lateralis; TPp, periventricular nucleus of posterior tuberculum; TS, torus semicircularis; V, ventral telencephalic area; V3, third ventricle; VII, sensory root of the facial nerve; VIII, octaval nerve; VCe, valvula cerebelli; Vd, dorsal nucleus of ventral telencephalic area; VL, ventrolateral thalamic nucleus; VM, ventromedial thalamic nucleus; VOT, ventrolateral optic tract; Vp, postcommissural nucleus of ventral telencephalic area; Vv, ventral nucleus of dorsal telencephalic area; ZL, zona limitans.

4 | RESULTS

4.1 | Adiponectin receptor expression during zebrafish development

Given the general lack of data concerning *adipor* expression in zebrafish, we first decided to investigate the expression of *adipor* during zebrafish development and compare it with mouse. Due to a genomic duplication occurring in Teleosts, numerous genes are duplicated in zebrafish. The gene coding for Adipor1 in mice (*Mus musculus*, mm) displays two orthologs in zebrafish (*D. rerio*, dr): *adipor1a* and *adipor1b*, and the one coding for *adipor2*, only one ortholog (Supporting Information Figure 3a). In zebrafish, there are also two orthologs for adiponectin: *adiponectin a* and *b* (www.ensembl.org). In mammals, it was previously shown that *Adipor1* and *Adipor2* were the product of the vertebrate specific duplication (Dehal & Boore, 2005; Nishio et al., 2008).

Given the lack of data about adiponectin and adiponectin receptors in zebrafish, we first investigated their temporal expression during development. We analyzed a recently published RNA seq data set providing a global transcriptomic profiling from zygote stage (1-cell) to 5 days postfertilization (dpf) (Supporting Information Figure 3). *adiponectin a* and *b* transcripts were almost not expressed during embryonic development. A weak expression was detected from blastula (128 cells stage) to gastrula (50% epiboly) for *adiponectin a*, and from the larval protruding mouth stage to 5 days post fertilization for both adiponectins. In contrast, *adipor* transcripts were detected at much higher levels from the zygote stage to the gastrula shield. Then, their expression decreased and stabilized until larval Day 5 except for *adipor2* which increased from the larval protruding mouth stage to 5 days post fertilization. These data show that the three adiponectin receptors exhibit an important maternal contribution and are dynamically expressed during zebrafish embryogenesis (Supporting Information Figure 3). These regulations have been observed in the whole embryo and could affect the periphery, the brain or both.

4.2 | Expression and distribution of adiponectin receptors in the brain of adult fish

Recent data document the neuroprotective effects of adiponectin and its positive impact on neurogenesis; we consequently decided to investigate whether *adiponectin receptors* were expressed in the brain

of adult zebrafish using different approaches: qPCR experiments and RNA seq data set reanalysis (Figure 1) as well as mRNA ISH to validate their spatial distribution (Figure 2 and Supporting Information Figures 4 and S5). Our qPCR experiments performed on three pools of three brains showed that *adipor1a* displayed the highest expression, whereas *adipor2* displayed the lowest (Figure 1a). A RNA seq data set analysis confirmed these results (Figure 1b). Taken together, these data demonstrated that *adipor* are expressed in the brain of adult zebrafish.

To study *adipor* distribution in the brain of adult zebrafish, we performed ISH. The specificity of the *in situ* staining was shown in Supporting Information Figure 4. Briefly, the hybridization without probe led to the absence of staining (Supporting Information Figure 4a-negative control), while the use of *id1* antisense probes as a positive control resulted in a clear and obvious labeling along the ventricular layer as previously described (Supporting Information Figure 4a-positive control). *Id1* is a transcriptional regulator that has been shown to be expressed only in neural stem cells (mainly Type 1) lining the ventricles in zebrafish (Diotel et al., 2015; Diotel, Beil, et al., 2015; Rodriguez Viales et al., 2015). In our experiments, *id1* ISH results in the same staining as previously described (Diotel, Beil, et al., 2015; Diotel, Rodriguez Viales, et al., 2015) and further demonstrates the efficiency and specificity of the staining. Given that sense probes are not always proper controls due to the presence of antisense transcripts from the targeted genomic locus (Katayama et al., 2005; Werner & Berdal, 2005), we performed ISH with two non-overlapping antisense probes for each gene of interest (Supporting Information Figure 4b). As evidenced in Supporting Information Figure 4b, the hybridization with the two non-overlapping probes for *adipor* (probe 1 and probe 2) resulted in a similar staining, such as shown in the hypothalamus, the corpus mamillare, the periventricular pretectal nucleus and the optic tectum. Consistent results were also obtained in the anterior brain (data not shown).

ISH, performed on more than six brains, revealed that *adipor* genes are widely distributed in the brain from the junction between the olfactory bulbs and the telencephalon to the cerebellum (Supporting Information Figure 5). In the anterior part of the brain, *adipor 1a/1b* and 2 were detected in the dorsal telencephalic area (D), along the ventricular layer but also more deeply in the brain parenchyma (Supporting Information Figure 5a–a3). All three receptors were also expressed in the telencephalon in the ventral (Vv) and dorsal (Vd) nuclei of the ventral telencephalon, as well as in the central (Dc), medial (Dm), lateral (Dl), and posterior (Dp) zones of the dorsal telencephalon (Supporting Information Figure 5b–b3; Figure 2a–c).

In the diencephalon, *adipor1a*, *adipor1b*, and *adipor2* gene expression was observed in the anterior (PPa) and posterior (PPp) part of the preoptic area, as well as in the suprachiasmatic nucleus (SC) (Supporting Information Figure 5c–d3; Figure 2d–f). They were also detected in the mediobasal and caudal hypothalamic nuclei (Supporting Information Figure 5e–g3; Figure 2g–i), as well as in the lateral hypothalamic nucleus (LH), the periventricular nucleus of the posterior tuberculum (TPp), the periventricular pretectal nucleus (PPv), the anterior preglomerular nucleus (PGa), and the periventricular gray zone of the optic tectum (TeO) (Supporting Information Figure 5e–g3; Figure 2j–o). The expression of *adipor* was also noticed in numerous other brain

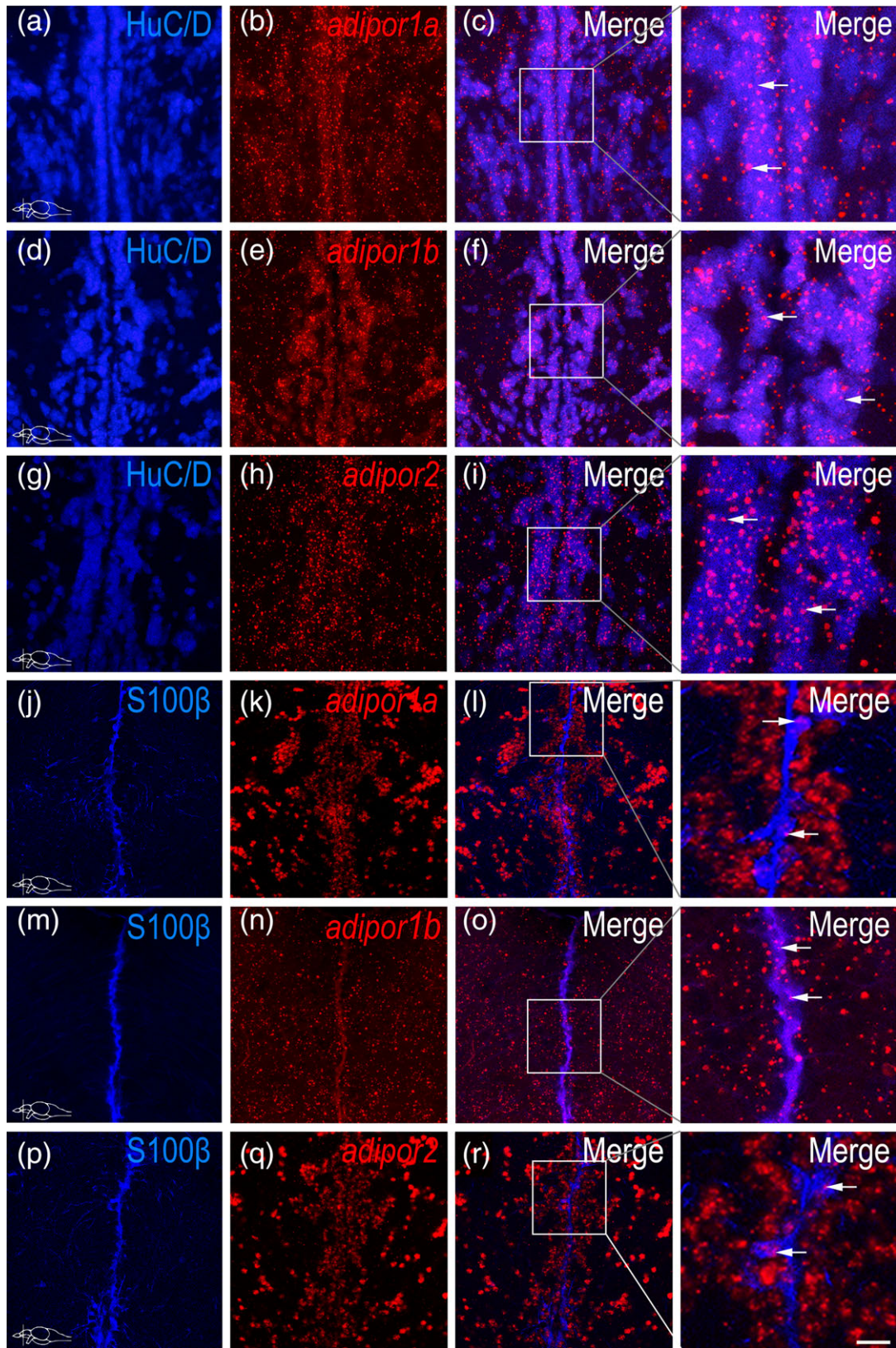


FIGURE 3 Adiponectin receptors are expressed by neurons and neural stem cells in the telencephalon of adult zebrafish. (a–i) *adipor* *in situ* hybridization (ISH) (red) followed by HuC/D immunohistochemistry (blue) showing that most *adipor*-positive cells correspond to HuC/D-positive neurons (junction between Dm and Vd/Vv). (j–r) *adipor* ISH (red) followed by S100β immunohistochemistry (blue) showing that radial glial cells weakly express *adipor* in the telencephalon (Dm). Arrows show examples of HuC/D-*adipor* and S100β-*adipor* colabelings. Micrographs have been taken in the telencephalon. Bar: 30 μm (a–r); 10 μm for high power views [Color figure can be viewed at wileyonlinelibrary.com]

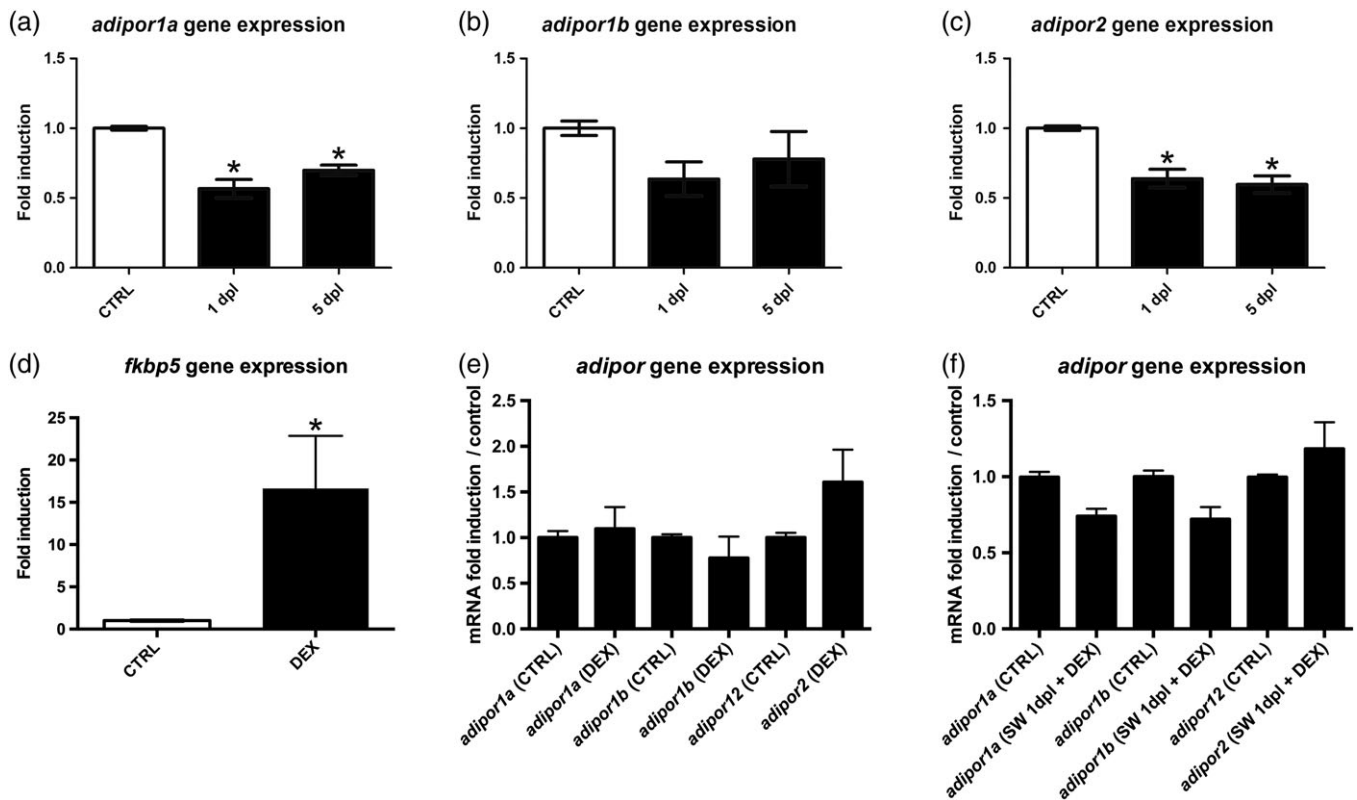


FIGURE 4 Injury-induced inflammation triggers the down-regulation of adiponectin receptors in the zebrafish telencephalon. (a–c) Stab wound injury of the telencephalon induces a significant decrease in *adipor1a* and *adipor2* gene expression at 1 and 5 days post-lesion (dpl). The results are expressed as relative fold induction to the control side normalized to 1 (white column). (d) *fkbp5* gene expression is up-regulated in the body of fish after a 7 days treatment with the anti-inflammatory compound dexamethasone (DEX), demonstrating the efficiency of the treatment (positive control). (e) *adipor* gene expression remains unchanged in uninjured telencephalon (CTRL) after 7 days of DEX treatment showing that DEX does not modulate *adipor* expression in homeostatic condition. (f) Anti-inflammatory treatment rescued the decreased expression of *adipor* gene expression induced by stab wound. SW: stab wound injury of the telencephalon. * $p < 0.05$

nuclei including ventrolateral (VL) and ventromedial (VM) thalamic nuclei, the periventricular nucleus of posterior tuberculum (TPp), along the rhombencephalic ventricle and in the cerebellum (Supporting Information Figure 5h–h3).

Our results demonstrated that all *adipor* exhibited an overall similar pattern of expression. They were detected in numerous cells localized deeply within the brain parenchyma in a way reminiscent to neurons and were also detected along the telencephalic and diencephalic ventricles suggesting expression in radial glial cells (Figure 2 and Supporting Information Figure 5).

4.3 | Adiponectin receptors are expressed in neurons and in neural progenitors in the brain of adult zebrafish

To identify the neuronal and neural progenitor identity of *adipor*-expressing cells, we performed *adipor* ISH followed by immunohistochemistry. As evidenced by confocal microscopy imaging from the telencephalon (notably in the Dm, Vv, and Vd), *adipor1a*, *adipor1b*, and *adipor2* transcripts were strongly detected in HuC/D-positive neurons (Figure 3a–i). In addition, *adipor1a*, *adipor1b*, and *adipor2* (Figure 3j–r) were also expressed in S100 β -positive cells corresponding to radial glial cells (neural progenitors). These results argue in favor of a potential role of adiponectin signaling in neural stem cell activity.

To further explore the potential involvement of adiponectin “signaling” during brain repair, *adipor* expression was investigated by qPCR following stab wound injury of the telencephalon (Figure 4). At 1 day post-lesion (dpl), *adipor* gene expression was consistently decreased compared to uninjured brains, reaching statistical significance for *adipor1a* and *adipor2* (Figure 4a–c). Inflammation is known to promote brain repair following stab wound injury of the telencephalon in zebrafish (Kyritsis et al., 2012). It also down-regulates adiponectin and/or adiponectin receptor expression in mammals (Anderson et al., 2007; Kadowaki & Yamauchi, 2005; Tsuchida et al., 2004; Venkatesh, Hickman, Nisbet, Cohen, & Prins, 2009). We consequently investigated whether inflammation occurring after stab wound injury of the telencephalon could be responsible for the decreased expression of *adipor*. To this aim, we first treated fish with the synthetic anti-inflammatory glucocorticoid DEX for 7 days and performed a stab wound injury of the telencephalon at Day 6. The efficiency of the DEX treatment was assessed by monitoring the up-regulation of *fkbp5* (FK506 binding protein 51) in the body. *Fkbp5* is a co-chaperone of hsp90 regulating glucocorticoid receptor sensitivity, and is known to be up-regulated under glucocorticoid stimulation (Rodriguez Viales et al., 2015; Scharf, Liebl, Binder, Schmidt, & Muller, 2011; Weger, Weger, Nusser, Brenner-Weiss, & Dickmeis, 2012). As shown in Figure 4d, treated fish display a strong and significant whole body up-regulation of *fkbp5* (fold induction >15). Under basal

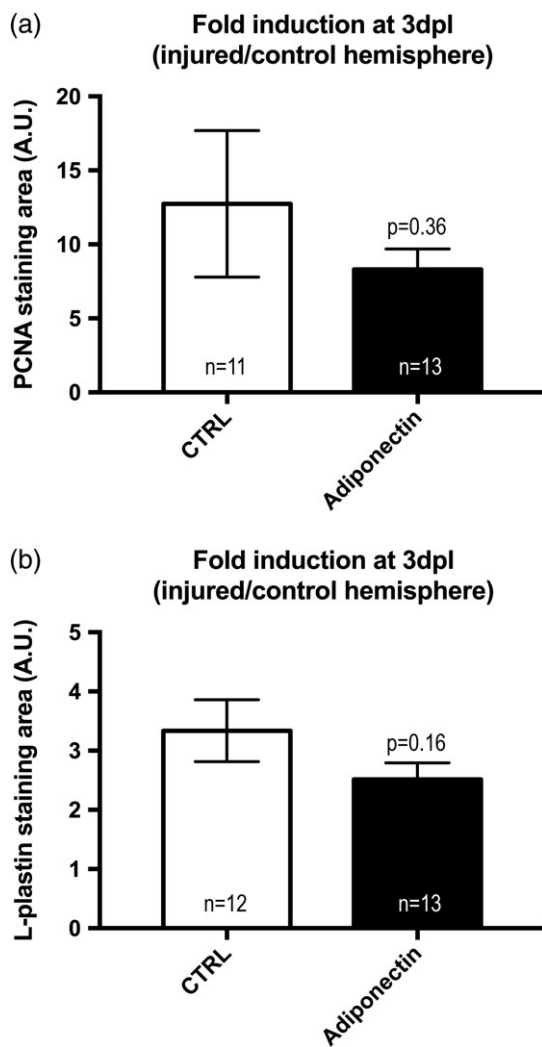


FIGURE 5 Adiponectin treatment tends to decrease injury-induced proliferation and microglial recruitment. Adult zebrafish were injected with recombinant adiponectin (100 µg/g of body weight), lesioned on the right telencephalic hemisphere and allowed to survive for 3 days. Cell proliferation (PCNA-positive area) was quantified at the ventricular surface where neural progenitors are localized; and microglial immunoreactivity (L-plastin-positive area) was quantified in the brain parenchyma. (a) Cell proliferation (PCNA) was increased in the ipsilateral hemisphere compared to the contralateral one in both control and adiponectin-injected fish. Note the decreasing trend in injury-induced proliferation in adiponectin-injected fish. (b) Microglia (L-plastin) recruitment was increased in the ipsilateral hemisphere compared to the contralateral one in both control and adiponectin-injected fish. Note the decreasing trend in L-plastin immunoreactivity in adiponectin-injected fish. The *n* indicates the total number of fish brain analyzed from three independent experiments. The quantification was performed on 3–4 sections for each brain and were averaged for normalization

conditions (without stab wound), DEX treatment did not result in any significant modification of *adipor* gene expression (Figure 4e). At 1 dpl, fish treated for 7 days with the anti-inflammatory compound did not exhibit any significant *adipor* down-regulation (Figure 4f). These results demonstrate that the inhibition of injury-induced inflammation blocks the decrease in *adipor* expression following brain injury at 1 dpl. In our experiments, *adiponectin a* and *b* were almost not

detected in the brain of zebrafish, and stab wound injury of the telencephalon did not increase their expression (data not shown).

To further explore the potential involvement of adiponectin in brain repair mechanisms in adult zebrafish, we performed intraperitoneal injection of murine adiponectin (100 µg/g) after stab wound injury of the telencephalon. This concentration was selected as it provides a strong anti-inflammatory effect *in vitro* (Supporting Information Figure 1). Mouse adiponectin shares a relatively strong homology with zebrafish adiponectin, particularly with the globular domain known to sustain neuroprotective effects (Supporting Information Figure 6). Three days after the lesion (3 dpl), adiponectin injection tended to reduce the number of proliferating neural progenitors (PCNA staining, *p*-value = 0.36) and the recruitment of microglial cells (L-plastin staining, *p*-value = 0.16) to the injury site observed in independent experiments (Figure 5). These results could argue for (a) a trend toward a decrease in microglia recruitment and in injury-induced neurogenesis and therefore (b) a possible neuroprotective effect of adiponectin, but these hypotheses need to be further explored.

4.4 | Adiponectin receptor expression in the brain of adult mouse

In a comparative approach, we next decided to investigate *Adipor* expression in mouse brain. To determine the sites of expression for both *Adipor1* and *Adipor2*, ISH was performed in the brain of adult mice. The specificity of the staining was ascertained by the use of a specific zebrafish probe that failed to generate any significant signal in mouse and with incubation in the absence of probes (Supporting Information Figure 7). Indeed, the zebrafish probes should not bind to any mouse mRNA. *Adipor1* and *Adipor2* were detected in the brain of adult mice, namely in the pallium (dorsal, lateral, ventral) including the cerebral cortex, the thalamus, the hypothalamus, and the septum (Figure 6 and data not shown). *Adipor1* expression was detected in the subventricular zone (SVZ) and in the dentate gyrus (DG) of the hippocampus that are known to be neurogenic regions (Figure 6c,d). In contrast, *Adipor2* was only detected in the DG (Figure 6o,p). Colabeling with the neuronal marker HuC/D and the astrocyte marker GFAP demonstrated a strong expression of *Adipor1* and *Adipor2* in neurons and almost no staining in astrocytes (Figure 6, see arrows and arrowheads). Our reanalysis of a published RNA seq data set performed in mouse cerebral cortex showed that *Adipor1* and *Adipor2* were expressed in neurons, immature and mature oligodendrocytes, in microglial as well as in astrocytes and in endothelial cells (Supporting Information Figure S8) (Zhang et al., 2014).

4.5 | Adiponectin receptor expression under inflammatory stimuli and brain ischemia in mouse

To investigate the potential implication of inflammation and pathological condition such as cerebral ischemia on *adiponectin* and *adipor* expression in mouse brain, we performed (a) LPS injection (100 µg/kg of body weight; sacrifice 6 hr postinjection) and (b) MCAO for 90 min (sacrifice at 24 hr). Intraperitoneal injection of LPS resulted in a significant increase in *Tnfa* gene expression in the hippocampus and in the cerebral cortex, demonstrating the efficiency of the stimulus.

However, it did not result in any significant change in *adiponectin* and *adiponectin receptor* expression (Figure 7a,b). After a 90 min MCAO, the efficiency of brain ischemia was confirmed using TTC vital staining. This showed a similar extent of brain infarction (TTC-negative area: 30–40% of brain section area; data not shown). The MCAO procedure results in a significant increase in *Tnfa* gene expression in the ipsilateral hemisphere compared to the contralateral one, without any significant change in *adiponectin* and *adipor* expression (Figure 7c). Consequently, in our experimental condition, inflammation and brain ischemia did not modulate *adiponectin* and *adipor* expression.

5 | DISCUSSION

Adiponectin signaling has been initially described for its implication in metabolic syndrome, namely in Type 2 diabetes mellitus and obesity (Bluher, 2014; Bluher & Mantzoros, 2015; Julia et al., 2014). It was also suggested to play roles in the central nervous system, regulating blood–brain barrier physiology (i.e., regulation of tight junction proteins, inhibition of inflammatory signaling across the BBB), and promoting neuroprotection. In this work, we took advantage of the zebrafish model to investigate the cerebral targets of adiponectin in a comparative manner with mouse. We documented *adipor* expression in neurogenic regions and we report for the first time their expression in neural stem cells (radial glia) in zebrafish.

5.1 | Adiponectin signaling and development

Given that there is little data on *adiponectin/adipor* gene expression in zebrafish, our developmental expression data analysis for *adiponectin* and *adipor* expression from fertilization to larva Day 5 provides novel insights into the behavior of the gene in this context. This RNAseq analysis is partly supported by the work of Nishio and colleagues (Nishio et al., 2008). In brief, *adipor* mRNA display an important maternal contribution, and appear dynamically up-regulated from segmentation to gastrulation (Supporting Information Figure 3). In mice, *Adiponectin* and *Adipor* mRNA are also detected throughout the first embryonic stages during the preimplantation from 2-cell to 8-cell embryonic stages, with a strong maternal contribution in a way reminiscent to zebrafish (Kim et al., 2011; Schmidt et al., 2008). These data argue in favor of some potential conserved regulation of adiponectin/adiponectin receptor expression during development, suggesting that adiponectin signaling plays similar functions between fish and mice during embryogenesis. However, this hypothesis should consider that regulatory mechanisms could be different at the central and peripheral level during embryogenesis and would benefit of further investigations.

5.2 | Adiponectin receptor expression in the brain and its involvement in neurogenesis

We evidenced that the three *adipor* are expressed in the brain of adult fish and display overlapping patterns notably in the telencephalon, the diencephalon (i.e., preoptic area and hypothalamus), and the rhombencephalon (i.e., cerebellum) (Figure 2 and Supporting Information

Figure 5). These data are supported by RT-PCR experiments performed in Orange-spotted grouper (*Epinephelus coioides*), showing *adipor* gene expression in these regions (Qin, Wang, Sun, Jia, & Li, 2014). We also demonstrated that *adipor1a* displays a higher expression than *adipor2*, fitting with the data obtained in rodents (Guillod-Maximin et al., 2009; Thundyil et al., 2010). All three receptors are strongly expressed in neurons and to a lower extent in radial glial cells known to behave as neural stem cells (Figure 3) (Diotel, Vaillant, Kah, & Pellegrini, 2016; Marz et al., 2010; Pellegrini et al., 2007, 2013). It is the first study documenting *adipor* distribution in the brain of fish and establishing the expression of *adipor* in neural stem cells. These data argue in favor of a potential role of adiponectin signaling in fish neurogenesis which has to be explored further.

In mice, we showed a wide expression of *Adipor1* and *Adipor2* in different brain regions/nuclei including the cerebral cortex (telencephalon), the thalamus, the hypothalamus, and the two main neurogenic regions: the DG of the hippocampus (*Adipor1* and *Adipor2*) as well as the SVZ of the lateral ventricle (*Adipor1*) (Figure 6). *Adipor1* and *Adipor2* proteins were previously detected in the DG of mice (Song et al., 2015), as well as in cultured adult hippocampal neural stem/progenitor cells (Zhang, Guo, Zhang, & Lu, 2011), which displayed increased proliferation following adiponectin treatment. In addition, adiponectin deficiency reduced dendritic length, spine density and branching of granule neurons of male mice, and reduced neural progenitor cell proliferation and differentiation (Zhang et al., 2016), supporting a role of adiponectin signaling in neurogenic activity. Furthermore, *Adipor1* and *Adipor2* expression in the other brain areas described above showed similar patterns as demonstrated in other studies and in the ISH database from the Allen Brain Atlas (Guillod-Maximin et al., 2009; Lein et al., 2007; Miranda-Martinez et al., 2017; Thundyil et al., 2012). Interestingly, both *Adipor* appear to be mainly expressed in neurons and almost not detected in astrocytes, as shown by ISH. However, RNA-seq analysis provides evidence of *Adipor1* and *Adipor2* expression in cortical astrocytes and neurons as well as in oligodendrocytes, microglia, and endothelial cells (Supporting Information Figure S8; C57BL/6 mice from RNA seq data from Zhang et al. [2014], suggesting either a lack of sensitivity of our hybridization technique, the decrease of the astrocytic-marker GFAP staining after the *in situ* protocol, or the existence of alternative splicing). We also confirmed by qPCR experiments the expression of both *Adipor1* and *Adipor2* genes using astrocytes (CLTT) and microglia (BV2) cell lines (data not shown). In accordance with our work, other studies have also shown *Adipor1* and *Adipor2* expression in astrocytes, notably in the rat olfactory bulbs and hypothalamus (Guillod-Maximin et al., 2009; Miranda-Martinez et al., 2017; Thundyil et al., 2012). Interestingly, it was also shown that *Adipor1* and *Adipor2* were expressed in tanycytes of the hypothalamic rat arcuate nucleus (Guillod-Maximin et al., 2009). Tanycytes are specialized ependymal cells, forming a blood-cerebrospinal fluid barrier in the hypothalamus, at the level of the median eminence (Langlet, Mullier, Bouret, Prevot, & Dehouck, 2013). These cells display characteristics of radial glial cells and also express tight junctions, a hallmark of central nervous system barriers (Clasadonte & Prevot, 2018; Guillod-Maximin et al., 2009). Tanycytes are of particular interest acting as blood glucose level sensors and as shuttles for metabolic signals involved in food intake (Prevot et al., 2018). In addition, they exhibit

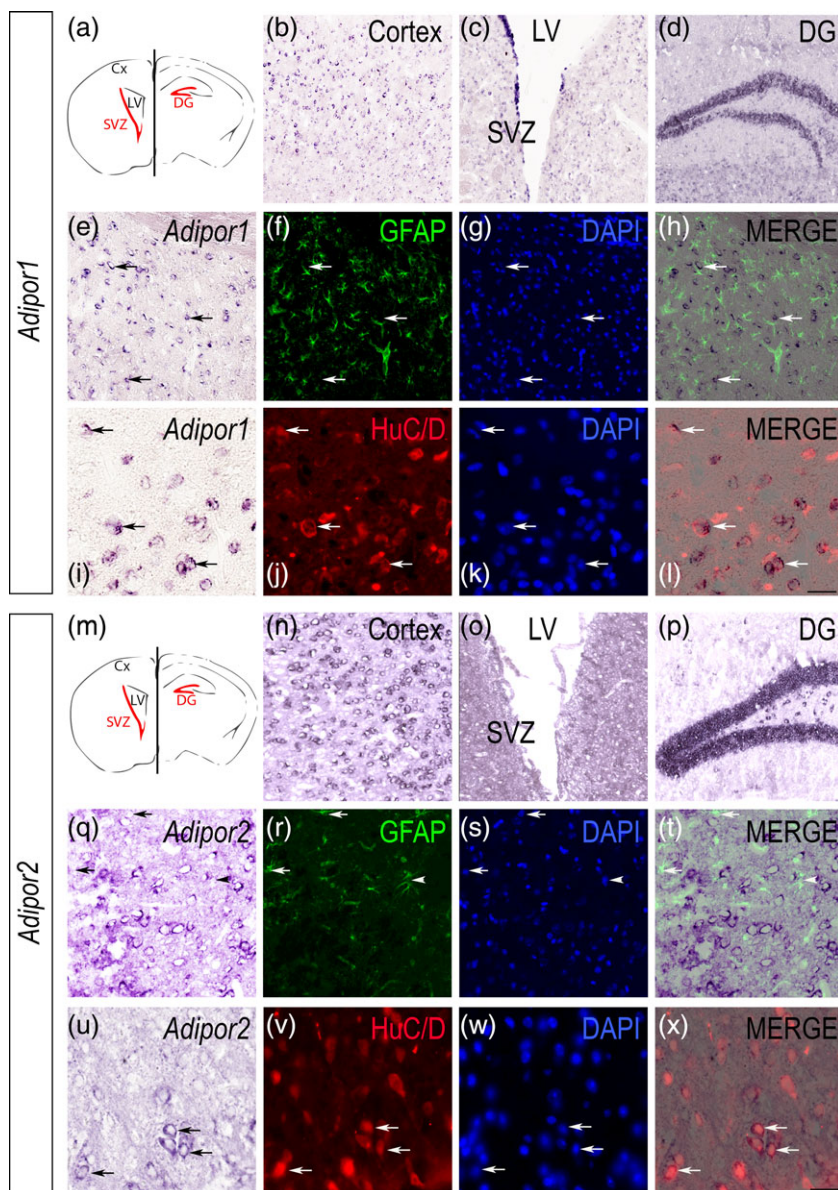


FIGURE 6 Adipor1 and Adipor2 are widely expressed in the brain of adult mouse including neurogenic regions. (a, m) Schematic views showing the different brain regions studied: the cortex (Cx), the dentate gyrus of the hippocampus (DG), and the subventricular zone (SVZ) of the lateral ventricle (LV). The regions in red are neurogenic areas. The left hemisphere corresponds to a coronal section through the LV/SVZ while the right one corresponds to a section through the DG of the hippocampus. (b–d) *Adipor1* mRNA expression is detected in the cerebral cortex and in neurogenic regions: the layer bordering the lateral ventricle (c) and the DG (d) of the hippocampus. (e–l) *Adipor1* *in situ* hybridization (ISH) followed by GFAP (green) or HuC/D (red) immunohistochemistry. Cell nuclei are counterstained with DAPI (blue). *Adipor1*-positive cells does not correspond to GFAP-positive astrocytes (green) as shown by arrows (e–h), while they mainly correspond to HuC/D-positive neurons (red) as highlighted by arrows (i–l). (n–p) *Adipor2* mRNA expression is detected in the cerebral cortex (n) and the DG (p) of the hippocampus, but not along the ventricular layer of the lateral ventricle (o). (q–t) *Adipor2* ISH followed by GFAP (green) or HuC/D (red) immunohistochemistry and nuclei counterstaining with DAPI (blue). Most *Adipor2*-positive cells do not correspond to GFAP-positive astrocytes (green) as shown by arrows, but few astrocytes seem to weakly expressed *Adipor2* (arrowheads). In contrast, most *Adipor2*-positive cells correspond to HuC/D-positive neurons (red) as highlighted by arrows (u–x). A total of three brains was investigated for each gene. Bar: 14 μ m (i–l and u–x), 28 μ m (n–p), 35 μ m (q–t), 55 μ m (e–h), 70 μ m (b–d) [Color figure can be viewed at wileyonlinelibrary.com]

neural stem cell properties and are a key component of hypothalamic neurogenesis (Bolborea & Dale, 2013; Prevot et al., 2018). In traumatic brain injury context, disruption of blood-cerebrospinal fluid barrier formed by tanycytes can occur in the median eminence in mice (Osterstock et al., 2014), and can cause neuroendocrine disorders.

Consequently, *Adipor* expression appears evolutionary conserved between fish and mice (telencephalon, diencephalon–thalamus and

hypothalamus, cerebellum) notably in neurogenic niches (Table 4). Indeed, *Adipor* expression has been reported in rodent neural stem cells and we demonstrated that radial glial cells, acting as neural stem cells, also express *adipor* in zebrafish. Taken together, these data strongly suggest that adiponectin could modulate neural stem cell activity in fish as partly evidenced in rodent. This assumption needs to be further explored.

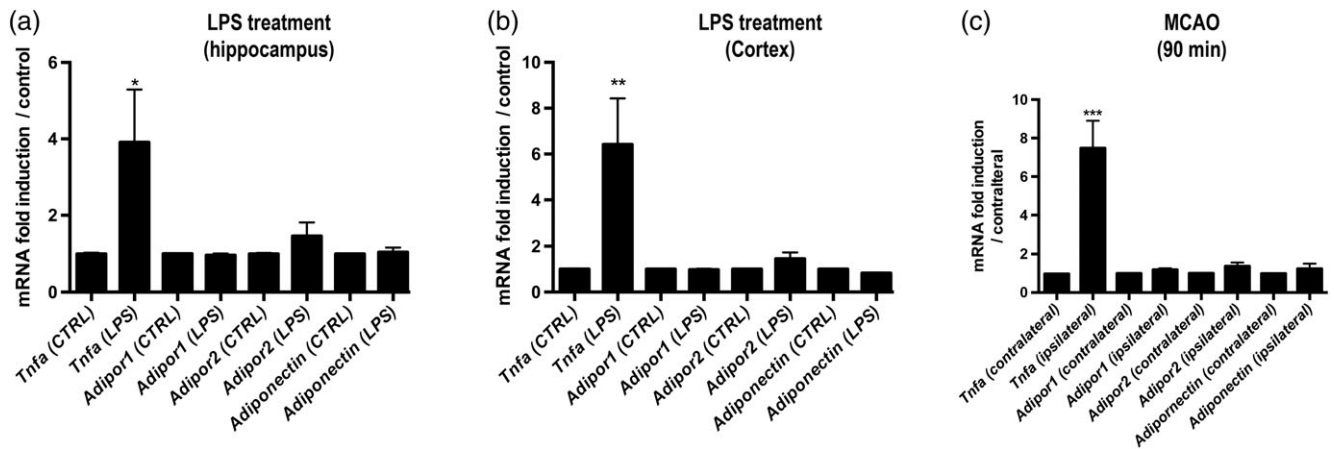


FIGURE 7 Lipopolysaccharide-induced inflammation and brain ischemia does not impair the expression of Adiponectin and Adipor in the brain. (a, b) Mice were intraperitoneally injected with PBS (CTRL) or with LPS (100 $\mu\text{g}/\text{kg}$ of body weight) and allowed to survive for 6 hr. In the hippocampus (a) and the cerebral cortex (b), LPS injection leads to a significant increase in *Tnfa* gene expression compared to the PBS injection (CTRL). No change was noticed for *Adipor1*, *Adipor2*, and *Adiponectin* expression. The results are expressed as relative fold induction to the PBS-injected mice (CTRL). (c) Mice were subjected to middle cerebral artery occlusion for 90 min and allowed to survive 24 hr. In the infarcted hemisphere (ipsilateral), a significant increase in *Tnfa* gene expression is observed compared to the contralateral one. No change was noticed for *Adipor1*, *Adipor2*, and *Adiponectin* expression. The results are expressed as relative fold induction to contralateral hemisphere ($n = 3$; $p < 0.05$). Note that individual cortex and hippocampus have been used for RNA extraction ($n = 3$)

5.3 | Adiponectin/adiponectin receptors and brain damages

We observed that stab wound injury of zebrafish telencephalon resulted in *adipor* down-regulation. In zebrafish, mechanical injury leads to an increase of proinflammatory cytokines (*il8*, *il1b*, and *tnfa*) which initiate injury-induced neurogenesis (Kyritsis et al., 2012). In our experimental conditions, inhibition of inflammation by DEX limited *adipor* down-regulation following injury (Figure 4). Our models of inflammation in mice induced by MCAO and LPS injection failed to modulate *Adiponectin* and *Adipor* expression (Figure 7). Consequently, different regulations of *adipor* expression seem to occur between fish and mice in these experimental models. However, it was demonstrated by Hall, Leuwer, Trayhurn, and Welters (2015) that LPS-injected mice exhibited a significant down-regulation of adiponectin receptors in adipose tissue, skeletal muscle, and liver. The used LPS concentration was significantly higher than in our experiments (25 mg/kg of body weight vs. 100 $\mu\text{g}/\text{kg}$ in our condition) (Hall et al.,

2015). It is also possible that the regulation of *adiponectin* and *adipor* expression in mice differs between the brain and peripheral tissues.

Interestingly, studies using hypoxia/MCAO/diabetic models reported that adiponectin exerted neuroprotective effects and reduced neuronal apoptosis, the size of the infarct and neurological deficits (Chen et al., 2009; Song et al., 2015). There are several potential mechanisms to explain the neuroprotective effects of adiponectin, such as the decrease in vascular cell adhesion molecule at the BBB and in immune cells recruitment after brain injury; increased survival and functions of BBB endothelial cells; stimulation of angiogenesis; decreased of excitotoxicity, oxidative stress and apoptosis (noticeably through increased AMPK signaling) and decreased neuroinflammation (Bloemer et al., 2018; Song et al., 2015, 2017; Xu et al., 2018). In our experimental conditions, injection of adiponectin in fish following stab wound injury of the telencephalon tended to decrease microglial recruitment and progenitor proliferation at the ventricular surface at 3 dpl. Such a decrease could be explained by a neuroprotective effect of adiponectin injection given that if the infarcted regions are reduced, the recruitment

TABLE 4 Comparative distribution of adiponectin receptors in the brain of mouse and zebrafish

		Mouse Adipor1	Mouse Adipor2	Zebrafish adipor1a	Zebrafish adipor1b	Zebrafish adipor2
Olfactory regions	Bulbs/tracts/area	+	+	+	+	+
Telencephalon	Subpallium	+	+	+	+	+
	Pallium	+	+	+	+	+
	Including hippocampus or "hippocampus-like" (lateral pallium in zebrafish)	+	+	+	+	+
Diencephalon	Preoptic area	+	+	+	+	+
	Hypothalamus	+	+	+	+	+
	Thalamus	+	+	+	+	+
Rhombencephalon	Cerebellum	+	+	+	+	+
	Pons	+	+	Nd	Nd	Nd

Nd: not determined.

of neural stem cells and microglia would be decreased too. However, this assumption would need to be confirmed. In addition, it is also possible that the affinity of murine adiponectin is not strong enough for zebrafish adiponectin receptors. The production of zebrafish adiponectin could be useful to fully document the role of adiponectin in brain repair mechanism and neuroprotection. In neonatal rats under hypoxia ischemia, it was recently shown that adiponectin treatment led to increased adiponectin, AdipoR1, and p-AMPK expression levels, resulting in reduced apoptosis (Xu et al., 2018). Such a mechanistic neuroprotective effect would be interesting to study in zebrafish.

6 | CONCLUSION

In conclusion, we show that *adipor* expression was highly similar between fish and mice. These data raise the question of the potential evolutionary conserved functions of adiponectin signaling between these two species particularly in the central nervous system. Further investigations have to be performed to better understand the impact of adiponectin signaling on adult neurogenesis and neuroprotection in zebrafish, and to establish zebrafish as an alternative model for studying the pleiotropic roles of adiponectin.

ACKNOWLEDGMENTS

We thank Luisa Lübke and Joseph Wragg for proof reading of the manuscript, Noenelle Marcelin and Anne-Claire Dorsemans for technical support, and M. Redd for kindly providing us the L-plastin antibody. This work was supported by grants from La Réunion University (Bonus Qualité Recherche, Dispositifs incitatifs), Conseil Régional de La Réunion, European Union (CPER/FEDER), Fédération BioSécurité en milieu Tropical (BioST), Philancia association and Fondation de France (for UMR1188 DéTROI). SR and US received fundings from the European Union's Horizon 3952020 research and innovation programme under the Marie Skłodowska-Curie grant agreement No. 643062 (ZENCODE-ITN) <<https://zencode-itn.eu>> and the programme BioInterfaces in Technology and Medicine of the Helmholtz foundation.

CONFLICT OF INTEREST

The authors declare that they have no conflict of interest.

AUTHOR CONTRIBUTIONS

N.D., C.L.d.H., O.G.M., S.R., A.P., W.V.: conception and design of the experiments; N.D., C.L.d.H., O.M., S.R., S.W., M.R., N.C.S., S.N.S., W.V., D.C., C.P.: acquisition of data; N.D., C.L.d.H., O.M., S.R., S.W., M.R., N.C.S., S.N.S., W.V., D.C., C.P.: analysis of the data. All the authors: writing and proof-reading of the manuscript.

ORCID

Avinash Parimisetty  <https://orcid.org/0000-0003-0174-4442>

Olivier Meilhac  <https://orcid.org/0000-0002-3740-7539>

Nicolas Diotel  <https://orcid.org/0000-0003-2032-518X>

REFERENCES

- Adolf, B., Chapouton, P., Lam, C. S., Topp, S., Tannhauser, B., Strahle, U., ... Bally-Cuif, L. (2006). Conserved and acquired features of adult neurogenesis in the zebrafish telencephalon. *Developmental Biology*, 295(1), 278–293.
- Anderson, P. D., Mehta, N. N., Wolfe, M. L., Hinkle, C. C., Pruscino, L., Comiskey, L. L., ... Reilly, M. P. (2007). Innate immunity modulates adipokines in humans. *The Journal of Clinical Endocrinology and Metabolism*, 92(6), 2272–2279.
- Baumgart, E. V., Barbosa, J. S., Bally-Cuif, L., Gotz, M., & Ninkovic, J. (2012). Stab wound injury of the zebrafish telencephalon: A model for comparative analysis of reactive gliosis. *Glia*, 60(3), 343–357.
- Berg, A. H., Combs, T. P., & Scherer, P. E. (2002). ACRP30/adiponectin: An adipokine regulating glucose and lipid metabolism. *Trends in Endocrinology and Metabolism*, 13(2), 84–89.
- Bloemer, J., Pinky, P. D., Govindarajulu, M., Hong, H., Judd, R., Amin, R. H., ... Suppiramaniam, V. (2018). Role of adiponectin in central nervous system disorders. *Neural Plasticity*, 2018, 4593530.
- Bluher, M. (2014). Adipokines - removing road blocks to obesity and diabetes therapy. *Molecular Metabolism*, 3(3), 230–240.
- Bluher, M., & Mantzoros, C. S. (2015). From leptin to other adipokines in health and disease: Facts and expectations at the beginning of the 21st century. *Metabolism: Clinical and Experimental*, 64(1), 131–145.
- Bolborea, M., & Dale, N. (2013). Hypothalamic tanycytes: Potential roles in the control of feeding and energy balance. *Trends in Neurosciences*, 36(2), 91–100.
- Chen, B., Liao, W. Q., Xu, N., Xu, H., Wen, J. Y., Yu, C. A., ... Campbell, W. (2009). Adiponectin protects against cerebral ischemia-reperfusion injury through anti-inflammatory action. *Brain Research*, 1273, 129–137.
- Clasadonte, J., & Prevot, V. (2018). The special relationship: Glia-neuron interactions in the neuroendocrine hypothalamus. *Nature Reviews. Endocrinology*, 14(1), 25–44.
- Couret, D., Bourane, S., Catan, A., Nativel, B., Planesse, C., Dorsemans, A. C., ... Meilhac, O. (2018). A hemorrhagic transformation model of mechanical stroke therapy with acute hyperglycemia in mice. *The Journal of Comparative Neurology*, 526(6), 1006–1016.
- Dehal, P., & Boore, J. L. (2005). Two rounds of whole genome duplication in the ancestral vertebrate. *PLoS Biology*, 3(10), e314.
- Diotel, N., Beil, T., Strahle, U., & Rastegar, S. (2015). Differential expression of id genes and their potential regulator znf238 in zebrafish adult neural progenitor cells and neurons suggests distinct functions in adult neurogenesis. *Gene Expression Patterns*, 19(1–2), 1–13.
- Diotel, N., Do Rego, J. L., Anglade, I., Vaillant, C., Pellegrini, E., Vaudry, H., & Kah, O. (2011). The brain of teleost fish, a source, and a target of sexual steroids. *Frontiers in Neuroscience*, 5, 137.
- Diotel, N., Le Page, Y., Mouriec, K., Tong, S. K., Pellegrini, E., Vaillant, C., ... Kah, O. (2010). Aromatase in the brain of teleost fish: Expression, regulation and putative functions. *Frontiers in Neuroendocrinology*, 31(2), 172–192.
- Diotel, N., Rodriguez Viales, R., Armant, O., Marz, M., Ferg, M., Rastegar, S., & Strahle, U. (2015). Comprehensive expression map of transcription regulators in the adult zebrafish telencephalon reveals distinct neurogenic niches. *The Journal of Comparative Neurology*, 523(8), 1202–1221.
- Diotel, N., Vaillant, C., Gabbero, C., Mironov, S., Fostier, A., Gueguen, M. M., ... Pellegrini, E. (2013). Effects of estradiol in adult neurogenesis and brain repair in zebrafish. *Hormones and Behavior*, 63(2), 193–207.
- Diotel, N., Vaillant, C., Gueguen, M. M., Mironov, S., Anglade, I., Servili, A., ... Kah, O. (2010). Cxcr4 and Cxcl12 expression in radial glial cells of the brain of adult zebrafish. *The Journal of Comparative Neurology*, 518(24), 4855–4876.
- Diotel, N., Vaillant, C., Kah, O., & Pellegrini, E. (2016). Mapping of brain lipid binding protein (Blbp) in the brain of adult zebrafish, co-expression with aromatase B and links with proliferation. *Gene Expression Patterns*, 20(1), 42–54.

- Dorsemans, A. C., Lefebvre d'Helencourt, C., Ait-Arsa, I., Jestin, E., Meilhac, O., & Diotel, N. (2017). Acute and chronic models of hyperglycemia in zebrafish: A method to assess the impact of hyperglycemia on neurogenesis and the biodistribution of radiolabeled molecules. *Journal of Visualized Experiments*, 124.
- Dorsemans, A. C., Soule, S., Weger, M., Bourdon, E., Lefebvre d'Helencourt, C., Meilhac, O., & Diotel, N. (2017). Impaired constitutive and regenerative neurogenesis in adult hyperglycemic zebrafish. *The Journal of Comparative Neurology*, 525(3), 442–458.
- Grandel, H., & Brand, M. (2013). Comparative aspects of adult neural stem cell activity in vertebrates. *Development Genes and Evolution*, 223(1–2), 131–147.
- Guillod-Maximin, E., Roy, A. F., Vacher, C. M., Aubourg, A., Bailleux, V., Lorisgnol, A., ... Taouis, M. (2009). Adiponectin receptors are expressed in hypothalamus and colocalized with proopiomelanocortin and neuropeptide Y in rodent arcuate neurons. *The Journal of Endocrinology*, 200(1), 93–105.
- Hall, A., Leuwer, M., Trayhurn, P., & Welters, I. D. (2015). Lipopolysaccharide induces a downregulation of adiponectin receptors in-vitro and in-vivo. *PeerJ*, 3, e1428.
- Hata, R., Mies, G., Wiessner, C., Fritze, K., Hesselbarth, D., Brinker, G., & Hossmann, K. A. (1998). A reproducible model of middle cerebral artery occlusion in mice: Hemodynamic, biochemical, and magnetic resonance imaging. *Journal of Cerebral Blood Flow and Metabolism*, 18(4), 367–375.
- Julia, C., Czernichow, S., Charnaux, N., Ahluwalia, N., Andreeva, V., Touvier, M., ... Fezeu, L. (2014). Relationships between adipokines, biomarkers of endothelial function and inflammation and risk of type 2 diabetes. *Diabetes Research and Clinical Practice*, 105(2), 231–238.
- Kadowaki, T., & Yamauchi, T. (2005). Adiponectin and adiponectin receptors. *Endocrine Reviews*, 26(3), 439–451.
- Katayama, S., Tomaru, Y., Kasukawa, T., Waki, K., Nakanishi, M., Nakamura, M., ... Consortium, F. (2005). Antisense transcription in the mammalian transcriptome. *Science*, 309(5740), 1564–1566.
- Kershaw, E. E., & Flier, J. S. (2004). Adipose tissue as an endocrine organ. *The Journal of Clinical Endocrinology and Metabolism*, 89(6), 2548–2556.
- Kim, S. T., Marquard, K., Stephens, S., Loudon, E., Allsworth, J., & Moley, K. H. (2011). Adiponectin and adiponectin receptors in the mouse preimplantation embryo and uterus. *Human Reproduction*, 26(1), 82–95.
- Kishimoto, N., Shimizu, K., & Sawamoto, K. (2012). Neuronal regeneration in a zebrafish model of adult brain injury. *Disease Models & Mechanisms*, 5(2), 200–209.
- Kizil, C., Kaslin, J., Kroehne, V., & Brand, M. (2012). Adult neurogenesis and brain regeneration in zebrafish. *Developmental Neurobiology*, 72(3), 429–461.
- Krishnan, J., & Rohner, N. (2019). Sweet fish. Fish models for the study of hyperglycemia and diabetes. *Journal of Diabetes*, 11(3), 193–203.
- Kyritsis, N., Kizil, C., Zocher, S., Kroehne, V., Kaslin, J., Freudenreich, D., ... Brand, M. (2012). Acute inflammation initiates the regenerative response in the adult zebrafish brain. *Science*, 338(6112), 1353–1356.
- Langlet, F., Mullier, A., Bouret, S. G., Prevot, V., & Dehouck, B. (2013). Tanycyte-like cells form a blood-cerebrospinal fluid barrier in the circumventricular organs of the mouse brain. *The Journal of Comparative Neurology*, 521(15), 3389–3405.
- Lein, E. S., Hawrylycz, M. J., Ao, N., Ayres, M., Bensinger, A., Bernard, A., ... Jones, A. R. (2007). Genome-wide atlas of gene expression in the adult mouse brain. *Nature*, 445(7124), 168–176.
- Lindsey, B. W., Darabie, A., & Tropepe, V. (2012). The cellular composition of neurogenic periventricular zones in the adult zebrafish forebrain. *The Journal of Comparative Neurology*, 520(10), 2275–2316.
- Lindsey, B. W., & Tropepe, V. (2006). A comparative framework for understanding the biological principles of adult neurogenesis. *Progress in Neurobiology*, 80(6), 281–307.
- Love, M. I., Huber, W., & Anders, S. (2014). Moderated estimation of fold change and dispersion for RNA-seq data with DESeq2. *Genome Biology*, 15(12), 550.
- Marz, M., Chapouton, P., Diotel, N., Vaillant, C., Hesel, B., Takamiya, M., ... Strahle, U. (2010). Heterogeneity in progenitor cell subtypes in the ventricular zone of the zebrafish adult telencephalon. *Glia*, 58(7), 870–888.
- Matsuzawa, Y. (2005). Adiponectin: Identification, physiology and clinical relevance in metabolic and vascular disease. *Atherosclerosis. Supplements*, 6(2), 7–14.
- Menuet, A., Pellegrini, E., Brion, F., Gueguen, M. M., Anglade, I., Pakdel, F., & Kah, O. (2005). Expression and estrogen-dependent regulation of the zebrafish brain aromatase gene. *The Journal of Comparative Neurology*, 485(4), 304–320.
- Miranda-Martinez, A., Mercado-Gomez, O. F., Arriaga-Avila, V., & Guevara-Guzman, R. (2017). Distribution of adiponectin receptors 1 and 2 in the rat olfactory bulb and the effect of adiponectin injection on insulin receptor expression. *International Journal of Endocrinology*, 2017, 4892609.
- Nishimura, M., Izumiya, Y., Higuchi, A., Shibata, R., Qiu, J., Kudo, C., ... Ouchi, N. (2008). Adiponectin prevents cerebral ischemic injury through endothelial nitric oxide synthase dependent mechanisms. *Circulation*, 117(2), 216–223.
- Nishio, S., Gibert, Y., Bernard, L., Brunet, F., Triqueneaux, G., & Laudet, V. (2008). Adiponectin and adiponectin receptor genes are coexpressed during zebrafish embryogenesis and regulated by food deprivation. *Developmental Dynamics*, 237(6), 1682–1690.
- Okamoto, Y. (2011). Adiponectin provides cardiovascular protection in metabolic syndrome. *Cardiology Research and Practice*, 2011, 313179.
- Okamoto, Y., Kihara, S., Ouchi, N., Nishida, M., Arita, Y., Kumada, M., ... Matsuzawa, Y. (2002). Adiponectin reduces atherosclerosis in apolipoprotein E-deficient mice. *Circulation*, 106(22), 2767–2770.
- Osterstock, G., El Yandouzi, T., Romano, N., Carmignac, D., Langlet, F., Coutry, N., ... Mery, P. F. (2014). Sustained alterations of hypothalamic tanycytes during posttraumatic hypopituitarism in male mice. *Endocrinology*, 155(5), 1887–1898.
- Ouchi, N., Parker, J. L., Lugus, J. J., & Walsh, K. (2011). Adipokines in inflammation and metabolic disease. *Nature Reviews. Immunology*, 11(2), 85–97.
- Pan, W., & Kastin, A. J. (2007). Adipokines and the blood-brain barrier. *Peptides*, 28(6), 1317–1330.
- Parimisetty, A., Dorsemans, A. C., Awada, R., Ravanan, P., Diotel, N., & Lefebvre d'Helencourt, C. (2016). Secret talk between adipose tissue and central nervous system via secreted factors—an emerging frontier in the neurodegenerative research. *Journal of Neuroinflammation*, 13(1), 67.
- Pellegrini, E., Mouriec, K., Anglade, I., Menuet, A., Le Page, Y., Gueguen, M. M., ... Kah, O. (2007). Identification of aromatase-positive radial glial cells as progenitor cells in the ventricular layer of the forebrain in zebrafish. *The Journal of Comparative Neurology*, 501(1), 150–167.
- Pellegrini, E., Vaillant, C., Diotel, N., Benquet, P., Brion, F., & Kah, O. (2013, 2013). Expression, regulation and potential functions of aromatase in radial glial cells of the fish brain. In J. B. Balthazart & F. Gregory (Eds.), *Brain aromatase, estrogens, and behavior*. Oxford, NY: Oxford University Press.
- Prevot, V., Dehouck, B., Sharif, A., Ciofi, P., Giacobini, P., & Clasadonte, J. (2018). The versatile tanycyte: A hypothalamic integrator of reproduction and energy metabolism. *Endocrine Reviews*, 39(3), 333–368.
- Psilopanagioti, A., Papadaki, H., Kranioti, E. F., Alexandrides, T. K., & Varakis, J. N. (2009). Expression of adiponectin and adiponectin receptors in human pituitary gland and brain. *Neuroendocrinology*, 89(1), 38–47.
- Qin, C., Wang, B., Sun, C., Jia, J., & Li, W. (2014). Orange-spotted grouper (*Epinephelus coioides*) adiponectin receptors: Molecular characterization, mRNA expression, and subcellular location. *General and Comparative Endocrinology*, 198, 47–58.
- Qiu, G., Wan, R., Hu, J., Mattson, M. P., Spangler, E., Liu, S., ... Zou, S. (2011). Adiponectin protects rat hippocampal neurons against excitotoxicity. *Age*, 33(2), 155–165.
- Ravi, V., & Venkatesh, B. (2008). Rapidly evolving fish genomes and teleost diversity. *Current Opinion in Genetics & Development*, 18(6), 544–550.
- Redd, M. J., Kelly, G., Dunn, G., Way, M., & Martin, P. (2006). Imaging macrophage chemotaxis in vivo: Studies of microtubule function in zebrafish wound inflammation. *Cell Motility and the Cytoskeleton*, 63(7), 415–422.
- Rodriguez Viales, R., Diotel, N., Ferg, M., Armant, O., Eich, J., Alunni, A., ... Strahle, U. (2015). The helix-loop-helix protein id1 controls stem cell

- proliferation during regenerative neurogenesis in the adult zebrafish telencephalon. *Stem Cells*, 33(3), 892–903.
- Rothenaigner, I., Krecsmarik, M., Hayes, J. A., Bahn, B., Lepier, A., Fortin, G., ... Bally-Cuif, L. (2011). Clonal analysis by distinct viral vectors identifies bona fide neural stem cells in the adult zebrafish telencephalon and characterizes their division properties and fate. *Development*, 138(8), 1459–1469.
- Scharf, S. H., Liebl, C., Binder, E. B., Schmidt, M. V., & Muller, M. B. (2011). Expression and regulation of the Fkbp5 gene in the adult mouse brain. *PLoS One*, 6(2), e16883.
- Schmidt, R., Beil, T., Strähle, U., & Rastegar, S. (2014). Stab wound injury of the zebrafish adult telencephalon: A method to investigate vertebrate brain neurogenesis and regeneration. *Journal of Visualized Experiments*, 90, e51753.
- Schmidt, T., Fischer, S., Tsikolia, N., Navarrete Santos, A., Rohrbach, S., Ramin, N., ... Fischer, B. (2008). Expression of adipokines in preimplantation rabbit and mice embryos. *Histochemistry and Cell Biology*, 129(6), 817–825.
- Song, J., Choi, S. M., Whitcomb, D. J., & Kim, B. C. (2017). Adiponectin controls the apoptosis and the expression of tight junction proteins in brain endothelial cells through AdipoR1 under beta amyloid toxicity. *Cell Death & Disease*, 8(10), e3102.
- Song, W., Guo, F., Zhong, H., Liu, L., Yang, R., Wang, Q., & Xiong, L. (2015). Therapeutic window of globular adiponectin against cerebral ischemia in diabetic mice: The role of dynamic alteration of adiponectin/adiponectin receptor expression. *Scientific Reports*, 5, 17310.
- Spranger, J., Kroke, A., Mohlig, M., Bergmann, M. M., Ristow, M., Boeing, H., & Pfeiffer, A. F. (2003). Adiponectin and protection against type 2 diabetes mellitus. *Lancet*, 361(9353), 226–228.
- Stefan, N., & Stumvoll, M. (2002). Adiponectin—its role in metabolism and beyond. *Hormone and Metabolic Research*, 34(9), 469–474.
- Sun, Y. Y., Yang, D., & Kuan, C. Y. (2012). Mannitol-facilitated perfusion staining with 2,3,5-triphenyltetrazolium chloride (TTC) for detection of experimental cerebral infarction and biochemical analysis. *Journal of Neuroscience Methods*, 203(1), 122–129.
- Thundyil, J., Pavlovski, D., Sobey, C. G., & Arumugam, T. V. (2012). Adiponectin receptor signalling in the brain. *British Journal of Pharmacology*, 165(2), 313–327.
- Thundyil, J., Tang, S. C., Okun, E., Shah, K., Karamyan, V. T., Li, Y. I., ... Arumugam, T. V. (2010). Evidence that adiponectin receptor 1 activation exacerbates ischemic neuronal death. *Experimental & Translational Stroke Medicine*, 2(1), 15.
- Tilg, H., & Moschen, A. R. (2006). Adipocytokines: Mediators linking adipose tissue, inflammation and immunity. *Nature Reviews. Immunology*, 6(10), 772–783.
- Tsushima, A., Yamauchi, T., Ito, Y., Hada, Y., Maki, T., Takekawa, S., ... Kadowaki, T. (2004). Insulin/Foxo1 pathway regulates expression levels of adiponectin receptors and adiponectin sensitivity. *Journal of Biological Chemistry*, 279(29), 30817–30822.
- Venkatesh, B., Hickman, I., Nisbet, J., Cohen, J., & Prins, J. (2009). Changes in serum adiponectin concentrations in critical illness: A preliminary investigation. *Critical Care*, 13(4), R105.
- Wan, Z., Mah, D., Simtchouk, S., Klegeris, A., & Little, J. P. (2014). Globular adiponectin induces a pro-inflammatory response in human astrocytic cells. *Biochemical and Biophysical Research Communications*, 446(1), 37–42.
- Waseem, N. H., & Lane, D. P. (1990). Monoclonal antibody analysis of the proliferating cell nuclear antigen (PCNA). Structural conservation and the detection of a nucleolar form. *Journal of Cell Science*, 96(Pt1), 121–129.
- Weger, B. D., Weger, M., Nusser, M., Brenner-Weiss, G., & Dickmeis, T. (2012). A chemical screening system for glucocorticoid stress hormone signaling in an intact vertebrate. *ACS Chemical Biology*, 7(7), 1178–1183.
- Werner, A., & Berdal, A. (2005). Natural antisense transcripts: Sound or silence? *Physiological Genomics*, 23(2), 125–131.
- White, R. J., Collins, J. E., Sealy, I. M., Wali, N., Dooley, C. M., Digby, Z., ... Busch-Nentwich, E. M. (2017). A high-resolution mRNA expression time course of embryonic development in zebrafish. *eLife*, 6.
- Whitehead, J. P., Richards, A. A., Hickman, I. J., Macdonald, G. A., & Prins, J. B. (2006). Adiponectin—a key adipokine in the metabolic syndrome. *Diabetes, Obesity & Metabolism*, 8(3), 264–280.
- Wilkinson, M., Brown, R., Imran, S. A., & Ur, E. (2007). Adipokine gene expression in brain and pituitary gland. *Neuroendocrinology*, 86(3), 191–209.
- Wong, R. Y., & Godwin, J. (2015). Neurotranscriptome profiles of multiple zebrafish strains. *Genomics Data*, 5, 206–209.
- Wullimann, M., Rupp, B., & Reichert, H. (Eds.). (1996). *Neuroanatomy of the zebrafish brain: A topological atlas* (pp. 1–144). Basel, Switzerland: Birkhäuser Verlag.
- Xu, N., Zhang, Y., Doycheva, D. M., Ding, Y., Zhang, Y., Tang, J., ... Zhang, J. H. (2018). Adiponectin attenuates neuronal apoptosis induced by hypoxia-ischemia via the activation of AdipoR1/APPL1/LKB1/AMPK pathway in neonatal rats. *Neuropharmacology*, 133, 415–428.
- Zang, L., Maddison, L. A., & Chen, W. (2018). Zebrafish as a model for obesity and diabetes. *Frontiers in Cell and Development Biology*, 6, 91.
- Zhang, D., Guo, M., Zhang, W., & Lu, X. Y. (2011). Adiponectin stimulates proliferation of adult hippocampal neural stem/progenitor cells through activation of p38 mitogen-activated protein kinase (p38MAPK)/glycogen synthase kinase 3beta (GSK-3beta)/beta-catenin signaling cascade. *The Journal of Biological Chemistry*, 286(52), 44913–44920.
- Zhang, D., Wang, X., & Lu, X. Y. (2016). Adiponectin exerts neurotrophic effects on dendritic arborization, spinogenesis, and neurogenesis of the dentate gyrus of male mice. *Endocrinology*, 157(7), 2853–2869.
- Zhang, Y., Chen, K., Sloan, S. A., Bennett, M. L., Scholze, A. R., O'Keefe, S., ... Wu, J. Q. (2014). An RNA-sequencing transcriptome and splicing database of glia, neurons, and vascular cells of the cerebral cortex. *The Journal of Neuroscience*, 34(36), 11929–11947.
- Zupanc, G. K. (2008). Adult neurogenesis and neuronal regeneration in the brain of teleost fish. *Journal of Physiology, Paris*, 102(4–6), 357–373.

SUPPORTING INFORMATION

Additional supporting information may be found online in the Supporting Information section at the end of this article.

How to cite this article: Rastegar S, Parimisetty A, Cassam Sulliman N, et al. Expression of adiponectin receptors in the brain of adult zebrafish and mouse: Links with neurogenic niches and brain repair. *J Comp Neurol*. 2019;1–17. <https://doi.org/10.1002/cne.24669>

Résumé

Le diabète est un problème majeur de santé publique. Il est caractérisé par une hyperglycémie, une résistance à l'insuline et est associé à des complications macro et micro vasculaires. En situation de diabète, la concentration de méthylglyoxal (MGO) est augmentée. Le MGO est un précurseur des produits avancés de glycation (AGE) et il induit un stress oxydatif, une inflammation et un stress du réticulum endoplasmique. Ces Stress jouent un rôle important dans les dysfonctions endothéliales et de la barrière hématoencéphalique ainsi que dans le retard de réparation des lésions.

L'objectif de ma thèse a été d'améliorer la délivrance de curcumine, une molécule d'origine végétale. La curcumine a plusieurs effets bénéfiques tel que des activités anti oxydantes et anti inflammatoires, mais ces effets sont limités par son hydrophobicité. Des nanovecteurs tel que des protéines de hautes densités (HDL) ou des micelles peuvent améliorer la délivrance de la curcumine.

L'effet de la curcumine, vectorisée par des HDL ou par des micelles, a été évaluée dans deux modèles différents : la protection de cellules endothéliales en présence de MGO *in vitro* et *in vivo*, la régénération de la nageoire caudale chez le poisson zèbre.

Des nanoparticules de rHDL associées avec la curcumine (Cur-rHDLs) ont été préparées par ultracentrifugation après avoir mélangé brièvement les HDL avec la curcumine. Une analyse par LC-MS/MS a permis de quantifier la curcumine associée aux HDL. Les cellules endothéliales cérébrales Bend3 ont été prétraitées 1 heure en présence de rHDL, de curcumine ou de Cur-rHDLs puis incubées en présence de MGO. Sur des cellules traitées par du MGO, la Cur-rHDLs a montré un effet protecteur en réduisant la cytotoxicité, la production d'espèces radicalaires d'oxygène, le stress du réticulum endoplasmique et la condensation de la chromatine. Elle améliore également l'intégrité des cellules endothéliales compromise par le MGO. La Cur-rHDLs a un effet synergique en comparaison des effets de la curcumine ou des rHDLs seuls.

Des micelles de polysaccharide d'algues (des carraghénanes) associées avec de la curcumine (Cur-micelles) ont été préparées en copolymérisant des oligocarraghénanes (carraghénanes digérées) avec du polycaprolactone. La curcumine a été associée aux micelles par la méthode d'évaporation de l'acétone. Les Cur-micelles ont été caractérisées par des analyses de spectroscopie de résonance magnétique nucléaire et de diffusion dynamique de la lumière. Dans ce modèle, les Cur-micelles augmentent le recrutement des macrophages et des neutrophiles au site de la lésion ainsi que la taille de la surface de la nageoire régénérée. Les Cur-micelles ont également un effet synergique en comparaison des effets de la curcumine ou des micelles seules.

Ces travaux montrent les effets bénéfiques des Cur- rHDLs sur des cellules endothéliales en présence de MGO et des Cur-micelles sur la régénérescence de la nageoire caudale des poissons zèbres. Ils permettent une meilleure compréhension de ces approches et ouvrent de nouvelles perspectives de recherche pour le développement de thérapies dans le cadre de complications vasculaires associées au diabète.

Abstract

Diabetes is a major health issue worldwide. It is characterized by hyperglycemia, insulin resistance and is associated with many microvascular and macrovascular complications. In diabetic conditions, methylglyoxal (MGO) levels are increased. MGO is a major precursor of advanced glycation end products (AGE) formation and it induces cellular oxidative stress, inflammation and endoplasmic reticulum (ER) stress. These cellular stresses play a crucial role in endothelial and blood brain barrier (BBB) dysfunctions and also delay the wound healing.

My thesis objective was to improve the drug delivery of a plant derived compound (Curcumin). Curcumin has several beneficial properties such as antioxidant and anti-inflammatory properties but its effects are limited due to its hydrophobic nature. Nanovectors such as High Density Lipoprotein (HDL) or micelles may help to improve the delivery of curcumin.

Curcumin vectorized by HDL or micelles were evaluated in two different models: *in vitro* brain endothelial cell protection from methylglyoxal and *in vivo* tail regeneration in Zebra fish.

Curcumin loaded rHDL nanoparticles (Cur-rHDLs) were prepared by mixing HDL and curcumin briefly followed by ultracentrifugation. Amount of curcumin loaded was quantified by LC-MS/MS analysis. Brain endothelial cells (Bend3), were pre-treated with rHDL, curcumin and Cur-rHDLs for 1h before co-incubating with MGO. Cur-rHDLs showed a protective effect by reducing the cytotoxicity, reactive oxygen species (ROS) production, ER stress, and chromatin condensation induced by MGO. It also improved the endothelial cell integrity impaired by MGO. Cur-rHDLs showed a synergistic effect compared to curcumin or rHDL alone.

Curcumin loaded carrageenan polysaccharide micelles (Cur-micelles) were prepared by using oligocarrageenan (digested carrageenan) copolymerized with polycaprolactone. Curcumin was loaded by acetone volatilization method. Cur-micelles were characterized by nuclear magnetic resonance analysis and dynamic light scattering analysis. On the Zebrafish tail amputation model, Cur-micelles increased macrophages and neutrophils recruitment to the site of tail injury and had a positive impact on the tail regeneration by increasing the tail regenerative area. Cur-micelles also showed a synergistic effect compared to curcumin or micelles alone.

These studies show the potential beneficial effects of Cur-rHDLs and Cur-micelles on MGO stimulated endothelial cells and on zebrafish tail regeneration, respectively. They open new research perspectives to further investigate and understand the mechanisms that can be used to develop therapeutics for diabetic vascular complications.